



Impact of GPS Navigational Errors on the Required Performance of GBAS Approach Service Type D/F (GAST-D/F)

Ahmad Alhosban¹

Doctoral (PhD) Dissertation

In

Defense Electronic Information Technology and Communication (ITC)

Doctoral School of Military Engineering (DSME)

University of Public Services (UPS/NKE)

Scientific Supervisor: Dr.Farkas Tibor²

Budapest, Hungary

2018-2022

¹Eng.Ahmad Alhosban: PhD Candidate, University of Public Service (UPS/NKE), Doctoral School of Military Engineering (DSME), Defense Electronic Information Communication Technology, Budapest - Hungary, ahmad_alhosban@yahoo.com, ORCID: <https://orcid.org/0000-0001-7494-6067>

²Dr. Farkas Tibor, University of Public Service (UPS/NKE), Signal Department, Budapest - Hungary, farkas.tibor@uni-nke.hu, ORCID: <https://orcid.org/0000-0002-8868-9628>

Acknowledgements

This PhD-Dissertation has many mentors who helped this work could become reality. It is of my pleasure to express my thanks at this place to all those who supported this work.

First of all, I would like to thank Dr. Farkas Tibor, My Supervisor at (UPS)/ Faculty of Communication/ Signal Department for opening the chance and the necessary doors towards the success of this work. I thank Dr. Farkas Tibor for his continuously reviewing the progress of the work and for his highly engaged criticism at all its stages, which allowed a significant enhancement for the work done so far. And I would like to thank him for his support during both the academic and research parts of this Hungarian International PhD program. His help was great to organize this work as an industrial and research project, following the “plan – act –check” principles throughout the work segments.

Secondly, I would like to thank Prof. Eng. Haig Zsolt (Head of the research field of the Defense Electronic Information Communication Technology), who firstly interviewed me, accepted and awarded my proposal in 2018, and he was continuously directing me during the main milestones in publications and research work.

I thank Mr. Oswald Glaser (Senior Systems Engineer SATNAV Ex-Thales engineer) for his very precise initial task description, and his guidance to me to refine the task description. I thank him for his remote support during the initial proposal design.

I thank Professor Christophe Macabiau (ENAC) University at Toulouse, France for having a first look on my draft document and for a special tutorial in developing the MATLAB modules to generate Multipath Error Envelopes (MEE) for code and phase measurements, and for his help in debugging those modules and explaining the theoretical background.

Dedication

I dedicate this Doctoral PhD Dissertation to:

My sincerely wife in Jordan - Mafraq
Mrs. Ebtessam Alhosban,
She was behind my motivations and physiological support.

The head of the research field of the Defense Electronic Information
Technology and Communication
Prof. Eng. Haig Zsolt,
Who was behind accepting and awarding the initial proposal of this dissertation

My Supervisor and his wife in Hungary – Budapest
Dr. Tibor Farkas and Mrs. Erika Farkasne Hronyecz
Who were behind the support of my staying in my second home Hungary

My twin brother
Eng. Jamil Alhosban
Who was behind the support for me and my family while abroad

My Eldest Son in Jordan - Mafraq
Eng. Emad Alhosban,
Who was behind my travelling efforts

My Two little daughters
Dr. Mai Alhosban and Dr. Shahd Alhosban
Who were behind the heart surviving and father tacking care

My little boys
Mohammad, Abdallah, and Zaid
Who were behind the hope of continuing the way to success

Finally, and Firstly, to My ***Parents' Souls*** in their life-after
For their long-life raising me to achieve this significant dream

Table of Contents

Acknowledgements	2
Dedication	3
Table of Contents	4
Chapter 1: Introduction and Motivations	9
1.1 Chapter Introduction	9
1.2 Literature Review Summary and Research Motivations.....	9
1.3 Formulation of the Scientific Problem	13
1.3.1 Signal in Space Continuity of Service Performance:.....	15
1.3.2 Signal in Space Integrity Performance:	16
1.3.3 Signal in Space Vertical Accuracy performance:	16
1.4 Dissertation Questions.....	19
1.5 The main Assumptions of the Dissertation	19
1.6 Dissertation Objectives and their related Research Methodologies	20
1.7 Dissertation Hypotheses	20
1.8 Dissertation Structure	21
1.9 Chapter Summary.....	22
Chapter 2: Balancing the Position in Space between GPS and Galileo.....	23
2.1 Introduction	23
2.2 Historical Background.....	23
2.3 The Technical and the Political Status of GLONASS in the NAVWAR	25
2.4 The Technical Differences between GPS and Galileo	27
2.5 Why Galileo Initiatives?.....	31
2.6 Galileo Implications	35
2.7 Conclusions	38
Chapter 3: Impact of the GPS Errors on the Availability of the GNSS-GBAS Landing Systems in CAT II/III (GAST -D/F) Performance	39
3.1 Introduction	39
3.2 Availability Calculations in GBAS Infrastructure	39
3.3 GBAS Parameters' Assumptions	45
3.4 Simulations Runs (planning topology and performing)	51
3.5 Results Analysis	56
3.5.1 Global Coverage of GNSS/GBAS	56
3.5.2 Regional Coverage over Europe/USA for GNSS/GBAS	62

3.6	Conclusions and Recommendations.....	68
3.6.1	The New Achieved Scientific Result.....	69
3.6.2	Recommendations.....	69
Chapter 4: Effectiveness of the Multiplexed Binary Offset Carrier (MBOC) Modulation on Multipath Error Envelope in GNSS Receivers		70
4.1	Introduction	70
4.2	Problematic Analysis of the Multipath Error	72
4.3	Receiver-Based Mitigation Methods/Multiplexed Binary Offset Carrier (MBOC) ..	74
4.4	Signal Processing of MBOC and MEE inside the GPS Receiver architecture	77
4.4.1	Costas PLL /Phase Tracking Multipath Error.....	79
4.4.2	Non-coherent DLL/Code Tracking Multipath Error.....	82
4.4.3	Coherent DLL/Code Tracking Multipath Error.....	85
4.5	Code /Phase Multipath Error Envelopes Algorithms.....	87
4.6	Program Validation Compared with Similar Software	90
4.7	Result Analysis.....	91
4.7.1	Chip Spacing and Relative Amplitude.....	91
4.7.2	Materialization waveform type: BPSK, BOC (1, 1), and BOC (2, 2)	92
4.7.3	Filter type Impact	93
4.8	Conclusions and Recommendations.....	96
4.8.1	The New Achieved Scientific Result.....	97
4.8.2	Recommendations.....	97
Chapter 5: Impact of Electronic Attacks on GNSS / GBAS Approach Service Types C and D Landing systems and their proposed Electronic Protection Measures (EPM).....		98
5.1	Introduction	98
5.2	Scientific Problem and the Observed Accidents/Deliberating.....	100
5.2.1	NATO military exercise on the 8th Nov 2018.....	101
5.2.2	EAs in South Korea, Ukraine and USA.....	102
5.3	GNSS/GBAS Signal Structure w.r.t Electronic Warfare	105
5.4	GNSS/GBAS Signal Processing w.r.t Electronic Warfare	109
5.5	Impact of EAs on GNSS/GBAS Using Multipath Approach	111
5.5.1	Jamming.....	111
5.5.2	Spoofing.....	112
5.5.3	Meaconing.....	112
5.6	Conclusions and Recommendations.....	120
5.6.1	The New Achieved Scientific Result.....	121

5.6.2	Recommendations.....	121
Chapter 6: GPS Characterization in Cyberspace between Vulnerability and Geo-encryption: Impact on GBAS Landing System (GLS)		
6.1	Introduction	122
6.2	Assessment of the Geo-Encryption Algorithm: Prospects and Implications	124
6.2.1	The successive geo-lock function of a predefined rout while in mobility.	125
6.2.2	The vulnerability of GPS using the Geo-Encryption while using the (C/A) code. 128	
6.3	The necessity of Geo-Encryption Algorithm for the GBAS Landing System	131
6.4	Assessment of implementation of the Geo- Encryption algorithm in the GBAS Landing System (GLS), special case study in Budapest International Airport.....	132
6.4.1	Results Analysis.....	136
6.5	Conclusions and Recommendations.....	137
6.5.1	The New Achieved Scientific Result.....	138
6.5.2	Recommendations.....	138
Chapter 7: Assessment of the GIS-Aided Precise Approach Using the GNSS-GBAS Landing Systems		
7.1	Introduction	139
7.2	Background	140
7.3	Geographic Information System (GIS) Implementation in the Aviation Domain ..	142
7.4	The technical differences between the GLS and the ILS insight of the GIS aiding	145
7.5	Assessment of the future performance of the GBAS Landing System (GLS).....	152
7.5.1	Result Analysis:	154
7.6	Special case implementation: Budapest Airport	154
7.6.1	Results Analysis:.....	157
7.7	Conclusions and Recommendations.....	158
7.7.1	The New Achieved Scientific Result.....	159
7.7.2	Recommendations.....	159
Chapter 8: Summarized Conclusions, and Recommendations		
8.1	Introduction	160
8.2	The New Achieved Scientific Results.....	160
8.3	Hypotheses' Answers.....	162
8.4	Practical Availability of the Scientific Results and Recommendations.....	162
Table of Figures		165
Table of Tables		167

Table of Equations	168
Appendix A-1: Bibliography and References	170
Appendix A-2: Author Publications.	174
Appendix B: Acronyms	177
Appendix C: Author CV (Resume).....	180
Appendix D: Matlab-Based Multipath Error Envelopes Software.....	184
Appendix E: Outputs of the Simulation Runs.....	203

This page is intentionally left blank

Chapter 1: Introduction and Motivations

1.1 Chapter Introduction

This chapter covers the following topics: Literature review and motivations, formulation of the scientific problem, the main dissertation questions, the main assumptions, and the main objectives associated with the related research methodology for each objective, the hypothesis, and finally, the main structure of the dissertation.

1.2 Literature Review Summary and Research Motivations

In this section, I address the four main motivations behind this dissertation, the research literature review and the speculated objectives based on them.

Firstly, In the Global Navigation Satellite System/ Ground Based Augmentation System (GNSS/GBAS) landing systems' domain, the first version of GNSS CAT I performance in what so called GNSS landing system (GLS) was certified in 2002, it was announced by the International Civil Aviation Organization (ICAO) as per (ICAO Annex 10, Volume 1, Amendment 77, 2002), (ICAOAnnex10, 2002), and it was fully technically detailed in (RTCA245A, 2004), this important event took place just after the Selectivity Availability (SA) had been removed in May 2001, then after, many systems were deployed in CAT I performance and had been operated successfully in France, Germany and USA using the GPS system or the GLONASS Russian System since 2002. The worldwide research had continued for achieving CAT II performance certification since that time, until it has been recently approved in Nov 2020 using the GPS single constellation as per (ICAOAmendment91&92, 2020), and it is still under foreseen for CAT III (or what newly called GBAS Approach Service Type F (GAST – F)), the latest performance of CAT III/ GAST-F is tended to be achieved - only and if only - dual constellation is being used.

Lately, a previous study (Rotondo, 2017) showed that the assumption of having dual constellation is subjected to the evaluation of certain significant factors that would restrict using it, such as: firstly, the delay in time due to phase measurements during phase combination at the receiving antenna, which might cause minimizing the accuracy of the Position Navigation and Timing (PNT) information or/and minimizing the margin below the stringent Vertical Alert Limits (VAL) in the integrity availability. Secondly, the complexity of using the multichannel receivers might also cause further delay in time. Thirdly, and above of all, depending on a

nation own GNSS constellation would add a significant value of independency in terms of Politics, Economics and Security, as per fully detailed in (Alhosban A. , 2019). On the other hand, President of the United States of America had recently signed a new Executive Order on Position, Navigation and Timing (PNT) services in Feb. 2020, in which he was encouraging the development of a resilient PNT infrastructure that isn't exclusively reliant on the U. S. Global Positioning System (GPS) only, its aim is motivating all providers to search for alternatives of such critical infrastructure, see (President of USA, (Order, 2020). Moreover, many of the recently published researches has conducted this domain individually for a certain airports, neither in a worldwide coverage manner, nor over Europe sky. In which it doesn't help significantly in the certification process needed by the high organizations bodies such as ICAO or FAA.

Based on above facts and motivations, the first objective of this dissertation was made to examine and evaluate the using of a Single Constellation (SC) in GBAS Landing Systems, particularly the European Galileo system over Europe Space. However, the Multipath error is considered a limiting factor to achieve the needed performance to meet the CAT II/III requirements in terms of Accuracy and yet availability. On the other hand, the BOC signals showed a better anti-multipath and anti-interference over the BPSK, in terms of better MEE. Moreover, the generic BOC modulation has been adopted in the modernized Global Positioning System (GPS) (JW, 2001), and the European Galileo System (Galileo, 2008), because of its good spectral isolation from heritage signals, its high accuracy, and its multipath interference resistance compared with BPSK modulation. Furthermore, and yet, the Multiplexed BOC (MBOC) modulation has been used for the Galileo E1-B/C and the GPS L1C at frequency (1575.42 MHz) to achieve enhanced accuracy and multipath interference resistance by using multilevel subcarrier symbols or combining different subcarrier symbols. Therefore, the first objective is more refined to assess the impact of these errors and enhancement in achieving CAT III/GAST-D/F performance of the GBAS landing systems.

Secondly; from the interference perspective; the Global Satellite Navigational Systems (GNSS) applications - which are using satellite signals in space - are currently and hugely subjected to Electronic Attacks (EAs) such as Jamming, Spoofing, and/or Meaconing, if it had not already been interfered unintentionally by other host applications. Many accidents were observed in the past decade especially with the huge dependency on GNSS applications in governmental and private critical infrastructure, in both civil and military aspects. The well-known GNSS

discrete frequencies (L1, L2, and L5, etc.) are too vulnerable to EAs, because of their extremely low level of power density, this is due to the reason that they are being propagated from long-distance satellites' orbits of about (22,000 Km) via Troposphere and Ionosphere layers. And they arrive the surface of ground at a weak power level. It's around (-160dBw for GPS L1, -154dBw for GPS L2 (Military), Speculated -155dBw for Galileo E1/E2). Saying that, any non-significant exceeded level of any transmitted power by a jamming transmitter would be harmful to them, this impact ranging either destructively at most, or electronically deceptively at least, consequently, the GNSS signals cannot be acquired or/and tracked anymore by the GNSS receivers.

Therefore, the Electronic Attacks were most critically observed by International Civil Aviation Organization (ICAO) and Federal Aviation Administration (FAA), they are in the GNSS/GBAS Landing systems more critical than other applications, because they are used for final landing phase of flights in both civil and military aviation domains, or during military operations in deployed theaters. However, the GBAS landing systems are satellite-based navigational aids used in the Critical Meteorological Conditions (CMC), such as heavy dust and heavy fog, where the visibility tends to zero in the final landing of an aircraft, in which their loss of service during the Final Approach Segment (FAS) is considered a catastrophic disaster to aviation safety-of-life in terms of assets, human and military operations. At those cases, the capability of service restoring on the proper time has very low probability. It is highly riskier in such safety-of-life applications of landing systems when compared with other safety-critical infrastructure applications such as banking or with non-critical applications of GNSS huge usages. Moreover, the GBAS stations are usually located in a well-known surveyed reference sites in the vicinity of the airport near the runways, which makes them more vulnerable to EAs, both the fixed ground reference stations and the downwind moving aircrafts while landing close to runway surface.

Moreover, It was observed a strong link between the concept of multipath and EAs, in terms of accumulating two or more signals at the receiving antenna in the so called technically signal interference. However, the over power jamming seems to be similar to the destructive multipath when the phases of the two signals are 180 degrees out of phase, assuming they were modulated and (authenticated) by the same navigation message of Position, Navigation and Timing (PNT). On other hand, spoofing/meaconing seems to be similar to the electronic deceptive side of the multipath signal with long delay time of the original signal that would cause the GNSS receiver

incapable to correlate them in proper time, it might mislead the pilots in terms of PNT information.

Based on that, the second objective of this dissertation was to evaluate the impact of the three different types of EAs (jamming, spoofing and meaconing) on the performance of GNSS/GBAS landing system, and to examine the latest proposed Electronic Protection Measures (EPM) for such EAs, providing the using of the three mitigation methods: the receiver-based mitigation methods, the antenna-based methods and the siting-based methods.

Thirdly, and from the perspective of the Geo-Encryption effectiveness, obviously, since the September 11, the terrorist attacks against the internet and servers' data base have noticeably increased, their tools took another path of the means' curve to achieve their ends and goals. Although the fact they have different levels of skills of hacking and computer knowledge, they were likely able to attack and growing their use of the internet as a digital battleground. As per (Denning, 2001), one of the main man-made cyberspaces is the aviation aspect, evidenced by the September 11 event. From which, it is clear that the aircrafts hijacking is possible anywhere and anytime. However, many data and voice messages transfer from the ground controllers to the aircrafts' computers and pilots could be attacked. Consequently, vast of encryption techniques have been developed using many Advanced Encryption Standards (AES) codes' generation process, most focused in this dissertation is the Denning Geo-Located Model (Denning&Scott, 2003), and its enhancements raised lately.

The Geo-encryption or the Geo-Located model is based on the established cryptographic algorithms to provide an additional layer of security. This added layer is enhancing the conventional cryptography, but not replacing it. It enables data encryption for a predefined place or a given geographic area in time and space. If an adversary, attempts to decrypt the data at different location or time, the decryption process would fail. The decryption device determines its location using some kind of location sensors like a GPS receiver or any positioning system. In all the process, it assumed the use of anti-jam and the anti-spoof receivers.

Based on that, the third objective of this dissertation is to assess the implementation of the geo-encryption (Denning&Scott, 2003) Model or the Mobile (Al-Fuqaha, 2007) Model in the approaching high-speed landing aircraft using GLS, and to examine to which extent the GPS signal is capable to be used in terms of immunity against spoofing/jamming in the geo-

encryption aiding and in terms of mobility as well, especially in final approach path in the GBAS Landing system application.

Fourthly and lastly, another perspective point of view, and in order to link the GBAS Landing System (GLS) to the Geographical Information System (GIS), a deeper investigation was performed in this aspect, which is the last objective of this dissertation, Historically, the navigational landing systems era had passed through a long way of developments and enhancements since the early 1970s, the major milestones in this development roadmap are the Instrument Landing System (ILS), the Microwave Landing System (MLS) and the GBAS Landing System (GLS). In early ILSs and MLSs stages, the Approach Instrument Plates (AIPs) were not aided by GIS. Recently, a new approach called RNAV (aRea NAVigation) has been used, it is totally depending on the WGS-84 coordinates system of the used beacons rather than their radiations. Consequently, the new GLS systems would be more effective if they have been used along with GIS-aided Approaches, in terms of accuracy and the capacity enhancing the ATM Management.

Based on that, the fourth objective here is to examine the GIS Aided precise approach trajectory using the signals of the GBAS Landing System (GLS) by comparing with the Non-GIS aided approach trajectories used in the current conventional ILSs. Furthermore, the available GIS infrastructure of the Budapest Airport (BUD) is strongly needed to be detailed, showing the future investment in GBAS landing system to optimize the accuracy, integrity, availability performance, as well as increasing the capacity of the air traffic of the airport handling.

With that is being into considerations, these four motivations have been converted to four objectives of this dissertation, from which this research effort took its importance, and its valuable scientific results so far.

1.3 Formulation of the Scientific Problem

In the satellite based navigation environment, so called Global Satellite Navigation Systems (GNSS) such as the US GPS, the Russian GLONASS, and the Future European GALILEO constellations, the Signals in Space (SIS) are being transmitted by the satellites vehicles in space and are received by the ground receivers through the ionosphere and troposphere layers, those signals when being used solely are currently not being monitored neither accurate enough

to meet the requirement of the precision approach of a landing aircraft as per International Civil Aviation Organization's (ICAO) standards Categories (CAT I to CAT III) of the needed performance to support flight safety Airworthiness. However, the augmentation technique is strongly needed to enhance their availability performance of accuracy, integrity, and continuity of service. The Ground Based Augmentation System (GBAS), which is one of the three Augmentation Systems globally used: Space Based Augmentation System (SBAS) and Airborne Based Augmentation System (ABAS), is intended to be used for precision approach from CAT I to CAT III. Although GBAS is currently been into operation at many airports globally, but to support CAT-I performance precision approaches only (Michael, 2015).

Basically, The Ground-Based Augmentation System (GBAS) provides corrections and integrity monitoring information along with the global navigation satellite system (GNSS) signals to provide navigation guidance for precision approach and landing for both civil and military aviation in all bad weather situations, GBAS is alike to (and will eventually and gradually supplement or/and replace) the currently used Instrument Landing System (ILS), it has been used since many years ago in all the controlled airports worldwide, ILS is used in order to guide the landing aircrafts to the centerline of a runway within a gliding angle (nominally 3 degrees) in the bad weather conditions where the visibility is very low. However, GBAS is based on the differential GNSS technique, where errors in GNSS range measurements are corrected in the range domain or area, the corrections delivered in real time are based on measurements by at least 2-4 ground reference GNSS receivers usually placed at or near an airport with their locations precisely known, those accuracy corrections for each satellite in view (within an elevation angle higher than 5 degrees above horizon) as well as integrity information are sent through VHF Data Broadcast (VDB) stations to (and are used by) the aircraft onboard receiver, then they are been applied to its real time position along the landing path vertically and laterally (Susumu, 2017).

GBAS will increasingly become a safety-critical application of GNSS for civil aviation requiring a high level of availability of (accuracy, integrity and continuity of service), so called performance. The performance requirements are defined by the International Civil Aviation Organization (ICAO) Annex 10 (ICAO 2014). Standards for avionics are further refined by relevant standardizing organizations such as RTCA (RTCA 2008a, b)/EUROCAE, EUROCAE also defined minimum operational performance standards for GBAS ground subsystem (EUROCAE 2013). However, GBAS has been standardized based on the use of single-

frequency GNSS (L1, centered at 1.57542 GHz) only (Susumu, 2017). Those performance requirements can be summarized (but not limited to) as follows, knowing that CAT I in ground ILS system is equivalent to GBAS Approach Service Type C (GAST-C) in satellite system, and CAT II is equivalent to GAST-D, and CAT III equals to GAST-F, see figure 1 below:

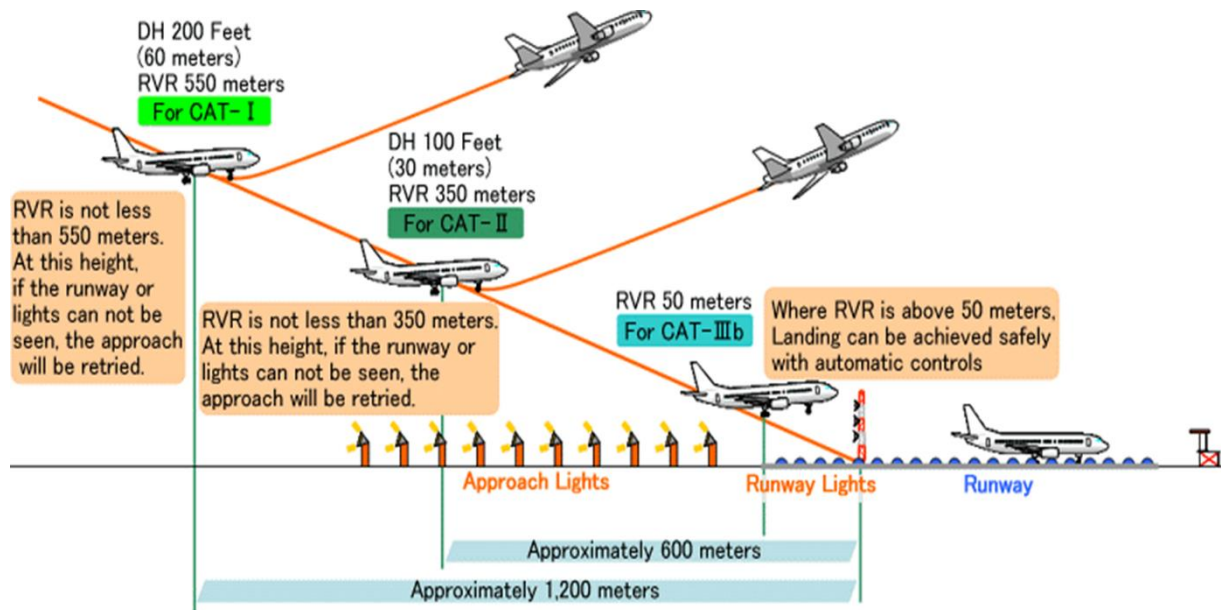


FIGURE 1: THE REQUIRED AERONAUTICAL REQUIREMENTS FOR ILS/GBAS LANDING SYSTEMS [OPEN SOURCE]

1.3.1 Signal in Space Continuity of Service Performance:

The GBAS Signal in Space continuity of service is defined by the probability that a fault-free aircraft subsystem provides valid outputs during any defined period of an approach, assuming that outputs were valid at the start of the period. Outputs are considered as valid if the Navigation System Error (NSE) is lower than alert limits and if there is no warning, and as follows:

- For CAT I operations: shall be greater than or equal to $1 - 8 \times 10^{-6}$ during any 15s period.
- For CAT II and CAT IIIA operations: shall be greater than or equal to $1 - 4 \times 10^{-6}$ during any 15s period.

- For CAT IIIB operations: shall be greater than or equal to $1- 2 \times 10^{-6}$ during any 15s period for vertical and greater than or equal to $1- 2 \times 10^{-6}$ during any 30 s period for lateral guidance.

1.3.2 Signal in Space Integrity Performance:

The GBAS Signal In Space (SiS) integrity risk is defined as the probability that the GBAS Ground Subsystem provides information, which when processed by a fault-free receiver, using any data that could be used by the aircraft, results in the position error exceeding the alert limit for a period longer than the maximum SiS time-to-Alert without annunciation, and as follows:

- For CAT I operations: is required to be less than 2×10^{-7} in any one operation.
- For CAT II and CAT III operations: is required to be less than 1×10^{-9} in any one operation.

1.3.3 Signal in Space Vertical Accuracy performance:

The GBAS vertical accuracy is defined in terms of vertical Navigation System Error (NSE). The vertical NSE is the difference between the measured and true vertical displacement from the final approach path. The probability that the vertical NSE value is within the limits shown below shall be at least 95% per approach. The vertical accuracy limits are given as a function of the height (H) above Landing Threshold Point / Fictitious Threshold Point (LTP/FTP) of aircraft position, (Lateral Accuracy is already identified by not mentioned due its compliance), and as follows:

- For CAT I operation:
 - Between 100ft HAT and 200ft HAT, a constant value of 4 m.
 - Between 200ft and 1340ft HAT, linearly varying from 4 to 17.3m.
- For CAT II operation:
 - Between 50ft HAT and 100ft HAT, a constant value of 1.4m.
 - Between 100ft and 1340ft HAT, a value linearly varying from 1.4 to 17.3m.
- For CAT III operation:
 - Between 50ft HAT and 100ft HAT, linearly varying from 0.7-1.4m.

- Between 100 feet and 1340 ft. HAT, linearly varying from 1.4 to 17.3 m.

GBAS Approach Service Type C (GAST-C) stations supporting CAT I operations have been fully developed and already certified with a 200ft decision height for precision instrument approach and landing, the first GBAS stations are currently operational in France, Germany, USA and other countries. Furthermore, the single-frequency GPS-based GBAS GAST-D, which is intended to support operations of CAT II, with lower than 100ft decision height, is still under development including automatic approaches and landings, requirements have been drafted, approved and are currently undergoing validation (Michael, 2015) (Yiping Jiang, 2016). Moreover, with the forthcoming GNSS environment, GAST-F has been designated to the provision of CAT III services using multi-constellation and dual-frequency corrections which will mitigate the issues raised under GAST-D and is being investigated within the European SESAR program (WP 15.3.7) (Yiping Jiang, 2016). Therefore, the dual constellation is the limiting factor for GAST-D/F implementations, especially in the case of Galileo delay.

The Ground Based Augmentation System (GBAS), as a new and alternative approach with high levels of performance in terms of navigation for aircraft, counters systematic errors in broadcast correction ranging measurements associated, such as Ionosphere Delay ID (IrfanSayim, 2017) and Multipath Errors ME (Yiping Jiang, 2016) when using a Global Positioning System (GPS) L1 frequency receiver. In principle, ID can be simply estimated with the aid of dual frequency receivers (GPS L1 and L2) or a new GPS signal (L5), ID is Low-latitude ionosphere disturbances dependent, and frequency depend as well, but the GBAS relies only on the L1 frequency as the L2 frequency is not protected by Aeronautical Radio Navigation Service (ARNS) and L5 is not fully functional yet, neither the new European Global Navigation System Galileo is fully operational yet (anticipated Full Operational Capability (FOC) in 2025 if not beyond, it was supposed to be FOC in Dec 2018 but the remaining 4 satellites out of 30 and the ground stations networking are still not contracted yet, see more details about the three main phases of Galileo navigation project as per (ESA, Galileo Navigation, 2018).

However, beyond Galileo FOC, a period of (5-10 years) is anticipated to be needed for the gradually transition phase for the new systems in, and the legacy ones out. Furthermore, and optimistically, the enhanced performance of the Galileo navigation system could enable worse performing aircraft, those with larger Flight Technical Errors (FTE), to meet the requirement,

based on the fact that total system performance depends upon both the navigation system error (NSE) and the Flight Technical Errors (FTE) (SARPs 2009).

Mainly, Ionosphere Delay (ID) and Multipath Error (ME) are the most errors challenge for GBAS Approach Service Type D (GAST-D) performance to be achieved using GPS L1, most the recently peer-reviewed published studies by the most experts and working groups in this domain are conducting methods of predictions and estimations of such errors and their effects on GBAS performance especially type D/F (CAT II/III). Moreover, some of those studies were being done and limited for a specific region or for a specific airports, and conducting one type of errors to determine its impact or its associated simulating software. At the same talking, my previous master dissertation study was conducting the user multipath effect on GBAS availability of integrity globally.

Later many multipath mitigation methods of such big threat were developed and did minimize the effect to be closer to achieve type D/F performance, other studies did conduct the ground multipath error impact in some airports due to tough terrain. In addition, and due to the medium term of minimum 5-10 years for the full operational capability (FOC) of Galileo, as the second satellite navigation system using L1, with an added another of 5 to 10 years of gradually transition period, saying that, it has been noticed that most of the studies recently published didn't conduct a comprehensive evaluation of the total error affecting achieving GBAS Type D/F performance. With that said, the total system performance of GAST-D/F GBAS, depending upon both the Navigation System Error (NSE) and the Flight Technical Errors (FTE), so called the total error budget (NSE +FTE), should be identified, determined and proved globally-wise and regionally-wise in terms of their dependency to achieve GAST- D/F Performance requirements.

From another perspective; the GPS L1C signal is not monitored yet, the signal integrity is not assured, it may mislead the pilots in terms of position information, especially in the final phase of flight landing, in which the probability of error should tend very low values, almost to less than 2×10^{-7} failure occurrence in any one operation is required to be for CAT I operations, and less than 1×10^{-9} failure occurrence in any one operation is required for CAT II/III, i.e. GAST –D/F. Also the interference impact may add another value for the errors and it should be modelled and identified, moreover, mitigated to its minimum probabilities as well.

Taking into consideration the mentioned motivations in section 1.2 above, and the rationale scientific problem formulation mentioned in section 1.3 above, all the above factors had led to the research objectives, in order to start, with a suitable methodology tools, to search for the best solutions to this scientific problem in the aviation domain. I tried my best to reach at the end of this research dissertation to the ultimate, optimized engineering scientific results.

By this is being taken into considerations, the questions, objectives hypotheses and their associated methodologies of the dissertation were addressed carefully as illustrated in the next sections.

1.4 Dissertation Questions

Based on the above literature review and motivations as well as the scientific problem formulation, the questions of the dissertation were as follow:

- How efficient the GBAS Landing systems (GLSs) to achieve the required performance of CAT II/III (or newly called GAST-D/F)?
- What is the impact of GPS Navigational errors on the required performance of GBAS GAST-D/F Landing systems?
- What is the impact of the Electronic Attacks on the GBAS GAST-D/F performance?
- How far the geo-encryption model and its mobility be implemented in the approaching high-speed landing aircraft using GLS?
- How to optimize and to enhance the use of the GIS-Aiding precision approaches in the GBAS Landing systems?

1.5 The main Assumptions of the Dissertation

The main assumptions of the dissertation are:

- Using single constellation of the EU Galileo Navigation system.
- Using dual frequency transmission to minimize the effect of Ionospheric and tropospheric errors.
- Using a limited coverage area over Europe with comparison with USA Area.

- Using a validated simulation tool to assess the needed availability for GAST D/F.
- Using a validated Matlab software to assess the Multipath Envelope Error (MEE).

1.6 Dissertation Objectives and their related Research Methodologies

In order to investigate the feasibility of achieving the GAST-D/F performance using GNSS Landing Systems, the main objectives of this PhD study are as stated and sequenced as below:

1. To investigate and define the impact of GPS/GNSS Navigational errors on the required performance of GBAS GAST-D/F landing systems. This was performed by using:
 - a. AVIGA validated Simulation Tool for the availability Assessment.
 - b. Matlab Code line programming for the Multipath Error assessment.
2. To investigate and model the impact of the Electronic Attacks on the performance GBAS GAST-D/F landing systems. This was performed by using modelling method for the interference caused by electronic-attacks, with analogy to Multipath errors estimations.
3. To assess the implementation of the geo-encryption model and its mobility in the approaching high-speed landing aircraft using GLS. This objective was performed by examining the model in different flight phases.
4. To optimize and enhance the use of the GIS-Aiding precision approaches. This was performed by a qualitative research method by examining the Budapest Airport (BUD) aerospace using GIS approach plates.

1.7 Dissertation Hypotheses

The following table 1 shows the hypotheses of my dissertation, those hypotheses have been tested throughout the progress of the work against their correctness, the results column intentional left blank until the end of the dissertation, and it is filled out in table 22 in chapter 8, in which the final results addressed, therefore the same table is shown twice, once in table 1 below without answers, and once in table 22 with answers.

#	Hypothesis	Results after testing
1	Single GNSS GBAS systems are capable to achieve GAST-D/F global performance in landing operations.	TBD (To be determined at the end the dissertation table 22 chapter 8)
2	Galileo/GPS each alone is capable to achieve GAST-D/F regional performance in Landing operations.	TBD
3	Galileo is more immune to Electronic Attacks than GPS	TBD
4	GEO- Encryption is not efficient with high speed mobility of the landing aircrafts that using GNSS.	TBD
5	GNSS Landing Systems (GLSs) have better performance with Geographic Information system (GIS) approaches plates than conventional ILSs.	TBD

TABLE 1: RESEARCH HYPOTHESES

1.8 Dissertation Structure

The main structure of this dissertation is detailed in the following table 2, The dissertation chapters were written based on the published papers/articles of each individual objective, each objective was planned to be dealt with during the 4-year research plan of the doctoral program, in which the research phase took place in the 3rd and the 4th years, while the academic phase took place in the 1st and the 2nd years along with some research activity as well.

Chapter No.	Chapter Title/objective	Publication Status
Ch.1	Introduction and Motivations	
Ch.2	Literature Review: Balancing the Position in Space between GPS and Galileo	Published
Ch.3	Obj.1: Impact of the GPS Errors on the Availability of the GNSS-GBAS Landing Systems in CAT III/ GAST-D/F Performance	Published

Ch.4	Obj.1: Effectiveness of the Multiplexed Binary Offset Carrier (MBOC) Modulation on Multipath Error Envelope in GNSS Receivers	Published
Ch.5	Obj.2: Impact of Electronic Attacks on GNSS / GBAS Approach Service Types C and D Landing systems and their proposed Electronic Protection Measures (EPM)	Published
Ch.6	Obj.3: GPS Characterization in Cyberspace Between Vulnerability and Geo-encryption: Impact on GBAS Landing System (GLS)	Published
Ch.7	Obj.4: Assessment of the GIS-Aided Precise Approach Using the GNSS-GBAS Landing Systems	Published
Ch.8	Summarized Conclusions and Recommendations	

TABLE 2: DISSERTATION STRUCTURE (CHAPTERS VERSUS OBJECTIVES)

The two phases were continuously linked together in a regular basis, and they were mile-stoned by the comprehensive Exam, which was designed to examine the academic knowledge and the research progress too. Figure 2 below shows the whole process of the dissertation building and the research activities.

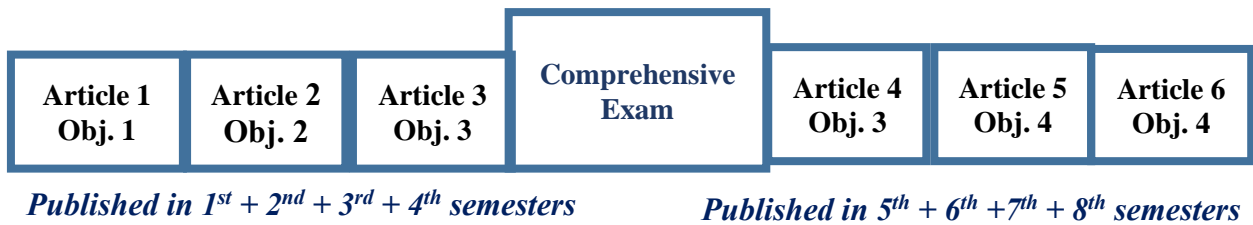


FIGURE 2: DISSERTATION PROGRESS (RESEARCH ACTIVITIES PHASE V_s ACADEMIC PHASE)

1.9 Chapter Summary

In this chapter, an introduction to the dissertation was produced, in terms of literature review summary, motivations, and formulation of the scientific problem, assumptions, hypotheses, the four objectives along with their research methodologies, and finally the dissertation structure.

Chapter 2: Balancing the Position in Space between GPS and Galileo

2.1 Introduction

In this chapter, the full justification of using the European GNSS constellation Galileo is addressed. However, in the concept of the Space Navigation Warfare (NAVWAR), balancing the position in space during the cold negotiations between the EU and the USA was the main aim in nullifying NAVWAR. Galileo, the new European navigational satellite system, will handle new potential operational fields and services, along with the existing U.S. navigational satellite system GPS. However, the so-called U.S. NAVSTAR GPS system is operating in the same unified space, and it is currently the dominant and the standard navigational system in the world, therefore, it is considered a monopoly in this domain. Meanwhile, the Galileo system will share the GPS system in this single space, it will enhance both the performance and the accuracy, and it will also share its benefits with civilians. Furthermore, the Europeans will pursue the EU independency from the U.S. and the economic share as well. The objective of this chapter is to identify the justifications and rationale of both stakeholders, the EU and the U.S., in having their interests in space. Those interests started initially as two separated independent systems and ended up eventually after long negotiations as two competitive and inter-operative systems. Furthermore, the chapter will identify the positive technical efforts progress done by both sides in order to maintain the two systems competitive, modernized and dynamic to become one efficient system, similarly to the Internet worldwide. However, there will be less focus on other systems such as the Russian GLONASS system, the Chinese Beidou system, and other augmented systems for the reasons explained later in this chapter.

2.2 Historical Background

In the satellite based navigational environment, the so-called Global Satellite Navigational Systems (GNSS) such as the American GPS, the Russian GLONASS, and the future European Galileo systems (also called constellations), the Signals in Space (SIS) are basically transmitted by the satellite vehicles in space, and then they are received by the ground receivers, after passing through the ionosphere and troposphere layers. Those Signals in Space (SIS) are intended to be used for many purposes, in both military and civilian domains, such as the communication relays with global coverage, the global navigational PVT: Position Velocity

and Timing, surveillance, and the metrological uses. Most importantly, the navigational signals are used for the common grid and the common timing especially for military operations, from where the original idea of the GPS concept came. It was very important for the U.S. army to unify the grid of the strategical, operational and tactical missions worldwide as well as the timing for the deployed forces globally in many theatres using those space sensors. Moreover, the GPS system was invented in the early 1970s and operated by the U.S. Air Force, Department of Defense DoD. Yet, its operation was shared with the Department of Transportation (DoT).

However, Russia, the other pole of the world at that time, would not be left behind, their idea of a Global Navigational Satellite System GLONASS was initiated and started to get operational in 1978, but using a different frequency band and different modulation scheme. Moreover, pursuing globalism was also their main hypothesis. Accordingly, the old continental Europe had its role also, the Europeans sought to have their independency in space. Therefore, their new born system, Galileo, was their hope and goal in sharing the space globally along with the U.S. and Russia. They started launching the first two satellites of the Galileo project, GIOVA A and B, at the end of 2005 after long debates and negotiations with the U.S. On the other hand, China launched their Beidou navigational system through three phases: B-1, B-2, and B-3, but even B-3 phase hadn't provide global coverage in terms of Full Operation Capability (FOC) yet. It is considered only regionally FOC focused over the Far East region (B. Eissfeller, 2007). And if becoming such FOC, then the Independency factor is a political restriction for all the world, especially after Covid-19 pandemic and the missing rotating Chinese rocket which scared the world population for one week in 2021.

Furthermore, the GPS satellites have got aged and deficiencies, Signals in Space (SIS) which came from the elder GPS Satellites are being received by the end-users without the required performance that meets the needs of both military and civilians; they are neither very accurate, nor being monitored. It was technically clear that the accuracy in position has suffered from many contributing errors such as the Ionospheric and the multipath errors (I. Sayim, 2017). Moreover, the accuracy had deviated about 100 meters before the selectivity availability (SA) was switched off by the declaration of the American President Bill Clinton in May 2000. Thereby, the accuracy became around 10 meters, but this was also not accurate enough for all the applications. More importantly, the integrity factor of the SIS was not feasible; this may

mislead or deceive the position information of the users without notifying them when the errors exceed the allowable limits of their tolerances.

Based on that, and due to such inaccurate and untrustable performance, the augmenting systems have been created over some regions by specific space agencies in order to compensate those drawbacks. Nevertheless, those augmentation systems are still using the same original GPS signals in a manner that they are corrected by the principles of the Differential GPS (DGPS). Those augmentations are classified into three main categories: The Space-Based Augmentation System (SBAS), the Ground- Based Augmentation System (GBAS), and the Airborne-Based Augmentation System (ABAS). However, the SBAS main systems are more covering the wide regions than the other two types, such as the European EGNOS system, the Indian GAGAN system, the U.S. WAAS system and the Japanese MSAS system. These systems will not be discussed under the scope of this chapter due to their dependency on the same original GPS signal in space; in other words, they are considered the subsystems of the GPS system itself.

On the other hand, the Beidou Chinese system is only a regional GNSS system owned and operated by the People's Republic of China. Moreover, China is currently expanding the system to provide a global coverage using 35 satellites anticipated to be fully operational by the year 2022. Nevertheless, the Beidou system – previously called Compass – is still currently not a globally based system; therefore, it will not be under the scope of this chapter.

2.3 The Technical and the Political Status of GLONASS in the NAVWAR

In order to examine the technical and the political status of the Russian GLONASS satellite system, the following questions are necessary to be answered: How can the GLONASS system be identified technically? What is its political status in the NAVWAR?

A short history of the GLONASS system is highlighted to be able to answer the above two questions. First of all, it is well known that the GLONASS system had been launched during the cold war era since 1978, its name stands for (GLObal NAvigation Satellite System), and it is a radio-based satellite navigational system, which was initially developed for the use of the Soviet military. Moreover, it was classified as the second generation of satellite-based navigational system of the Soviets, and was intended to improve their first generation (Tsikada) system. Furthermore, the Tsikada system suffered deficiencies; it required one to two hours of signal processing to calculate the location with high accuracy. Moreover, the time of observing

more than 4 satellites in the sky-view was limited, because it did not form a complete GNSS system at that time in spite of the fact that it was proposed to be fully operational by the year 2010, and to be compatible and interoperable with the GPS and the future Galileo systems.

Originally, the goal of developing the GLONASS system was to create more opportunities for the developers of the GNSS applications, allowing them to provide value-added services to the end-customers. Therefore, the development on the GLONASS system began in 1976, with a goal of a global coverage by 1991. Hence, numerous satellite launches had been completed since the year 1982, until the constellation of 26 satellites was obtained by the year 1995. Unfortunately, after its completion, the system rapidly fell into decay with the collapse of the Russian economy; therefore, the older satellites were taken out of service after their design lifetime expired without being replaced. In the end, only 8 satellites remained in the GLONASS orbits. Yet, and to change this situation, Russia decided to restore the system in major milestones that would end by the year 2011. Based on that, a federal program named “Global Navigation System” was undertaken by the Russian Government on 20 August 2001 with the Indian Government joining the program as a partner in both funding and services. Accordingly, both countries emphasized again the civilian side of the provided services, in particular the geodetic use of GLONASS. Later, on the 18th of May 2007, Russian President Vladimir Putin signed a decree providing open access to the civilian navigation signals of the GLONASS system to both Russian and foreign consumers free of charge and without limitations (B. Eissfeller, 2007). This was due to the competition with the charges and fees assumed by the Modernized GPS Block III and the potential Galileo at that time. However, this decree was considered another economic side of the global NAVWAR conducted by the Russian President.

Technically wise, the development and maintenance of the GLONASS system was conducted by the Federal Space Agency (FSA) (ROSCOSMOS, MOD). FSA had developed the second, and current generation of satellites called Uragan-M (also called GLONASS-M) in the beginning of 1990 and launched them for the first time in 2001. These satellites possess a substantially increased lifetime of 7 years and weigh slightly more (about 1,480 Kg). Furthermore, laser corner-cube reflectors were installed as aids for precise orbit determination and geodetic research. After that, 8 satellites were launched as of April 2007, and then an extra 14 satellites were launched by the year 2010. With that said, the total of 22 satellites of GLONASS-M was completed and fully operational. Next, the third generation satellites Uragan-K (GLONASS-K) started to be launched; they were designed with a lifetime of 10 to

12 years, at a reduced weight of only 750 Kg, they offered an additional L-Band navigational signal, and entered service following the Uragan-M inventory depletion in 2008. Eventually, the fourth generation “GLONASS-KM” was decided to be in space, but unfortunately, this was not meant to be. It had been in the requirement definition phase since 2002 and proposed to be available by 2025 (B. Eissfeller, 2007). Politically wise, the United States and Russia initiated a cooperation in 2004, with the primary goal of enabling a civilian interoperability at the user level between both the GPS and Russia’s GLONASS systems. Therefore, two working groups had been established to address two objectives: the first one was the radio frequency compatibility and interoperability for enhanced Positioning, Navigation, and Timing (PNT); and the other one was the technical interoperability between the Search-and- Rescue capabilities planned for the GPS and GLONASS systems. Nevertheless, all U.S.–Russia cooperation in this area was on hold status as of April 2014 (GPS, 2006).

In conclusion, the Russian GLONASS system is currently occupying the space along with the GPS system, but with no interference between their technical operations due to the fact that they are using different technologies and different frequencies, the space racing between Russia and USA had smoothly increased in the cold war era, and it has formulated another technical dimension of the NAVWAR concept. Furthermore, they had been operated without any real cooperation between the U.S. and Russia since 2014.

2.4 The Technical Differences between GPS and Galileo

There are differences and similarities between the two navigational systems, GPS and Galileo, a full technical and operational comparison is needed to be identified which would help to evaluate their strengths and weaknesses. Specifically, the GPS operational deficiencies from a European perspective and the extent to which level can Galileo intend to improve its performance in order to overcome those deficiencies. The main aspects of the comparison are the following:

Firstly, and in terms of purpose and sponsorship, the U.S. places priority on the security of the allied military capabilities when using GPS system, but the EU places priority of the Galileo system on the commercial viability for the civilians. In sponsorship wise, the GPS system was originally driven by the military’s need for the increased weapon accuracy. Yet, the U.S.

Government had established the Interagency GPS Executive Board (IGEB) since 1996. The IGEB manages senior-level policy for GPS and is chaired jointly by both the Department of Defense (DOD) and the Department of Transportation (DoT) whilst the U.S. Air Force is still operating the system. On the other hand, Galileo emerged as a joint system of the European Commission (EC) and the European Space Agency (ESA). Furthermore, the Galileo system is funded through a public-private partnership in which the EC and ESA provide funding in tandem with private companies participating in the project. In addition, the Galileo system is being operated by the so-called Galileo Operating Company (GOC) (Beidleman, 2006). Later, it is being operated by European Space Agency (ESA).

Secondly, and in terms of infrastructure, both the GPS and Galileo systems are subdivided into three parts: the space segment (also called satellite vehicles); the ground control segment (also called the command and control infrastructure); and the user segment (also called the end user or customer). The detailed comparison in this domain is as follows:

- The GPS space segment is comprised of 24 up to 30 satellites in a (Walker constellation) at an altitude of 10,898 nautical miles (roughly 20,200 Km), they are equally spaced in 6 orbital planes in right ascension around the earth, with an inclination of 55 degrees. The design of the GPS constellation guarantees that at least 5 satellites with good geometry are always seen in the sky-view to users worldwide in order to meet the accuracy requirements. Moreover, GPS currently uses two carrier signals, known as L1 (at 1575.42 MHz) and L2 (at 1227.6 MHz). Furthermore, GPS phases are historically as follow: Block I, Block II, Block IIA, and Block IIR (replenishment), Block IIF, IIR-M (for military uses on L5 separated), and finally the future modernized GPS Block III which is proposed to be fully operational in 2022. On the other hand, the proposed Galileo space segment will perform the space navigation mission with only minor differences; therefore, the Galileo system will employ more satellites in fewer orbital planes with a slightly higher altitude and inclination. Literally, the Galileo system will consist of up to 30 satellites in a Walker constellation at an altitude of 23,616 Km, they are equally spaced within three orbital planes with a 56-degree inclination. Furthermore, it plans to employ the following signals: two signals on the E5A band centered at 1176.45 MHz, two signals on E5B band at 1207.14 MHz, three signals on E6 band at 1278.75 MHz, and three signals on E2-L1-E1 band at 1575.42 MHz (see Figure 3 below). Hence, the Galileo satellites are physically smaller,

lighter and more covering the world than the GPS ones (European Space Agency, ESA, 2018), (ESA, ESA / Applications / Navigation, 2018).

- The ground control segments of the two systems are very similar in operation, infrastructure and the way they are controlling the space segments to maintain them operational and healthy.
- Concerning the end-user segment (or the customer receivers), the U.S DOD initially developed the GPS system to support national security. The U.S. armed forces are still the primary intended customers for the GPS system for the Precise Positioning Service (PPS) with higher accuracy (less than 15 ft.), but the other users of the rest of the world are using the Standard Positioning Service (SPS) with less accuracy (10–20 m), especially after President Clinton’s declaration to turn off the Selective Availability (SA) in May 2000, before the SA turning off, the accuracy was around 100 m. On the other hand, the EU marketed Galileo as a public GNSS dedicated to the civilian and the commercial users, and reduced Galileo’s military utility. Furthermore, the Galileo provided services are more accurate and more precise than the current given services by the GPS system.

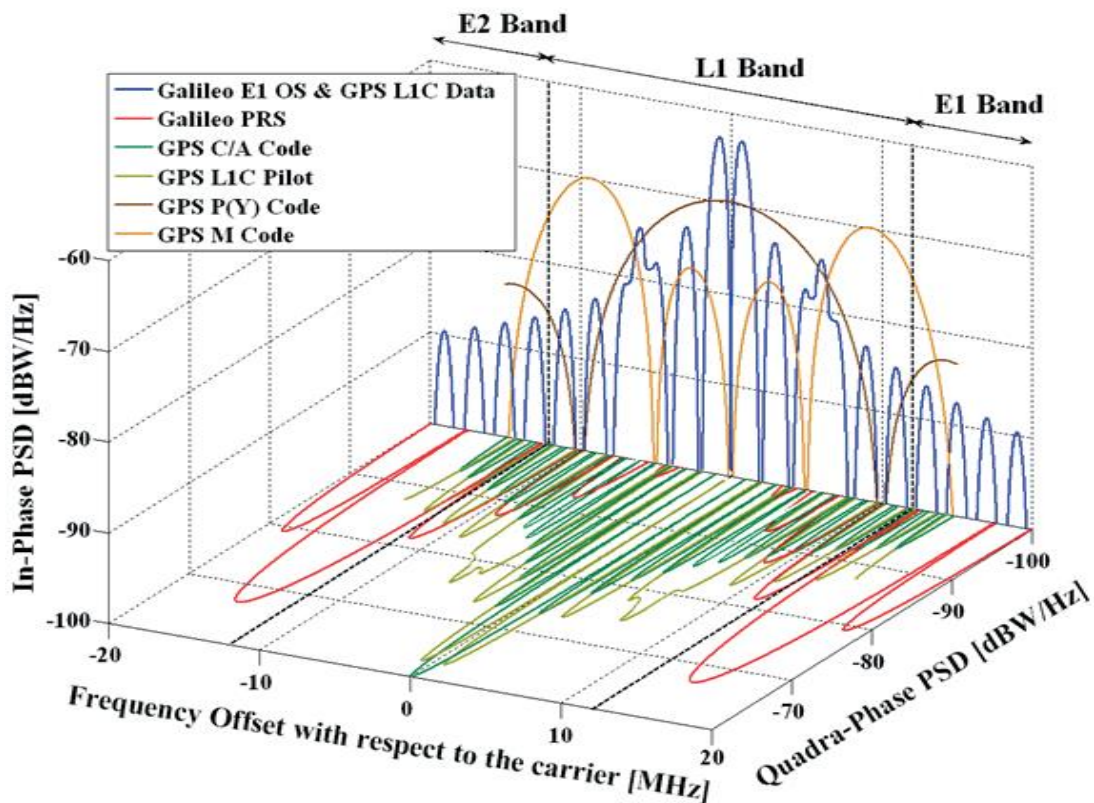


FIGURE 3 : NEW MODERN GNSS SIGNAL STRUCTURE ((B. EISSFELLER, 2007)

Thirdly, and in terms of services, there are differences between the two systems, especially the services of the Galileo system, and in specific their potential effects on the GPS system. In short, the GPS system provides the Position, Navigation, and Timing (PNT) services with two different levels of accuracy: The Standard Positioning Service (SPS) level and the Precise Positioning Service (PPS) level. The unencrypted SPS offers PNT services free of charge to all users without any alerts to users when being out of their tolerances' limits, while the PPS is dedicated for military purposes only. In contrast to GPS, Galileo plans to offer five types of services: The Open Service (OS), the Commercial Service (CS), Safety-of-Life (SoL) Service, the Public Regulated Service (PRS), and the Search and Rescue (SAR) Support Service. All of them guarantee alerts to users but not free of charge (with the exception of the Open Service [OS], which will be free). Saying that, both GPS and Galileo systems provide the basic PNT (Positioning, Navigation and Timing) services open to all users as well as the augmented services restricted to authorized users. Nevertheless, Galileo plans to offer additional features such as: the service guarantees, the global-integrity monitoring, and the additional data services supporting commercial markets; doing this for the sake of an attempt to overcome the GPS limitations from a civilian perspective.

Fourthly and lastly, in terms of limitations and vulnerabilities, both systems are identified to be vulnerable to jamming and Electronic Attacks (EA) because they are both using the electromagnetic energy in their SIS in low power level; this limitation may prevent using them in some critical applications such as the final phase of landing of an aircraft on a runway, or in other military precise missions that need weapons' high accuracy and sustainability of the used SIS. However, Galileo experimental trials showed more immune signal structure to jamming than GPS. This immunity is due to the fact of using the Binary offset Carrier (BoC) modulation scheme, and due to higher transmitted power that can mitigate high power jammers. Nevertheless, the proposed GPS Block III promises an enhanced performance as good as Galileo in this domain (Alhosban A. , 2019).

The above comparison evaluates both systems, and sheds light on how the Galileo system will be competitive to the GPS system especially in terms of the civilian services and their proposed quality. That means the initiatives of Galileo from the European perspective are highly justified and touch the top of the competitiveness as well as Galileo worthiness to share the space with the other navigational systems in the concept of NAVWAR. The following sections of this chapter show those initiatives and justifications.

2.5 Why Galileo Initiatives?

The intention of the European Union (EU) and the European Space Agency (ESA) is to establish the Galileo system. However, some questions and assumptions need to be answered in this domain: Why is Europe pursuing the development of Galileo while a free to all global space-based radio navigation system already exists? Despite the high costs of developing and deploying its own redundant system, Europe is pressing ahead. Does GPS have deficiencies that Galileo will fix or improve? Are there any motives that have not yet been made public (Beidleman, 2006, p. 2)?

In order to answer the above questions, Europe's rationale to build a separate satellite navigation system was identified as follows: improved performance, independence from the United States, and economic opportunity.

Firstly, and in terms of the improved performance, the Europeans' basic assumption was that the GPS system may not be upgraded to meet the future needs; their debates were that the enhanced GPS B-III was planned to begin launching in 2012 (Beidleman, 2006), but unfortunately, it was anticipated to be launched in 2022 or may be beyond as per (GPS, 2006), but it hasn't been launched yet, The fifth satellite in the GPS III series out of 10 was launched in June 17, 2021 by Lockheed Martin (LockheedMartin, 2021). Hence, the GPS current performance in the form of accuracy, reliability and vulnerability became a primary concern and a strong motive for the European development of Galileo. Furthermore, the GPS accuracy still degrades at high latitudes and in urban areas; the five-meter accuracy of GPS is available only 17% of the time, also the GPS civilian service (SPS) cannot be guaranteed worldwide all the times. For example, in 2000, GPS satellite malfunctions deprived the areas of Oklahoma, Kansas and Nebraska from navigational signals for 18 minutes. Consequently, if the satellite navigation is considered a keystone of transportation infrastructure, then even minor service discontinuities would cause severe consequences on the safety of people and assets. Based on that, Galileo is foreseen to be the promising global navigational satellite system, which will overcome all these deficiencies and GPS Block III will also overcome most of them and free of charge to the users.

Furthermore, and in terms of GNSS importance, it has obviously been noted that no single NATO mission had been performed without using the current GPS systems; it is being used in every single air force, land and Maritime's missions. Therefore, the GPS system has been the

essence and the core of many operational needs since its announcement date, such as: the digital mapping, the unified timing and the common synchronizations especially in the deployable operations. Furthermore, and from a military perspective, signal officers on duty whilst the planning phase of operation should investigate the applicable technologies and the possible technical devices in order to give the needed suggestions for the implementation. Moreover, the digital soldier must nowadays be the best-equipped soldier of the battlefield who is connected to the theatre of war/ operations with all it is needed of the latest technologies such as computers, wireless communication and by using GPS receivers. Therefore, the personal communication system should provide the ability to perform all the tasks with the appropriate support such as the digital GPS maps, the picture and voice commands and the messaging options (Hronyecz, 2015). Hence, it is important in place, that the EU operational decision-makers to seek for the optimal best technologies that meet their missions accomplished precisely and successfully, depending on their own secure timing and synchronization of the potential Galileo system.

However, it was definitely clear for the EU that they can successfully proceed in their own Research and Development R&D efforts. Moreover, and according to NATO and EU, a newly owned GNSS system with an improved technical performance higher than the given GPS SPS services by USA to NATO allies in joint Operations, is strongly needed.

Secondly, and in terms of the independence from the United States, the rationale behind it was identified as follows:

- The political independence: Europe plans to employ a GNSS to aid the implementation of a broad set of policies that includes regulating agriculture, fisheries and transportation services. Therefore, without Galileo, European critical infrastructure will rely on a system owned and operated by a foreign military power. However, the United States concluded that this idea was not in its best interest. Nevertheless, the final negotiations with the U.S. showed their conditioned approval, especially after China's involvement in funding the Galileo project, in a way that would not affect the interest of U.S. interests. Yet, China's involvement was used by the EU as a pushing card towards the final approval.
- The security independence: The European security perspective has changed over the past years. Therefore, Galileo will play an important role in the future defense of the EU. Historically, Europe has depended on the United States for security since the end of World

War II. Yet, the EU security was faded by America's reluctance to prosecute the war in Kosovo, as the American priority changed in the absence of the USSR. Furthermore, it was certainly noted that the post-9/11 environment refocused America's priorities on homeland defense and the war on terrorism. Hence, Europe insists that the Galileo system is designed specifically for the civilian purposes – as compared to GPS, which was designed during the Cold War for military purposes only. Consequently, the EU implies that Galileo will be the best choice for security of the European civilians, due to the fact that: meeting civilian needs is not the Pentagon's top priority any more.

- The technological independence: It has been approved that Galileo is not the first European venture designed to overcome the technological dominance of the U.S. For example, the Europeans independently pursued the development of the Ariane launch booster against the U.S. Delta, the Airbus against the Boeing aircraft, and the land communications Ericsson switches against the U.S. ones, all of these are good examples of the EU's ability of competition. Therefore, the U.S. dominance in satellite navigation technology once again threatens Europe in the technological dependence.

Thirdly, and in terms of the EU economic opportunity share in the worldwide market, it was anticipated that if the EU will establish a foothold in space racing, then the sales of the Galileo receivers are expected to increase from €100 million in 2010 to about €875 million by 2020 or even more and this represents market penetration rising from 13% up to more than 52%. It will also drive the creation of jobs ranging from 100,000 jobs by 2020 to about 146,000 by the year 2025. In addition to driving up market share and creating jobs, Galileo will gain more and more profits through royalties and service charges (Beidleman, 2006). In conclusion, with Galileo, Europe does not only secure a degree of political, security and technological independence from the United States, but also, it will provide Europe with an economic window of opportunity to seize the satellite navigation market away from the United States market dominance and to set a new global standard (Beidleman, 2006, p. 45). Table 3 below summarizes all the mentioned rationale and justifications.

Improved performance	Independence from the U.S.	Economic Opportunity
<ul style="list-style-type: none"> • The GPS performance of accuracy, reliability, and vulnerability has become a primary concern and motive for European development of Galileo. • GPS five-meter accuracy was available only 17% of the time. • The GPS civilian service, the SPS, is not guaranteed worldwide at all times • Even GPS Block III will overcome most of such deficiencies and free of charge to the civilian users, but it was tented to be launched by 2012, delayed to 2018, and then started in 2019, only 2 out of the 10 satellites were launched, the second on 25 August 2019. (USAF, 2019), the 5th was in 2021, (LockheedMartin, 2021) 	<p>Political Independence: Europe plans to employ a GNSS to aid the implementation of a broad set of policies that includes infrastructure, regulating agriculture, and transportation services. Which cannot be relied on a system owned by foreign military power.</p> <p>Security Independence: Europe security has faded as an American priority in the absence of the USSR by America’s reluctance to prosecute the war in Kosovo. The post-9/11 environment refocused American priorities on homeland defense and the war on terrorism. EU implies that Galileo is the best choice for security of the civilians, due to meeting civilian needs is not any more the Pentagon’s top priority.</p> <p>Technical Independence: The Galileo is not the first European venture designed to overcome US technological dominance. Europeans independently pursued development of the Ariane launch booster, and Airbus against Boing aircrafts, land communications Ericson switches, and are all good examples of EU ability of competition.</p>	<p>Market share: Sales of the Galileo receivers are expected to increase from €100 million in 2010 to about €875 million by 2020, representing market penetration rising from 13% up to 52 %.</p> <p>Creating jobs: Ranging from 100,000 jobs by 2020 to 146,000 by 2025.</p> <p>Royalties and Service Charges: The Galileo will gain more and more profits through royalties and service charges.</p>

TABLE 3. EUROPEAN RATIONALE SUMMARY [COMPILED BY THE AUTHOR]

2.6 Galileo Implications

In order to examine the implications of the Galileo system, the following two questions are needed to be answered: What are the implications of the proposed Galileo system for the United States? How should the United States respond?

Basically, the national security and economic concerns generated by the emergence of Galileo reviewed the U.S. policy towards Galileo and provided recommendations for the future. The Galileo system has attracted the interests and the investments from many non-European nations, including the People's Republic of China since its announcement date. This reflects the fact that Galileo is a fast-becoming technology that gets into reality rapidly. Although its Initial Operation Capability (IOC) has recently started, its Final Operation Capability (FOC) has not started yet; the FOC has delayed since the announcement of its estimated time due to some financial constraints in the EU economic share.



FIGURE 4. COLLISION OF THE NORWEGIAN FRIGATE “KNM HELGE INGSTAD” AFP (SEIDEL J. , 2018)

In terms of implications, the EU has claimed some technical issues in the performance of the GPS system in order to succeed in nullifying the NAVWAR concept born since 1996. One of those technical issues was the vulnerability of the GPS system to jamming. The EU claimed that not only the civilian L1 frequency is vulnerable to jamming, but also the military L2 frequency, because the L2 is basically using the L1 frequency in the acquisition process to calculate the position in the PPS service. Saying that means that both the military and the

civilian users would be at a risk especially when they are jammed by the adversary within the operation theatre. The U.S. security would also be risked. On the other hand, Galileo will not face those issues as designed. One example for this technical issue has recently and clearly appeared in the huge NATO Exercise called “Trident Juncture” in 2018; the Norwegian frigate “KNM Helge Ingstad” suffered a navigation failure leading to a collision with the tanker “Sola TS” on the 8th of November 2018 in the Hjeltefjord near Bergen, as seen in Figure 4 above. This exercise involved about 50,000 personnel, tens of thousands of vehicles, and dozens of ships and aircraft. All participants were forced to practice their skills in and around Norway in the freezing waters and the icy mountains. The exercise was labelled as the Alliance’s largest exercise since the Cold War, with a total of 29 NATO members plus the non-NATO members Finland and Sweden. Actually, the GPS signals that were guiding the ships, the aircraft (both civilian and military), the tanks, the trucks and the troops started to fail. Nevertheless, the U.S. forces declared less damage. It was most likely due to their using of the PPS service that had higher accuracy and was more immune to jamming compared with other forces who were using the SPS service only (Seidel J. , 2018).

Moreover, the other main technical issue concerning Galileo is that the U.S. started to design GPS BLOCK III F-M military code, with a higher power on a separated L5 frequency. Meanwhile, the International Telecommunications Union (ITU) had authorized Galileo to transmit its PRS and OS signals in the same frequency range as the GPS M-code, because the Europeans intended to plan transmitting the PRS signal using the same modulation scheme as the GPS M-code, and directly overlaying Galileo’s PRS signal on top of the GPS M-code signal so that to interfere with GPS signals. Therefore, any attempt by the United States to jam the PRS would also jam their M-code signal. This means effectively nullifying the NAVWAR with the U.S. GPS system. With that done, neither the monopoly of the U.S. concept in space navigation would be valid anymore, nor its superiority in space control.

In response, a third technical issue was raised as well. NATO highlighted concerns regarding the integrity of the Galileo PRS encryption regime, fearing that the PRS signals could be compromised and exploited by any adversary. Likewise, the United States feared that rogue states, terrorists, or even states acting against the U.S. interests could use the Galileo PRS to their advantage. Nevertheless, the EU asserted the expertise to design and implement an effective governmental encryption. Taking into consideration that the resulting technology could be made available only to the European authorities who are controlling the Galileo PRS

signal and the U.S. should trust the EU regarding this issue. In this manner, Galileo would mitigate fears of the PRS encryption. By saying and proving that, the EU could face challenges implementing Galileo, but the U.S. would not make this happen, at least initially.

Nevertheless, things have currently been changed, interoperability and cooperation do exist in both systems.

From the U.S. perspective, the history of negotiations is summarized as follows:

- Initially, the U.S. policy employed a “wait-and-see” approach towards Galileo, downplaying the need for another system and doubting Europe’s ability to pull it off.
- Officially, the United States saw “no compelling need for Galileo” because the GPS system would continue to meet the needs of users worldwide; there was a tendency in the U.S. planning to confuse the unfamiliar with the improbable.
- In February 1999, the EU announced the plans to pursue an independent system, and they obtained the approval and the funding to launch the Galileo program starting from 2002.
- In May 2000, the United States stopped degrading the GPS civilian accuracy by turning off the Selective Availability (SA) in an effort to make the GPS system more responsive to the civilian and the commercial users worldwide.
- In September 2000, the U.S. accelerated the GPS modernization phase by upgrading 12 out of the 20 Block IIR satellites, and included an additional civilian signal (L2C) and other two military signals (M-code), that were one of the root causes of the famous crisis of the U.S. economy at that time.
- Once the United States accepted that, the EU would build the Galileo system, whether the U.S. liked it or not, the policy was softened from blocking Galileo’s progress to ensuring its compatibility and interoperability with the GPS system, similarly to the internet network.
- Lately, the United States recommended a specific signal structure to be shared by Galileo’s OS and GPS B-III.
- In February 2004, the EU positively responded to the U.S. offer, and was potentially removing the last major obstacle.

Finally, and as per published by the EU Publication website in 2014, the U.S.– EU Agreement on GPS–Galileo cooperation was signed in 2004, and it had laid down the principles for the cooperation activities between the United States of America and the European Union in the field of satellite navigation. That agreement resolved all the technical, trade and security issues. Therefore, it eventually nullified the NAVWAR between both of them.

2.7 Conclusions

In conclusion, the proposed Galileo satellite navigation system challenges the U.S. national security and economic productivity. The European system currently threatens the U.S. space superiority because it could interfere with GPS signals and nullify the concept of NAVWAR. However, the questionable security of the Galileo PRS encryption scheme and broad international participation heighten the fear of the future hostile use of Galileo against the U.S. interests. Economically, Galileo erodes GPS's status as the world standard. The EU's need to generate revenue raises concerns regarding access to the signal specifications, the fair-trade practices and the proliferation of space technology. In response, the United States should work with the EU to develop a common standard for the satellite navigation as a framework of cooperation and competition similarly to the Internet worldwide. Within this framework, the United States must strengthen GPS's competitiveness by two actions; the first is the accelerating of the GPS modernization phase wherever possible to minimize Galileo's appeal, and the second is the separating of the military and the civilian services in order to enable both sectors to minimize conflict within a dual use system and focus on their own specific needs. In this manner, the United States can reach to the extent of: cooperating where it can be done, and competing where it must be done, in order to maintain a global leadership status in the satellite navigation and uphold its position in space.

Chapter 3: Impact of the GPS Errors on the Availability of the GNSS-GBAS Landing Systems in CAT II/III (GAST -D/F) Performance

3.1 Introduction

This chapter handles the impact of the GPS errors on the availability of GBAS Landing systems in GAST-D/F performance. An assessment of the availability parameters for GAST-D/F performance is conducted by using the upcoming Galileo constellation signals only and over Europe Only. A simulation tool was used to estimate to which level of integrity and accuracy is needed to meet the requirements of the current approved CAT II/GAST-D performance and the intended future requirements of CAT III/GAST-F, considering the new modulation scheme called Binary Offset Carrier (BOC) and the increased power of +6dB in Galileo signals. The availability results showed a promising better and a more stable performance of achieving those requirements over Europe space compared with the modernized GPS BIII system performance.

The structure of this chapter starts with the availability calculations in GBAS infrastructure, followed by the GBAS Parameters' Assumptions for the errors' contributions in the total error budget, then an explanation of the Simulations Runs (planning topology and performing) is illustrated, afterwards, the Results of the availability of the GBAS System is analyzed in both ways, first globally over the whole world for the sake of certification process and to comply with the needed international standards, and second over Europe and USA each alone in terms of using GPS and Galileo constellations each alone, for the sake of partially certifications. Finally, the conclusions are summarized and addressed along with the recommendations.

3.2 Availability Calculations in GBAS Infrastructure

In accordance to the recent studies (Lewis, 2015), and (G. Gluschke, 2018), the Critical Space Infrastructure (CSI) was deeply illustrated, shedding the light on the Navigational Space, which utilizes the satellites that are most likely providing critical services, basically in GBAS Systems' infrastructure, as shown in Figure 5 below, the aircraft subsystem corrects its own pseudorange measurements for each satellite with the differential correction data received from the ground subsystem. The corrected pseudorange measurements are then used to more accurately determine the aircraft's position relative to the selected FAS (Final Approach Segment) or FAP (Final Approach Path). The Aircraft subsystem is developed to minimize the

aircraft system integration, so it based on ILS look-alike scaling and deviation outputs, it has two modes of operation: Optional Position Service: Position, Velocity and Time (PVT) data that can be used as an input to a non-board navigator. Or Multi Mode Receiver (MMR) that's offers a high flexibility to use (ILS/MLS/GLS), so called XLS, and when there are no differential corrections the receiver can be used in GPS or SBAS mode.

Analogy to Communication Infrastructure (CI) protection techniques (G. Gluschke, 2018), the GBAS system is broken down to four types of data links that are established in order to examine its performance availability; Space-Ground Data Downlink, Space-Aircraft Data Downlink, Ground-Aircraft Data Uplink and Ground-ATC Data link. GBAS VDB has the following Characteristics: VHF NAV band (108-117.975 MHz), with channel spacing of 25 kHz, D8PSK (Differential 8 States Phase Shift Keying) modulation, Pseudorange Corrections update rate of 2 Hz, 8 slots Time Division Multiple Access Technique, Horizontal (Standard) or Elliptical Polarization, 50 Watt ground transmitter output power (47 dBm signal level), Omni-directional antenna coverage, Horizontal radius of 20 NM.

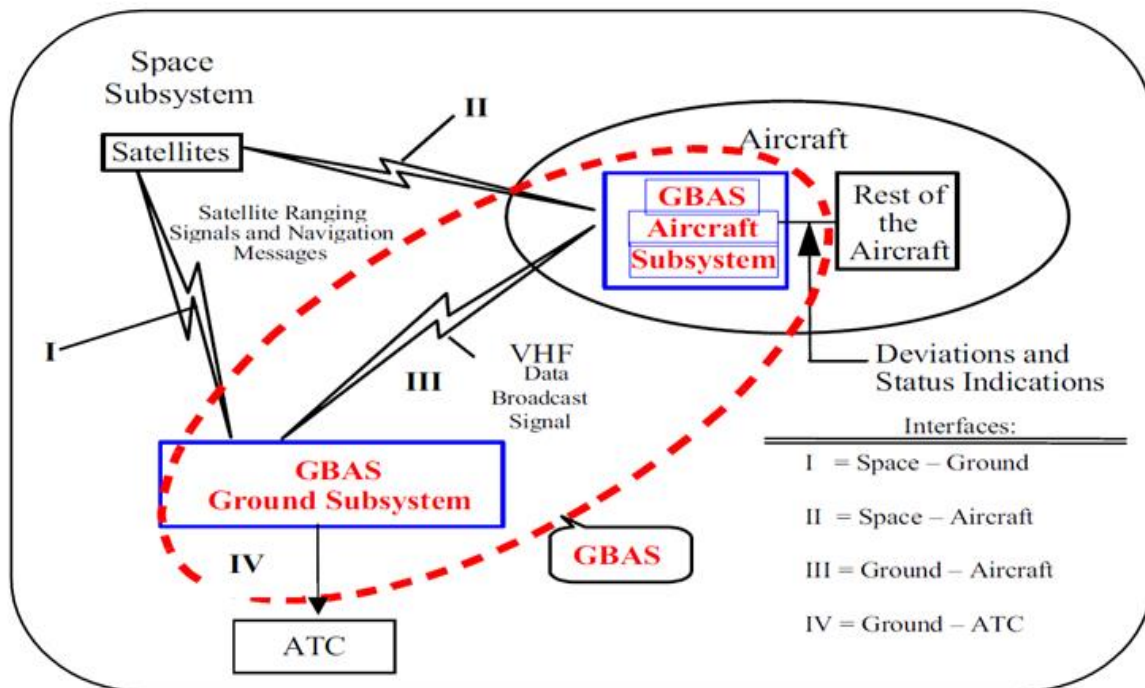


FIGURE 5: GBAS SYSTEM INFRASTRUCTURE OVERVIEW [EDITED BY AUTHOR]

In specific, the GBAS data are broadcasted through different GBAS messages types (MT-x), these messages are transmitted by GBAS ground station (GS). Currently only 8 of the 256

available message types have been defined, with the intent that future needs can be addressed in the remaining message types., they are shown in the following table, only the highlighted messages are used for CAT I performance (ICAO, 2020) (ICAOAmendment91&92, 2020), The Type 1 message provides the differential correction data for individual GNSS ranging sources. The Type 2 message has two purposes: Identifies the location of the GBAS reference point at which the corrections provided by the GBAS apply: Latitude, Longitude and Height, it also gives other GBAS-related data. The Type 4 message contains one or more sets of FAS data, each defining a single precision approach.

However, the required performance for GBAS system is summarized in the table 4 below as derived from (RTCA245A, 2004) (ICAOAmendment91&92, 2020) (ICAOAnnex10, 2002)(ICAO, 2020 and RTCA-245) called REF [1] and REF [2] in all related chapters:

Performance Requirements Category	GBAS Approach Service Type (GAST)	Accuracy		Integrity				Continuity
		Lateral NSE 95%	Vertical NSE 95%	Integrity Probability	Time to Alert	Lateral Alert Limit	Vertical Alert Limit	Continuity Probability
APVI	A	16.0 m (52 ft.)	20 m (66 ft.)	1-2 x 10 ⁻⁷ In any 150 s	10 s	40 m (130 ft.)	50 m (160 ft.)	1-8 x 10 ⁻⁶ In any 15s
APV II	B	16.0 m (52 ft.)	8.0 m (26 ft.)	1-2 x 10 ⁻⁷ In any 150 s	6 s	40 m (130 ft.)	20 m (66 ft.)	1-8 x 10 ⁻⁶ In any 15s
CAT I	C	16.0 m (52 ft.)	4.0 m (13 ft.)	1-2 x 10 ⁻⁷ In any 150 s	6 s	40 m (130 ft.)	10 m (33 ft.)	1-8 x 10 ⁻⁶ In any 15s
CAT II/IIIB	D	5.0 m (16 ft.)	2.9 m (10 ft.)	1-1 x 10 ⁻⁹ In any 15 s vet, 30 s let	2 s	17 m (56 ft.)	10m(USA) 5/2.5m EU	1-8 x 10 ⁻⁶ In any 15s
	E	5.0 m (16 ft.)	2.9 m (10 ft.)	1-1 x 10 ⁻⁹ In any 15 s vet, 30 s let	2 s	17 m (56 ft.)	10m(USA) 5/2.5m EC	1-4 x 10 ⁻⁶ In any 15s
	F	5.0 m (16 ft.)	2.9 m (10 ft.)	1-1 x 10 ⁻⁹ In any 15 s vet, 30 s let	2 s	17 m (56 ft.)	10m(USA) 5/2.5m EC	1-2 x 10 ⁻⁶ In any 15 s vet, and 1-2 x 10 ⁻⁶ In any 30 s let

TABLE 4: GSL REQUIRED PERFORMANCE [EDITED BY AUTHOR]

Availability is the portion of time during which the service can be used for a CAT I, CAT II or CAT III operations with reliable navigation information presented to the crew, autopilot, and other system managing the flight of the aircraft. Furthermore, GBAS service is defined to be

available when all the conditions needed to initiate a CAT I, CAT II or CAT III operation i.e. Accuracy, Integrity and Continuity of Service performances better than required, are met throughout the coverage service volume. Lately in 2018, those categories CAT I, II, III were replaced by GAST – C/D/F for GBAS satellite based landing systems, and they were kept for conventional ground based Instrumental Landing Systems by ICAO. (ICAOAmendment91&92, 2020).

For GBAS, the availability is given by a combination of the space subsystem availability and ground and aircraft subsystems availability. The ground and aircraft subsystems loss of availability results from constraints due to Accuracy, Integrity and Continuity of Service requirements. No additional requirement is made on these subsystems related to availability. Availability can be predicted from considerations on statistical performance of the system, considering the effect of system failures.

In order to provide the same level of performance as equivalent to ILS system, the availability for the different operations supported by the GBAS system shall meet the requirements defined in table 5 seen below. In addition, the operational effect of the critical satellite concept needs to be verified before being incorporated. The current availability figures as stated here relate to unavailability due to failures, not constellation geometry with a nominal constellation.

Operation Mode	Availability Probability Level
CAT I or (GAST - C)	0.9975
CATII or (GAST - D)	0.9999
CAT III or (GAST -F)	0.9999

TABLE 5: GBAS REQUIRED AVAILABILITY PERFORMANCE

Any landing system availability can be defined by the following equation, Eq.1, as per its committees' experts:

$$A = A_P \times A_F \times A_M \quad \text{EQUATION 1}$$

Where; For ILS CAT I, the following values has been considered by the experts in GBAS infrastructure evaluations:

$$A = 0.9975$$

For the following assumed values:

A_P : Fault free system availability, is set to 1.

A_F : Availability of the ground and aircraft subsystems, as determined by MTBO and MTTR. For ILS Cat I, ICAO Annex 10 requires 500hrs MTBO for the ground subsystem (1000hrs for the Localizer and 1000hrs for the Glide Path), which results in a 0.998 factor and AWOP considers a 2000hrs MTBO for the airborne subsystem, and with 1hr MTTR, which gives 0.9995. The product is 0.9975.

A_M : Availability of the ground and aircraft subsystems, taking into account scheduled maintenance operations. This factor is set to 1, considering that maintenance is performed when the system is not needed.

For GBAS CAT-I Case, Equation above can be used for GBAS also, if: A_P takes into account the ranging sources constellation and the accuracy performances of the ground and airborne subsystems. This could be considered as the « Geometry dependent » component of availability. Also, the Scheduled maintenance operations for the space segment are included in A_P

To be consistent with the continuity of service requirement of 1 to 3.3×10^{-6} , the ground subsystem MTBO will be better than 1263hrs. (Continuity of service is given by the ratio of exposition time (15s) over MTBO). Considering a 1hr MTTR, this gives the following ground subsystem availability in Eq.2 below:

$$\frac{MTBO - MTTR}{MTBO} = 0.9992 \qquad \text{EQUATION 2}$$

Where:

MTBO: is the Mean Time Between Outages

MTTR: Is the Mean Time To Repair

Considering an aircraft subsystem availability of 0.9995, that would be equivalent to ILS receiver, the resulting figure of A_F would be: $A_F = 0.9987$

Considering an aircraft subsystem availability of 0.9995 that would be equivalent to ILS receiver, the resulting figure of A_F would be: $A_F = 0.9987$

In order to achieve a global availability figure of 0.9975, the minimum value for A_P is: $A_P = 0.9988$

For CAT III Systems availability, ILS CAT III Case, A_P is the fault-free system availability, set to 1 for an ILS. A_F is the availability of the ground and aircraft sub-systems, determined by MTBO and MTTR values. For an ILS CAT III, the requirement [ICAO] for MTBO is 4000hrs (LLZ) and 2000hrs (GLIDE), and MTTR is 1hr Eq.3 below:

$$A_{gnd} = 1 - \left[\left(1 - \frac{MTBO_{LLZ} - MTTR}{MTBO_{LLZ}} \right) + \left(1 - \frac{MTBO_{GLI} - MTTR}{MTBO_{GLI}} \right) \right] = 0.99925 \quad \text{EQUATION 3}$$

(Equivalent MTBO of 1333hrs for a unique system, with a MTTR of 1hr), for the airborne part, the MTBO is 2000hrs, $A_{air} = 0.9995$. Therefore, $A_F = 0.99875$ (99.875 %).

A_M : Is the availability of the ground and airborne sub-systems, taking into account scheduled maintenance operations. This factor is set to 1, considering that the maintenance is performed when the system is not needed. Therefore, for ILS CAT III, the required availability is $A = 99.875$ %.

In GBAS Case; A_P is the fault-free system availability (set to 1 such as for an ILS). It takes into account the ranging sources geometry and the accuracy performance of the ground and airborne sub-systems. This could be considered as the 'geometry dependent' component of Availability. Scheduled maintenance operations for the space segment are included in A_P , A_F is the availability of the ground and aircraft sub-systems. In order to be consistent with the continuity of service requirement1 ($1-2 \times 10^{-6} / 15s$, i.e. MTBO of 2083hrs), and considering a MTTR of 1hr., the ground sub-system availability will be: $A_{gnd}=0.99968$. Conserving the same airborne sub-system availability (0.9995, MTBO 2000hrs), then $A_F = 0.99918$. In order to meet a global availability figure equivalent to the CAT III ILS one (99.875%), then: $A_P \geq 0.99957 \approx 99.96\%$

This figure assumes that there is a unique operation at a given time, and the alternate airport is equipped with an available means of landing in case of rerouting. The multiple and

simultaneous landing operations are not addressed. However, additional margins should be added to this a priori requirement. For this reason, even if the initial aim is to meet the availability figure of 99.96 %, the more symbolic figure of 99.99 % will be demanded.

$$\text{So, Recommended } A_p \geq 0.9999 \rightarrow A \geq 99.99\%$$

The information of this section are used as background and input for the other next sections and it is used in the result analysis process also, that's to reach the level of better understanding and investigation of the GNSS errors impact on the availability of integrity in GBAS applications.

3.3 GBAS Parameters' Assumptions

The currently used error models described in standards documents REF [1] and REF [2] have been defined for airborne and ground receivers in the configuration of GPS L1 C/A signal with a first order code-carrier filter (100s time constant).

It's assumed that the UDRE error Budget for GPS/GBAS System will be the same as UDRE error Budget for GALILEO/GBAS system during the simulations to be combatable with the other studies. It's assumed also to shorten the simulations on the vertical alert limit values only due the sensitivity of this parameter in the final approach over the lateral alert limit values. It's assumed also that simulations will be performed on each GNSS constellation alone, no combined different constellations will be considered, that's for the reason of hypothesis of using one constellation as nominal operating GNSS constellation and keeping other GNSS constellations as hot standby. It's assumed that the mask angle for GPS will be 5 degrees and for Galileo will be 10 degrees for the global simulation work. For the special cases of comparisons, they may change to be comparable with other studies.

The derived error models in the documents above with specific change were applied to serve the main goal of the research. Some of those additional assumptions were proposed by the working groups 28 and 62 in Eurocontrol publications. This was assumed due to the improved expected signals that will take place in GNSS world in the few next years. New signals will have different radio frequency characteristics (bandwidth, location, power, modulation type). Important differences between the current GPS L1 signal and the new expected signals to establish the model of expectable ranging measurement performance are summarized in the following table 6 below:

	Galileo			GPS	
	L1	E5a	E5b	L1 C/A	L5
Chipping Rate (MHz)	2	10	10	1.0	10
Power (dBw)	-155	-155	-155	-160	-154

TABLE 6: RANGING MEASUREMENT PERFORMANCE

Error models for these signals do not exist. The same methodology for the one used to develop current GPS L1 C/A models will be reused taken into account the specific characteristics of the GPS L5 and GALILEO L1/E5 signals. The following characteristics may have a significant impact on the error models:

- Transmitted power (+6dB compared to GPS C/A), code chipping rate (2MHz for GALILEO L1 and 10MHz for GALILEO E5), code modulation (BOC for GALILEO E1), frequency band E5 and its major interference (DME/TACAN in GALILEO E5).
- CAT II/III specific multipath environment (vicinity of the ground and potential impact of the ground multipath on airborne receiver).
- Different possibilities to correct Ionospheric propagation errors, to filter thermal noise and multipath.
- The advantages of using a narrow correlator with a BOC signal with a 2MHz chipping rate signal
- Multiplexed BOC as a new concept to be implemented versus BOC in the future GNSS2.

In GBAS Applications, and as derived from REF [2], the GPS Differentially Corrected Pseudorange Measurement Model for satellite i is given by the following equation 4:

$$\sigma_i^2 = \sigma_{pr-groundi}^2 + \sigma_{troboi}^2 + \sigma_{iono i}^2 + \sigma_{airi}^2 \quad \text{EQUATION 4}$$

Where:

$\sigma_{pr-groundi}^2$ is the total (post correction) fault free noise term provided by the ground function (via VDB) for satellite i .

$\sigma_{tropo_i}^2$ Is a term which is computed by the airborne equipment to cover the residual Tropospheric error for satellite i.

$\sigma_{iono_i}^2$ Is the residual Ionospheric delay (due to spatial decorrelation) uncertainty for the i^{th} ranging source.

$\sigma_{air_i}^2$ is the standard deviation of the aircraft contribution to the corrected pseudorange error for the i^{th} ranging source, the aircraft contribution includes the receiver contribution and standard allowance for airframe multipath.

The standard deviation of the aircraft contribution error is given by Equation 5 below:

$$\sigma_{air,i}^2 = \sqrt{\sigma_{receiver}^2(\theta_i) + \sigma_{multipath}^2(\theta_i)} \quad \text{EQUATION 5}$$

Where:

$\sigma_{receiver}^2(\theta_i)$ Is the standard allowance for the receiver error.

$\sigma_{multipath}^2(\theta_i)$ Is the standard allowance for the multipath error.

Due to the new expectation of enhanced performance of the GPS/Galileo constellations, the GBAS parameters assumptions will be applied to the following Designators:

- Ground Accuracy Designator Parameters (GAD)
- Airborne Accuracy Designator Parameters (AAD)
- Airframe Multipath Designator (AMD)

For the Ground Accuracy Designator Parameters (GAD), The RMS of the total non-aircraft contribution to the GPS/GBAS error as a function of the elevation angle is given in RTCA - 245 standard page 31, Equation 6 below:

$$RMS_{pr_{grdGPS}}(\theta_i) \leq \sqrt{\frac{(a_0 + a_1 e^{-\theta_i/\theta_0})^2}{M}} + a_2^2 \quad \text{EQUATION 6}$$

Where:

M is number of ground reference receiver subsystem

i : Is the i^{th} ranging source

a_0 , a_1 , a_2 and i are parameters determined by the table shown below.

The table 7 shown below is assumed to present the basic GPS error model and it's taken from Ref [2], page 31, each letter of the ground accuracy designator letters A, B, or C is associated with performance of the ground subsystem reference receiver and a number that indicates the number of the reference receivers. These values will be assumed to represent the single frequency configuration of the ground subsystem, or in other words the low/mid accuracy configuration, if they mitigated by 2 (divided by 2), then they will be assumed to represent the dual frequency configuration (or high accuracy configuration) as seen in table 8 below and plotted in figure 6 below.

Ground Accuracy Designator (GAD)	θ_i (degrees)	a_0 (meters)	a_1 (meters)	θ_0 (degrees)	a_2 (meters)
Letter A	>5	0.5	1.65	14.3	0.08
Letter B	>5	0.16	1.07	15.5	0.08
Letter C	>35	0.15	0.84	15.5	0.04
	≤ 35	0.24	0.24	-	0.04

TABLE 7: BASIC GBAS PERFORMANCE (LOW ACCURACY/SINGLE FREQUENCY)

Ground Accuracy Designator (GAD)	θ_i (degrees)	a_0 (meters)	a_1 (meters)	θ_0 (degrees)	a_2 (meters)
Letter A	>5	0.25	0.825	14.3	0.04
Letter B	>5	0.08	0.504	15.5	0.04
Letter C	>35	0.075	0.42	15.5	0.02
	≤ 35	0.12	0.12	-	0.02

TABLE 8: ADVANCED GBAS PERFORMANCE (HIGH ACCURACY/DUAL FREQUENCY)

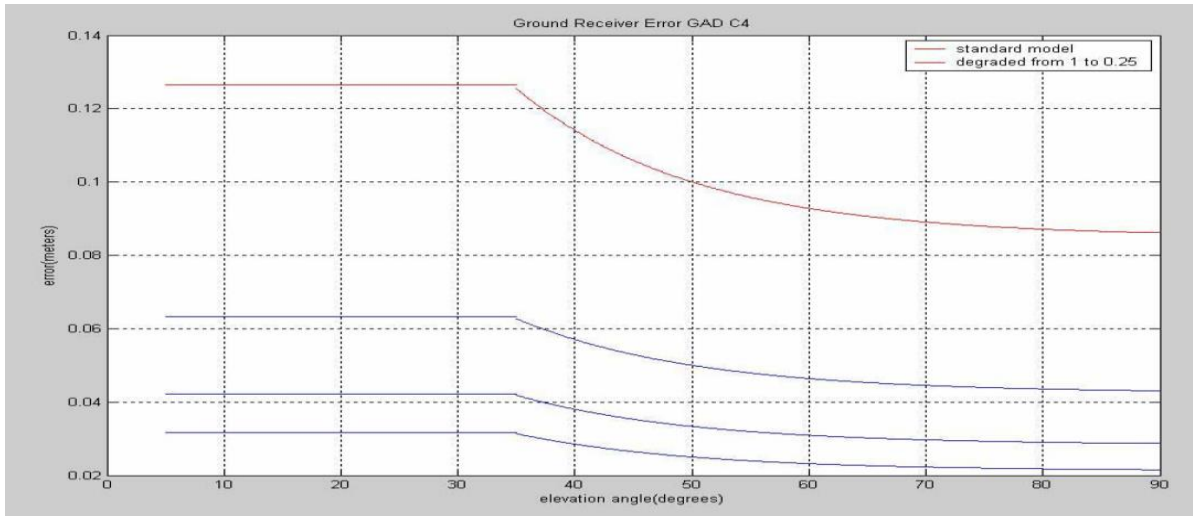


FIGURE 6: MITIGATED GAD GROUND ACCURACY DESIGNATOR CONFIGURATION [EDITED BY AUTHOR]

The same technique has been done for the other two equations 7 and 8 for Airborne Accuracy Designator Parameters (AAD) and Airframe Multipath Designator (AMD) to 0.25 and 0.10 respectively as seen in the figure 7 below.

$$RMS_{pr-air GPS}(\theta_i) = a_0 + a_1 \cdot e^{-\theta_i/4} \quad \text{EQUATION 7}$$

And

$$RMS_{multipath}(\theta_i) = a_0 + a_1 \cdot e^{-\theta_i/10} \quad \text{EQUATION 8}$$

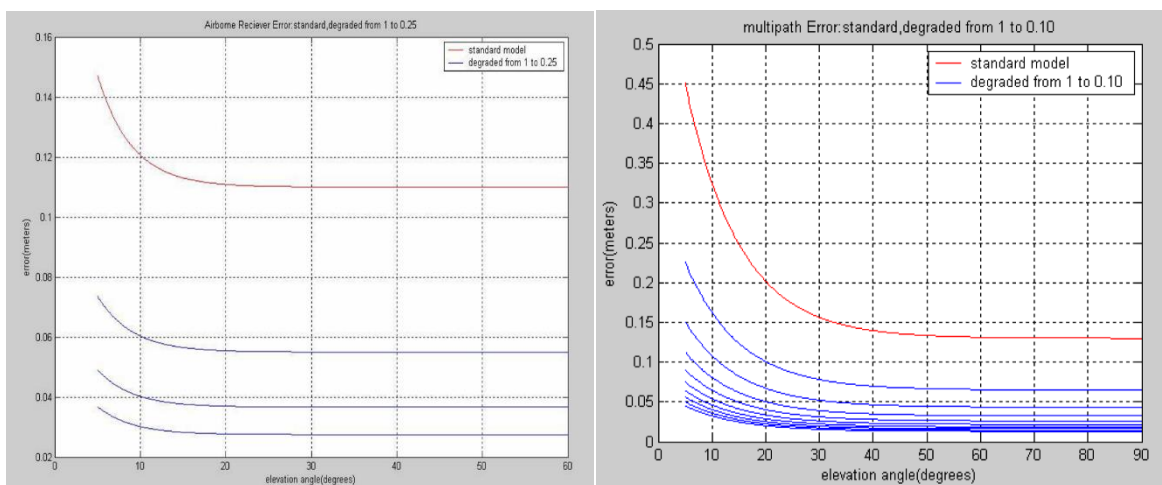


FIGURE 7: MITIGATED AAD (LEFT)/AMD (RIGHT) ACCURACY DESIGNATORS CONFIGURATION [EDITED BY AUTHOR]

In which the Multipath mitigation levels were assumed to be extended to four levels, and varies with other combinations to investigate its impact on them, it is necessary to vary one parameter while others are fixed, and the user multipath error was chosen to be varied because it is the only error with major effect in the user side as per observed during the landing phase of flights:

- A: the standard
- A/2(B): currently used
- A/4: its visible by the modified mitigation methods
- A/10: the far future expectations

Furthermore, for the Tropospheric and Ionospheric Parameters, table 9 below, it is assumed to be taken as follows according to the international Standards ICAO and RTCA-245 for both GPS and Galileo constellations' simulations to offset the comparison between them, by dual frequency usage both of them will be less effect on the needed performance availability.


	Parameter	Value of the parameter	Reference
1	Convergence time of the smoothing filter (tau)	100 seconds	REF [2]-Appendix-F, page F-2
2	$K_{md_e_CATI, GPS}$	5 ,(0 to 12.75) Or 4.47 (ED114)	REF [1], Table B-71, Page APP B-89
3	$V_{vert_iono_gradient}$	4E10-6 Or 2.1E10-5(ICA0 Annex 10 ATTD-23)	REF [2]-Appendix-F, pageF-5 (Eq 3-76, sec3.3.2.15, page 64)
4	x_{air}	5400m,for GSL=D&F (6000m, for GSL=C)	REF [2]-Appendix-F, page F-5 (Eq 3-76, sec3.3.2.15, page 64)
5	v_{air}	72m/s , for GSL D&F (77m/s , for GSL C)	REF [2]-Appendix-F, page F-5 (Eq 3-76, sec3.3.2.15, page 64)
6	V_{tropo}	$V_N =0$	REF [2]-Appendix, pageF-5 (Eq 3-75, sec3.3.2.14, page 64)
7	Decorrelation factor, P	0.00015m/m	REF [2]-Appendix-F,pageF-2
8	 h	200 m,(500m, for FAF 15m, for CAT III)	REF [2]-Appendix, page C-2

TABLE 9: IONOSPHERIC AND TROPOSPHERIC PARAMETERS' ASSUMPTION [EDITED BY AUTHOR]

Table (9) notes:

1. The confidence factor for the ephemeris data in the CAT I case Kmd_e_CAT1, GPS was selected to be 5 for GPS and Galileo. According to ICAO-Annex 10 Table B-71Page APP B-89 values in the range of 0 to 12.75 are possible. EURCAE ED 114 proposed 4.47 that is nearly the same value as used here.

2. The Convergence time of the smoothing filter (tau) is set to 100s for all the single frequency simulations according to RTCA-DO245 A-Appendix-F, pageF-2. It will be doubled for Dual Frequency (DF). This parameter has minor impact on the performance results as was shown in previous investigations.

The following table 10 shows the parameters which are common to all simulations concerning the all the subsystems;

	Parameter	Value of the parameter	Reference
1	Max. Service volume	43 Km(23 NM)	REF [1], Amendment 77 Sec:(3.7.3.5.4.4.2.2, note, page42F) REF [2]-Sec2.3.2, page 17
2	Runway Heading	100°	Arbitrary
3	Glide path angle	2.7°	REF [2]-Sec2.3.2, page 17
4	Time of approach Phase(FAS)	150 sec	REF [2]-Appendix, page C-2
5	Critical satellites	Max=2 for GSL =D, Max= (6) for GSL =F, High enough	REF [2], Table 3-13
6	Availability threshold	VNSE=2.9 m LNSE=5 m	REF [2]-sec 2.3.11, page (15+16), Tables 2-2, and 2-3.
7	Reference receivers	4	REF [1], Table B-71, Page APP B-89
8	Geographic Coverage Area	90° N to 90° S 180° E to 180° W	Global Coverage Assumption./Over Europe alone

TABLE 10: COMMON PARAMETERS' ASSUMPTIONS [EDITED BY AUTHOR]

3.4 Simulations Runs (planning topology and performing)

Simulations operations have been planned in a systematic method that takes into account grouping the selected parameters in a suitable and methodical approach that eases performing and saving both the calculated output and the input scenarios files, this was done for all the

possible combinations of subsystems performance parameters based on the background information and standards documents. For all the groups of the performed simulations results, the analysis procedure shall show the following dependency indicators, and as shown in the figure 8 below (group tree):

- Dependency on constellation (Galileo 27, GPS 29)
- Dependency on Vertical Alert limits (10m, 5m, and 2.5m).
- Dependency on Receiver(s) Accuracy Designators GAD/AAD (AA, BB, CB)
- Dependency on GS/User Receivers Performance (SF, DF)
- Dependency on the User Multipath Error (UMPE) /Airborne Multipath Designator (AMD) mitigation level (A, A/2, A/4, A/10)

Furthermore, the simulations steps were done in the following order:

1. Input Parameters as they ordered in AVIGA Tool:
 - Geographic Coverage Area
 - Constellation Trajectory Type and GSL service Level
 - Reference Receivers
 - GAD Letter, AAD letter, AMD Letter, and VAL /LAL
 - Maximum Service radius, RWY, GPA
 - Tropospheric/Ionospheric Parameters
 - AMD multipath Parameters Table
 - GAD parameters Table and AAD parameters Table
2. Saving Input (Scenario) Files, Calculate Scenarios, Editing Output Files, Saving Output Files, and finally the documentation of the Output Files (Tables and Figures)

Performing simulation groups is a time consuming process, it depends on the following factors:

- Periodic of Constellation (10 days for Galileo (Actual Definition), 3 Days for Galileo (Initial Definition till 2018) and 12 hours for GPS)

- Number of Used Satellites: (29 satellites for GPS, 27satellites for Galileo) one of each constellation was left as a prediction of malfunctions/initially launched as realistic process.
- Latitude and Longitude grid (5° X5°, 2° X 2°, 1° X1°).
- Calculation step (300s or 60s)

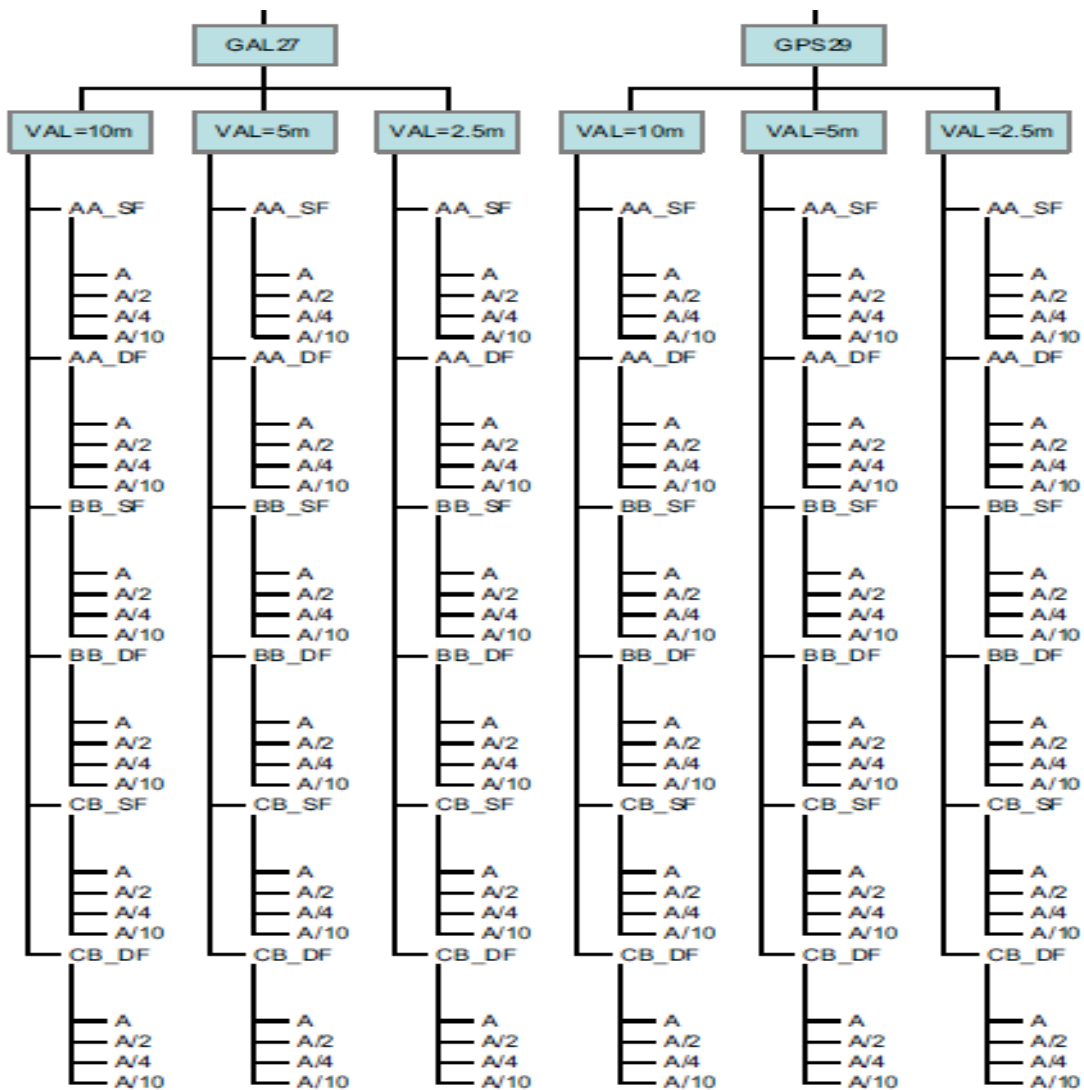


FIGURE 8: SIMULATION GROUP TREE COMBINATIONS [EDITED BY AUTHOR]

The following table 11 shows the average time that needed for each simulation process:

Simulation Operation type	Operation time
Simulation with Galileo 27 satellites constellation 10 days' trajectory, 60 sec step, 5° X 5° grid	9 hours
Simulation with Galileo 27 satellites constellation 2.33 days trajectory, 60 sec step, 5° X 5° grid	3 hours
Simulation with GPS 29 satellites constellation 1 day trajectory, 60 sec step, 5° X 5° grid	1 hour
Simulation management (preparing, interning parameters, editing after completing the calculation, saving)	5 minutes

TABLE 11: THE AVERAGE TIME THAT NEEDED FOR EACH SIMULATION PROCESS [EDITED BY AUTHOR]

The following table 12 shows the numbers of the performed simulation in this study.

Simulation operation type	Number of single Operations
Test and Validation of the AVIGA	25
Galileo 27	75
GPS 29	75
WG-28 (Galileo + GPS)	50
Special Cases	40
Repeated	25
Not Needed(due to iterative processes)	80
Total	370

TABLE 12: THE PERFORMED NUMBER OF SIMULATIONS' RUNS [EDITED BY AUTHOR]

The used simulation tool called AVIGA, AVIGA is a program for: Analysis of Visibility, Integrity, Geometry, and Availability of Global Navigation Satellite Systems, AVIGA is running under WIN98/NT/2000/XP and requires approximately about 30 MB of disk space. AVIGA has the following functions: Prediction of GPS, GLONASS and Galileo satellites' positions/velocities in ECEF frame computation of precise satellites' positions. Also the Analysis of satellite Visibility & DOP characteristics at a given space-time point for mask angles specified by the user in addition to regular space-time points within a definable geographic area. Furthermore, AVIGA analyzes the position accuracy based on DOP values and views satellite positions on the azimuth/elevation sky plot. However, it analyzes the Integrity/Continuity characteristics, XPL/XNSE characteristics, Availability characteristics and the GBAS/ Galileo LE characteristics.

AVIGA has two Calculation Steps can be summarized as seen in figures 9 and 10 below:



FIGURE 9: AVIGA STEP 1: TRAJECTORY CALCULATION [EDITED BY AUTHOR]



FIGURE 10: AVIGA STEP 2: SPECIFIC OPERATION CALCULATION [EDITED BY AUTHOR]

Availability algorithm that used in AVIGA simulation tool is shown in the following figure 11, this algorithm is widely used among the similar simulation tools like AVIGA with some differences. The sub models that are used for GBAS application are as per its software designers:

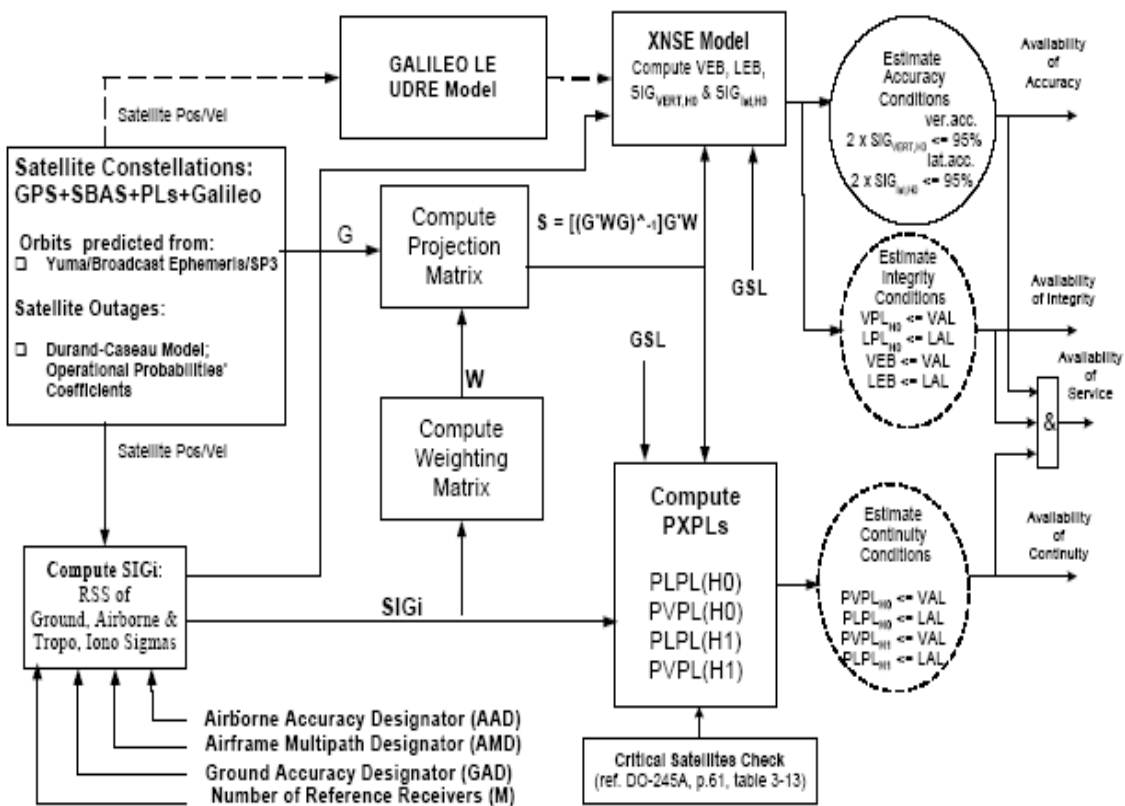


FIGURE 11: AVIGA GBAS MODEL SCHEME/ ALGORITHM [AS PER DESIGNER]

3.5 Results Analysis

3.5.1 Global Coverage of GNSS/GBAS

First of all, the following table 13 shows the input parameters used for this research, these parameters are entered to the simulation tool as scenario files, changing the ones of independency variation each time, as explained in the simulation planning section. The most frequently variation is the Multipath parameters, this for the sake of investigating its impact in all the used combinations, the lowest varied parameters are the allowable critical satellites number, which was made to be 6 only. Other parameters are varied according to the arranged sub-groups for specific configuration of the GBAS system.

Parameter	Value(s)
Number of critical satellites	6
Constellation type	GALILEO 27, GPS 29,
GSL(GBAS Service Level)	D/F
VAL (Vertical Alert Limit)	10m, 5m , or 2.5m
GAD(Ground Accuracy Designator)	A, B, or C
AAD (Airborne Accuracy Designator)	A or B
AMD(Airframe Multipath Designator)	A, A/2(B),A/4, and A/10
GS &User Performance Type	Single or/and Double Frequency(SF or DF)

TABLE 13: THE INPUT PARAMETERS VARIATION [EDITED BY AUTHOR]

The critical satellite number was chosen to be moderate, it was chosen to be 6, the critical satellites are those satellites which when being removed from the protection level XPL computations would cause the XPL to rise above the alert limit. This decreases the availability of the system. But at the same time allowing more critical satellites in the XPL availability computation will reduce the continuity. A previous study investigated impact of critical satellite number to be reduced to 2 once, and then to be 10 another time, on availability, the study resulted in assuming the compromise between both performances, continuity and integrity.

The following table 14 shows the meanings of the parameters abbreviations used in the input parameters in all the groups and graphs:

Parameters Combinations	Meaning
AA_SF	GAD=A,AAD=A, Single Frequency performance type(standard values)
BB_SF	GAD=B,AAD=B, Single Frequency performance type (standard values)
CB_SF	GAD=C,AAD=B, Single Frequency performance type (standard values)
AA_DF	GAD=A,AAD=A, Dual Frequency performance type(divided by 2)values)
BB_DF	GAD=B,AAD=B, Dual Frequency performance type (divided by 2 values)
CB_DF	GAD=C,AAD=B, Dual Frequency performance type (divided by 2 values)

TABLE 14: THE MEANING OF THE ABBREVIATIONS OF INPUT PARAMETERS VARIATION [EDITED BY AUTHOR]

The main raw results for Galileo GBAS availability are shown in table 15 below, while the main raw results for GPS are shown in table 16 below after, both are shown in figure 12 just after:

GAL27_10m	AA_SF	BB_SF	CB_SF	AA_DF	BB_DF	CB_DF
A	100,000000	100,000000	100,000000	100,000000	100,000000	100,000000
A/2	100,000000	100,000000	100,000000	100,000000	100,000000	100,000000
A/4	100,000000	100,000000	100,000000	100,000000	100,000000	100,000000
A/10	100,000000	100,000000	100,000000	100,000000	100,000000	100,000000
GAL27_5m	AA_SF	BB_SF	CB_SF	AA_DF	BB_DF	CB_DF
A	23,995509	93,499658	99,892565	95,920615	100,000000	100,000000
A/2	38,281423	99,919057	100,000000	99,939689	100,000000	100,000000
A/4	41,380565	99,939321	100,000000	100,000000	100,000000	100,000000
A/10	42,232003	99,947210	100,000000	100,000000	100,000000	100,000000
GAL27_2.5m	AA_SF	BB_SF	CB_SF	AA_DF	BB_DF	CB_DF
A	0,000000	1,083954	15,584790	1,940423	36,484341	46,349066
A/2	0,000000	14,866188	56,418665	21,533050	76,369480	85,489091
A/4	0,000000	23,736165	66,804131	31,420162	85,470464	93,117284
A/10	0,000000	26,455902	69,702587	34,308464	87,799825	94,928447

TABLE 15: GBAS AVAILABILITY FOR GALILEO CONSTELLATION [EDITED BY AUTHOR]

GPS29_10m	AA_SF	BB_SF	CB_SF	AA_DF	BB_DF	CB_DF
A	99,803784	99,997559	99,999717	99,998715	100,000000	100,000000
A/2	99,868813	99,999974	100,000000	100,000000	100,000000	100,000000
A/4	99,885950	100,000000	100,000000	100,000000	100,000000	100,000000
A/10	99,893144	100,000000	100,000000	100,000000	100,000000	100,000000
GPS29_5m	AA_SF	BB_SF	CB_SF	AA_DF	BB_DF	CB_DF
A	45,533628	95,319517	99,005380	96,829586	99,714116	99,799596
A/2	56,477759	98,885806	99,839291	99,194222	99,961101	99,971943
A/4	59,026662	99,277672	99,901468	99,519056	99,973433	99,980165
A/10	59,741130	99,374868	99,917294	99,606977	99,976465	99,985689
GPS29_2.5m	AA_SF	BB_SF	CB_SF	AA_DF	BB_DF	CB_DF
A	0,000000	0,000000	1,799712	0,505681	14,373576	25,251108
A/2	0,000000	0,942062	34,383223	5,281909	60,158055	75,984287
A/4	0,000000	5,078033	42,997695	11,924407	79,157762	88,215655
A/10	0,000000	6,600341	46,019981	13,802275	82,384696	90,390007

TABLE 16: GBAS AVAILABILITY FOR GPS CONSTELLATION [EDITED BY AUTHOR]

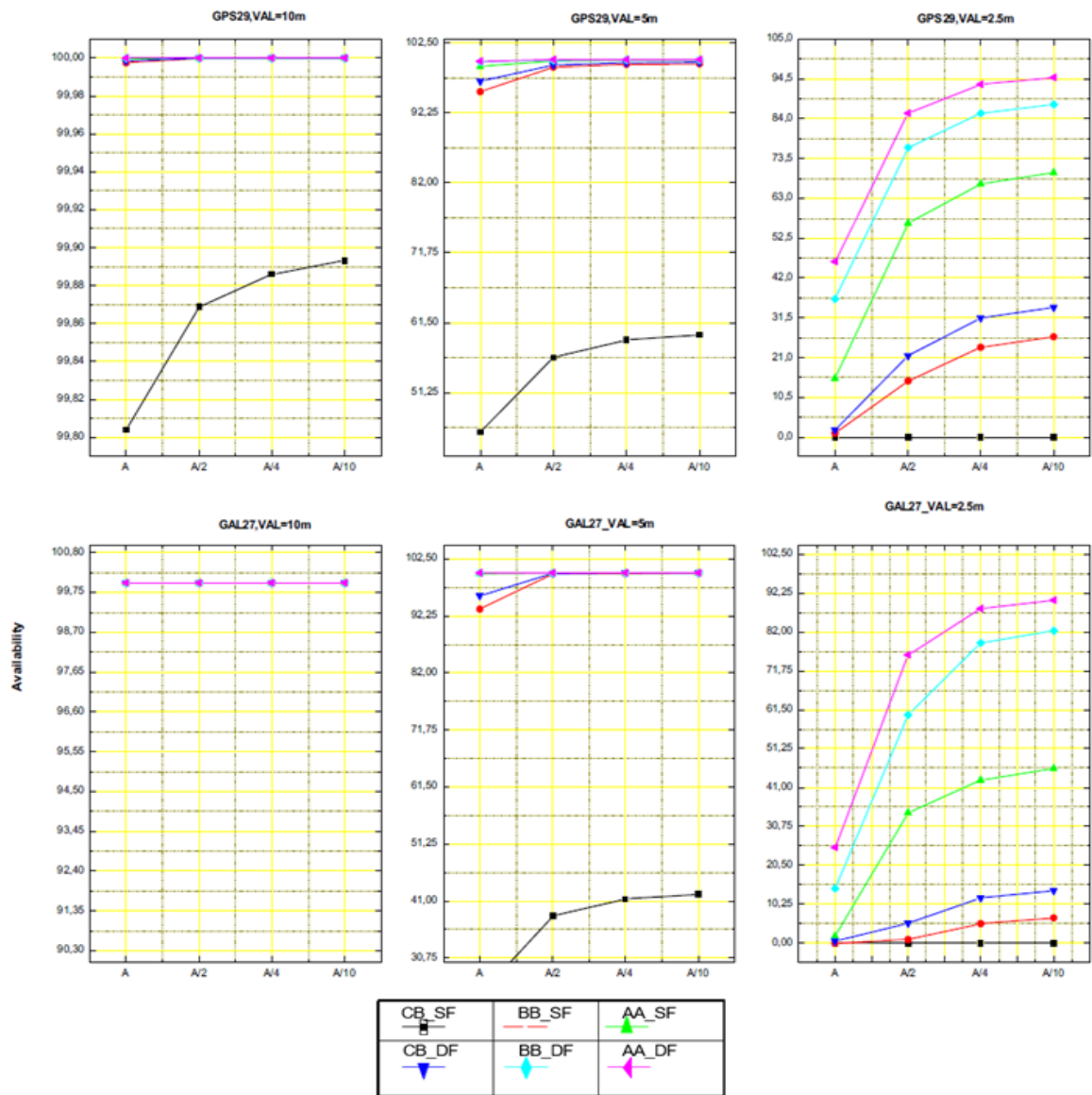


FIGURE 12: MAIN RESULTS AVAILABILITY AGAINST USER MULTIPATH ERROR FOR GPS / GALILEO [EDITED BY AUTHOR]

Simulations showed that GBAS system availability performance could meet the aeronautical availability requirements of 99.75% and 99.99% for an integrity risk of $10E^{-9}$ (using the same K-factor according to GBAS Service Level definition) for an assumed Vertical Alert Limit (VAL) of 10 m and 5m if a certain level of user multipath mitigation was applied. However, table 16 below shows to which level this multipath mitigation is needed for each GBAS configuration to reach or closely reach those requirements, or for which conditions these

requirements cannot be achieved. This table 17 was analyzed carefully by interpretations methodology illustrated below it, and it is considered the main analyzed results for this chapter.

VAL	Constellation Type	User Multipath mitigation level needed to meet Aeronautical Availability Requirements											
		99.99%						99.75%					
		AA_SF	BB_SF	CB_SF	AA_DF	BB_DF	CB_DF	AA_SF	BB_SF	CB_SF	AA_DF	BB_DF	CB_DF
10 m	GALILEO	A	A	A	A	A	A	A	A	A	A	A	A
	GPS	VC	A	A	A	A	A	A	A	A	A	A	A
5 m	GALILEO	NV	VC	A/2	A/4	A	A	NV	A/2	A	A/2	A	A
	GPS	NV	VC	VC	VC	VC	A/10	NV	VC	A/2	VC	A/2	A
2.5 m	GALILEO	NV	NV	NV	NV	NV	V	NV	NV	NV	NV	NV	V
	GPS	NV	NV	NV	NV	NV	V	NV	NV	NV	NV	NV	V

TABLE 17: UMPE MITIGATION LEVELS NEEDED TO MEET REQUIREMENTS PER CONFIGURATION [EDITED BY AUTHOR]

The letters A, A/2, A/4, or A/10 are the needed UMPE mitigation levels with associated parameters to meet the desired availability of 99.75% or 99.99%. in GBAS applications, they are illustrated as follows; A: is the standard UMPE model given by the REF [1] and REF [2], A/2: is the 1st UMPE mitigation level, divided by a factor of 2, due the expected improvements in GNSS signals and new UMPE mitigation techniques (refer to parameters assumptions section), A/4: is the 2nd UMPE mitigation level, divided by a factor of 4, due the same reasons above, and A/10: is the 3rd UMPE mitigation level, divided by a factor of 10, due the same reasons above

The letters VC: means VERY CLOSE to the 3rd UMPE Mitigation Level A/10 (Availability >99.00%), and that's means, further mitigations and/or changing to one higher level of accuracy configuration(GAD,AAD) could make it possible to meet the aeronautical requirements, these cases of VC are of a high degree of interest where more investigations should be applied for them , other parameters can be varied to check that , but this work is beyond the scope of this study, however , some suggestions are listed in this research later to be investigated in the future to see the visibility of meeting CAT II/III requirements with a single constellation.

The letter C: means CLOSE to the 3rd UMPE Mitigation Level A/10 (98.00 % < Availability <99.00%), That's mean, these C cases need even more mitigations in other parameters or changing some configuration to upper level of accuracy the same wording can be said as in Note 2, but with more care and investigations.

The letter V: mean VISIBLE (<95.00% Availability <98.00%), this means, these cases noted V are visible to meet the requirements but not with the means of UMPE mitigation, it could be possible with other subsystems configuration or other parameters improvements. While the letter NV: mean NOT VISIBLE (Availability <95.00%), in these cases of NV are not close at all to be achieved by the UMPE mitigation levels and not even visible, they are low level availability performance out of range being satisfying the required aeronautical availability.

These eight levels of the classified mitigation levels and those levels which are beyond them are shown in the following two charts, the first shows the different approaches of the simulated configuration of GBAS subsystems in achieving 99.99% availability, and the second for 99.75% availability.

3.5.1.1 Results of the Globally Coverage of Galileo /GPS

The main results can be summarized into three categories as per VAL values and as follows:

1. For VAL = 10m, globally, all the Dual Frequency (DF) GBAS configurations using all single GNSS constellations have achieved both 99.75% and 99.99% Availability Requirements, i.e. GAST D/E/F. On the other hand, all Single Frequency (SF) CB configurations with all single GNSS constellations have achieved 99.75% availability only, i.e. GAST-C only. Which is compliant with ICAO declarations.
2. For VAL =5m, globally, Galileo constellation achieved 99.75% availability with all DF GBAS configurations. While GPS 29 achieved 99.75% availability with CB-DF configuration only, it needs A/2 UMPE mitigation level with BB-DF configuration. But, Galileo constellation achieved 99.99% availability in all GBAS configuration except in AA-DF configuration (it needs A/4 UMPE mitigation level). While, GPS 29 constellations are very close (VC) to achieve 99.99% availability and could achieve it with A/10 UMPE mitigation level in CB-DF configuration. On the other hand, and for Single Frequency SF Configuration, All GNSS constellations couldn't achieve 99.75% availability nor 99.99% availability with AA-SF configuration. All GNSS constellations are very close (VC) to achieve 99.99% and 99.75% availability with BB-SF configuration, except Galileo could achieve 99.75% availability only with A/2 UMPE mitigation level. All constellations are very close (VC) to achieve 99.99% availability using CB-SF configuration, but Galileo

constellation could achieve it by A/2 UMPE mitigation level. Galileo constellation achieved 99.75% availability with CB-SF configuration, whereas GPS constellation could achieve it by A/2 UMPE mitigation level. Which is also compliant with ICAO.

3. For VAL =2.5m, All GNSS constellations with all GBAS configurations are not visible (NV) to achieve 99.75% nor 99.99% availability on both SF and DF for VAL = 2.5m with the exception of CB-DF configurations in GPS 29 and Galileo Constellations, they are somehow visible to achieve the 99.75% or 99.99% availability requirements. Which is also compliant with ICAO.

In general, there was strong positively impact on availability of GBAS system in the lower VAL values against visible impact in the middle VAL values and minor Impact in higher VAL values, Furthermore, No significant difference in the way of how different GNSS constellations response to the variation of user Multipath error levels, But more sensitive response of Galileo over GPS performance. Also the DF receivers have higher increment in availability, higher improvement, in both the maximum and the average than the SF receiver when UMPE decreases. It was clear to see major availability improvement responses to UMPE error mitigation in CB, BB, types against less improvement responses in AA type.

By this said, it is clearly resulted that any single GNSS constellation, like Galileo or Modernized GPS, or even those which are not involved in this study, like GLONASS or Beidou, none of the them as a single constellation will be able to globally achieve GAST-E/F GBAS performance, even that the best expected configuration is achieved by the technical improvement, it might achieve GAST-D performance as stated in the introduction of this research, but to achieve higher performance it needs dual combination of constellation. This result is recently notified by other researchers and announced by ICAO recently, it is not new to have it, but the aim of this study is - as mentioned earlier- to build on and validate it, the other step of the next sections is investigating more in the single constellation whether it can be able or not to achieve the higher performance of GAST-D/F over Europe/USA region and not globally wise, and this will ease its certification by ICAO standards at least partially in some airports during the landing phase on them, because not all the terrain of the world operates airports, for example, certification of GAST D/F is not needed in Northern Pole (beyond 80 degree) where are no airports exist.

3.5.2 Regional Coverage over Europe/USA for GNSS/GBAS

During result analysis in the past section, it was noticed that some of the cases are very close to fulfil the aeronautical requirements of 99.99% or 99.75% availability, as we performed the simulation globally, these special cases could meet the requirement if one or more of the following factors has been varied in such way to increase the availability: Some parameters are changed to better configuration of GBAS subsystems including: (1) the optimized number of the allowed critical satellites, (2) a certain level of User Multipath Error (UMPE) mitigation is applied, and (3) the size of the geographic areas is reduced.

It was noticed the effect of the geographic factor in achieving the requirements, when simulations are performed globally, the simulation tool averages all geographic areas, including the non-related parts of GBAS applications like wide oceans, the north and south poles, and the dead reception areas, in reality it doesn't give the true indication of the true availability over the sensitive airports final approach segments, as it considered the operational field of GBAS applications, but this assumption, global coverage, was taken into account for the sake of the user (airborne) multipath error (UMPE) study in order to perform comprehensive study.

Based on that the input assumptions for the AVIGA Simulation tool was modified to cover Europe and USA regions with best combination of configuration expected to be achieved by both GBAS subsystems and using the GPS 29 and Galileo 27 constellations separately, and as follows:

In the case of Galileo 27 satellites constellation, using the following GBAS parameters: Constellation of Galileo 27 Satellites, Step Calculation Grid of $5^{\circ} \times 5^{\circ}$, Mask angle = 10° , Ground Accuracy Designator (GAD) = C, Airborne Accuracy Designator (AAD) = B, Receivers (ground and airborne) performance = Dual Frequency (DF), Ground Service Level (GSL) = D, No. of Critical satellites = 6, Vertical Alert Limit (VAL) = 2.5m, Airborne Multipath Designator (AMD) = A, and User Multipath Error (UMPE) mitigation level = A/10.

To start with a logic analysis for this investigation of Galileo Constellation over Europe, we followed the following order Sequence in simulation Runs:

1. Case 1: Investigating and comparing the initial global Galileo Coverage in terms of GBAS with its Europe coverage, using the above input parameters.
2. Case 2: As first reduction in geographic area was performed from the globally coverage down to the following area which represent Europe and a part of the un guaranteed areas, using the same parameters with Step Calculation Grid of Lat. X Long. = $5^{\circ} \times 5^{\circ}$, Latitude = 30° N to 70° N, Longitude = 12° W to 55° E.
3. Case 3: Reducing the grid calculation step from Lat. X Long. = $5^{\circ} \times 5^{\circ}$ in the previous case 2 to Lat. X Long = $2^{\circ} \times 2^{\circ}$ in order to have more calculation nodes which lead to more accurate calculations when they are being averaged.

In Case 1: Investigating the globally coverage For Galileo as seen in Figures 13 +14 below in both 3D and 2D showed that the availability was 92.750941%, it was noticed that the constellation guaranteed the availability of 100% over a fixed areas of the globe, these areas look like stripes belts bounding the earth over a certain latitudes depending on the input parameters that have been used, in the case of the used parameters above for GBAS CAT III performance the un guaranteed availability stripes are the red bars. The nonguaranteed sectors are located in the north part of the earth and the south part also; in the north part from Lat. of 06° N up to 30° N, nearly northern the Equator, and from Lat. 74° N up to the North Pole. And in the south part of the earth from Lat. 10° S down to 34° S, nearly southern the Equator and from Lat. 80° S down to the South Pole.

These areas have the following characteristics:

- They are fixed over the same geographic areas and not varying (moving) with constellation status or with time.
- They are bounding the earth along the 360 Longitudes
- They have the same availability values, so they could be Equal-availability areas.
- They are sloped (inclined) cliff shape, not 90° cliff shape.
- Their position is GBAS configuration dependent.

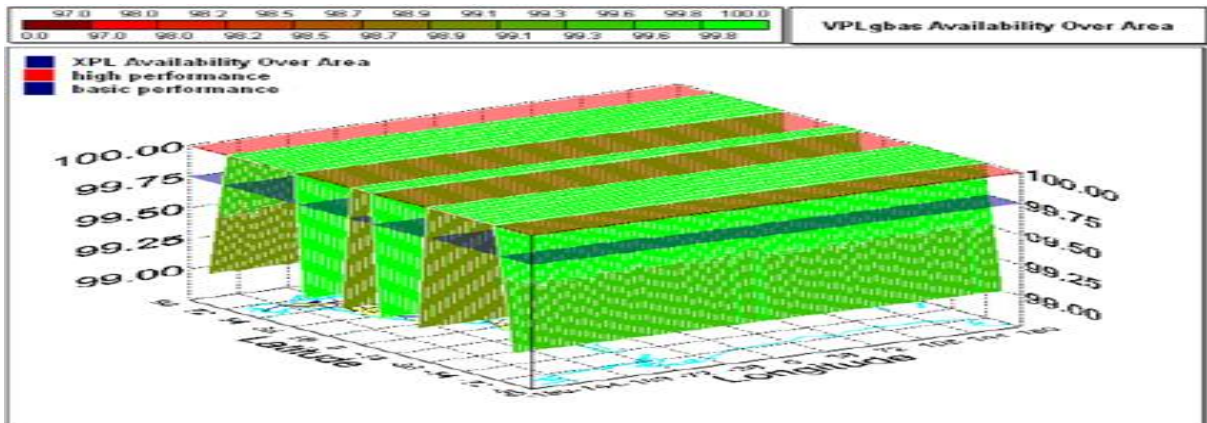


FIGURE 13: 3D GLOBALLY AVAILABILITY FOR GALILEO [EDITED BY AUTHOR]

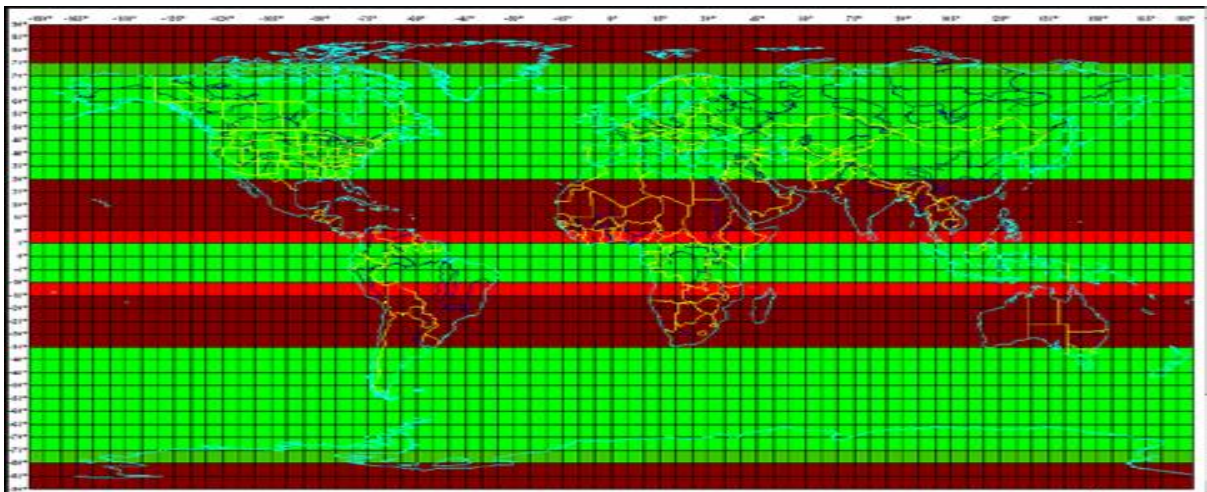


FIGURE 14: 2D GLOBALLY AVAILABILITY FOR GALILEO [EDITED BY AUTHOR]

These fixed and Equal availability stripes could be said that it's a Galileo property constellation, which is consist of three orbits 120° apart, each orbit has 9 operating satellites and 1 spare satellite, periodicity of 10 days. The advantages of the fixed Equal-Availability areas could be:

- The possibility of operating GBAS systems on guaranteed availability areas.
- The possibility of avoiding the nonguaranteed availability areas.
- Optimizing the usage of Galileo constellation in all applications
- Help in the standardization process of Galileo-based GBAS system.

In Case 2, As first reduction in geographic area was performed from the globally coverage down to Europe and a part of the un guaranteed areas, the availability improved from 92.750941% in global case 1 to 99.501282% in this case, as shown in figure 15 below, as we see, we still have a small part of the un guaranteed areas, then for sure, which cause a reduction in availability over Europe.

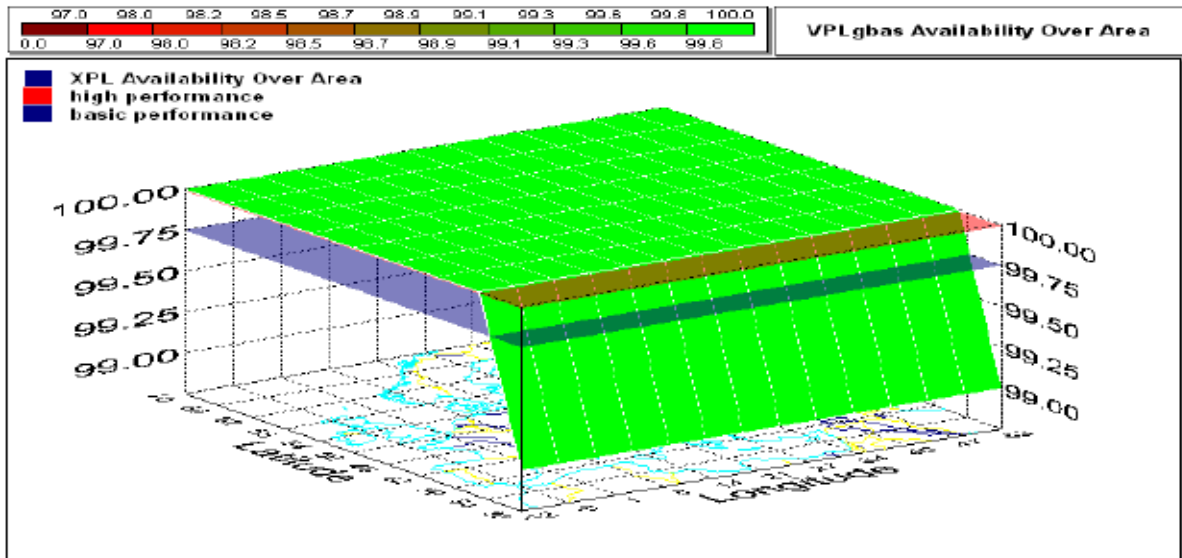


FIGURE 15: AVAILABILITY OVER EUROPE 30N TO 70N, 5°X5° GRID FOR GALILEO [EDITED BY AUTHOR]

In case 3, when we have reduced the grid calculation step from Lat. X Long. = 5°X5° in the previous case to Lat. X Long. = 2°X2°, as shown figure 16 below, the availability has increased in a slight percentage from 99.501282% to 99.674383% using the same parameters over the same previous area over Europe. This is due to the increase of the number of nodes or calculation points, in less grid calculation steps more point will be considered in availability calculation process, and then this will increase the accuracy of averaged results of the calculated points and then the overall availability will slightly increase.

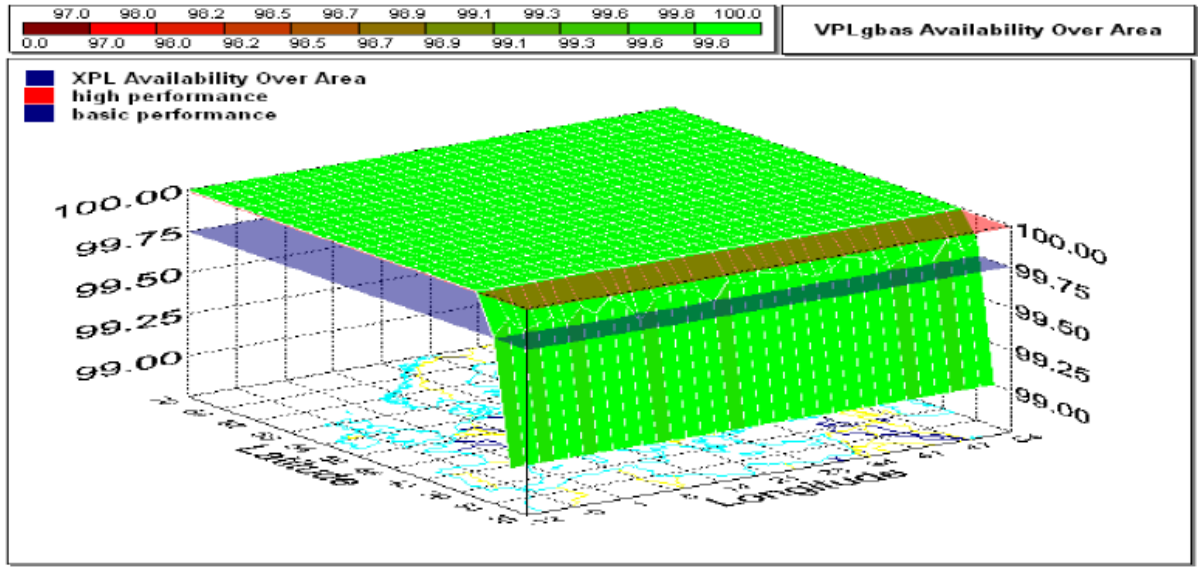


FIGURE 16: AVAILABILITY OVER EUROPE 30N TO 70N, 2°X2° GRID FOR GALILEO [EDITED BY AUTHOR]

Furthermore, as a second reduction in the geographic areas of Europe, we have chosen the following restricted area which covers Europe exactly: Lat. = 39° N to Lat. = 70° N and Long. = 12° W to Long. = 55° E Step Grid 5°X5°, and 2°X2°, the resultant availability has increased to 100% for both step grids, so it now fulfils the aeronautical availability requirements. As shown in Figure 12 below, the availability has increased due to the best parameters of the used configuration of GBAS subsystems, and the A/10 level of User Multipath Error (UMPE) mitigation is applied, as well as the size of the geographic areas is reduced to be within the guaranteed areas.

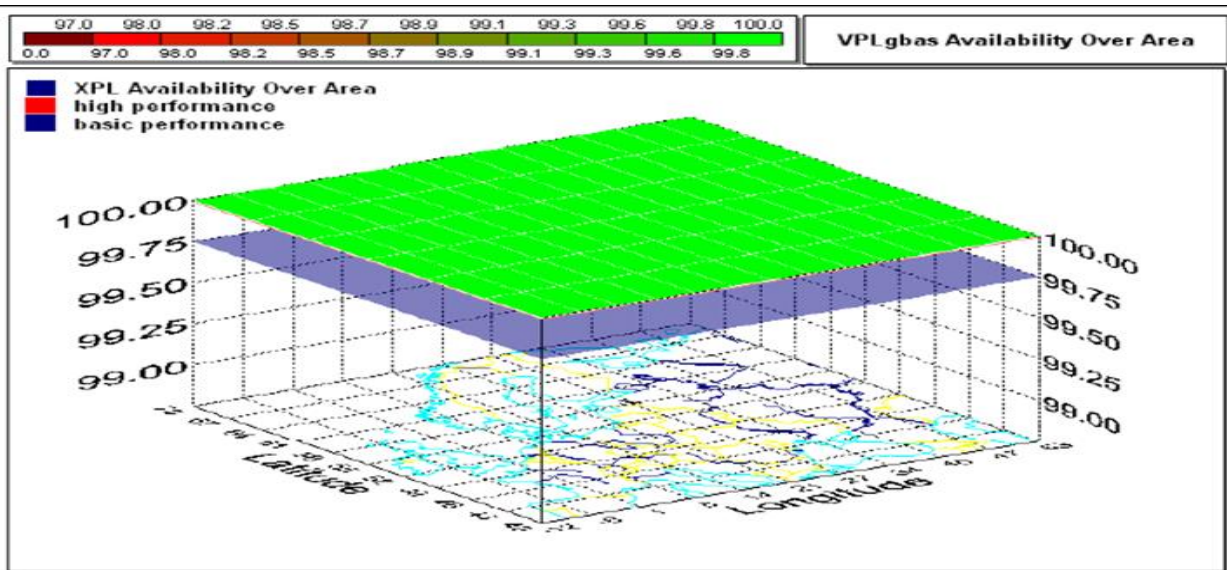


FIGURE 17: AVAILABILITY OVER EXACT EUROPE 39N TO 70N, GRID 5°X5°, AND 2°X2° FOR GALILEO [EDITED BY AUTHOR]

In order to investigate the Galileo performance over USA region as well, the same analysis steps were done for USA region, with same input parameters and with Galileo constellation also, and nearly similar results were achieved, the achieved availability over USA region (99.40465%.) in the best case of GBAS input parameters(CB-DF), Optimized coverage areas, UMPE mitigation level (A/10). So that it couldn't meet the aeronautical availability requirements of 99.99% for GAST D/E/F, but it is very close to achieve it if more improvements have been made in the aspect of GBAS parameters only or dual constellation solution. Finally, it can be said that Availability of Galileo constellation in terms of GBAS application over Europe is better than over USA.

A further investigation where done for GPS 29 constellation over both Europe and USA using the same criteria and inputs, the resultant availability was not able to achieve neither 99.99% nor 99.75% threshold, i.e. GAST-D/E/F, explanation of this could be due to the difference in modulation scheme used in both.

3.5.2.1 Results of the Regional Coverage of Galileo/GPS over Europe and USA

This final result of this section can be summarized that Galileo 27 constellation was able to meet the aeronautical requirements of both 99.99% and 99.75% (GAST-D/E/F) over Europe only with the given input parameters of the best GBAS configuration of CB-DF and for VAL= 2.5m (CAT III/GAST - E/F requirements), and it was very close (99.404%) over USA. But GPS 29 was not capable to meet these requirements

3.6 Conclusions and Recommendations

The requirements of GNSS/GBAS Landing System CAT III performance (GAST-F) are tended to be approved using dual Constellation by adding the European Galileo signals in the near future. The assumption of having dual constellation is subjected to the evaluation of certain factors such as the delay in time due to phase measurements during phase combination, the complexity of using the multichannel receivers, and political reasons. Based on that, the main assumption of this research was made on using a Single GNSS Constellation (SC) GBAS Landing System, and to examine, by usage of a simulation tool, the capability of the newly European Galileo system to meet the GAST-D/F requirements over at least Europe Space. Due to the improved signal in space availability of using the BOC modulation scheme and the increased power of +6dB in Galileo signal structure, the resultant availability was promising and stable in terms of the accuracy and Integrity designators which were chosen to the best combination. The results of this research approved clearly that any single GNSS constellation, like Galileo or Modernized GPS, or even those which are not involved in this study. However, the results have also approved, by using the same simulation tool, that the European Galileo Navigation system can meet the aeronautical requirements of the higher performance of GAST-F over Europe region. So that, the final result of this research can be summarized that Galileo constellation was able to meet the aeronautical requirements of both 99.99% and 99.75% (GAST-D/E/F) over Europe only with the given input parameters of the best GBAS configuration of CB-DF and for VAL= 2.5m (CAT III/GAST –E/F requirements), and it was

very close (99.404%) over USA. But the modernized GPS constellation was not able to meet these requirements, this due to different modulation scheme used in both.

3.6.1 The New Achieved Scientific Result

- New scientific result # 1a: Global coverage: I have approved that the global availability of the GBAS Landing System in GAST-D/F performance of 99.99% using a single constellation simulator (Galileo or GPS) is not feasible in Single Constellation/ Dual Frequency (SC/DF), but Galileo is more visible when CB-DF precision configuration is reached, which is characterized being newly updated result than a recently announced in 2020 by ICAO in Annex 10/V.1/Amendment 92. It is more precise and fully validated than the previously conducted studies.
- New scientific result # 1b: Regional coverage: I have innovated a regional coverage selection, and I approved that Galileo constellation is able to fulfil the aeronautical requirements of both 99.99% and 99.75% (GAST-D/E/F) over Europe sky using GBAS precise configuration of CB-DF, and it is very close (99.404%) over USA, but the GPS constellation is not able to fulfil these requirements, which is characterized being a new, approved, validated and efficient regional operational concept of GBAS system not being conducted by any other previously studies except as individual airports.

3.6.2 Recommendations

A further investigations in this aspect is recommended when Galileo system comes to its full operation capability of 30 satellites. As well as the modernized GPS Block III comes to its full 20 satellites capability, this would be anticipated by 2025.

Since Budapest International Airport is located in the same tested Europe region, then the

Chapter 4: Effectiveness of the Multiplexed Binary Offset Carrier (MBOC) Modulation on Multipath Error Envelope in GNSS Receivers

4.1 Introduction

This chapter handles the objective of the previous chapter but from another point of view, it is the enhancements encountered in the Galileo and GPS Block III constellations, and how they positively affecting the availability of GBAS landing systems, However, and as reminder, The GNSS Ground-Based Augmentation Systems (GNSS/GBAS) has recently been widespread, and they were approved in CAT II performance (GBAS Approach Service Type D (GAST-D)) for the precision landing system. However, it was noticeable that the main constraint factor of achieving CAT III/GAST-E/F performance in a single constellation usage is the multipath error and/or the interference from other same-frequency users, especially in GPS L1C and Galileo E1 open services. Moreover, the Binary Offset Carrier (BOC) techniques have been adopted in Galileo and GPS BIII as one of the efficient mitigation methods to decrease the multipath error and to increase both the Position Accuracy and the immunity of GNSS interferences. In addition, the Multipath Error Envelope (MEE) is considered as the assessing tool to compare performances of such techniques in terms of error delay/displacement. This chapter aims to present a software method of assessing the improvements of the Accuracy, and yet the Availability, by producing the MEE for each used technique. Afterwards, assessing the GNSS-GBAS availability to achieve the CAT III/GAST-E/F requirements for aviation worthiness. The used methodology is based on analyzing the theoretical equations behind the multipath error envelopes in BPSK and BOC signals, then programing in Matlab to assess the Multipath error delays. The Resultant software could be used as a simulating tool for manipulating multipath parameters, manipulating materialization waveforms, and testing filter types. It concludes to which level of multipath mitigation is needed to meet the higher performance of GAST-E/F in GNSS/GBAS landing systems.

Based on above facts and motivations, the main aim of this chapter is made to examine the using of a Single Constellation (SC) in GBAS Landing Systems, particularly Galileo system. In which the Multipath error is considered a limiting factor to achieve the needed performance to meet the CAT II/III requirements in terms of Accuracy and yet availability. On the other hand, the BOC signals showed a better anti-multipath and anti-interference over the BPSK, in

terms of better MEE. The generic BOC modulation has been adopted in the modernized Global Positioning System (GPS) (JW, 2001) and the European Galileo System (Galileo, 2008), because of its good spectral isolation from heritage signals, high accuracy, multipath interference resistance compared with BPSK modulation. Furthermore, and yet, the Multiplexed BOC (MBOC) modulation has been used for the Galileo E1-B/C and GPS L1C (frequency (1575.42 MHz) signals to achieve enhanced accuracy and multipath interference resistance by using multilevel subcarrier symbols or combining different subcarrier symbols.

Recently, a new proposed Frequency-Hopping BOC (FH-BOC) scheme as per Jian gang et al, in 2020, (J. Ma, 2020) might improve the anti-interference performance and mitigates the ACF ambiguity problem of BOC modulation, the proposed FH-BOC modulation combines the most two practical and dominant spread spectrum techniques; the direct-sequence spread spectrum (DSSS) and the frequency-hopping spread spectrum (FHSS) techniques. because the acquisition time and complexity of the receiving process for the proposed FH-BOC signal are the same for the BOC signal with the same Main Lobe Bandwidth MLB. This new proposed modulation may be used as a new technique for the next-generation GNSS signal design, especially military signal design, but it is not used to yet, and needed to be deeply experimented as well. Furthermore, another new technique for MBOC is also proposed by Xin et al, in 2021, (X. Zhao, 2021), called MBOC-POS, where the subcarrier periodic shifting binary offset carrier modulation is used as the lower-order component instead of sine binary offset carrier modulations. In which, different proposed implementations of MBOCPOS modulations were compared with traditional multiplexed binary offset carrier (MBOC) signals in multipath mitigation, tracking accuracy, anti-interference and compatibility. Then, resulted in reduction of 35% of the multipath error envelope MEE is with the filter bandwidth of 10 MHz, also, it said that it may be used as a new option for MBOC modulations in next-generation signal design. But it should be subjected to a common test tool for examining its efficiency in terms of MEE envelope.

The results showed that the chip spacing and the relative amplitude are the key factors in multipath mitigation in the code tracking loop, but the relative amplitude is the key factor in decreasing the multipath error in the phase tracking error. Moreover, in terms of the multipath error, the BOC (2,2) modulations has the best performance among all, BOC (1,1) has better performance than the currently used BPSK. More results can be found for other new schemes that would be used in the future new signal generations.

The chapter structure illustrates the problematic analysis of the multipath error, followed by shedding the light on the Receiver-Based Mitigation Methods – especially the Multiplexed Binary Offset Carrier (MBOC), then after, a detailed explaining of the MBOC and MEE theoretical signal processing inside the GPS Receiver, followed by the Code /Phase Multipath Error Envelopes Algorithms which are used in my software, and the Program Validation Compared with Similar Software, lastly concluding the results of this chapter/objective.

4.2 Problematic Analysis of the Multipath Error

In general, Multipath is the propagation phenomenon that results in radio signals reaching the receiving antenna by two or more paths; this could affect the original signal in constructive (when the reflected phase angle is 0) or destructive (when the reflected phase angle is 180), However, interference in terms of amplitude varying and/or phase shifting. This interference can be formulated intentionally or unintentionally. The intentionally cause is considered as a spoofing in the Electronic Warfare (EW), this Electronic Attack has been approved in (Alhosban A. , 2019) that there is an Analogy of interference of signals at the Receiving Antenna and inside Receiver Signal processing from one side, and Multipath interference from the other side. Basically, the causes of the unintentionally multipath could be mainly reflection wise or/and diffraction wise in both specular and diffuse, the reflection and the diffraction are generated by the existing of the obstacles nearby the receiving antenna. However, there are two important assumptions underlying most GNSS-receiver multipath mitigation Approaches: firstly, is the Multipath components are being delayed relative to the direct path signal, because they have to travel a longer distance, and secondly is the Multipath signals are being weaker than the direct path signal, since some power will be lost due to the reflection. So the accumulated signal at the receiving antenna can be given by the following equation 9 below:

$$r(t) = A_0 \cdot d(t - \tau_0) \cdot c(t - \tau_0) \cdot \cos(2\pi f_{L1} t - \theta_0) + A_1 \cdot d(t - \tau_1) \cdot c(t - \tau_1) \cdot \cos(2\pi f_{L1} t - \theta_1) \quad \text{EQUATION 9}$$



Where:

$r(t)$ is the received GPS signal at the antenna.

A_0, τ_0, θ_0 : are the amplitude , the propagation delay, and the carrier phase shift respectively of the direct signal. And A_1, τ_1, θ_1 : are for the one reflected multipath signal. The phase rate of change is assumed to be zero, and The delay of the ground reflection is a dependent factor on the altitude of the aircraft (user) antenna and the elevation angle is given by the following equation 10 below:

$$D= 2. H. \text{SIN} (\text{ELEV.}) \quad \text{EQUATION 10}$$

Where D is the delay of the ground reflection, h is the altitude of the aircraft antenna, and elev. is the elevation angle. After Matlab simulation, the resultant signal will be analyzed inside the receiver, it will be auto correlated then entered the discriminator, the discriminator will be affected in all the above parameters, figure 18 below shows the affected discriminator my multipath.

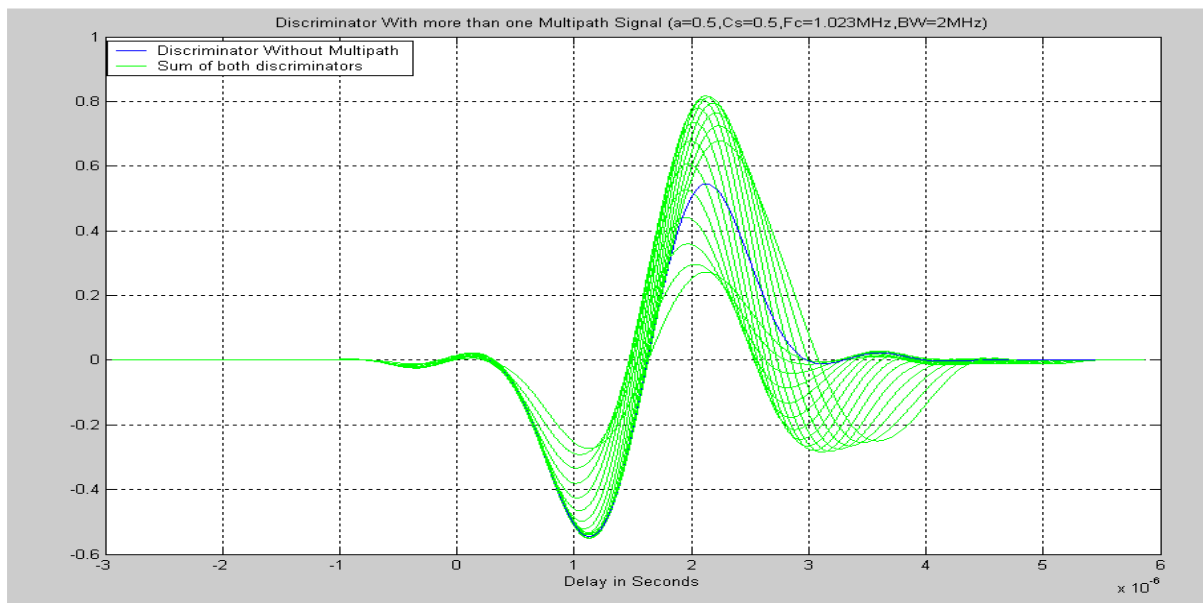


FIGURE 18: DISCRIMINATOR AFFECTED BY MULTIPATH [EDITED BY AUTHOR]

On the other hand, Mitigation methods could be classified to the following three types: Receiver-based mitigation methods, Antenna-based mitigation methods and Sitting-based mitigation methods. The first two methods could be applied for both the User (aircraft) receivers, and the Ground stations receivers. However, some classifications refer to the hardware and software based mitigation methods also, they are located in the domain of

Receiver-based methods. The sitting-based method would be applied to the ground station receivers only in GBAS application, due to the mobility of the aircraft, where the antennas are already sited once in the structure of the aircraft, and almost no control on the aircraft movement during the last phase of flight. In the same manner, the landing aircraft will be in a stable position with respect to the constellation space segments and what's needed is only the best position of the antenna in the aircraft structure, a lot of studies have investigated this point deeply and they have a satisfied results in mitigating the effect of the aircraft structure in terms of multipath, Upon these mitigation methods, it can be said that the multipath phenomena could be classified also to two types: the User multipath (mobile user i.e. aircrafts), and Ground station receiver's multipath, it can be resembled by the Ground Accuracy Designator (GAD).

Concerning the antenna-based and the sitting-based mitigation methods, they need to be experimentally dependent, improvement jumps are little and short in this aspect, but the Last two types of Chock ring and MLA (Multipath Limiting Antenna) could improve the performance of the Ground stations in GBAS stations from GAD letter A to better B or C letters. Researches fulfilled this domain (Braasch, 2002), (Jean-Pierre, 2003), particularly (Mathews, 2005), it compared the following antenna array types, each of them were assumed to have 7 antenna elements: Flat Antenna Array, Curved Antenna Array. Stack Antenna Array, and Curved (B) Antenna Array. In which, the results of this research approved, based on the simulation results, that the 3-D antenna array (7 elements) had the best multipath rejection performance in both the horizontal and vertical dimensions. Most importantly, and related to this research the focus will be on the Receiver-Based Mitigation Methods in the next section.

4.3 Receiver-Based Mitigation Methods/Multiplexed Binary Offset Carrier (MBOC)

In general, the receiver-based mitigation methods are those techniques used to reduce the multipath effect using the signal processing methods inside the receiver, specifically the ways implemented to enhance the performance of the tracking loops. However, there are two methods: The Correlator Techniques and the Signal Structure Techniques, our MBOC modulation technique is located under the signal structure technique, but it is strongly linked with the correlator technique after the signal comes in from the front end to the signal processor

/tracking channels in the GNSS receivers, thus, both of them will be analyzed in this section in order to build up the MEE software.

Conceptually, The Binary Offset Carrier (BOC) means to form the spectral shape (power distribution over frequency) of a transmitted signal. BOC type signals are usually expressed in the form $BOC(f_{\text{shift}}, f_{\text{chip}})$ where frequencies are indicated as integer multiples of the GPS C/A Code chip rate of 1.023 Mcps. For example, a BOC (10, 5) signal has actually a sub-carrier frequency of $10 \times 1.023 \text{ MHz} = 10.230 \text{ MHz}$ and a code chip rate of $5 \times 1.023 \text{ MHz} = 5.115 \text{ MHz}$, the ratio of the $2 \times f_{\text{shift}}/f_{\text{chip}}$ is the n ratio which could be even or odd, this n number is one of the factors that contribute inside the equation of signal itself as it will be mentioned in the next section. Figure 19-left panel below shows the two modulation schemes and how the power is spread over the frequencies, and figure 19-right panel shows its effect in the Autocorrelation Function ACF. Thus, the key parameter of a signal structure with respect to multipath is the signal bandwidth, because large bandwidth leads to a small amplitude of the multipath error.

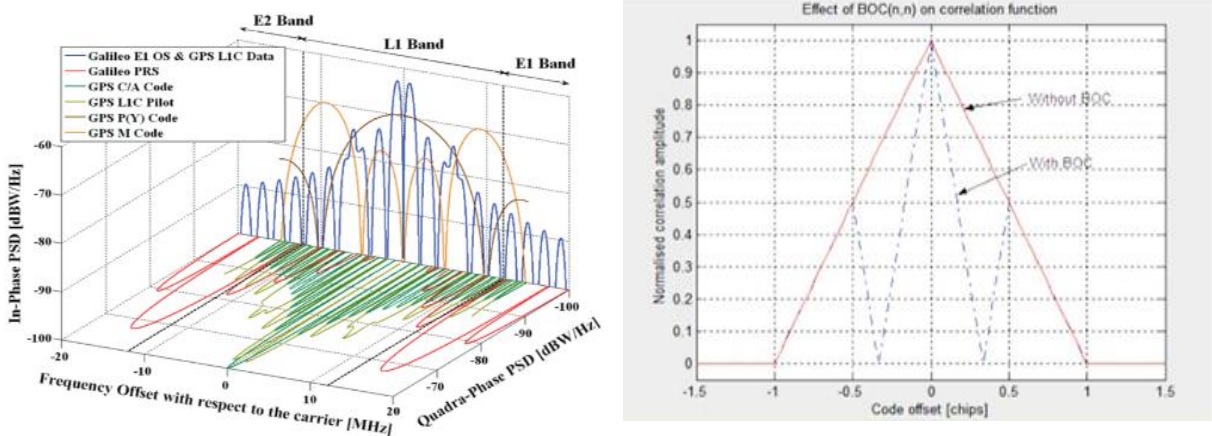


FIGURE 19: LEFT PANEL: NEW MODERN GNSS SIGNAL STRUCTURE [16], RIGHT PANEL: EFFECT ON THE AUTOCORRELATION FUNCTION ACF [EDITED BY THE AUTHOR]

However, the Multiplexed BOC (MBOC) is a new design, it introduces the multiplexed binary offset carrier (MBOC) spreading modulation recently recommended by the GPS-Galileo Working Group on Interoperability and Compatibility for adoption by Europe's Galileo program for its Open Service (OS) signal at L1 frequency, and also by the United States for its modernized GPS L1 Civil (L1C) signal. Its idea is based on various investigations that may be

led to candidates for a L1 Open Service optimized signal structure which is called a CBCS solution also (Composite Binary Coded Symbols). It can be expressed by a superposition of BOC (1, 1) and a BCS (Binary Coded Symbol) waveform with the same chip rate, equation 11 below:

$$CBCS = \alpha \cdot BOC(1,1) + \beta \cdot BCS(n,1) \quad \text{EQUATION 11}$$

Where α and β are values in percentage (%) under the condition $\alpha + \beta = 100\%$, and n represents the number of symbols. However, the BCS signal is a generalization of the BPSK-R and BOC modulation (except for BOC ($k \cdot n/2$, n) with k odd) in both the sine and cosine versions. Thus, the well-known BPSK and BOC modulations can be understood as a particular case of the BCS modulation. For more information, [ION GNSS 18th, Hein, Jose-Angel Avila Rodriguez]. Both BOC and MBOC had enhanced the Multipath Error Envelope delay dramatically from 250-300 meters in BPSK down to less than 10 meters in MBOC and less than 50 meters in BOC, figure 20 below, where the black colored curve is BOC (2,2), the red is BOC (14,2), and the blue is BPSK (1), but with some drawbacks; a larger bandwidth for BOC signals is still needed with comparison the BPSK, this may reach 32 MHz, and may impact the design of the receivers.

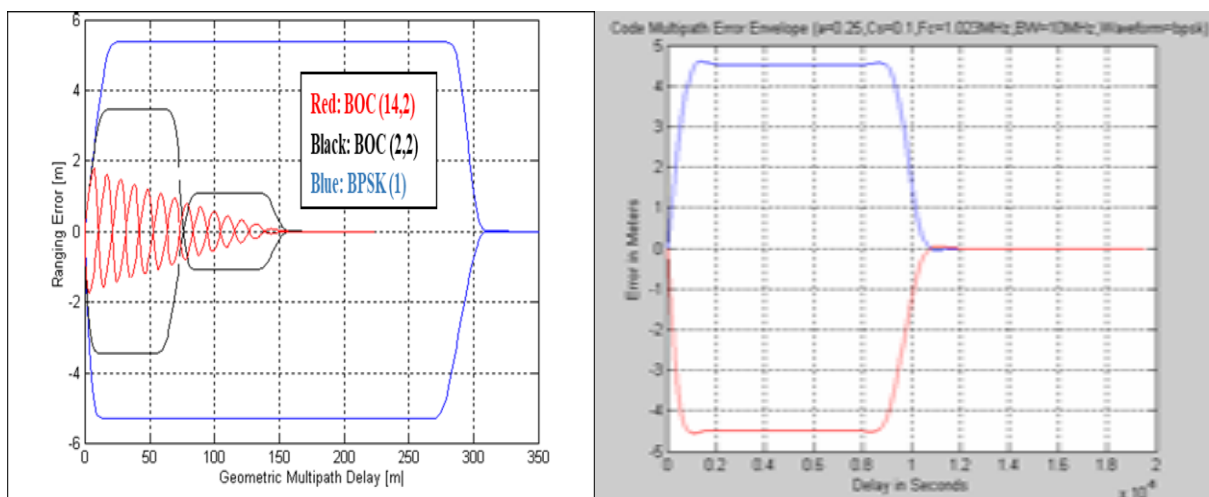


FIGURE 20: EFFECT OF BOC AND BPSK ON THE MULTIPATH ERROR ENVELOPE MEE
[OPEN SOURCE, EDITED BY AUTHOR]

4.4 Signal Processing of MBOC and MEE inside the GPS Receiver architecture

In order to produce formula of both phase and code error envelopes, first, we processed the accumulated signal at the front end of the global general GPS receiver architecture shown in Figure 21 below in a simple way that serves this goal.

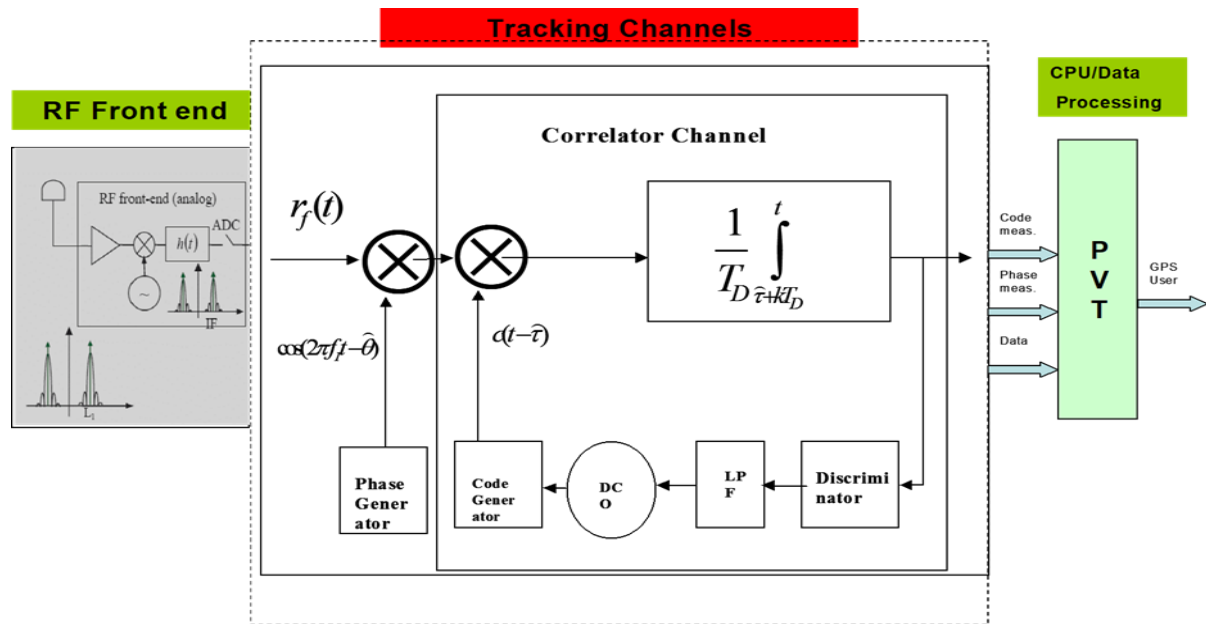


FIGURE 21: BLOCK DIAGRAM FOR GENERAL GNSS RECEIVER [EDITED BY AUTHOR]

The receiver consists of three main parts: the front end, the tracking channels and the PVT solution to the user. In the front end part, the functions of Analog to digital converting (ADC), Sampling, Encoding, and the Selective Filtering ($h(t)$) is taking place. The input of this stage is the GPS received signal from each satellite in view through the antenna, as seen in Equation 12 below:

$$r(t) = A \cdot d(t - \tau) \cdot c(t - \tau) \cdot \cos(2\pi f_{L1} t - \theta) + n(t) \quad \text{EQUATION 12}$$

Where $r(t)$ is the received GPS signal, A is the amplitude of the received signal, $d(t)$ is the GPS navigation message, $c(t)$ is the Gold spreading code, τ is the propagation delay, θ is the carrier phase shift, includes the Doppler effect, and the $n(t)$ is the white Gaussian noise.

In the presence of the multipath error, the GPS received signal will be as follows under the assumption of one reflected ray and neglecting the noise (noiseless channel) as a first approximation as seen in Equation 13 below again:

$$r(t) = A_0 \cdot d(t - \tau_0) \cdot c(t - \tau_0) \cdot \cos(2\pi f_{L1} t - \theta_0) + A_1 \cdot d(t - \tau_1) \cdot c(t - \tau_1) \cdot \cos(2\pi f_{L1} t - \theta_1)$$

EQUATION 13



Where: $r(t)$ is the received GPS signal at the antenna, A_0, τ_0, θ_0 : are the amplitude, the propagation delay, and the carrier phase shift respectively of the direct signal. And A_1, τ_1, θ_1 are for the one reflected multipath signal. The output of the RF front end is the same signal but filtered and sampled, under the assumption of neglecting the quantization errors as seen in equation 14 below:

$$r(t) = A_0 \cdot d(t - \tau_0) \cdot c_f(t - \tau_0) \cdot \cos(2\pi f_I t - \theta_0) + A_1 \cdot d(t - \tau_1) \cdot c_f(t - \tau_1) \cdot \cos(2\pi f_I t - \theta_1)$$

EQUATION 14

Where the small (f) denotes the filtered signal and the (I) denotes the Intermediate Frequency (IF) frequency conversion. The front stage is not simulated by the produced program, neither the last stage which the data processing unit that finalized the navigation solution (PVT: Position, Velocity, and Time) in its readable form by the user. The only simulated stage is the tracking channels. Equation 6 above is the input to the tracking channels (Auto Correlator Function ACF), which consists of the following circuitry:

- Carrier Tracking Loop (PLL/FLL): to generate an instantaneous carrier replica of the incoming signal.
- Code Tracking Loop: (DLL) to generate an instantaneous code replica of the incoming signal, it could be coherent or non-coherent with phase tracking loop. The most frequent architecture is FLL (if the phase pseudo range measurement is not needed), because it's more robust, and the non-coherent DLL loop. DLL loops generates usually the early and the late autocorrelation functions; in this case a discriminator is needed.

- Discriminator: it has the function of generating the error voltage produced by the early and late correlators with different ways (could be differencing or multiplying) this error voltage drives the DCO, the Differential Controlled Oscillator to generate the difference in phase or code error that compensates the errors in the loop by iterative process.
- Low Pass Filter: is needed to get rid of the unwanted generated frequencies due to the autocorrelation functions.
- Integrator: is accumulating the power in the spread GPS incoming signal each time of the loop process and over the interval of the 1ms (the navigation message period).

4.4.1 Costas PLL /Phase Tracking Multipath Error

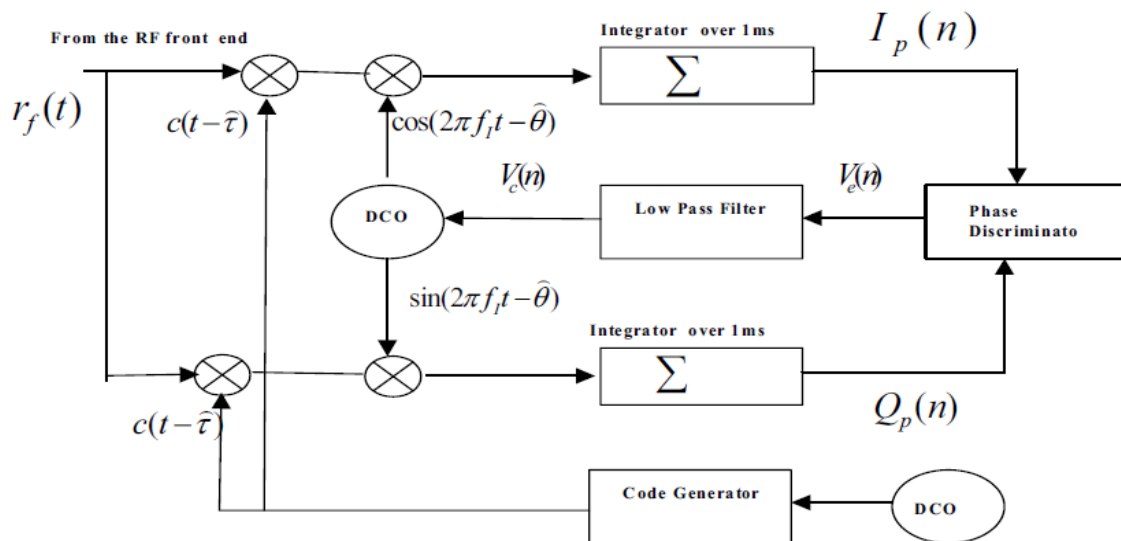


FIGURE 22: COSTAS PLL LOOP [EDITED BY AUTHOR]

As a first step we can consider the PLL is not locked, that incoming phase is not the same as the estimated phase in the Costas PLL loop shown in Figure 22 above, the input signal is Equation 14 above with the multipath error embedded in it.

Where $t = kT_D$, then;

$$r(t) = A_0 \cdot d(kT_D - \tau_0) \cdot c_f(kT_D - \tau_0) \cdot \cos(2\pi f_I kT_D - \theta_0) + A_1 \cdot d(kT_D - \tau_1) \cdot c_f(kT_D - \tau_1) \cdot \cos(2\pi f_I kT_D - \theta_1) \text{ EQUATION 15}$$

$$\theta - \hat{\theta} = K_{DCO} \int_0^t V_c(v) dv \quad \text{EQUATION 16}$$

The phase is the integration of the DCO command voltage.

$$I_p(n) = A/2 \cdot d(n) \cdot K_c(\tau - \hat{\tau}_0) \cdot \cos(\theta - \hat{\theta}_0) + \alpha \cdot A/2 \cdot d(n) \cdot K_c(\tau - \hat{\tau}_1 + \Delta\tau) \cdot \cos(\theta - \hat{\theta}_1 + \Delta\theta) \text{ EQUATION 17}$$

$$Q_p(n) = A/2 \cdot d(n) \cdot K_c(\tau - \hat{\tau}_0) \cdot \sin(\theta - \hat{\theta}_0) + \alpha \cdot A/2 \cdot d(n) \cdot K_c(\tau - \hat{\tau}_1 + \Delta\tau) \cdot \sin(\theta - \hat{\theta}_1 + \Delta\theta) \text{ EQUATION 18}$$

Where: $K_c(\tau - \hat{\tau}_0)$ is the autocorrelation function of the in-phase /Quadrature-phase of the LOS signal, $K_c(\tau - \hat{\tau}_1 + \Delta\tau)$ is the autocorrelation function of the in-phase /Quadrature-phase of the reflected signal, $\Delta\tau$ is the time delay due to multipath, and $\Delta\theta$ is the phase delay due to multipath, assuming negligible Doppler Effect

The phase discriminator could be either: Product or Costas discriminator, Arc tangent Discriminator, or 4-quadrant discriminator. In the Product or Costas Discriminator;

$$V_e(n) = I_p(n) \cdot Q_p(n) \text{ EQUATION 19}$$

$$V_e(n) = A^2/4 \cdot K^2(\tau - \hat{\tau}_0) \cdot \sin(\theta - \hat{\theta}_0) \cdot \cos(\theta - \hat{\theta}_0) \text{ EQUATION 20}$$

When the loop is locked; $\theta - \widehat{\theta}_0 = 0 (\pi)$

$$V_e(n) = A^4 / 8 \cdot K^2 (\tau - \widehat{\tau}_0) \cdot \sin(2(\theta - \widehat{\theta}_0)) \text{ EQUATION 21}$$

So, the discriminator is not linear and not normalized and with ambiguity of π , it can be normalized by dividing the last output by the power of the both punctual correlators:

$$V_e(n) = \frac{I_p(n) \cdot Q_p(n)}{(I_p^2(n) + Q_p^2(n))} \text{ EQUATION 22}$$

Normalized as follows:

$$V_e(n) = 1/2 \cdot \sin(2(\theta - \widehat{\theta}_0)) \text{ EQUATION 23}$$

For the 4-quadrant Discriminator: $V_e(n) = \arctan(2 \cdot Q_p(n) / I_p(n))$, the ambiguity of π is removed.

For the Arctangent Discriminator:

$$V_e(n) = \arctan\left(\frac{Q_p(n)}{I_p(n)}\right) \text{ EQUATION 24}$$

$$V_e(n) = (\theta - \widehat{\theta}_0)(n) \text{ EQUATION 25}$$

Which is normalized and linear but still with ambiguity of π . Finally, it was fully demonstrated that the phase tracking error due multipath is:

$$\varepsilon_\theta = \theta - \widehat{\theta}_0 = \arctan\left[\frac{\alpha \cdot K_c(\tau_0 - \widehat{\tau}_0 + \Delta\tau) \cdot \sin(\Delta\theta_1)}{K_c(\tau_0 - \widehat{\tau}_0) + \alpha \cdot K_c(\tau_0 - \widehat{\tau}_0 + \Delta\tau) \cdot \cos(\Delta\theta_1)}\right] \text{ EQUATION 26}$$

And the last equation, Eq. (26), was used in the Matlab program to be simulated with company of the equations that are needed in the following section.

4.4.2 Non-coherent DLL/Code Tracking Multipath Error

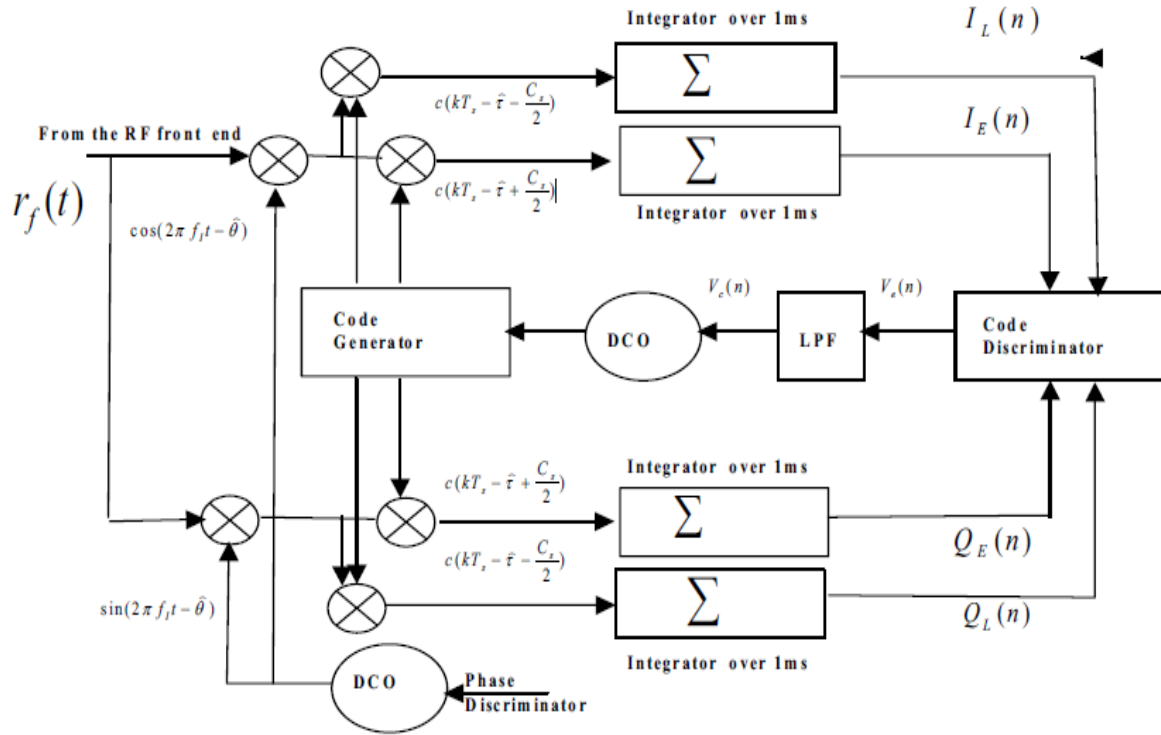


FIGURE 23: NON COHERENT DLL LOOP [EDITED BY AUTHOR]

$$I_L(n) = A/2 \cdot d(n) \cdot K_c(\varepsilon_\tau - C_s/2) \cdot \cos(\varepsilon_\theta) + \alpha \cdot A/2 \cdot d(n) \cdot K_c(\varepsilon_\tau - C_s/2 + \Delta\tau) \cdot \cos(\varepsilon_\theta + \Delta\theta)$$

EQUATION 27

$$I_E(n) = A/2 \cdot d(n) \cdot K_c(\varepsilon_\tau + C_s/2) \cdot \cos(\varepsilon_\theta) + \alpha \cdot A/2 \cdot d(n) \cdot K_c(\varepsilon_\tau + C_s/2 + \Delta\tau) \cdot \cos(\varepsilon_\theta + \Delta\theta)$$

EQUATION 28

$$Q_L(n) = A/2 \cdot d(n) \cdot K_c(\varepsilon_\tau - C_s/2) \cdot \sin(\varepsilon_\theta) + \alpha \cdot A/2 \cdot d(n) \cdot K_c(\varepsilon_\tau - C_s/2 + \Delta\tau) \cdot \sin(\varepsilon_\theta + \Delta\theta)$$

EQUATION 29

$$Q_E(n) = A/2 \cdot d(n) \cdot K_c(\varepsilon_\tau + C_s/2) \cdot \sin(\varepsilon_\theta) + \alpha \cdot A/2 \cdot d(n) \cdot K_c(\varepsilon_\tau + C_s/2 + \Delta\tau) \cdot \sin(\varepsilon_\theta + \Delta\theta)$$

EQUATION 30



Where:

$\varepsilon_\tau = \tau_0 - \hat{\tau}$ Is the LOS code tracking error

$\varepsilon_\theta = \theta_0 - \hat{\theta}$ Is the LOS phase tracking error

$\Delta\tau = \tau_1 - \tau_0$ Is the code tracking error due to multipath

$\Delta\theta = \theta_1 - \theta_0$ Is the phase tracking error due to multipath

τ_0, θ_0 are for the LOS direct signal

τ_1, θ_1 are for the reflected multipath signal

The second part of the equations represent the multipath contribution to the early late correlator, and here we have two types of discriminators: The Dot-Product discriminator, and the early minus late power discriminator one, in the dot-product one, which won't be used in the program this time, its resultant output signal is:

$$V_e(n) = I_p(n) \cdot (I_E(n) - I_L(n)) + Q_p \cdot (Q_E(n) - Q_L(n)) \quad \text{EQUATION 31}$$

But for the Early- minus- late discriminator:

$$V_e(n) = (I_E^2(n) + Q_E^2(n)) - (I_L^2(n) + Q_L^2(n)) \quad \text{EQUATION 32}$$

$$V_e(n) = A^2/4 \cdot (K^2(\varepsilon_\tau + C/2) - K^2(\varepsilon_\tau - C/2)) + \alpha^2 \cdot A^2/4 \cdot (K^2(\varepsilon_\tau + C/2 + \Delta\tau) - K^2(\varepsilon_\tau - C/2 + \Delta\tau)) \quad \text{EQUATION 33}$$

As an approximation, we will consider no effect due to filter on the correlation function, it can be offset if its delay time has been known.

So, $K_{cf} = K_c$, and then,

$$K_c(\varepsilon_\tau) = \begin{cases} K_c(\varepsilon_\tau) = 1 - \frac{|\varepsilon_\tau|}{T_c}, & \text{if } |\varepsilon_\tau| \ll T_c \\ K_c(\varepsilon_\tau) = 0, & \text{elsewhere} \end{cases} \quad \text{EQUATION 34}$$

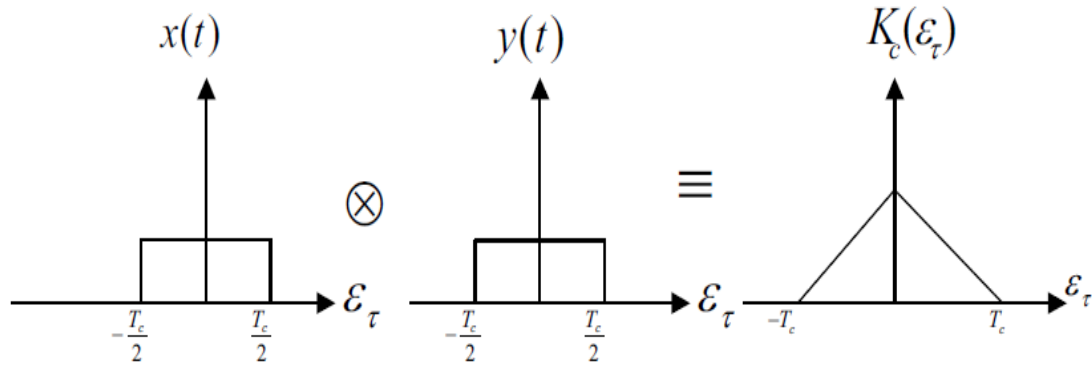


FIGURE 24: CORRELATION PROCESS [EDITED BY AUTHOR]

As seen in the figure 24 above the correlation process, when $x(t)$, represents the code rect (t) wave, and $y(t)$ the local generated code, replica and shifted t_0 , $\text{rect}(t-t_0)$, are convoluted with each other the form the correlator function, $K_c(\epsilon_\tau)$, with twice the time interval than any one of them, but if the code is not rectangular waveform, the autocorrelation will be different, in the simulation Matlab program, BOC(binary offset carrier) signals are used, their power spectrum is different, it provides spectral isolation and leads to a significant improvements in terms of tracking and multipath mitigation, a full demonstration of BOC signals are presented in[Macabiau, ION NTM,2005], from this reference we have taken the following BOC equations:

$$G_{BOC}(f) = \frac{1}{T_c} \left(\frac{\sin(\frac{\pi f T_c}{n}) \sin(\pi f T_c)}{\pi f \cos(\frac{\pi f T_c}{n})} \right)^2 \text{ FOR THE SINE PHASED EVEN N} \quad \text{EQUATION 35}$$

$$G_{BOC}(f) = \frac{1}{T_c} \left(\frac{\sin(\frac{\pi f T_c}{n}) \cos(\pi f T_c)}{\pi f \cos(\frac{\pi f T_c}{n})} \right)^2 \text{ FOR THE SINE PHASED ODD N} \quad \text{EQUATION 36}$$

According to the reference above, both BOC (1, 1) and BOC (2, 2) are both even, for BOC (p, q)

$f_s = p \cdot 1.023\text{MHz}$ And $f_c = q \cdot 1.023\text{MHz}$, then $n = 2 \frac{f_s}{f_c} = 2 \frac{p}{q}$, if n is even, Equation 36 will be used. And the result will be calculated by a sub function of the program

Then it can be demonstrated that: $V_e(n) = \frac{A^2}{4} \cdot \left(2 - \frac{C_s}{T_c}\right) \cdot \frac{2\varepsilon_\tau}{T_c}$, which is linear discriminator in ε_τ and non-coherent.

4.4.3 Coherent DLL/Code Tracking Multipath Error

It is the second type of the DLL loops that is dependent on the phase error also, it uses the early minus late correlator, as illustrated in Figure 25 below:

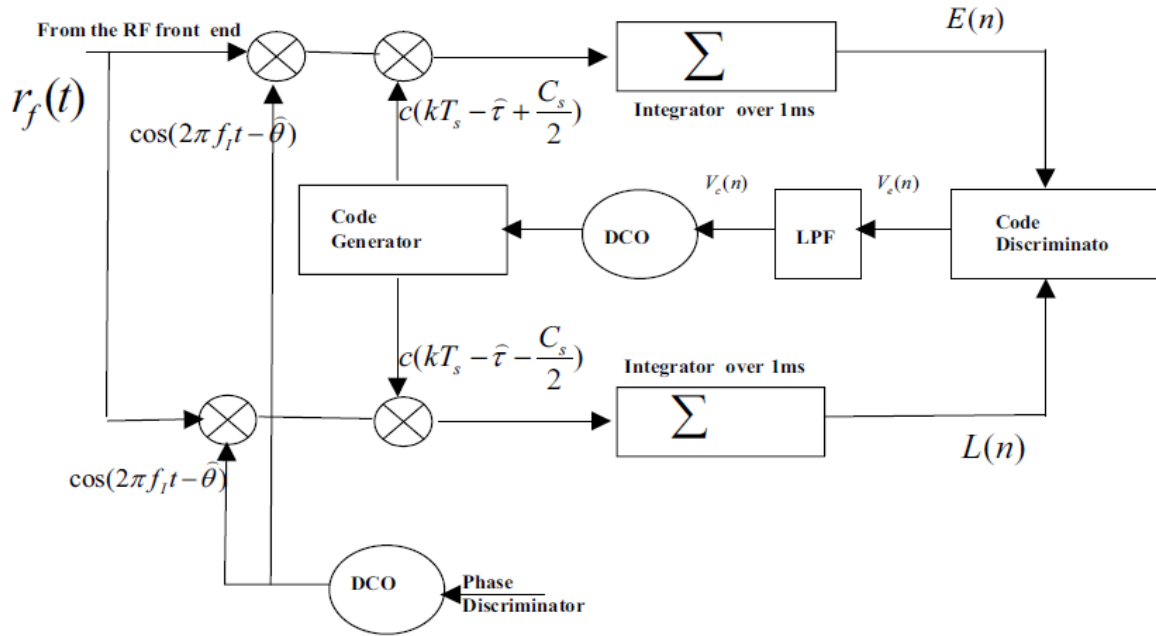


FIGURE 25: COHERENT DLL LOOP [EDITED BY AUTHOR]

$$E(n) = \frac{A_0}{2} \cdot K_{cf} \cdot \left(\varepsilon_\tau + \frac{C_s}{2}\right) + \frac{A_1}{2} \cdot K_{cf} \cdot \left(\varepsilon_\tau + \frac{C_s}{2} + \Delta\tau\right) \cdot \cos(\Delta\theta) \quad \text{EQUATION 37}$$

$$L(n) = \frac{A_0}{2} \cdot K_{cf} \cdot \left(\varepsilon_\tau - \frac{C_s}{2}\right) + \frac{A_1}{2} \cdot K_{cf} \cdot \left(\varepsilon_\tau - \frac{C_s}{2} + \Delta\tau\right) \cdot \cos(\Delta\theta) \quad \text{EQUATION 38}$$

Early - minus - Late discriminator assuming $\varepsilon_\tau=0$ will be $V_e(n) = E(n) - L(n)$

$$V_e(n) = \frac{A_0}{2} K_{cf} \left(\varepsilon_\tau + \frac{C_s}{2}\right) - \frac{A_0}{2} \cdot K_{cf} \left(\varepsilon_\tau - \frac{C_s}{2}\right) + \left(\frac{A_1}{2} \cdot K_{cf} \left(\varepsilon_\tau + \frac{C_s}{2} + \Delta\tau\right) - \frac{A_1}{2} K_{cf} \left(\varepsilon_\tau - \frac{C_s}{2} + \Delta\tau\right)\right) \cos(\Delta\theta) \quad \text{EQUATION 39}$$

If we set: $V(\varepsilon_\tau) = K_{cf} \cdot \left(\varepsilon_\tau + \frac{C_s}{2}\right) - K_{cf} \cdot \left(\varepsilon_\tau - \frac{C_s}{2}\right)$, Then;

$$V(\varepsilon_\tau) = \frac{A_0}{2} \cdot V(\varepsilon_\tau) + \frac{A_1}{2} \cdot V(\varepsilon_\tau + \Delta\tau) \cdot \cos(\Delta\theta) = 0 \quad \text{EQUATION 40}$$

A stable Lock point will be when $V_e(n) = 0$, then $\frac{A_0}{2} \cdot V(\varepsilon_\tau) + \frac{A_1}{2} \cdot V(\varepsilon_\tau + \Delta\tau) \cdot \cos(\Delta\theta) = 0$

If $C_s = T_c$, then no more steady point. Then $\alpha = \frac{A_1}{A_0} \leq 1$, is the relative amplitude,

$\Delta\tau \geq 0$: should be positive because there is no delay comes before the LOS signal arrive, LOS signal comes first directly to the antenna, then after the reflected waves follow it. Then the cross point occurs when:

$$V(\varepsilon_\tau) = -V(\varepsilon_\tau + \Delta\tau) \cdot \cos(\Delta\theta), \text{ in the interval } \left[-\frac{C_s}{2}, \frac{C_s}{2}\right]$$

Looking for the zero crossing of the discriminator function is the goal of the Matlab programming, at the envelope then can be resolved to be as close as the following theoretical shape in figure 26 below:

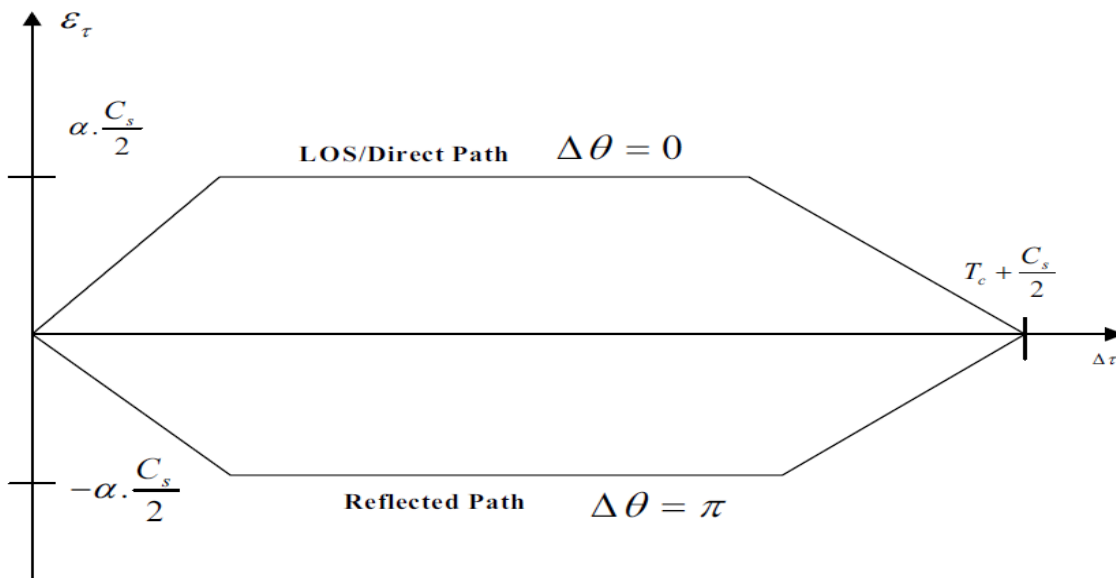


FIGURE 26: CODE ERROR ENVELOPE OF THE MULTIPATH [EDITED BY AUTHOR]

4.5 Code /Phase Multipath Error Envelopes Algorithms

After the theoretical part of the Multipath Error Envelopes MEE has been illustrated in the previous sections, in this section, and in order to show the different impacts of the materialization signals on the mitigation of the multipath error, the main functions were used in the Matlab simulating software are: Firstly, the autocorrelation function for: BPSK, BOC (1, 1) and BOC (2, 2) wave forms. Then, the discriminator function of the Early-minus-late for the code tracking error envelope and the Early -minus-late power for the phase tracking error envelope. Afterwards, the filtering functions using the FIR Boxcar, FIR hamming, Butterworth and the Chebyshev filters. Furthermore, different types of filters were designed in the program to show the different delays of each on the discriminator function as well as the power reduction due to excluding side lobes during the filtering process, most of the studies uses infinite bandwidth, that means they neglect the effect of filters, in reality filters are exist, but as soon, their effect is known, i.e. delay time, then it can be offset, so both assumptions are correct and gives nearly the same final results.

There are two functions considered as the heart of the program: The Error-Finding function for the BPSK and the filters, and the Error-Finding function for BOC signals, their function is to find the zero crossing points of the discriminator with the τ axis, then these crossing point are converted to error-wise terms in meters (by multiplying with light speed) in case of code envelope or radians (by multiplying by fractions of $\pi /2$ of the wave length of the L1 GPS frequency (19cm)) in case of phase envelope, and then being plotted versus τ to produce both envelopes. Hereafter, in figures 27 and 28 below, the whole flow chart of the program structure for the code tracking error envelope due to multipath:

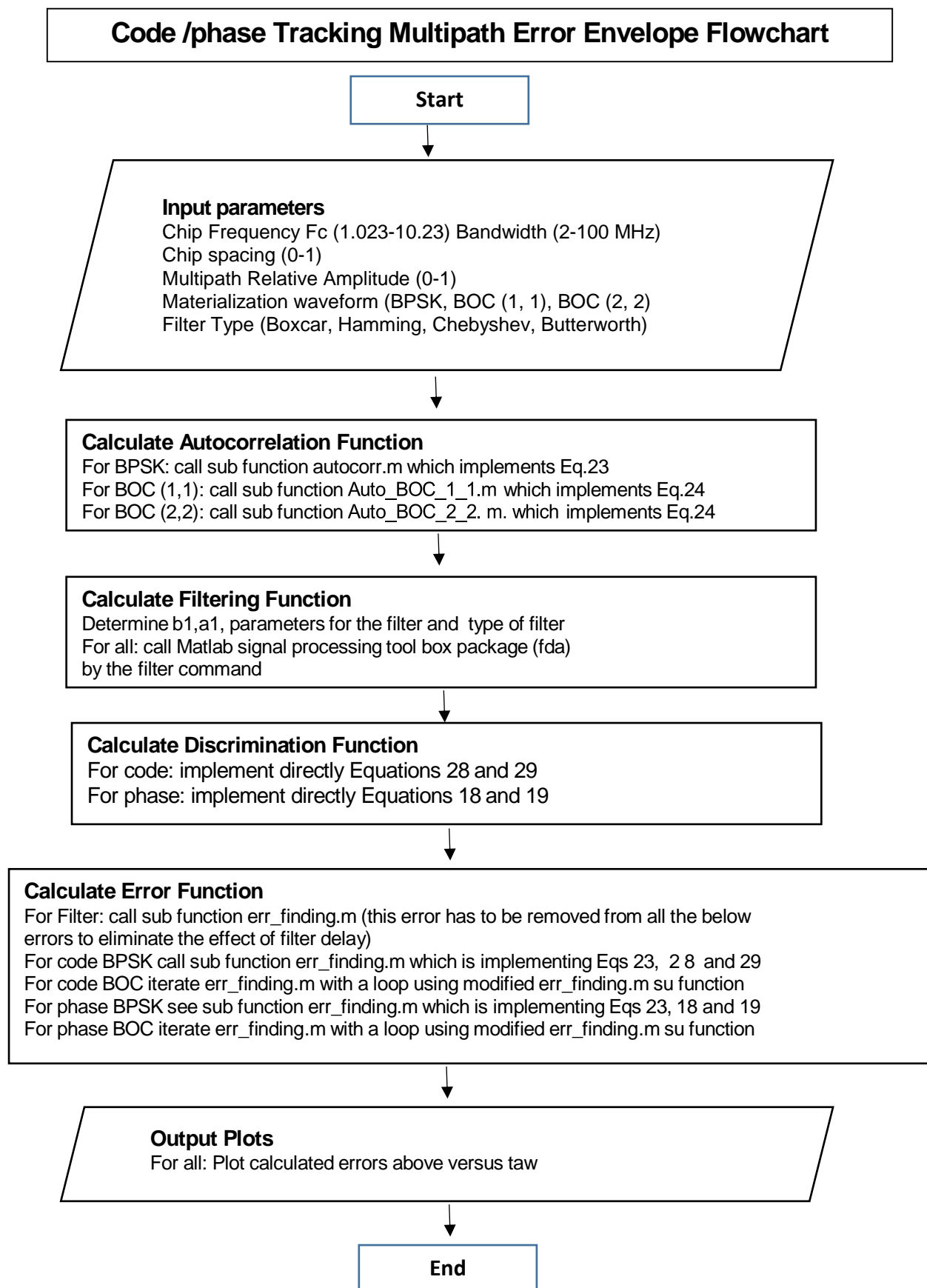


FIGURE 27: ERROR FINDING FUNCTION AND ENVELOPE ERROR FLOWCHART [EDITED BY AUTHOR]

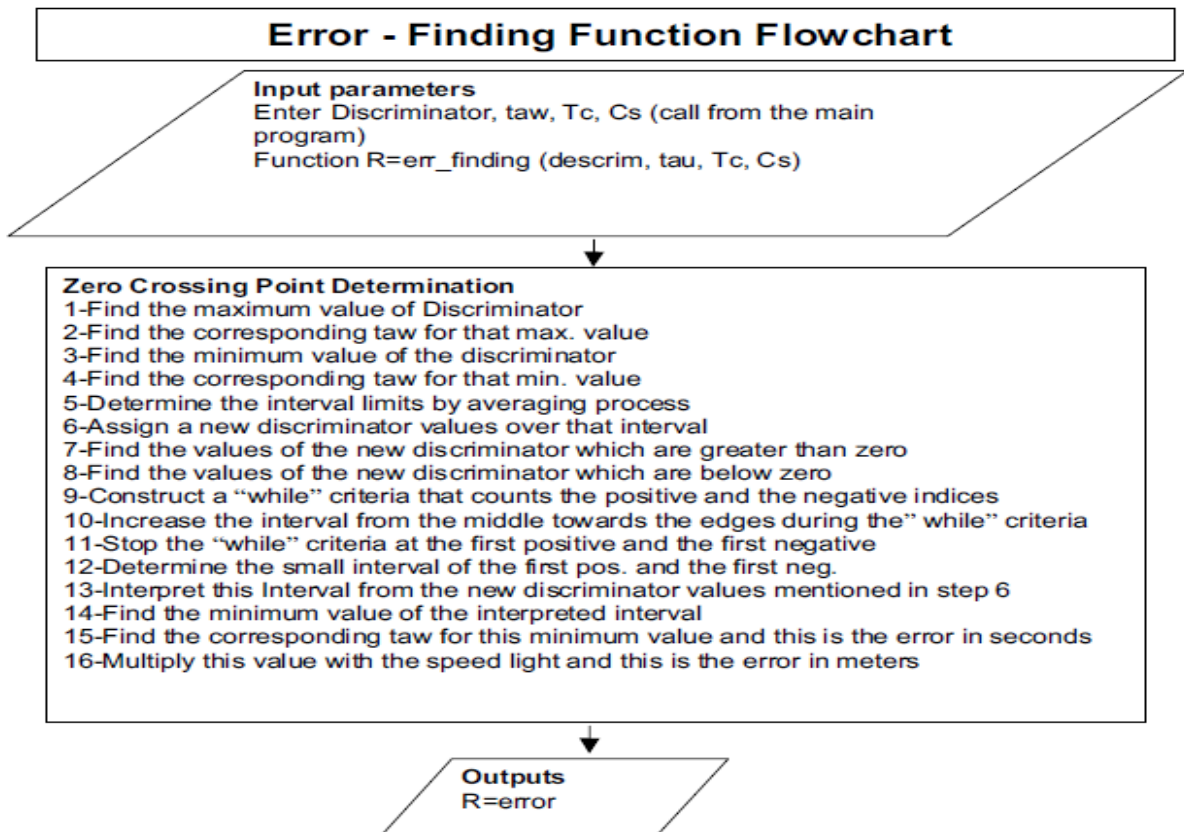


FIGURE 28: ERROR – FINDING FUNCTION FLOW CHART [EDITED BY AUTHOR]

This error finding sub function mentioned above is designed for the BPSK waveform only, it can work properly if there is one zero-crossing point of the discriminator with τ axis, but in the case of BOC signals where there are more than one zero-crossing point with the τ axis, another algorithm is used, it is almost the same with some differences in the way of prediction of the zero-crossing points. However, both algorithms are working very well for the code multipath error envelopes after being validated as it will be explained in the next section. For the phase multipath error envelopes, the above algorithm works well also, but the modified BOC modulation needs more improvements and validations, so the phase envelopes for both BPSK and BOC were skipped for future work. Furthermore, due to the fact that the BOC waveform modified error finding algorithm needs to be iterated many times to determine the zero-crossing point for BOC signals, it was difficult to work as external sub function, so it was better to include it within the main program code lines. In addition, other sub functions are

directly accessing the implementation of the equations that are already mentioned in the theoretical part and according to the main algorithm above. So they can be easily understood from the code lines directly.

4.6 Program Validation Compared with Similar Software

Actually, our software was validated against similar software done by a worldwide publication paper submitted by Dr. Braasch [Braasch, ION 59th, 2003]. He has used 4 cases of interest in the carrier-phase multipath error envelope:

- Standard correlator spacing ($C_s=1$), with Relative amplitude (M/D) = -2dB.
- Narrow correlator spacing ($C_s=0.1$), with Relative amplitude (M/D) = -10dB.
- Standard correlator spacing ($C_s=1$), with Relative amplitude (M/D) = -2dB.
- Narrow correlator spacing ($C_s=0.1$), with Relative amplitude (M/D) = -10dB.

In which M/D : is the Multipath to Direct ratio in dB, but we have converted his M/D in dB values to relative delay ratios under the assumption that Braasch had used:

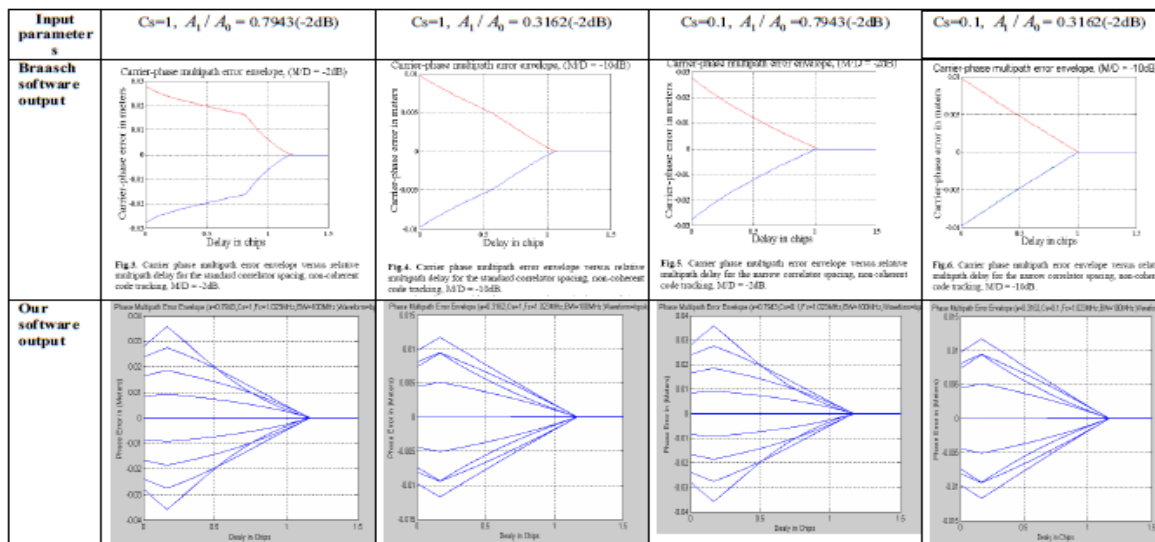


FIGURE 29: COMPARISON WITH SIMILAR SOFTWARE [EDITED BY AUTHOR]

$$\frac{M}{D} (dB) = 10 \log \left(\frac{A_1}{A_0} \right)^2, \text{ So, } \frac{A_1}{A_0} = 10 \left[\frac{M/D (dB)}{2 \times 10} \right] \quad \text{EQUATION 41}$$

M: is the Multipath reflected signal amplitude, this is Equivalent to 1 A in our notes and D: is the direct signal amplitude, this is equivalent to 0 A in our notes. So, for $M/D = -2 \text{ dB}$, $A1/A0 = 0.7943$ and for $M/D = -10\text{dB}$, $A1/A0 = 0.3162$ to be applied in our software, figure 29 above, and comparison as follows:

Similarities: Nearly the same output in terms of envelope shape, that's both, have decreasing error with increasing in tau. In addition, both has the same maximum carrier-phase error for the same input parameters taking onto account our software plots more than one curve.

Differences: The knee point takes occur at $\tau = 0.8$ chips in Braasch curves, but in ours at $\tau = 0.2$ chips, and as chip spacing decreases his curves goes smoothly, but ours still has the same knee at the tau. Justifications: It could be that Braash's curves are plotted according to the approximation formulas not the exact ones that we have used.

4.7 Result Analysis

4.7.1 Chip Spacing and Relative Amplitude

The software could be used to any values, but we have taken into account the following parameters assumptions: Varying the chip spacing into two values for the BOC (n, n) and BPSK waveforms: In which both Standard Correlators $C_s = 0.3$, and Narrow correlators $C_s = 0.1$. and the relative amplitude value: $\alpha = 0.1$, in which the first assumption was chosen to be comparable with the other studies and to be compatible with the existing correlators.

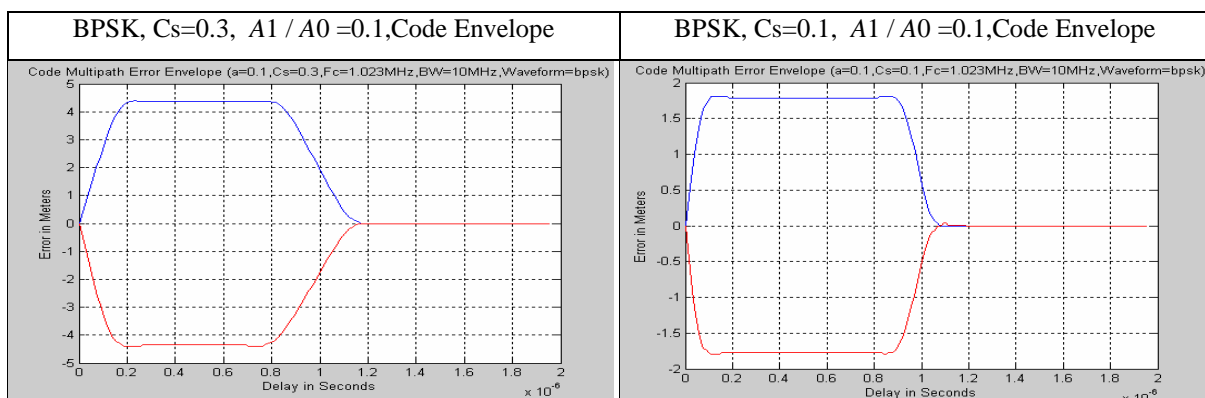


FIGURE 30: BPSK, CODE MULTIPATH ERROR ENVELOPES [EDITED BY AUTHOR]

Results analysis: Using the BPSAK waveforms, figure 31 above, the chip spacing and the relative amplitude are the key factors in multipath error reduction, when they decreased, the multipath error decrease as shown in the figure 31 above, the Reduction of 0.2 chip spacing (from 0.3 to 0.1) causes the multipath error to be decreased to more than the half.

4.7.2 Materialization waveform type: BPSK, BOC (1, 1), and BOC (2, 2)

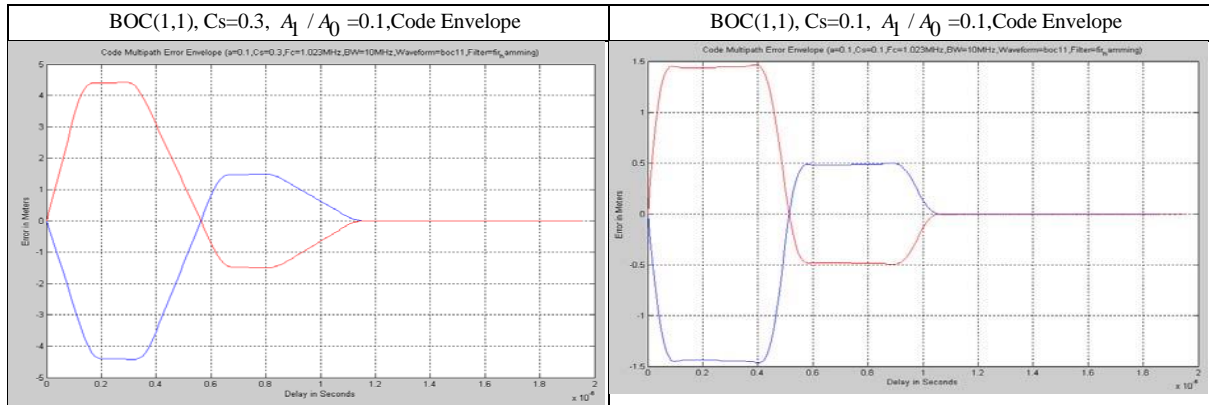


FIGURE 31: BOC (1, 1), CODE MULTIPATH ERROR ENVELOPES [EDITED BY AUTHOR]

Results analysis: Using the BOC (1, 1) waveforms, as well as BPSK, the chip spacing and the relative amplitude are the key factors in multipath error reduction, when they are decreased, the multipath error decrease as shown in the figure 32 above, the curve starts as BPSK curves then it crosses the zero in nearly $C_s/2$, then ends as the BPSK curve again. The reduction of 0.2 chip spacing (from 0.3 to 0.1) causes the multipath error to be decreased to more than one half, also the same can be said for the relative amplitude knowing that the relative amplitude is not controllable factor. The multipath error nearly negligible after the (1) chip delay.

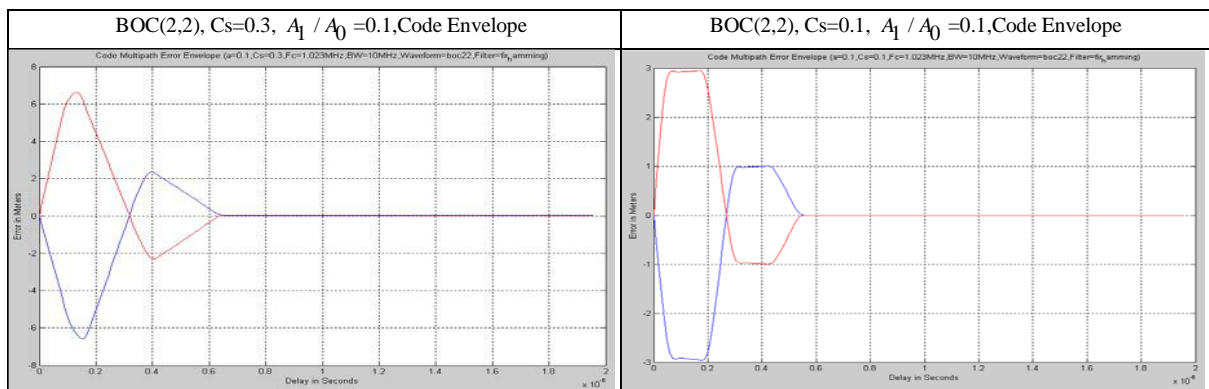


FIGURE 32: BOC (2, 2), CODE MULTIPATH ERROR ENVELOPES [EDITED BY AUTHOR]

Results analysis: Using the BOC (2, 2) waveforms, as well as BPSK and BOC (1, 1), the chip spacing and the relative amplitude are the key factors in multipath error reduction, when they decreased, the multipath error decrease as shown in the figure 33 above, However, Reduction of 0.2 chip spacing (from 0.3 to 0.1) causes the multipath error to be decreased to more than the half. The multipath error nearly negligible after the (0.5) chip delay. In addition, the error envelope consists of two parts: the first one overlaid the first half of the affected chip delay with a value near to the achieved one in BPSK, but during the second half period the error is reduced to less than the half for all selected parameters, and this the improvement added by the BOC signals in general.

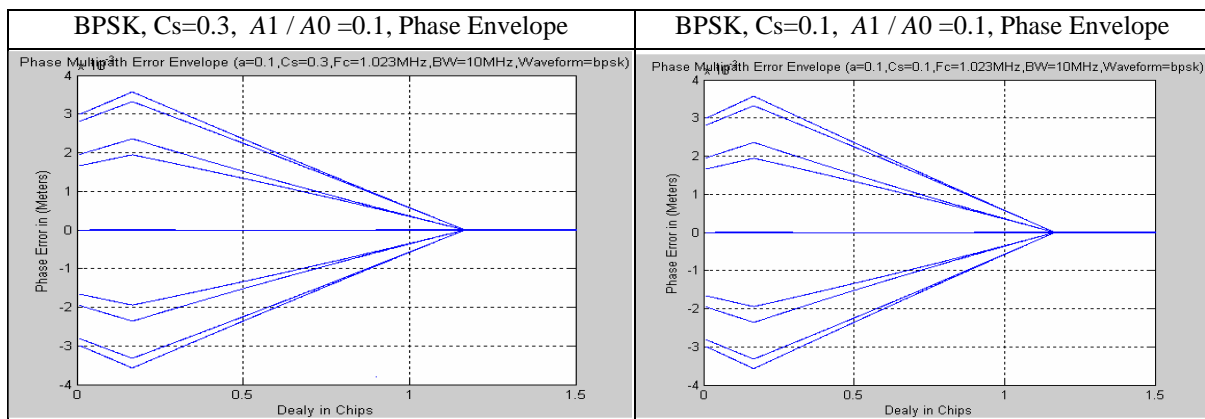


FIGURE 33: BPSK, PHASE MULTIPATH ERROR ENVELOPES [EDITED BY AUTHOR]

Results analysis: Using the BPSK waveforms, the relative amplitude is the key factors in multipath error reduction, when it decreased, the multipath error decrease as shown in the figure 34 above, but the chip spacing no more has influence on the multipath error reduction in the phase measurement. The multipath error nearly negligible after the (1) chip delay. The multipath error is less than 1 cm in its highest value, the curve as mentioned previously has a knee (change) around $\tau = 0.2$, then it decreases dramatically towards the zero crossing point at 1.2 chip delay.

4.7.3 Filter type Impact

In order to show the filter type impact, we have chosen 4 types of filters; the impact of filter on the discriminator is falling in two areas:

- The amplitude reduction due to the window cut of the minor lobes in the signal.
- The induced delay of the discriminator which will be added to the multipath delay also.

The actual filters used in the GPS type are of the type of FIR (Finite Impulse Response) which they are in less impact on the discriminator. The developed software shows these effect in separate figures displayed before the final error envelopes, and then the impact of the filter is calculated in terms of delay in seconds and removed from the final calculation of the multipath error, which the real case in GPS receiver, that means once the filter delay is known, then it can be removed. However, any type of the produced Matlab filter can be used by changing only the a_1 and the b_1 parameters according to the used one. So, the final delay will be only:

$$\text{FINAL DELAY} = \text{THE PROPAGATION DELAY (PSEUDORANGE)} + \text{THE MULTIPATH DELAY} - \text{FILTER DELAY} \quad \text{EQUATION 42}$$

Sometimes there are ripples in the error envelopes due to the filter type used. This can also be removed by changing to the most appropriate type of filters. Anyway, the impact of filter is beyond of the domain of this study but it was advised to be mentioned as subtitle for completeness, the impact of the filter on three cases: the Impact on the multipath error envelopes (see figure 35 below), the Impact on the Discriminator delay (see figure 36 after), and the Impact of the filter band width on the envelope (see figure 37 after)

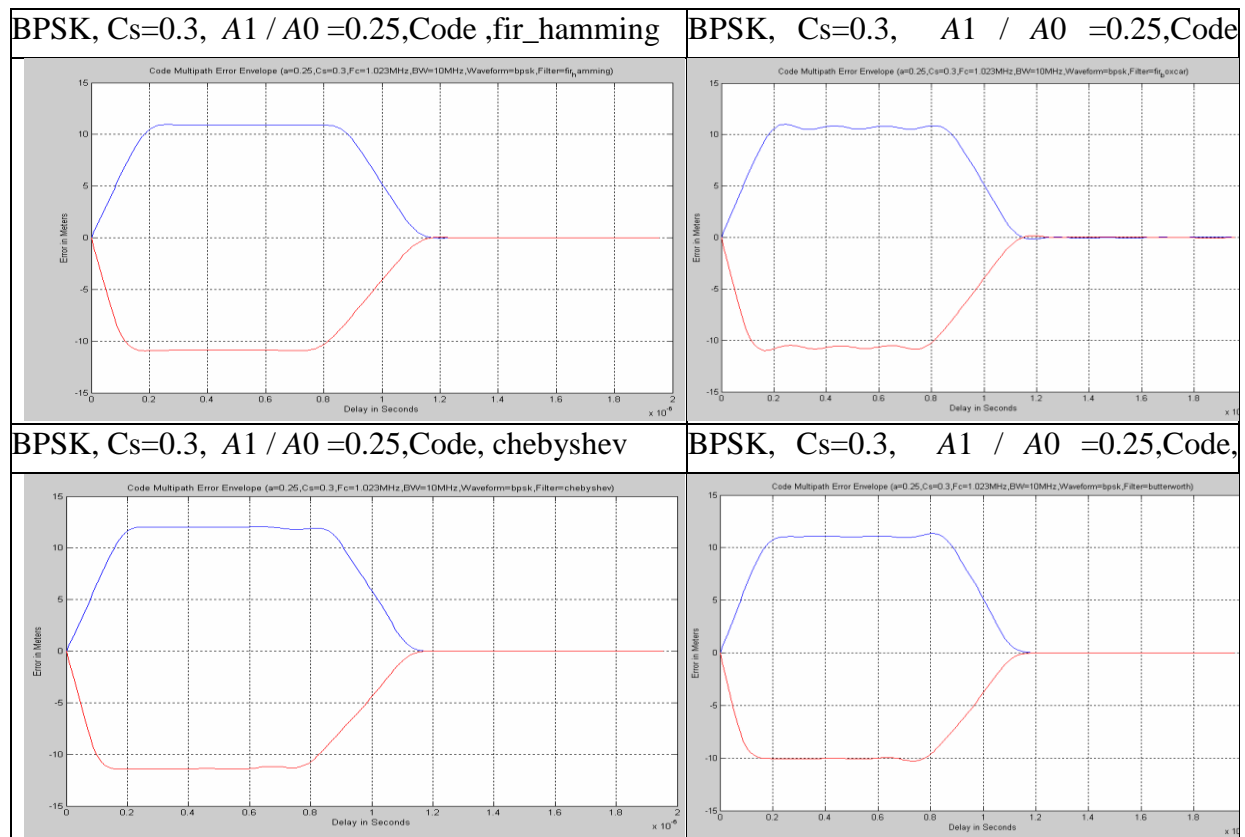


FIGURE 34: BPSK, CODE MULTIPATH ERROR ENVELOPES/DIFFERENT FILTERS [EDITED BY AUTHOR]

Figure 34 above shows the impact of the filters on the multipath error envelope for the same set of parameters, it clear that some types of FIR filter could cause ripples in the envelope and others didn't, but mainly all the used filters are close to each other in terms of error magnitude.

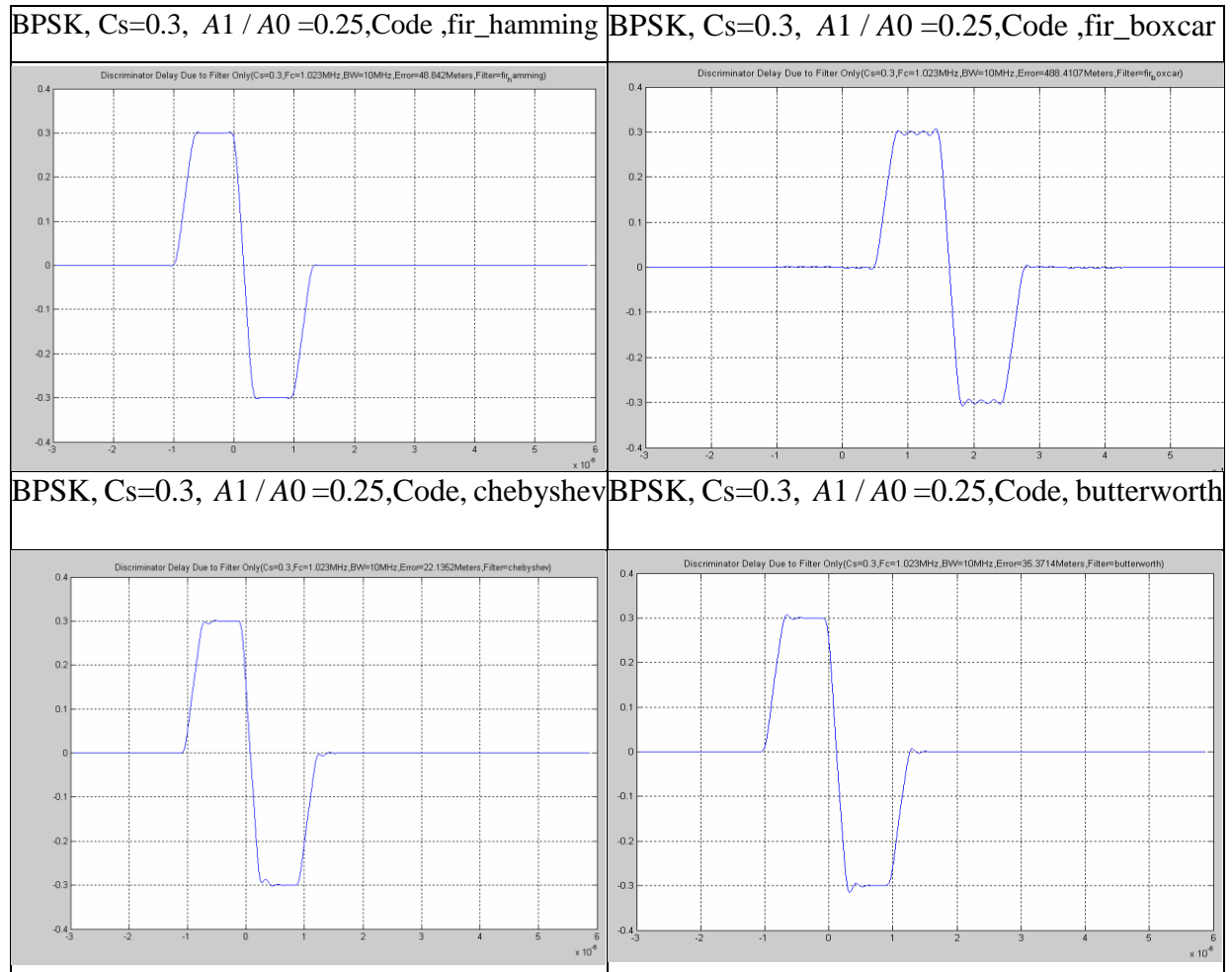


FIGURE 35: BPSK, DISCRIMINATOR DELAY DUE TO FILTER [EDITED BY AUTHOR]

Figure 35 above shows the induced delay (in meters) on the discriminator due to the filter type, the least one is the Chebyshev, and the largest one is the boxcar, for the same set of parameters. And figure 36 below shows the impact of the bandwidth on the multipath error and it clear that the large bandwidth the less error up to the 10 MHz, then the error seems to be fixed but the envelope gets close to the ideal theoretical curve.

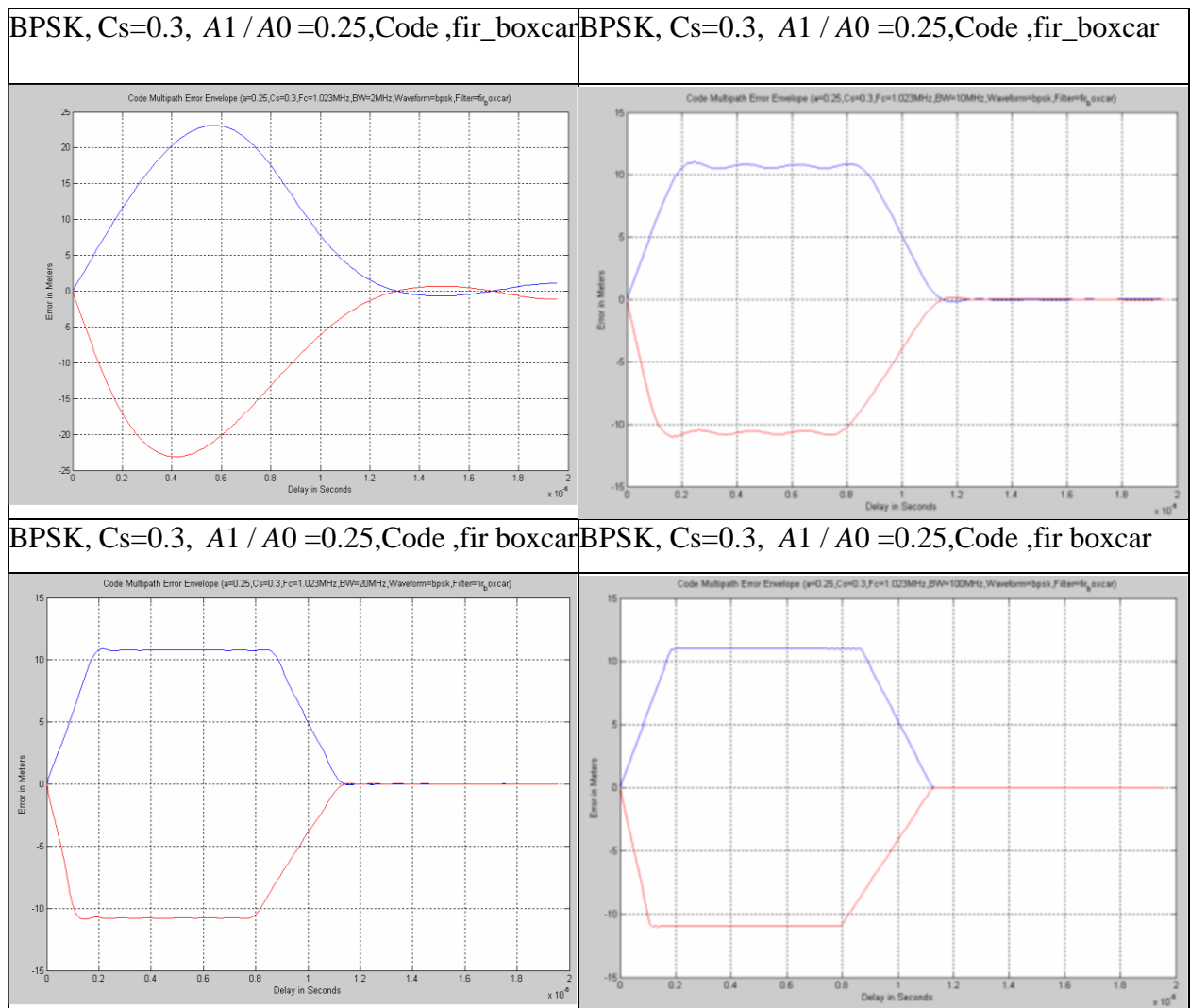


FIGURE 36: BPSK, IMPACT OF THE FILTER BANDWIDTH [EDITED BY AUTHOR]

4.8 Conclusions and Recommendations

In this chapter, the developed new software in Matlab language which was based on the theoretical bases of the signal processing of the receiver, was validated and tested, then it was applied as a simulating tool for the key factors that control the multipath error in the tracking loops, a new BOC signals was implemented in the software for the code tracking loops, with different types of filters. The relative amplitude is the key factor in decreasing the multipath error in the phase tracking error. The future BOC (2, 2) waveform impacts the multipath error in such a way that has the best performance among all, BOC (1, 1) has better performance than the currently used BPSK. The increase of bandwidth causes a decrease in the multipath error

to a certain limit. The type of filter used affects the multipath envelope with ripples. Finally, the software is capable to be modified and improved for more purposes due to its simple structure and its dependency on different sub function that can added easily according to the needed mission.

4.8.1 The New Achieved Scientific Result

The new scientific result # 2: I have developed a structural Matlab software of nearly 1000 code lines to assess the impact of the new BOC signals and filters on the MEE errors in the GPS receivers based on the theoretical multipath error equations, which is characterized being a new, validated, more comprehensive and more customized software than those being recently used by the Chinese researchers in 2020. It is more capable of being customized to assess any new GPS signal process analysis in the future.

4.8.2 Recommendations

I recommend to use this software for researches as it is capable to be customized and improved for more purposes due to its simple structure and its dependency on different sub function that can added easily according to the needed mission

Chapter 5: Impact of Electronic Attacks on GNSS / GBAS Approach Service Types C and D Landing systems and their proposed Electronic Protection Measures (EPM).

5.1 Introduction

As we have seen in the last two chapters, the unintentional errors contributed in lack of GBAS availability had been evaluated, tested and assessed. But in this chapter, the impact of the intentional imposed errors such as the Electronic Attacks on the GBAS landing system performance is examined and modelled, the used methodology was using modelling analogy to the multipath behave, then it was simulated and assessed. However, the Global Satellite Navigation Systems (GNSS) applications - using different satellite signals in space - are currently and hugely subjected to Electronic Attacks (EAs) such as Jamming, Spoofing, and/or Meaconing. Many accidents were observed in the past decade, while huge dependency on GNSS applications in governmental and private critical infrastructure, in both civil and military aspects. The EAs could be expensive and high-power such as the military-grade jammers, which are an integral pillar of navigation warfare (NAVWAR) strategies. On the other hand, EAs could be cheap and low-power such as the so-called Personal Protection Devices (PPD), which they are widely available. Electronic Attacks, most critically observed by ICAO and FAA, are in Ground Based Augmentation System -(GNSS/GBAS) Landing systems, in which is riskier and more critical than other applications due to the sensitivity of the final landing phase of all flights. The objective of this study is to evaluate the impact of the three different types of EA on the performance GNSS/GBAS landing system. On the other hand, to address and examine their latest proposed Electronic Protection Measures (EPM).

The EAs could be expensive, sophisticated and high-power such as the military jammers, which are an integral pillar of navigation warfare (NAVWAR) strategies. As other EW aspects, EAs are affecting the GNSS Position, Navigation and Timing (PNT) usage before and during any kinetic fight, Examples of such attacks were experienced in South Korea and Ukraine, in South Korea, GPS Signals were disrupted in many military aircrafts and ships between August 2010 and May 2013 by the deliberating Military-effect jammer from North Korea. In Ukraine, the Organization for Security and Cooperation in Europe (OSCE) has recently reported a military-grade GPS jamming on the UAVs missions, as the report (Novatel, 2015).

On the other hand, EAs could be cheap, low-power, and widely available such as the so-called Personal Protection Devices (PPD), which are been considered more and more frequently source of EAs; PPDs are small, light-weight jammers that are easily available in the internet market, their usage is forbidden in the majority of countries; but their possession is not regulated everywhere with the same strictness level. Examples of such attacks GBAS landing system at Newark Liberty International Airport/USA in 2012, when the certification process was disturbed by a truck jammer driving in a road nearby the airport as per Federal Aviation Administration (FAA) reported, (Novatel, 2015), (InsideGNSS, GNSS Jamming and Spoofing: Hazard or Hype?, 2018). And also reported in the Future Security Conference -7th in 2012, (ESA, Galileo_Future_and_Evolutions, The reference for Global Navigation Satellite Systems, 2018).

Electronic Attacks, most critically observed by International Civil Aviation Organization (ICAO) and Federal Aviation Administration (FAA), are in GNSS/GBAS Landing systems, which are used for final landing phase of flights in both civil and military aviation domains, or during military operations in deployed theaters. However, GBAS landing systems are satellite-based navigational aids used in Critical Meteorological Conditions (CMC), such as heavy dust and heavy fog, where the visibility tends to zero in the final landing of an aircraft, in which their loss of Service during the Final Approach Segment (FAS) is considered a catastrophic disaster to aviation safety-of-life in terms of assets, human and military operations. At those cases, capability of service restore on the proper time has very low probability. Its highly risker in such safety-of-life applications of landing systems when compared with other safety –critical infrastructure applications such as banking or non-critical applications of GNSS huge usages. Moreover, GBAS stations are usually located in a well-known surveyed reference sites in the vicinity of the airport near the runways. Which makes them more vulnerable to EAs, both the fixed ground reference stations and the downwind moving aircrafts when being landing close to runway surface.

It was observed a strong link between the concept of multipath and EAs, in terms of accumulating two or more signals at the receiving antenna in the so called technically interference. However, the over power jamming seems to be similar to the destructive multipath when the phases of the two signals are 180 degrees out of phase, assuming they were modulated and (authenticated) by the same navigation message of Position, Navigation and Timing (PNT). On other hand, spoofing/meaconing seem to be similar to the electronic deceptive side of the

multipath signal with long delay time of the original signal that GNSS receiver would be unable to correlate in proper time, that will mislead PNT information.

The objective of this research in this chapter is to evaluate the impact of the three different types of EAs (jamming, spoofing and meaconing) on the performance of GNSS/GBAS landing system. On the other hand, to address and examine the latest proposed Electronic Protection Measures (EPM) for such EAs, based on the three mitigation methods: the receiver-based mitigation methods, antenna-based methods and the siting-based methods.

The methodology used in this objective of research is the scientific analysis of the GNSS signal structure and signal processing, comparing EAs techniques versus Multipath effect by its nature of interference of the genuine signal, and finally using the results from a simulating tool applied in GBAS application to assess to which level this effect could be harmful. Those simulations were done over Europe including the main airports, with special concentration is focused on Liszt Ferenc International Airport in Budapest, Hungary. Followed by examining of the Electronic Protective Measures (EPM) being used to mitigate the signal damage/loss, which eventually cause at least the loss of service if not been electronically deceived.

5.2 Scientific Problem and the Observed Accidents/Deliberating

Firstly; EA threats could be professionally intentionally, using expensive, sophisticated and high-power such as the military-grade jammers. Those are considered an integral pillar of navigation warfare (NAVWAR) strategies. Many accidents were observed and had been reported to higher authorities and related organizations such as ICAO and FAA, but here the most two importantly are:

5.2.1 NATO military exercise on the 8th Nov 2018

During the NATO military exercise on the 8th Nov 2018, in Finland and Norway: navigation failure lead to collision of frigate with a tanker. There was collateral damage. Civilian airliners, cars, trucks, cargo ships and smart phones operating in and around experienced similar disruptions. The airline said its aircraft carried alternate navigation systems. A US defense official told CNN that the jamming had "little or no affect" on US military assets. (Seidel, 2018). This little or no effect is due using the military P/Y code that it's much more immune against jamming as it will be illustrated later in this study. The Norwegian frigate "KNM Helge Ingstad" suffered a navigation failure leading to a collision with the tanker "Sola TS" on November 8, 2018 in the Hjeltefjord near Bergen. Figure 37 below: AFP Source: AFP



FIGURE 37: THE NORWEGIAN FRIGATE SUFFERED NAVIGATION FAILURE [(SEIDEL, 2018)]

5.2.2 EAs in South Korea, Ukraine and USA

Secondly; EAs were experienced in South Korea and Ukraine: In South Korea, GPS Signals were disrupted in many military aircrafts and ships between August 2010 and May 2013 by the deliberating Military-effect jammer from North Korea. In Ukraine, the Organization for Security and Cooperation in Europe (OSCE) has recently reported a military-grade GPS jamming on the UAVs missions, (InsideGNSS, 2018). Furthermore; EAs could be unprofessionally intentionally occurred, using cheap, low-power, small, light-weight jammers. Those are widely available such as the so-called Personal Protection Devices (PPD). They are considered more frequently source of EAs, and easily available in the internet market, their usage is forbidden in the majority of countries. The most related accident to be addressed here is the GBAS landing system (Honeywell SLS-4000) which was approved by the FAA at Newark Liberty International Airport/USA in 2012 as CAT I (GAST C). While the certification process was disturbed by a truck jammer driving in a road nearby the airport as per FAA reported, (InsideGNSS, 2018) (Novatel, 2015). And also reported in the Future Security Conference -7th in 2012, (B. Hofmann-Wellenhof, 2001), [p 197]. As seen in the Figure 38 below, the airport is fully and closely surrounded by crowded traffic roads. This increased its GBAS vulnerability of being interfered or attacked. When the geographic vicinity of the Liszt Ferenc International Airport in Budapest Hungary is compared with Newark Airport, as seen in Figure 39 below after, its little better but not significantly much differ from. The nearest road is about 350 meters from any of the two proposed suggested sites of any future GBAS system would be installed in.

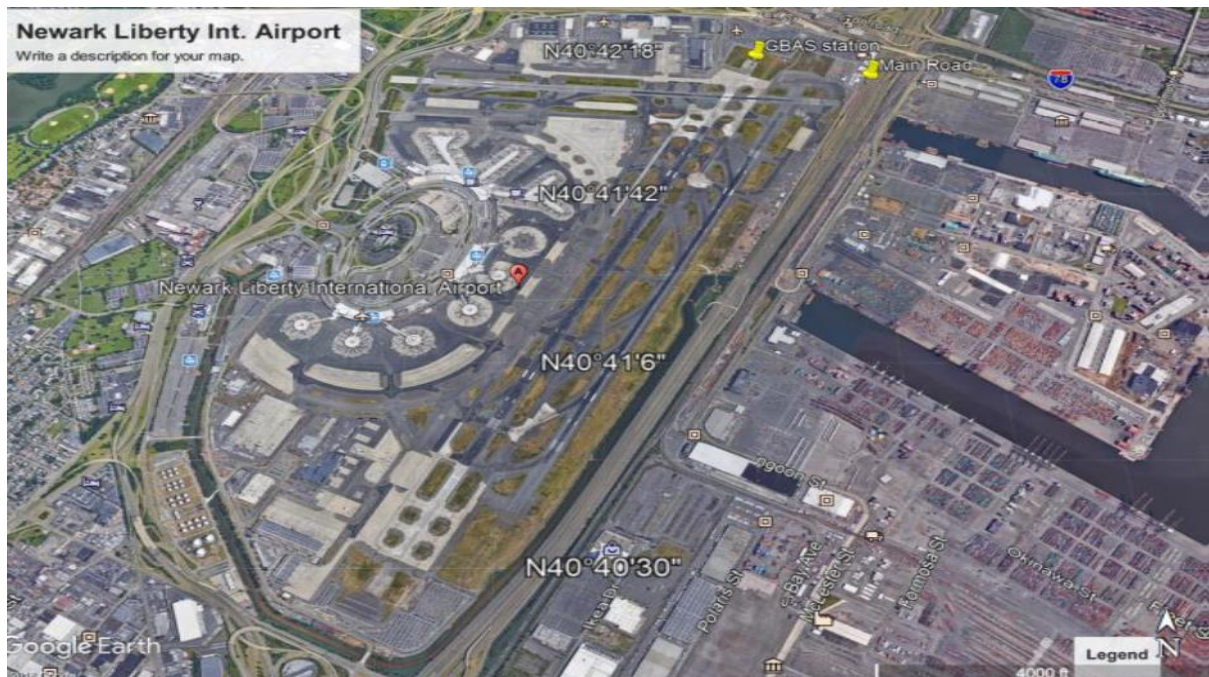


FIGURE 38: NEWARK AIRPORT LAYOUT (EDITED BY THE AUTHOR)



FIGURE 39: LAYOUT OF LISZT FERENC AIRPORT AT BUDAPEST (EDITED BY THE AUTHOR)

The real scientific problem is not only the citing criteria, but also that the GNSS signals are so vulnerable to EAs because of their extremely low level of power density, satellites transponders' are orbiting about (22,000 Km) above the Ground level, and they are transmitting their signals via Troposphere and Ionosphere layers, so that the signals arrive the earth surface to users in a weak signal to noise ratio, around -160dBw for GPS L1, - 154dBw for GPS L2 (Military), Speculated -155dBw for Galileo E1/E2). The other part of the problem is that capability of service restore on the proper time has very low probability. It's so high risky in safety-of-life applications of landing systems when compared with other safety –critical infrastructure applications such as banking or non-critical GNSS applications. Furthermore, GBAS stations are usually located in a well-known surveyed reference sites in the vicinity of the airport near the runways. Which makes them more vulnerable to EAs. Anyhow, currently GBAS systems are hardly achieving CAT I/GAST C performance, only due to other system errors originally invoked by other than interference or EAs.

Finally, EAs could be unintentionally, such as some GNSS bands are shared with certain radars, amateur radio. Other sources are Distance Measuring Equipment (DME). Also the TV harmonics, malfunctioning electronic equipment.

5.3 GNSS/GBAS Signal Structure w.r.t Electronic Warfare

In the concept of Electronic Warfare (EW), the Electronic Attack (EA) is defined as the use of the electromagnetic energy, directed energy, or anti-radiation weapons to attack personnel, facilities, or equipment with the intent of degrading, neutralizing, or destroying enemy combat capability and is considered a form of fires. Electronic attack includes reducing an enemy's effective use of the electromagnetic spectrum, the use of either electromagnetic or directed energy as a primary destructive mechanism, and the use of countermeasures, (FieldManual(FM)-3-36, 2012). Electronic warfare is integrated and synchronized with lethal fires in order to disrupt and increase the enemy's decision making reaction time. It supports friendly forces with different kinds of information about the enemy's electronic systems. Electronic countermeasures can be offensive or defensive. Offensive activities are generally conducted at the initiative of friendly forces. Defensive electronic countermeasures protect personnel, facilities, capabilities and equipment. Including communications systems such as wireless networks, cyberspace networks and radios, as well as the non-communications systems such as radars, Air Traffic Control and navigation, etc., (Haig, 2015).

EW's produces NAVWAR effects by protecting or denying transmitted global navigation satellite system (GNSS) or other radio navigation aid signals. EA is used to create NAVWAR effects by degrading, disrupting, or deceptively manipulating positioning, Navigation, Timing (PNT) transmissions. Electronic Support Measures (ESM) assist NAVWAR through DF and geolocation of intended or unintended transmissions that interfere with effective and timely PNT signal reception. EPM is used to deliver NAVWAR capabilities protecting space, control, or user segments of the GPS/GNSS architecture from disruption or destruction. (FieldManual(FM)-3-36, 2012).

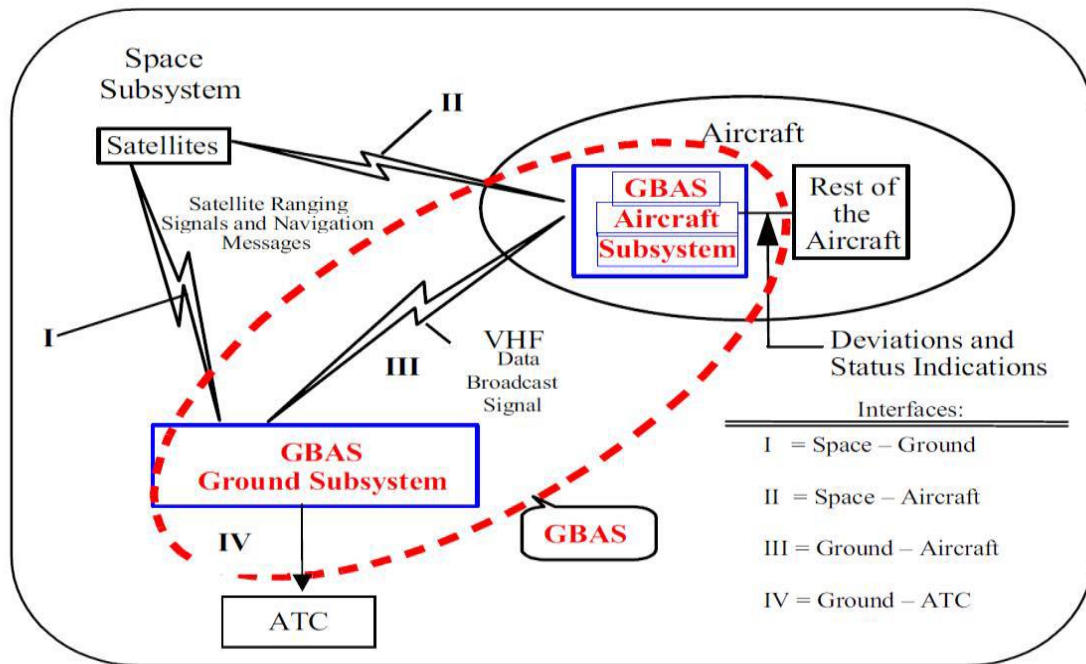


FIGURE 40: GBAS SYSTEM LINKS, [EDITED BY AUTHOR]

In GBAS landing systems, there are four types of links, shown in Figure 40 above (repeated figure for simplicity of referring):

- Space- Ground GBAS Downlink, with weak GNSS signal (Currently GPS): S/N is -160dB. It's more vulnerable to EAs due to fixed position. The GPS errors included are: Ionosphere, Multipath, Rx, hardly achieving GAST-C (CAT I) performance of 99.74% A_p . Moreover, Electronic protection techniques as LPI, is used such as spreading the spectrum and antenna based but still experienced accidents.
- Space – Aircraft Downlink: It's also a weak GNSS signal (Currently GPS): -160dB. And it's less vulnerable to EAs due to mobile dynamic position, due to higher altitude about at least 200 feet above ground level makes it more immune to ground jammers but not UAVs based ones. Furthermore, using Up-looking MLA GPS Antenna somehow mitigates interferences. GPS errors: Ionosphere, Multipath, Rx, hardly achieving GAST-C (CAT I) performance of 99.74% A_p . The Electronic Protection Techniques as LPI, is used as well, such as spreading the spectrum and antenna based but still experienced accidents.

- Ground – Aircraft Uplink: it's a Protected VHF link carrying the continuously sent integrity and corrections messages. It's characterized by its higher power to noise S/N, so more immune to EAs.
- Ground – ATC Link: which is a secured land lines that nit in the scope of EW electromagnets attacks. And really doesn't affect the operation of the system as it informative link to ATC about the health status of the system.

At the satellite transponder side, which is the space segment, the GPS signal structure is sent by the satellites Space Segment, (B. Hofmann-Wellenhof, 2001)[p77], consists of Two Carrier Frequencies (L1 and L2) and Two codes, both characterized by a pseudorandom noise (PRN) sequence Figure 41+42 below. The first is the course/acquisition or (clear/access) code (C/A-code). It has the frequency $f_0/10$ and is repeated every millisecond. The codes of the two registers are not classified, and the C/A-code is available to civilian users. The other code is the precision (or protected) code (P-code). It has the frequency f_0 and is repeated approximately once every 266.4 days. It is also not classified, but the P-code is encrypted to the Y-code by Anti spoofing (A-S). Since the Y-code is the sum of the P-code and the encrypting W-code, access to the P-code is only possible when the secret conversion algorithm is known, so its jamming immunity is better. A third code called the W-code is used to encrypt the P-code to the Y-code when A-S is implemented. The coding of the navigation message requires 1500 bits and, at the frequency of 50 Hz, and it's transmitted in 30 seconds.

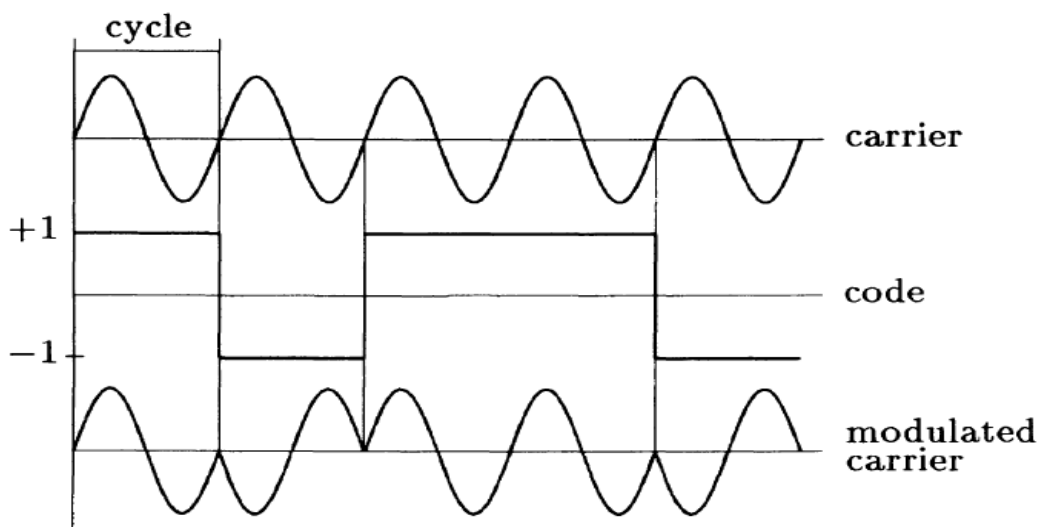


FIGURE 41: GPS CODING STRUCTURE [(B. HOFMANN-WELLENHOF, 2001)]

Component	Frequency (MHz)	
Fundamental frequency	f_0	= 10.23
Carrier L1	$154 f_0$	= 1575.42 ($\hat{=}$ 19.0 cm)
Carrier L2	$120 f_0$	= 1227.60 ($\hat{=}$ 24.4 cm)
P-code	f_0	= 10.23
C/A-code	$f_0/10$	= 1.023
W-code	$f_0/20$	= 0.5115
Navigation message	$f_0/204\,600$	= $50 \cdot 10^{-6}$

FIGURE 42: GPS SIGNAL COMPONENTS [(B. HOFMANN-WELLENHOF, 2001)]

Pseudo Random Noise Codes PRN is the generation of the PRN sequences in the codes and it is based on the use of hardware devices called tapped feedback shift registers. While the Navigation Message essentially contains information about the satellite health status, the satellite clock, the satellite orbit, and various correction data. Moreover, it contains the predicted satellites orbital elements (broadcast ephemerides) necessary to compute satellite coordinates in WGS84 system, and directly used to process receiver coordinates. It's subdivided into five sub-frames, each sub-frame is transmitted in 6 seconds and contains 10 words with 30 bits. More details about GPS signal structure are found in (B. Hofmann-Wellenhof, 2001).

In general, GNSS world includes four main satellite systems, the USA GPS system, the Russian GLONASS system, the European Galileo system, and the Chinese Beidou System. There are differences in signal structure among them, but they used the same principle of producing the position, velocity and time (PVT) solution to the different users. More detailed information about differences in signal structure and performance for GPS, GLONASS and the Galileo systems can be found in (Bernd Eissfeller, 2007). The new European Global Navigation System Galileo is not fully operational yet. It is anticipated to be in Full Operational Capability (FOC) in 2024 if not beyond. More details about the three main phases of Galileo navigation project in (ESA, Galileo_Future_and_Evolutions, 2018). Moreover, GLONASS system uses different

frequencies and different modulation scheme. On the other hand, China has launched their Beidou navigational system but not globally, it is up to date a regionally covering the far-east region only, (B. Eissfeller, 2007). Figure 43 below shows a new projected GNSS signals structure.

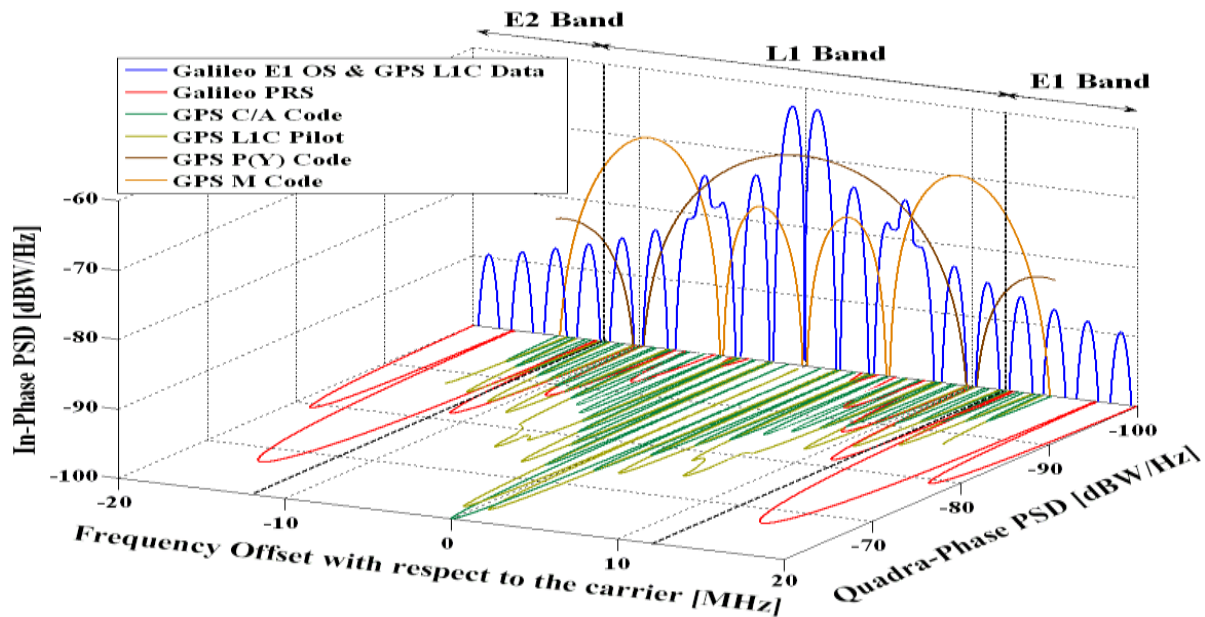


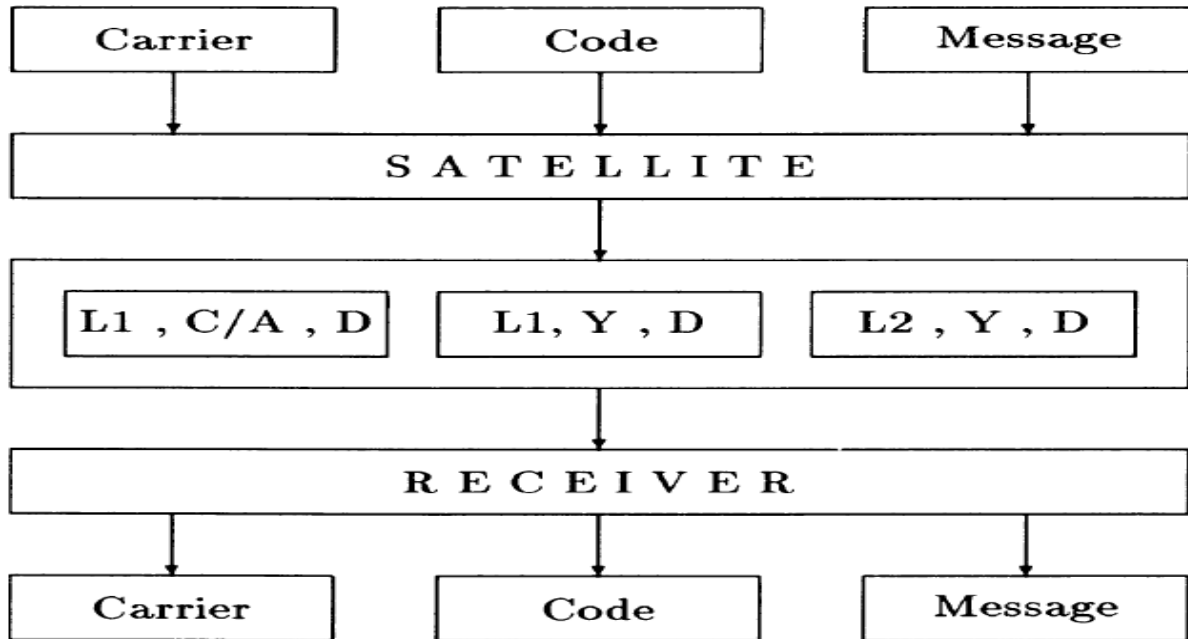
FIGURE 43: NEW MODERN GNSS SIGNAL STRUCTURE [(B. EISSFELLER, 2007)]

All the GPS receivers uses fixed-tuned receiver type because the satellites within the 24/29 GPS constellation are broadcasting at the same frequency. But with spreading codes that allow selection of one satellite's signal by a receiver, or a channelized receiver. The Direct Sequence spread Spectrum DSS is used in both the BPSK modulation scheme and the Galileo BOC modulation scheme as basic LPI technique, (Adamy, 2009)[p 84].

5.4 GNSS/GBAS Signal Processing w.r.t Electronic Warfare

At the receiver side, which is mainly the ground segment (here in GBAS system the ground station or the Aircraft receiver), the carrier, code and the navigation message is decoded and demodulated to form the useful information of the PNT using the code correlation techniques. Such as: Code correlation narrow and wide, squaring technique, Cross correlation technique, Code correlation plus squaring technique, and the Z-tracking technique. The Data Acquisition

is done by: Either the Code pseudorange in which the precision of roughly 3 m and 0.3 m is achieved with C/A-code and P-code pseudorange respectively. Or the Phase pseudorange: can



be measured to better than 0.01 cycles which corresponds to millimeter precision, (B. Hofmann-Wellenhof, 2001) [p83]. See Figure 44 below.

FIGURE 44: GPS SIGNAL PROCESSING FLOWCHART [(B. HOFMANN-WELLENHOF, 2001)]

Code	Strength reduction		Technique	dB
	at L1	at L2		
C/A-code	-156 to -160	-	Squaring	-30 dB
Y-code	-159 to -163	-162 to -166	Cross correlation	-27 dB
			Code correlation plus squaring	-17 dB
			Z-tracking	-14 dB

TABLE 18: S/N RATIO AGAINST EAS IN CORRELATION TECHNIQUES [(B. HOFMANN-WELLENHOF, 2001)]

Comparing the S/N ratio with respect to different correlation techniques in terms of the used EPM of the DSSS signal, the Z-tracking is the strongest among them against EAs. Table 18 above. These receiver-based techniques of data acquisition are not only used to retrieve the useful information of PNT, but also considered mitigation methods of interference or EAs if intentionally invoked. Even though they are not so efficient if the taking into consideration the

occurred accidents mentioned previously. However, the new signal structure and the new signal processing in Galileo and the modernized GPS are hopefully will add another value in receiver based mitigation methods.

5.5 Impact of EAs on GNSS/GBAS Using Multipath Approach

The well-known EAs types are classified technically into three main categories. They could be spot or chirp or swept or continuous wave affect. Depending on their utilizing of frequencies coverage and electromagnetic power density over those frequencies. (InsideGNSS, GNSS Jamming and Spoofing: Hazard or Hype? , 2018), (Adamy, 2009):

5.5.1 Jamming

It's the Intentional interference deliberate radiation of electromagnetic signals at GNSS frequencies. The aim is to overpower the extremely weak GNSS signals so that they cannot be acquired and tracked anymore by the GNSS receiver. They cause loss of LOCK (Destroy/ Neutralizing). And as said they could be Military grade jammers dual band, denial system, 10km-150 km or PPDs: civilian, dual band, with range of 30-350 Km. Figure 45 below.



FIGURE 45: PPDs LOW POWER WIDELY AVAILABLE [(INSIDEGNSS, GNSS JAMMING AND SPOOFING: HAZARD OR HYPE?, 2018)]

5.5.2 Spoofing

It's the generation and transmission of fake GNSS signals. The aim to lead a GNSS receiver astray (Deception), possibly without the GNSS receiver being aware of the attack. Technically they are more challenging than jamming, according to the complex GNSS signal structures especially for several GNSS signals in parallel (InsideGNSS, GNSS Jamming and Spoofing: Hazard or Hype? , 2018)

5.5.3 Meaconing

It's the little brother of spoofing, it is the re-transmission of received GNSS signals (Deception). This avoids the burden of implementing the generation of the complex GNSS signal structures. Also it causes the GNSS receiver to provide erroneous PNT information, because the reception and re-broadcast process changes the relative delays of the GNSS signals as seen by the receiver, compared to the relative delays of the authentic GNSS signals at the receiver's location. (InsideGNSS, GNSS Jamming and Spoofing: Hazard or Hype? , 2018)

In general, The Model of Jamming in EA for any communication system including GNSS down links, [(Adamy, 2009), p 253] is given by equation 43 below:

$$J/S = ERP_J - ERP_S - L_J + L_S + GR_J - GR \quad \text{EQUATION 43}$$

Where:

J/S : the ratio of jammer power to the desired signal power (Here the received power *from* satellite) at the input of the receiver being jammed in dB

ERP_J : the effective radiated power of the jammer in dBm

ERP_S : the effective radiated power of desired signal transmitter (Satellite) in dBm

L_J : the propagation loss from the jammer to the targeted receiver (GBAS or Aircraft) in dBi

L_S : the propagation loss from the desired signal transmitter (Satellite) to the targeted receiver (GBAS or Aircraft) in dBi

GR_J : the receiving antenna gain (GBAS Antenna or Aircraft Antenna) in the direction of the jammer in dBi

GR: the receiving antenna gain (GBAS or Aircraft) in the direction of the desired signal transmitter (Satellite) in dBi

In comparison with Multipath phenomenon which is the propagation phenomenon that results in radio signals reaching the receiving antenna by two or more paths; in other words, it's an interference in its nature. (Alhosban A. , 2015). The multipath can be:

- Constructive (when the reflected phase angle is 0) \approx resemble the Spoofing and Meaconing (deceptive) in EA
- Destructive (when the reflected phase angle is 180) \approx resemble the brute force jamming (destroy) in EA
- Interference in terms of both amplitude varying and/or phase shifting \approx resemble both.

And it's given by the following equation 44:

$$r(t) = A_0 \cdot d(t - \tau_0) \cdot c(t - \tau_0) \cdot \cos(2\pi f_{L1} t - \theta_0) + A_1 \cdot d(t - \tau_1) \cdot c(t - \tau_1) \cdot \cos(2\pi f_{L1} t - \theta_1)$$

EQUATION 44

The equation is annotated with two blue brackets below it. The first bracket, labeled 'LOS/DIRECT SIGNAL', spans the first term: $A_0 \cdot d(t - \tau_0) \cdot c(t - \tau_0) \cdot \cos(2\pi f_{L1} t - \theta_0)$. The second bracket, labeled 'REFLECTED SIGNAL', spans the second term: $A_1 \cdot d(t - \tau_1) \cdot c(t - \tau_1) \cdot \cos(2\pi f_{L1} t - \theta_1)$.

Where:

$r(t)$ Is the received GPS signal at the antenna.

A_0, τ_0, θ_0 : are the amplitude , the propagation delay, and the carrier phase shift respectively of the direct signal. And A_1, τ_1, θ_1 : are for the one reflected multipath signal. The phase rate of change is assumed to be zero

Analyzing both equations in terms of power, time of action and data affect, the results, as seen in table 19 below, could be interpreted:

Parameter	EA (jamming, spoofing, meaconing) level	Multipath Interference level	Mitigation level
Power J/S	<ul style="list-style-type: none"> • Jamming CW • Jamming Chirp 	MP level A destructive at least	<ul style="list-style-type: none"> • CW by filtering almost negligible • Chirp is deceptive without Authentication • Loss of signal track and lock • Power level at receiver end
Time of action	<ul style="list-style-type: none"> • CW continuously during landing • Chirp depends on frequency scanning process 	<ul style="list-style-type: none"> • For fixed stations is continuously • For a moving aircraft is temporarily 	<ul style="list-style-type: none"> • By Signal structure • By power level at time of affect
Data affecting	Deceptive misleading information , degrading of availability of integrity and accuracy	High error , deceptive and degrading availability of integrity and accuracy	<ul style="list-style-type: none"> • By signal structure, receiver power level and coding. • P/Y code is more immune

TABLE 19: COMPARISON TABLE BETWEEN EAS AND MULTIPATH [EDITED BY THE AUTHOR]

The mitigation levels of the EAs in compare with Analogy of the Multipath Error can be categorized in three domains: the power level impact, the time of action impact, and the data effect impact, and as follows:

- Power level: The Continuous Wave (CW) and the chirp Jamming is look like in behave similarity the level (A) destructive signal in Multipath impact, its mitigation level controlled by filtering is almost negligible, the Chirp jamming is deceptive without Authentication, and would cause Loss of signal track and lock due to Power level reduction at receiver end.
- Time of action: the CW is continuously during landing and the Chirp depends on frequency scanning process, therefore it is look like affecting the fixed stations continuously, but for a moving aircraft is temporarily impact. Its mitigation is depending only by GPS Signal structure and by the power level at time of affect, so nothing can be done in this case if the new higher power +6dB new signals has not been used in the Galileo or the modernized GPS Block III.
- Data Affecting: The data would be deceived as a misleading information look like, which causes degrading of availability of integrity and accuracy of the GPS signal, that is look like occurrence of high error impact, deceptive impact and degrading information impact on the correlation process, Again, its mitigation would be the same as in time of action part, by signal structure itself, the power level at receiver, and the coding hardening. Therefore, the USA military P/Y code is more immune to data loss.

In order to analogy resemble the above impacts on GPS signals, the Airborne multipath model will be used, which modules the Airborne multipath Designator (AMD): is the Multipath level, 0 to 1 levels, the 1 level is the highest value and could be constructive or destructive depending the phase θ_i , (Alhosban A. , 2015). Going toward zero by $B = A/2$, or further $A/4$ resemble mitigation level optimistically depending on mitigation techniques for evaluation purpose of Impact on Availability using simulator tool, and it's given by the following equation 45:

$$RMS_{multipath}(\theta_i) = a_0 + a_1 \cdot e^{-\frac{\theta_i}{10}} \text{ EQUATION 45}$$

Where: i : Is the i^{th} ranging source

a_0 , a_1 , and θ_i are parameters determined by the table 20 shown below:

Ground Accuracy Designator (GAD)	θ_i (degrees)	a_0 (meters)	a_1 (meters)
Letter A	10	0.13	0.53
Letter B	10	0.065	0.265

TABLE 20: AMD PARAMETERS [(ALHOSBAN A. , 2015)]

Based on that, those parameters and assumption were run in a simulating tool, over some important areas over Europe:27E-9W&34N-62N and USA:65E-127E&23N-50N, the results also were compared with previous study within the same area but using different simulating tool, as shown in Figure 46 below, for the purpose of validation.

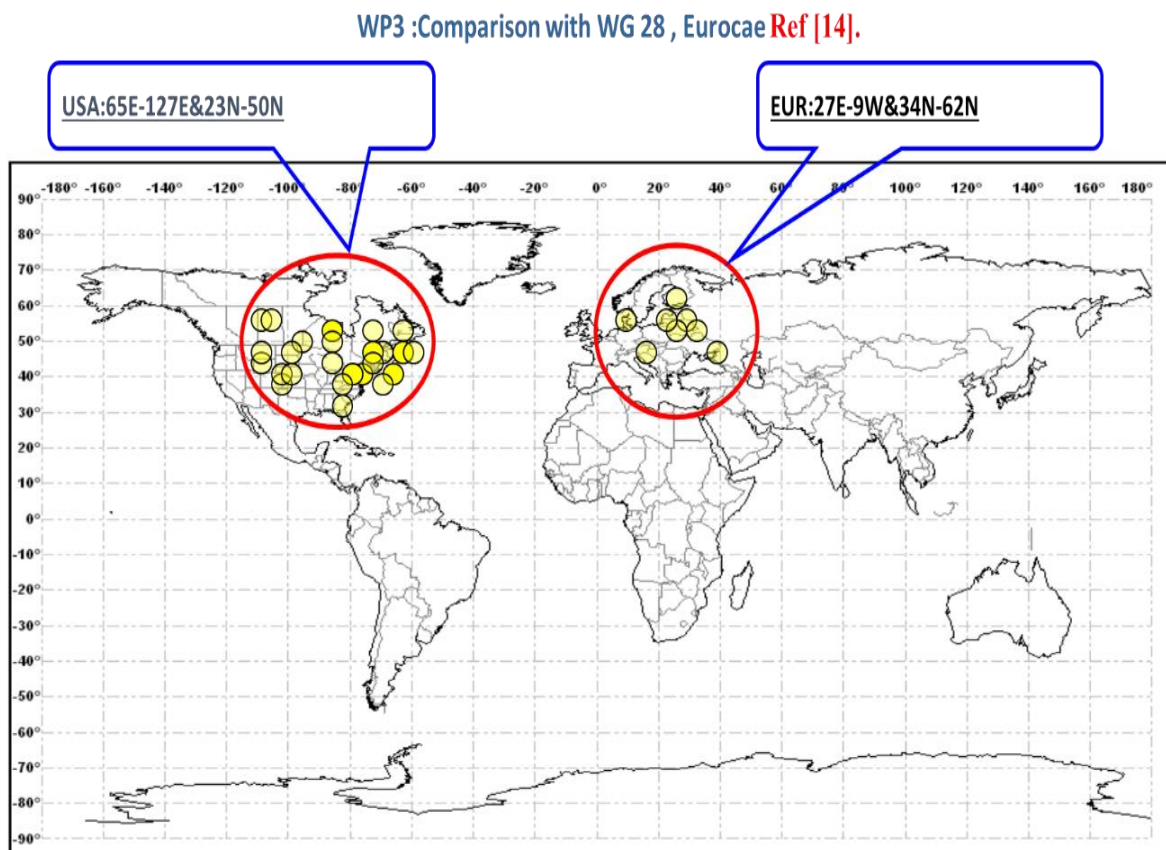


FIGURE 46: THE SIMULATED AREAS IN EUROPE AND USA [(ALHOSBAN A. , 2015)]

The Impact of the Analogy Multipath was examined against the GBAS availability to see to which mitigation level the CAT II/III can be achieved. And the results were as shown in Figure 47 below, (Alhosban A. , 2015).

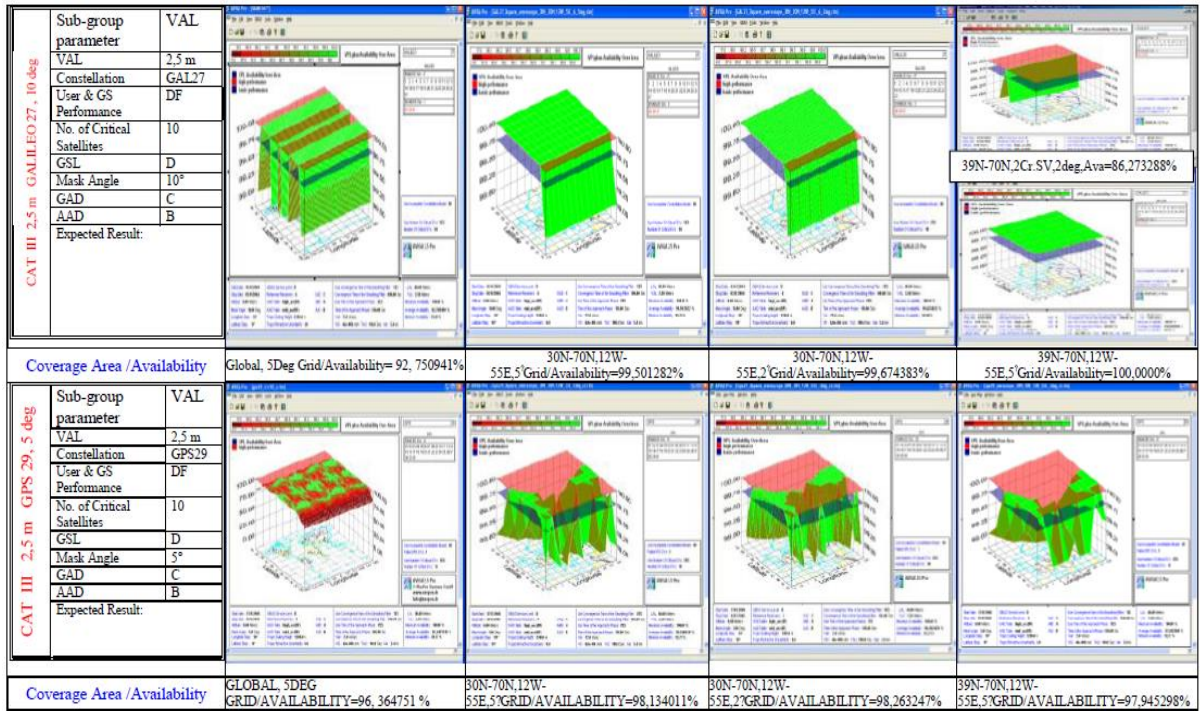


FIGURE 47: SIMULATION RESULTS [EDITED BY THE AUTHOR]

And they can be summarized as follows:

1. Due to the higher power level (+6dB) used in Galileo signal, and the new BOC signal modulation scheme, which is not the case in GPS signals, then, Galileo was able to meet the aeronautical requirements of both 99.99% and 99.75% over Europe with the given input parameters of the best GBAS configuration of CB-DF and for VAL= 2.5m (CAT III requirements), and it was very close (99.404%) over USA. But GPS signal was not able to meet these requirements.
2. GPS constellation is not guaranteed, this means that the green spot of good availability is continuously moving and cannot be assured over a certain geographic area like a specific airport for example, while we can warrantee that using Galileo Constellation.

3. Galileo constellation guaranteed the availability of 100% over a fixed areas of the globe, these areas look like stripes belts bounding the earth over a certain latitudes depending on the input parameters that have been used.

4. Availability of Galileo constellation in terms of GBAS application over Europe is better than over USA.

5. Results were validated with the results of WG-28 using the same parameters but different simulator tool. They are similar (with 0.02%) due to the parameters used to compute the availability; this ensures and validates the work also.

However, mitigation methods could be classified to the following three types:

- Receiver-based mitigation methods: Which includes; firstly, the Correlator Techniques such as the Standard Correlator in which the early-late autocorrelations spaced with (1) one chip spacing; and the Narrow Correlator in which the early-late autocorrelations spaced with (0.1) of chip spacing. Secondly, the Signal Structure Techniques; mainly the new Binary Offset Carrier (BOC) Spreading of the power spectrum, that places a small amount of additional power at a higher frequency in order to improve the signal tracking performance, that leads to the decreasing the multipath error. Also the (BPSK) spreads the power with a rectangular pulse shape and spreading code chip rate of 1,023 MHz around the center frequency L1. BOC type signals are usually expressed in the form BOC (f_{shift} , f_{chip}) where frequencies are indicated as integer multiples of the GPS C/A.
- Antenna-based mitigation methods: such as Flat Antenna Array, Curved Antenna Array Stack Antenna, and the Array Curved (B) Antenna Array. Those types are basically creating Nulls toward the chirp jammers and reduces their effect on the main lobe, its functional looks like as protection by deception. Figure 49 below.

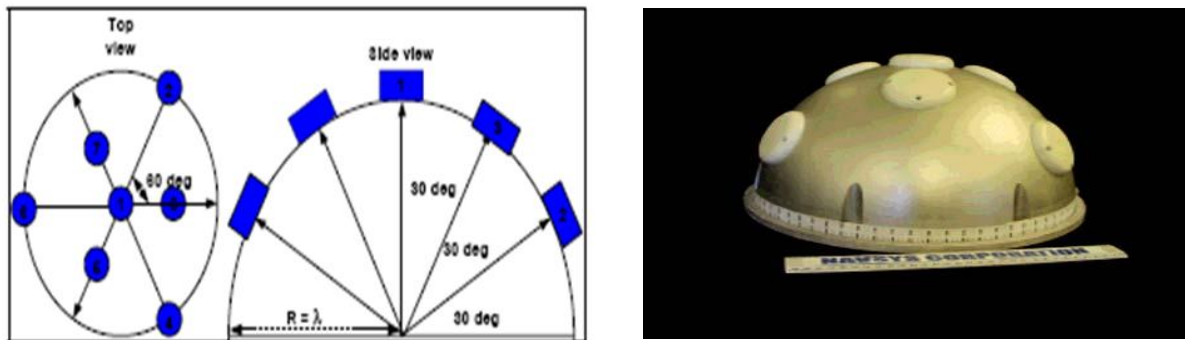


FIGURE 48: CURVED B NAVSYS PROTOTYPE 3-D 7-ELEMENT [(ALHOSBAN A. , 2015)]

- And finally; the Sitting-based mitigation methods: As per the Sitting Criteria proposed by ICAO or FAA regulations concerning GBAS systems. They were put mainly to prevent multipath reflections and unintentionally interferences caused by the nearby obstacles and metal surfaces. As well as other Harmonics of Adjacent transmissions of Radars and common used frequencies bands.

Inasmuch of the promising new signal structures and higher power coming down the road, the interference (both Multipath and EAs) impact on GBAS availability is expected to be mitigated to a significant degree. In this study, this mitigation level was simulated optimistically as A/10 value (one tenth of the amplitude of the genuine desired signal). Figure 50 below. The GNSS modernization will be 6dB more power with new modulation schemes (BOC) as follows:

- GPS block IIF/M, P/Y code, used currently by US Army, but they are classified.
- GPS Block III satellites carrying GPS 2022, (OfficialUSgovGPS, 2019).

- Galileo, new planned signal structure 2022, (ESA, Galileo_Future_and_Evolutions, The reference for Global Navigation Satellite Systems, 2018)[8].

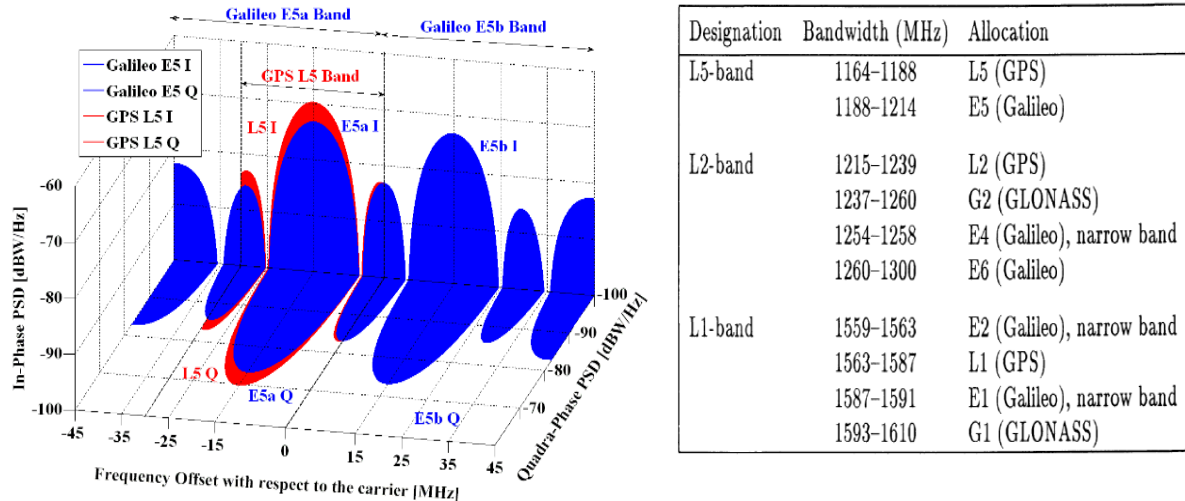


FIGURE 49: GALILEO AND GPS NEW FREQUENCY PLAN FOR DIFFERENT SERVICES [(OFFICIALUSGOVGPS, 2019) (ESA, GALILEO_FUTURE_AND_EVOLUTIONS, 2018)]

5.6 Conclusions and Recommendations

In this chapter; the Electronic Attacks EA in NAVWAR was evaluated in terms of concept, impact and mitigation techniques. The Analogy of interference of signals at the Receiving Antenna and inside the Receiver Signal processing were addressed between the different types of EA and the Multipath interference. Furthermore, the Impact of EA on GBAS was analyzed over Europe and USA using The Multipath approach mitigation levels. The required performance of GBAS for aviation Requirements can be met by Galileo, but not by the current GPS, especially for CAT-II/III (GAST D/F) performance. This is because of the less errors affecting the availability of Accuracy and Integrity invoked by EA or (MP Analogy) compared to GPS. However, Galileo will use more signal power and better Signal structure than Current GPS. Current Military GPS uses P/Y coding which is less affected by EA, but not open to non-USA folks. That's means the EA mitigation techniques using robust signal structure and robust signal processing are more effective than those techniques used in Antenna based or sitting

based, nevertheless, both are important and have their significant contribution in Interference (Multipath and EAs) mitigation.

5.6.1 The New Achieved Scientific Result

New scientific result # 3: I have developed a new methodology in assessing the impact of the Electronic Attacks on the GPS signal using the Multipath analogy approach in terms of power level, time of action and data affecting, which is characterized being a new methodology and more efficient than other empirical assessing methods in GBAS protection domain. It assesses by a simulating tool to which level of protection is needed in each configuration.

5.6.2 Recommendations

I recommend using the analogy method of interference between the unintentional multipath error and the intentional electronic attacks in order to assess to which extent the electronic equipment could be affected constructively or destructively.

Chapter 6: GPS Characterization in Cyberspace between Vulnerability and Geo-encryption: Impact on GBAS Landing System (GLS)

6.1 Introduction

While in the previous chapter intentional Electronic Attacks (EAs) were modelled and examined, in this chapter, a deeper examination and assessment in the domain of GNSS Cyberspace is conducted. In the cyberterrorism concept, whoever was the type of terrorist group: Religious, New-Age, Ethno-nationalist separatist, Revolutionary, and Far-right extremist, the most efficient deterrence solution locates in the end-user's protection and hardening. In the cyberterrorism activities, either disruptive and/or destructive, people tend to be the weakest link in security. Therefore, the threat source would be less important compared with the way of protection. Many efforts have been performed in strengthening the far-end-recipients' infrastructure of communications and critical information systems. Amongst, is the Geo-Encryption Cryptographic algorithm. It depends on adding a new layer of security by using the most vulnerable signals to cyber-attacks, which is the GPS signals. Hence, its strength came out from its weakness. The Geo-encryption technique assumes the use of anti-jam and anti-spoof GPS receivers, which without, the model would be of no added value to the end-users' security. In this chapter, an assessment of the model performance among vulnerability challenges is conducted, showing the characterization of the GPS tool in such model being a solution while it is simultaneously a vulnerable target. A special focus was put in the GBAS Landing System (GLS) performance, in both military and civilian aviation aspect.

Obviously, since the September 11, terrorist attacks against the internet and servers' data base have increased, their tools took another path of the means' curve to achieve their ends and goals. Although the fact they have different levels of skills of hacking and computer knowledge, they were likely able to attack and growing their use of the Internet as a digital battleground. As per (Denning, 2001), one of the main man-made cyberspaces is the aviation aspect, evidenced by the September 11 event. From which, it is clear that the aircrafts hijacking is possible anywhere and anytime. However, many data and voice messages transfer from the ground controllers to the aircrafts' computers and pilots, could be attacked. Consequently, vast of encryption techniques have been developed using many Advanced Encryption Standards

(AES) codes' generation process. The most focused and relevant in the aviation domain is the Denning Geo-Located Model. (Denning&Scott, 2003).

The Geo-encryption or the Geo-Located model is built on established cryptographic algorithms and protocols to provide an additional layer of security. This added layer is beyond that provided by conventional cryptography, but not replacing it. It allows data encryption for a specific place or broad geographic area and supports constraints in time as well as space. If someone, attempts to decrypt the data at another location or different time, the decryption process fails and reveals no details about the original plaintext information. The device performing the decryption determines its location using some sort of location sensor such as a GPS receiver or any radio frequency positioning system. In all process, it assumed the use of anti-jam and anti-spoof receivers.

Following the innovation of this model, many researchers had developed a new enhancing approaches and added features to its original performance. However, all of the previous studies were assuming the same basic hypothesis of using of anti-spoof receivers. Amongst the previous studies in Geo-encryption model, the most relevant study to this chapter is the Geo-Encryption Protocol for Mobile Networks model, which was proposed by (Al-Fuqaha, 2007). Basically, the researchers claimed that they have not seen the details of mobility support in Denning's geo-encryption model, and therefore they proposed a model for mobility when using GPS-based encryption. Simply their proposed model characterised the mobility in certain parameters within an ellipse shaped receiving area. However, their results showed low efficiency in mobile encryption process, there was decryption decline with increase in mobility, and also there was a decrease in decryption ratio with an increase of network traffic due to increased message queuing delay. Furthermore, their future recommended improvements of this model were the using of the next position prediction at the sender or the receiver based on the history of movement parameters such as speed and direction to be sent by the receiver to the sender.

The objectives of this chapter are to assess the implementation of the geo-encryption (Denning&Scott, 2003) Model or the Mobile (Al-Fuqaha, 2007) Model in the approaching high-speed landing aircraft using GLS. In addition, to examine to which extent the GPS signal is immune against spoofing/jamming to be used as geo-encryption aiding, especially in final approach path.

6.2 Assessment of the Geo-Encryption Algorithm: Prospects and Implications

Basically, the proposed algorithm of the (Denning&Scott, 2003) Geo-Encryption, or so called the Geo-Codex Geo-Encryption algorithm, addresses new protocols. Referring to Figure 50 below, the approach modifies the hybrid algorithm to include a Geo-Lock. On the originating (encrypting) side, a Geo-Lock is computed based on the intended recipient's Position, Velocity, and Time (PVT) block. The PVT block defines where the recipient needs to be in terms of position, velocity & time for decryption to be successful. The Geo-Lock then uses the XOR logic gate with the session key (Key_S) to form a Geo-Locked session key. The resultant is then encrypted using an asymmetric algorithm and conveyed to the recipient.

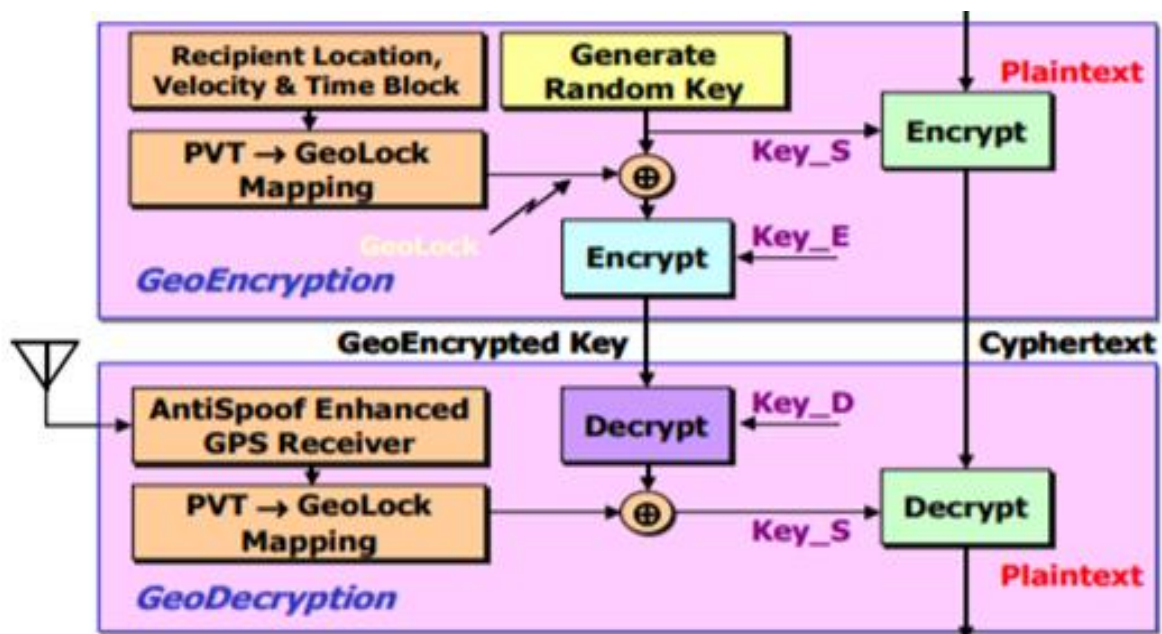


FIGURE 50: THE GEO-CODEX GEO-ENCRYPTION ALGORITHM (DENNING&SCOTT, 2003)

In this section of the chapter, the Geo-encryption concept is assessed by examining two important factors: (1) the mobility of such cryptographic especially in flight mode, and (2) the vulnerability of the GPS coordinates used as keys in terms of Continuity of Service (CoS) and Accuracy, which both contributed in the Availability of the GPS system from one side and the security robustness of the model itself.

6.2.1 The successive geo-lock function of a predefined rout while in mobility.

Basically, and as per definition in (Denning&Scott, 2003), the PVT-geo-lock function is a function of Position(Lat/Long), Velocity, and Time of each used key at a given time of usage, so it can be interpreted by the following equation 47 below:

$$\text{PVT-GEO-LOCK} = f(\text{POSITION (LAT. /LONG.)}, \text{VELOCITY}, \text{TIME}) \text{ EQUATION 46}$$

It can be represented/mapped as shown in Figure 51 below:

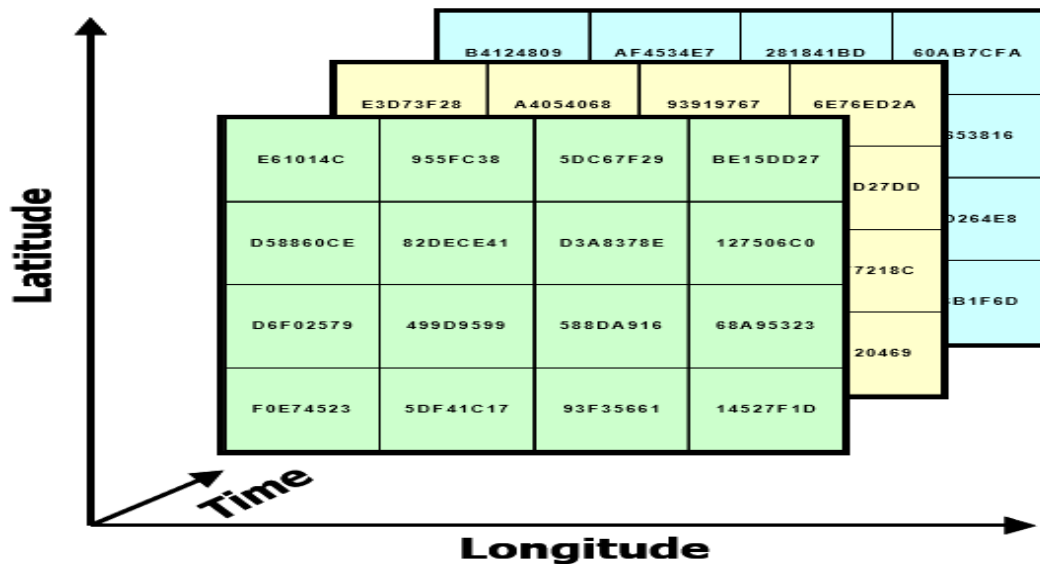


FIGURE 51: THE PVT GEO-LOCK MAPPING (DENNING&SCOTT, 2003)

Therefore, and while in mobility, the geo-lock concept changes little, a successive Geo-encryption can be used to force data and/or keys to follow a specific geographical path before it can be decrypted. It can be achieved by applying multiple geo-locks at the origination node prior to transmitting. As each required node is traversed, one layer of Geo-Locking is removed, thus ensuring the desired path has been followed. Therefore, supposing that we have a route of three successive predefined waypoints or (Locations), L1, L2, L3, then the geo lock equation of each waypoint would be as follows in equation 48 below:

$$L1 = (RK), L2 = L1(RK), \text{ AND } L3 = L2(L1(RK)) \text{ EQUATION 47}$$

Where L1 is location 1, L2 is location 2, and L3 is location 3

And the full route can be geo-encrypted as seen in left panel of Figure 52 below, and it is decrypted and authenticated as seen in the right panel of Figure 52 below:

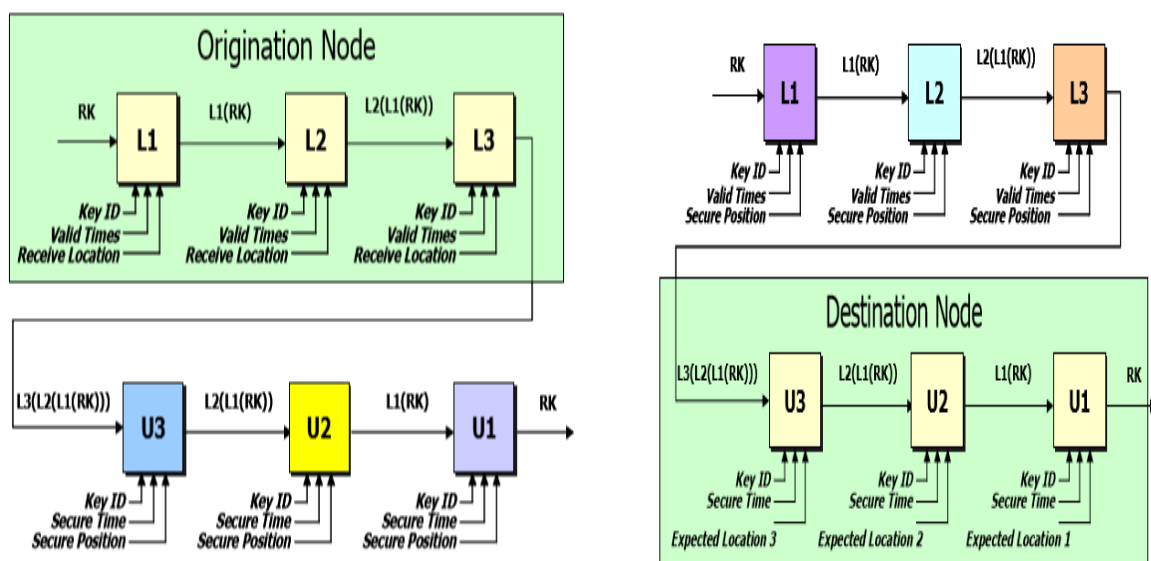


FIGURE 52: THE SUCCESSIVE PVT GEO-LOCK WAYPOINTS: ENCRYPTED (LEFT PANEL), DECRYPTED (RIGHT PANEL) (DENNING&SCOTT, 2003)

The shown waypoints, as per the (Denning&Scott, 2003) Model, does not mean to be a single point only, it may include the surrounding points as well. Hence, when applying this concept on a real route or a path, as seen in (left panel) of Figure 53 below, there is no particular requirement that the PVT-Geo-Lock mapping function be based on a regular grid, therefore, polygonal shapes were chosen based on mission needs. Also, the Geo-Lock regions can overlap; they do not have to be geographically disjoint from one another. Furthermore, time and velocity window requirements could also be imposed. Also an added refinement, a “keep waypoints” safe region could be defined. On the other hand, more focus of the shape of waypoint area was illustrated by (Al-Fuqaha, 2007), trying to reach a proper model of its four parameters; the four mobility parameters of an ellipse zone shape are: velocity (v), direction

(θ), speed maneuverability (y-axis β), and breadth maneuverability (x-axis α) as shown in the (right panel) of Figure 53 below.

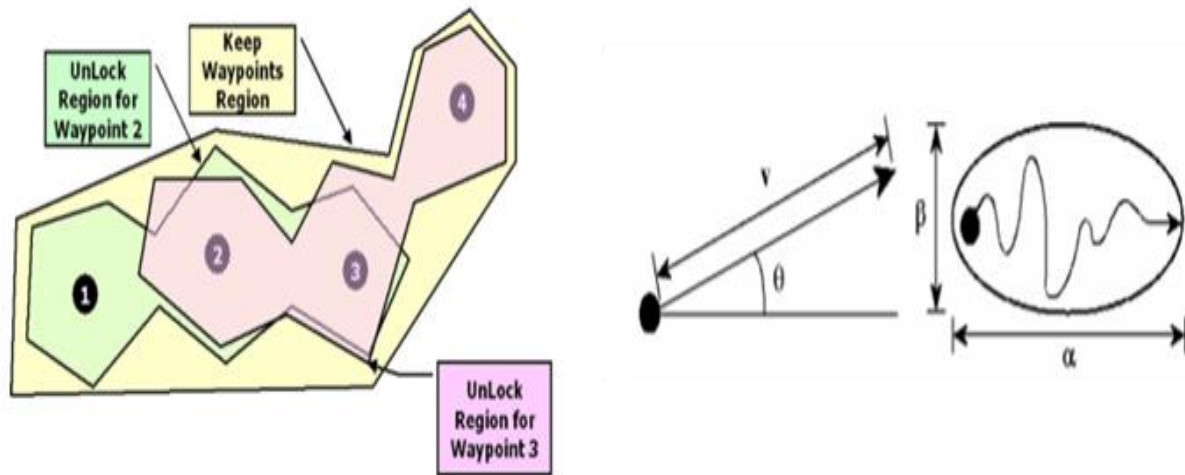


FIGURE 53: THE SUCCESSIVE PVT GEO-LOCK WAYPOINTS TO SECURE THE INFORMATION IN A PREDEFINED ROUTE OF POLYGON SHAPE, (LEFT PANEL) (DENNING&SCOTT, 2003) MODEL, DIAGRAM ILLUSTRATING THE FOUR MOBILITY PARAMETERS OF AN ELLIPSE ZONE SHAPE: VELOCITY (V), DIRECTION (θ), SPEED MANOEUVRABILITY (Y -AXIS B), AND BREADTH MANOEUVRABILITY (X -AXIS A), (RIGHT PANEL) (AL-FUQAHA, 2007) MODEL

By examining both models shown above, the mobility concept has not seen fully described nor characterised, for example, in the (Denning&Scott, 2003) model, the sender is stationary while the receiver is moving in a discrete waypoints path within some predefined decryption areas surrounded by an extra safe zones that couldn't be exceeded, in where the receiver should receive the PVT geo-lock to decrypt the added layer of security. On the other hand, in (Al-Fuqaha, 2007) model, the sender should require to have knowledge of the position, velocity and time of all the moving nodes by means of a "movement update message", this message is intended to be sent back to the sender whenever and wherever it exceeds the predefined tolerances in the sender pre-set map, which is not the possible case in flight encryption methods, where it should be one-way encryption algorithm from the sender to the receiver as per described in (Denning&Scott, 2003) Model.

6.2.1.1 Results' Analysis

However, the results of this part can be concluded as follows in both models:

- The mobility concept hasn't been seen fully characterised in Denning Model of Geo-encryption, but it is an added significant value for the stationary senders and receivers, more or less, can be applied in a well-defined decryption zones discretely and not in continuous moving objects especially in high speeds.
- The mobility concept in (Al-Fuqaha, 2007) Model of Geo-encryption was characterised deeper, but in slow moving objects (buses in crowded areas not exceeding 20-30Km/h), it was interpreted from their results that the decryption ratio falls with an increase in mobility. This is due to the fact that higher mobility means that nodes move more often away from their perceived positions at the sending nodes, as a result, more messages are not decrypted. Also, the overhead decreases with increased pause times. This behaviour is typical of a protocol that is reactive to movement. If there is no movement then there is no need for movement updates.

6.2.2 The vulnerability of GPS using the Geo-Encryption while using the (C/A) code.

In general, the Coarse/Acquisition or (Clear/Access) code (C/A-code) in GPS is considered a vulnerable signal, the real scientific problem is not only the citing criteria, but it is also the GNSS signal structure, the GNSS signals are weak to resist higher power of the Electronic Attacks (EAs) as detailed in a previous chapter. This is due to their extremely low level of power density; because satellites' transponders are orbiting about (22,000 Km) above the ground level, and they are transmitting their signals via Troposphere and Ionosphere layers, hence, the signals arrive to users on the earth surface in a very weak signal to noise ratio, it is around -160dBw for GPS L1C, and -154dBw for GPS L2 (Military), and speculated -155dBw for Galileo E1/E2). The other part of the problem is that the capability of services' restoring on the proper time, when disrupted, has very low probability. This may cause a high risk in safety-of-life applications of GLS landing systems when compared with other safety –critical infrastructure applications such as banking, or the non-critical GNSS applications. However, the GBAS stations are usually located in a well-known surveyed reference sites in the vicinity

of the airport near the runways, which makes them more vulnerable to EAs as well. Full detailed technical data are available in (Alhosban A. , 2019), and (B. Hofmann-Wellenhof, 2001) book.

6.2.2.1 GPS's Signal Structure

In this part a dedicated review of the GPS signal structure is focused on, especially in purpose to serve the objective of this chapter. Therefore, at the satellite transponder side, which is the space segment, the GPS signal structure is sent by the satellites Space Segment, see (B. Hofmann-Wellenhof, 2001) book, consists of two Carrier frequencies (L1 and L2) and two codes, both characterized by a pseudorandom noise (PRN) sequence as shown in Figure 54 below. The first is the Coarse/Acquisition or (Clear/Access) code (C/A-code). It has the frequency $f_0/10$ and is repeated every millisecond. The codes of the two registers are not classified, and the C/A-code is available to civilian users. The other code is the precision (or protected) code (P-code). It has the frequency f_0 and is repeated approximately once every 266.4 days. It is also not classified, but the P-code is encrypted to the Y-code by Anti Spoofing (A-S). Since the Y-code is the sum of the P-code and the encrypting W-code, access to the P-code is only possible when the secret conversion algorithm is known, hence, its jamming immunity is better. A third code called the W-code is used to encrypt the P-code to the Y-code when A-S is implemented. The coding of the navigation message requires 1500 bits and, at the frequency of 50 Hz, and it's transmitted in 30 seconds.

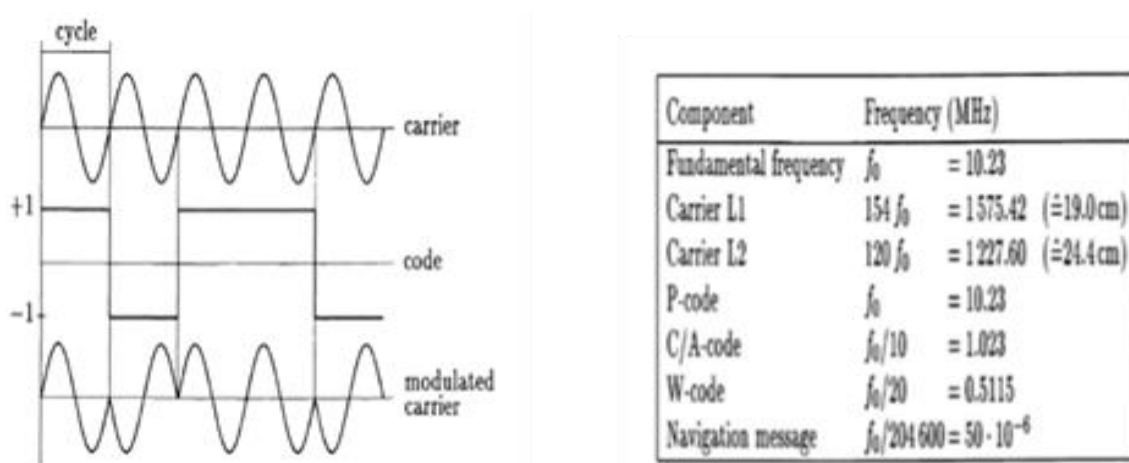


FIGURE 54: GPS CODING STRUCTURE (LEFT PANEL), GPS SIGNAL COMPONENTS (RIGHT PANEL) HOFMANN (2001)

At the receiver side, which is mainly the ground segment (here is GLS system the ground station or the Aircraft receiver), the carrier, code and the navigation messages are decoded and demodulated to form the useful information of the PVT using the code correlation techniques. Such as: Code correlation Narrow and wide, squaring technique, Cross correlation technique, Code correlation plus squaring technique, and the Z-tracking technique. The Data Acquisition is done by: Either the Code pseudorange in which the precision of roughly 3m and 0.3m is achieved with C/A-code and P-code pseudorange respectively. Or the Phase pseudorange: can be measured to better than 0.01 cycles which corresponds to millimetre precision, for more mathematical details refer to the book of (B. Hofmann-Wellenhof, 2001) However, the new signal structure and the new signal processing in Galileo and the modernized GPS Block III will hopefully add another protection value by the receiver-based mitigation methods.

6.2.2.2 Characterization of GPS Jamming Model

In general, the model of jamming in EA for GPS/GLS down links, is modelled as in following equation 49 as per (Adamy, 2009) stated in his book and modified by this study accordingly:

$$J/S = ERP_J - ERP_S - L_J + L_S + GR_J - GR \quad \text{EQUATION 48}$$

Where:

J/S: the ratio of jammer power to the desired signal power (Here the received power from satellite) at the input of the receiver being jammed in dB

ERP_J: the effective radiated power of the jammer in dBm

ERP_S: the effective radiated power of desired signal transmitter (Satellite) in dBm

L_J: the propagation loss from the jammer to the targeted receiver (GLS or Aircraft) in dBi

L_S: the propagation loss from the transmitter (Satellite) to the receiver (GLS or Aircraft) in dBi

GR_J: the receiving antenna gain (GLS/Aircraft Antennas) in the direction of the jammer in dBi

GR: the receiving antenna gain (GLS/Aircraft) in the direction of the transmitter (Satellite) in dBi.

6.2.2.3 Results Analysis

However, using the C/A GPS code, the open civilian code, has a higher potential tendency to be jammed or spoofed more than the military restricted P/Y code due to power level. Therefore, the GPS coordinates are not guaranteed and could be easily attacked. The drawbacks of the Geo-encryption algorithm in terms of using the Lat. /Long. Coordinates of the GPS system can be summarized as follows:

- The necessity of using the anti-spoof GPS receivers. Otherwise, the added layer of security would be shortened to the conventional algorithm only.
- The encryption file would reveal the physical location of the intended recipient, especially in the military usages. It may provide vital information to someone who wants to spoof the device.
- If the device is vulnerable to tampering physical attack, it may be possible to be modified as to completely bypass the location check parameter. The potential modified device would decrypt all the received data without acquiring its location and verifying that it is correct. Alternatively, an adversary might compromise the keys and build a modified decryption device without the location check. Either way, the potential modified device could be used anywhere and yet the location would be irrelevant.

6.3 The necessity of Geo-Encryption Algorithm for the GBAS Landing System

By principle, the GBAS Landing System GLS requires that both the ground and aircraft subsystems use exactly the same ephemeris and satellite clock corrections. Because the differential principle removes all the ranging errors that are common to the ground and the aircraft subsystems. Mainly, the GBAS Ground Subsystem provides the Final Approach Segment Data (FAS), as per (Alhosban A. , 2015). The GBAS ground subsystem stores data, related to the serviced runway end(s), in the form of Final Approach Segment (FAS) path construction data blocks. It broadcasts data continuously for reception by the approaching aircraft. However, each GBAS station has data processing and integrity units that are

responsible for GBAS Messages Elaboration (MT1, MT2, MT4). Most importantly, the Type 4 message contains one or more sets of FAS data, each defining a single precision approach, including the coordinates of the Landing Threshold Point/Fictitious Threshold Point (LTP/FTP). On the other side, the aircraft subsystem then corrects its own pseudorange measurements for each satellite with the differential correction data received from the ground subsystem. The corrected pseudorange measurements are then used to more accurately determine the aircraft's position relative to the selected FAS. More details can be found in (Alhosban A. , 2015). Based on the above description, it is clear that the GBAS /GLS system is fully capable to be operated by the GIS-aided precision approach procedures, it is more relevant to data transmission that is timely sent to the approaching aircraft without any delay. Any encryption process, either conventional or added layer as Denning geo-encryption, would not be of an added value, it may cause disruption of waypoint coordinates, and could cause a negative impact rather than being of an added security value, let alone the critical final situation of hosting the aircraft safely to the runway surface. Next section illustrates this in depth.

6.4 Assessment of implementation of the Geo- Encryption algorithm in the GBAS Landing System (GLS), special case study in Budapest International Airport.

In order to examine where the Denning Geo-Encryption can be potentially implemented, the phases of flights of any aircraft should be identified and illustrated. Most importantly, in which flight phase the airborne equipment is most likely vulnerable to be attacked by hackers or intruders. The intended or unintended jamming or spoofing may impact the communication voice messages from the controllers to pilots. As seen before, the navigation messages in those phases are comparatively secured by the GPS structural encryption methods whether it is enough or not. A special case study of the Budapest International Airport was taken as an example, but it can be applied for all airports procedures. In general, there are three modes of phases of flight, the terminal phase mode (both departure and arrival), the Enroute phase mode, and the final approach phase mode, as shown in Figure 55 below, each phase has an operational requirements of navigation that are supported by a certain type of equipment, the radio navigation equipment such as (VOR, DME, ILS), they will be gradually replaced by the GNSS technical solutions such as (ABAS, GBAS, SBAS) systems.

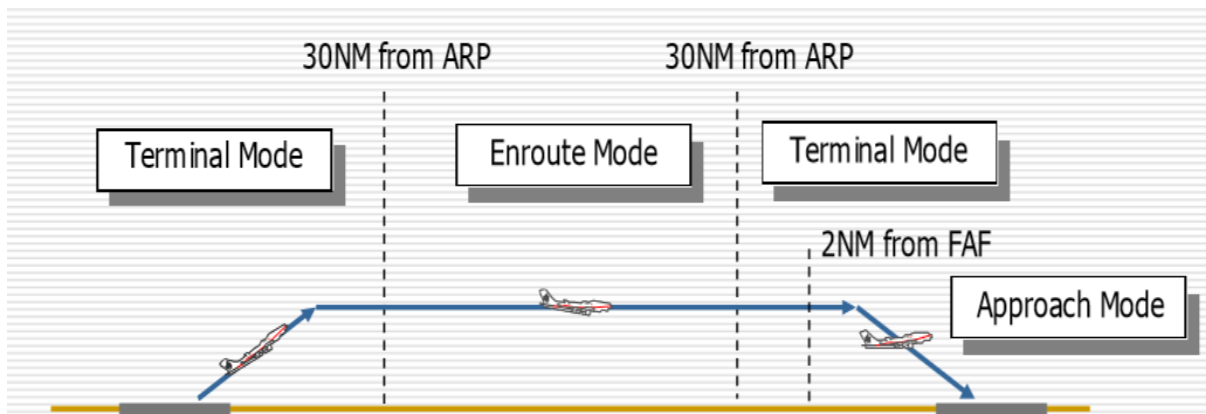


FIGURE 55: THE FLIGHT PHASES MODES (EDITED BY AUTHOR)

In terms of existing infrastructure for Budapest airport BUD, the following figures, taken from the official website and have been published since May 2018, data are listed in the official websites of www.hungaryairport.hu and www.ais.hungarocontrol.hu. Hence, In Figure 56 below, there are three GIS-aided holding areas in the terminal mode in the BUD airport. The holding areas are used in case of the heavy traffic to delay the coming aircrafts until the runway is clear to land. In those three holding areas, many voice messages can take place between the controller and the pilot, in which adding the extra layer of security by using the Denning geo-encryption could be in possible usage.

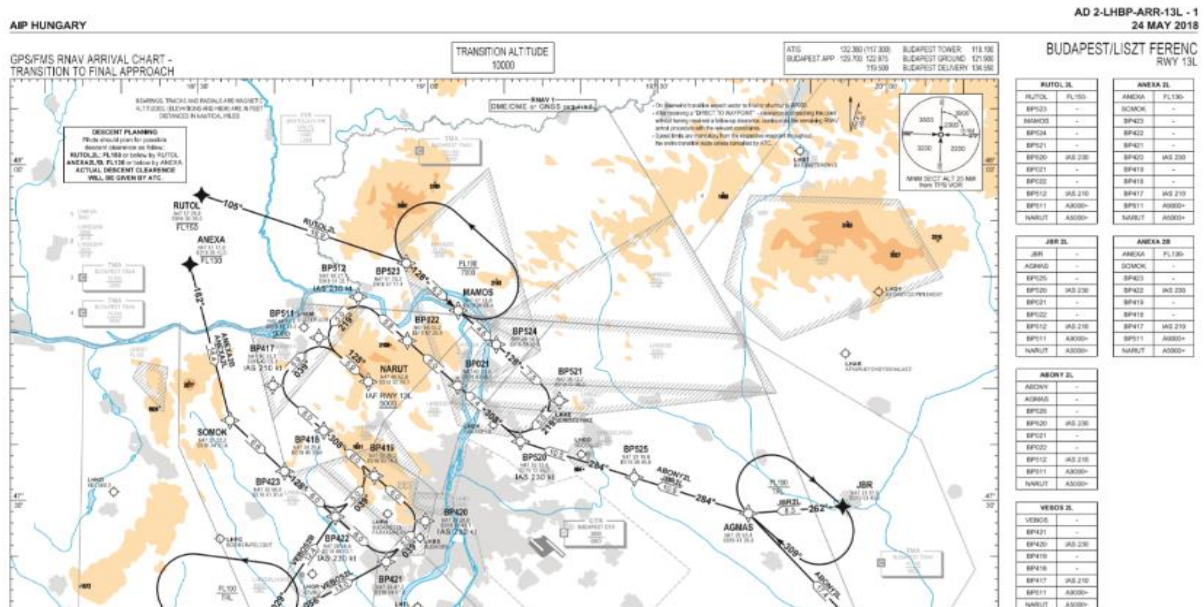


FIGURE 56: THE TERMINAL RNAV DATA FOR BUD AIRPORT 13L INCLUDING THREE HOLDING AREAS FOR TRANSITION TO FAS

Then, In Figure 57 below, showing the final approach segment data, it contains four (4) Way Points (WP), the three Initial Approach Fix (IAF) WPs resemble the three potential coming directions; the straightforward WP named (NARUT), the left one (GIGAN), and the right one (KESID). All the three WPs lead the approaching aircraft to the Initial Final (IF) WP which is the start point to the FAS descending glide path where the ILS and the GLS turn to be used in bad weather of low visibility. Actually, some voice messages may happen, but more likely the navigation messages dominate. Furthermore, the relatively high speed of a traversing aircraft not less than 320Km/h, those waypoints may cause a restrictions and limitations of ciphering the voice messages by the use of geo-encryption model. Due to the fact that its mobility is shortened by high speeds of movement compared by mobility speed of 20Km/h in (Al-Fuqaha, 2007).

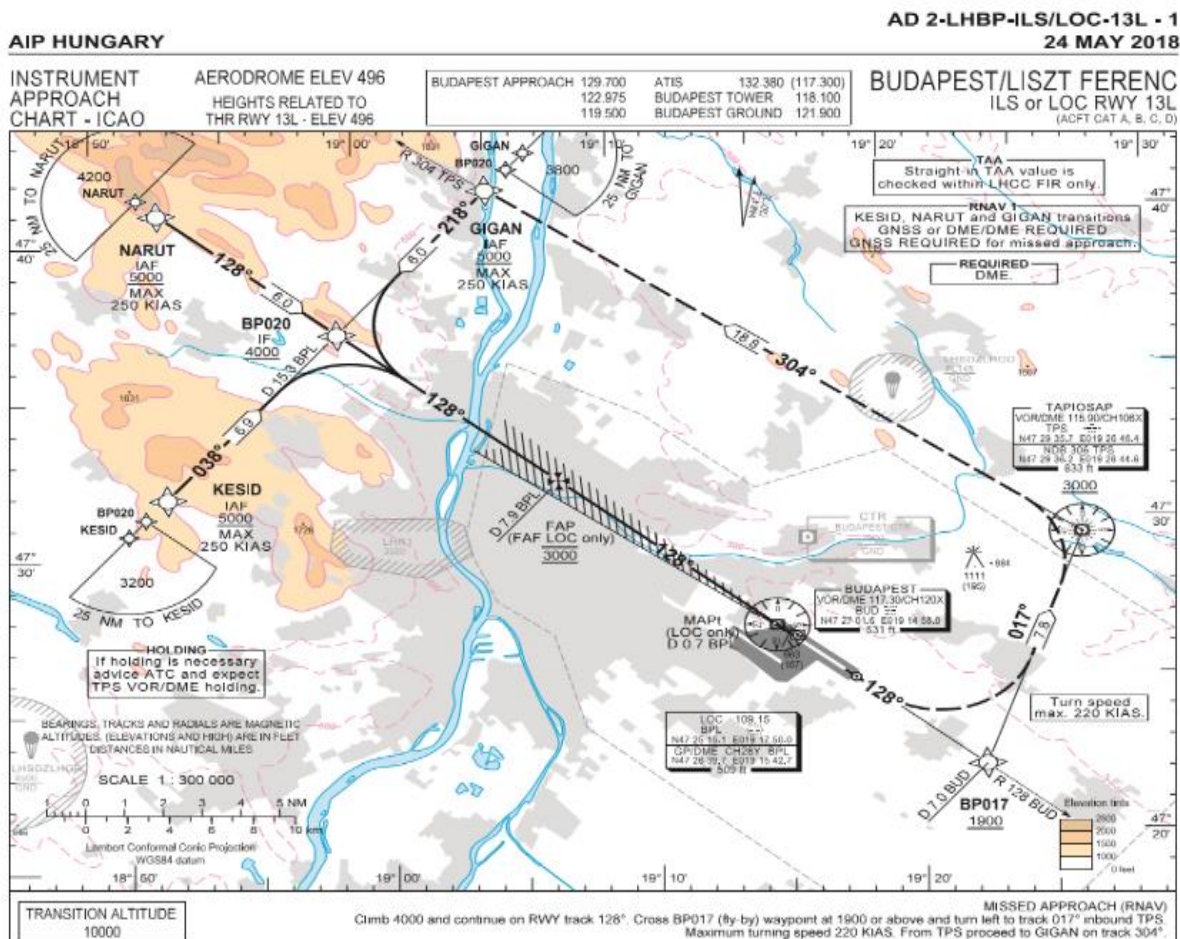


FIGURE 57: THE START OF THE FINAL APPROACH SEGMENT INSTRUMENT RNAV DATA FOR BUD AIRPORT 13L

Finally, and as shown in Figure 58 below, the final approach fix (FAF) started to be used in the final segment, extended to the 13R Runway's Touch Height (TCH) point called MAPT. In this final segment, the use of ILS or GLS is dependent on the availability of integrity, accuracy and continuity of the system, especially in bad weather or night flights. Hence, the voice messages are so limited and the only guidance would be the GLS system data and coordinates in the navigation message.

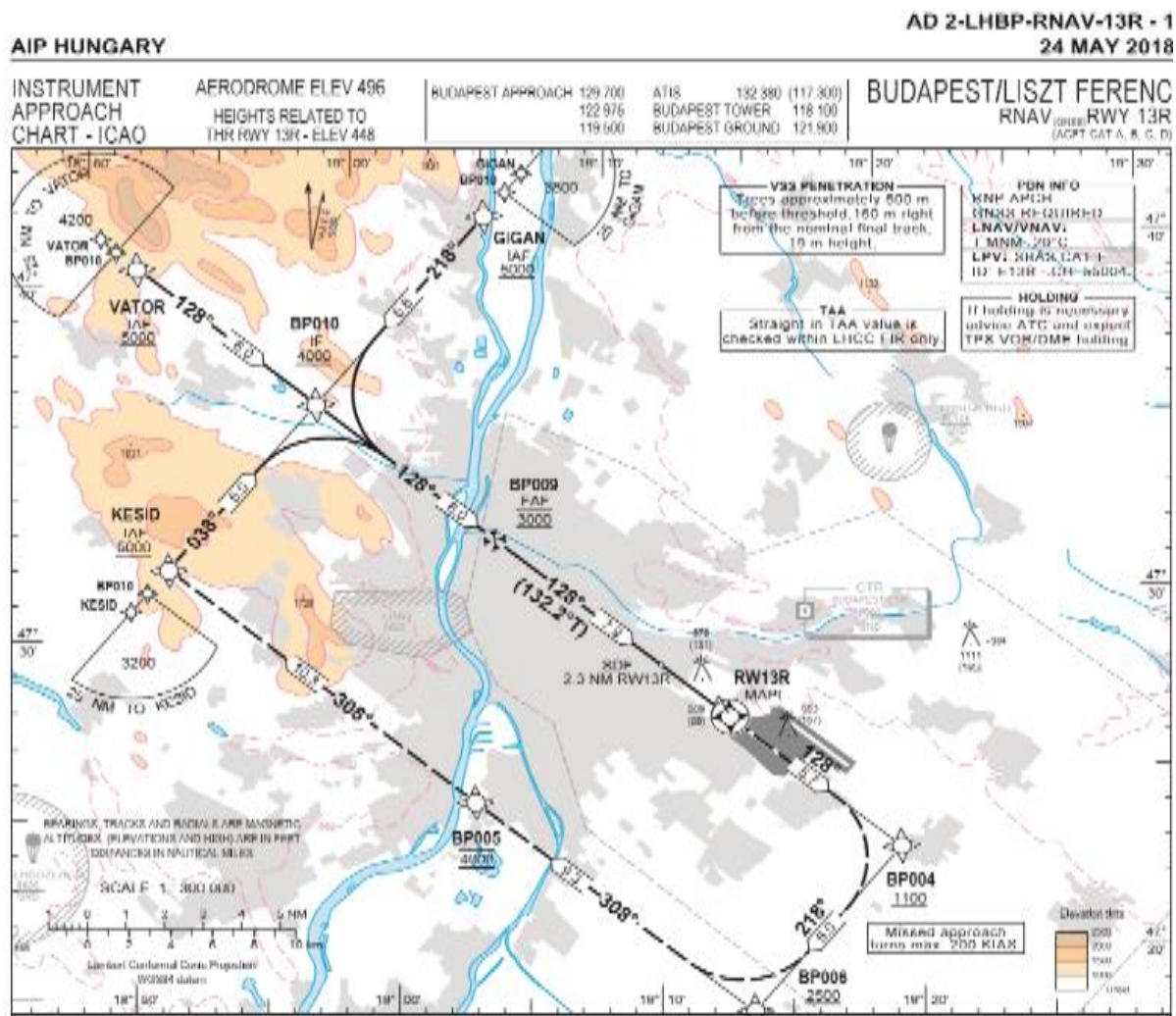


FIGURE 58: THE FINAL APPROACH SEGMENT INSTRUMENT RNAV DATA FOR BUD AIRPORT 13L

From another perspective, a recent study of (Gurtov, 2018) has shown that the importance of improving Controller–Pilot Data Link Communication (CPDLC) security stems from the need to create a secondary VHF communication channel. It should be trustworthy enough to

alleviate the already congested communication VHF voice communication and to enable ATC continued growth.

The study of (Gurtov, 2018) showed that the implementation of any encryption methods therefore needs to have minimum impact on the system's performance as possible while still providing an all-round security protection. They proposed utilizing the current flight plan and AIP information systems to provide a root of trust for authenticating CPDLC encryption. Identity-defined networking was proposed also as a generic solution to be applied to the air traffic communication system as a whole, including CPLDC and all the communication means. It can be incrementally deployed without the need to change the existing hardware.

However, the study unfortunately didn't propose the Denning Geo-encryption method amongst their solutions. And their study lacks to any best approach for security in the CPDLC link, that's approved my study results of existing of challenging constraints in applying any type of encryption during the terminal and final approach phases of flight. Although the encryption is needed in order to strengthen the security of the communication in this phase of flight, but it should be optimized and compromised with other negative impacts may cause disruption of its generic function. The geo-encryption method could be used, with more investigation, in the holding areas prior the final approach is conducted, in which a lot of traffic of voice messages being transferred between the pilot and the controller while descending in the well-defined holding area.

6.4.1 Results Analysis

The descent profile computed by the Flight Management System (FMS) in the aircraft is a very efficient and useful tool to help the flight crew in managing the aircraft energy during the descent and approach phases, the descent speed for Airbus A320, A330, A340 commonly used types of aircraft is 160 – 180mph, as per (Airbus, 2017), it is almost about 320 – 360Kmh, However, this speed is impacted with the wind during the landing phase, that added a compensating ΔV continuously by FMS, see Figure 59 below. Therefore, the descent path computed by the FMS uses the forecasted wind, and the actual conditions may vary from the predicted ones. As a consequence, the difference between the predicted descent wind and the actual wind (Δwind) affects the aircraft's behavior, the aircraft tends to leave the FMS computed idle path.

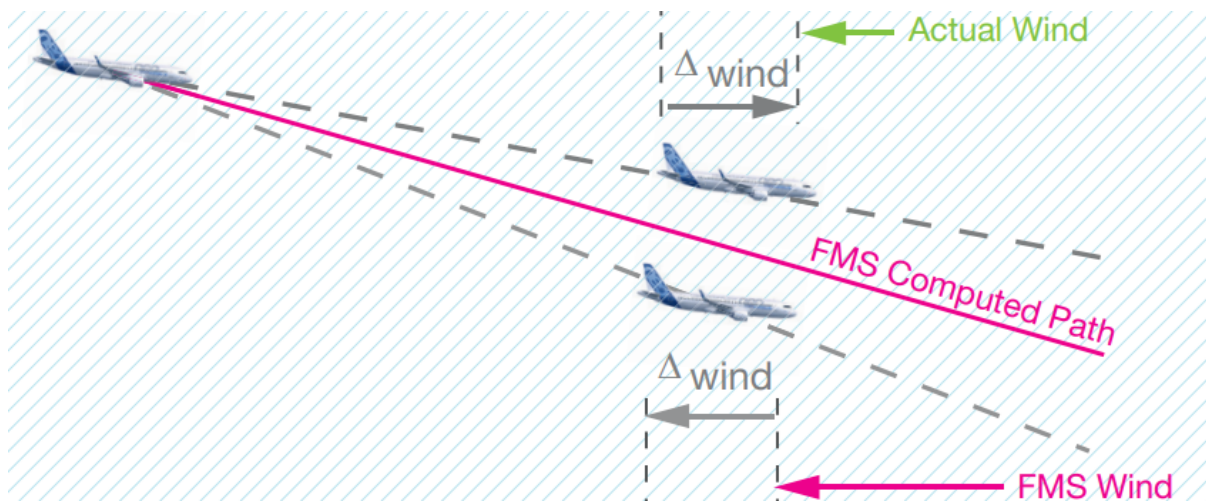


FIGURE 59: THE WIND IMPACT IN THE DESCENT SPEED [(AIRBUS, 2017)]

By saying that, the actual speed is not only high, but varying also, therefore, the mobility of the descending status is more complicated in terms of high speed and varying speed, moreover, adding this to the vulnerable GPS navigational message and its slow rate of updates relatively to the geo-encryption principles, it makes the usage of such model more and more inefficient when compared to (Al-Fuqaha, 2007).

6.5 Conclusions and Recommendations

In conclusion, this research argued and examined the possible ways of using the innovated Geo-encryption model in flight phases. The chapter also analysed the concept of its mobility and the potential limitations. There is a tendency to use this model in a stationary receiver rather than mobility, moreover, it can be used in a semi-moving object in a predefined zone in a pre-set safe areas designed in a well-defined path or route of relatively slow movement. One potential use could be, with more investigation, in the well-defined holding areas, in which a lot of traffic of voice messages being transferred between the pilot and the controller. Above all of this, the model is most likely depends on the assumption of jamming/spoofing free GPS receivers. The added value of the geo encryption method is an extra layer of security, locked to a geographic location, time and limited velocity, which in case of not being met, the conventional encryption could be in use, otherwise, no benefit or information loss will be blamed. It was approved that it is good to have it under certain conditions in flight phases, without negatively affecting the operation of the generic function of communication performance. It's recommended to have further investigations of such better concept of geo-

encryption in flight phases should be conducted by experimental flight tests, which is beyond the capability of the scope of this PhD Dissertation.

6.5.1 The New Achieved Scientific Result

New scientific result # 4: I have approved that the innovated Denning Geo-Encryption model and its mobility enhancement is not efficient in flight modes, it cannot be characterized to be safely used in approach and landing phases due to the high speed mobility of the landing aircrafts, vulnerable and weak GPS signal, slow navigational message update rate, and the wind-varying descent speed. But it can be used with more added value in stationary or semi-moving modes only, which is characterized being safer and less risky than the similar geo-encryption mobility model created by Alfugaha model.

6.5.2 Recommendations

I recommend that further investigations of such better concept of geo-encryption in flight phases should be conducted by experimental flight tests, which is beyond the capability of the scope of this PhD Dissertation.

Chapter 7: Assessment of the GIS-Aided Precise Approach Using the GNSS-GBAS Landing Systems

7.1 Introduction

In this chapter, the last chapter, The Assessment of the GIS-Aided Precise Approach Using the GNSS-GBAS Landing Systems is conducted, the GIS-aided precise Approach Plates are being used worldwide, because the radio navigational Instrument Landing Systems (ILSs) are currently intended to guide the aircrafts in lateral and vertical dimensions to the runway surface safely and precisely. Therefore, they are strongly related to the geographic location of an airport and its runway(s). The ILS systems use the aids of the radio frequency radiation to achieve this purpose, depending on the ground emitting stations, and providing the guidance to the runway centerline location along with the glide slope guidance during the Final Approach Segment (FAS). Furthermore, the new ILS systems are fully aided by the coordinates of the Global Positioning System (GPS) instead of the ground radiations, they use the waypoint fixes during the landing phase of flight by means of transmitting their corrections to the on-board receivers. Those new invented Ground Based Augmentation Systems (GBAS) are more precise and trustable, they also increase the capacity of the huge air traffic demands nowadays by multiple and non-straight approaches. As a result, the Geographic Information System (GIS) of any airport supported by the GBAS system is intended to be fully used and implemented in both instrumental and procedural aids. Many previous studies had indicated that the old procedural approaches should be changed to the new GIS aided ones, but without pointing out when and how to implement such important transfer. The objective of this chapter is to assess the performance of the GIS aided precision procedures using the GBAS stations, and to identify to which extent they can enhance the navigational aviation in the air traffic management domain. A special focus will be put on the Hungarian Budapest international airport in terms of both capability motivating factors and the current GIS infrastructure aiding. Results showed a promising chance for more investment in installing the GBAS stations in the airport. That will enable more capacity and easier approaches in all weather conditions.

7.2 Background

Due to the reason that the GIS approaches are geographically linked to the ILS systems, then a background about their evolvments is strongly needed for this chapter. Historically, the navigational landing systems era has passed through a long way of developments and enhancements since the early 1970s; the major milestones in this development roadmap are the Instrument Landing System (ILS), the Microwave Landing System (MLS) and the GBAS Landing System (GLS). In the following paragraphs, the light is shed on their advantages and drawbacks.

The ILS has been safely guiding aircraft on the final approach for about 70 years; it was chosen by the International Civil Aviation Organization (ICAO) as the international standard for navigation aids, and has been operated in most airports since the 1950s. Basically, it consists of two VHF transmitters, of which one provides the lateral guidance and the other provides the vertical guidance; The first VHF transmitter supports the precision approach and landing of flights by providing information on the lateral deviation (flight landing around the center of the runway) using the difference in the depth of modulation (DDM) of the directional radio wave radiated from the ground, while the second transmitter supports the vertical deviation (flight landing above and below the Glide Path Angle (GPA), and provides also the distance between the runway threshold and the location of the approaching flight. (M. Jeong, 2016). However, the most noticeable shortages in the ILS systems are: (1) both transmitters are necessary for each runway end to which the precision approach is provided, and this makes the system expensive, because multiple installations are necessary at one airport, depending on how many runways it operates; (2) since the air traffic is continuously increasing, the existing ILS is shortened to fulfil the capacity needs; (3) the ILS design only allows the definition of straight-in approach trajectories to a fixed point, which makes operations inflexible. Therefore, there was a need for research on a new technology to overcome those shortages within the limited airspace.

Then, the MLS was developed in the 1980s. It allowed more flexibility, mainly by allowing the definition of multiple approach tracks to one runway threshold. The only installed system was in London Heathrow airport, although it was certified by ICAO as Category CAT III performance during all kinds of bad weather, especially fog. (T. Dautermann M. F., 2012). Unfortunately, the development of the MLSs was ceased when the GNSS/GBAS systems had

been started to be developed since 1990s in the USA and Europe, the MLS system was the victim of the GNSS system in its early stages. Nonetheless, when MLS was about to be widely used, many of the on-board fleets' equipment had to be modified, if not been changed accordingly; this change was because of the difference of frequencies used in MLSs over the ILSs. Therefore, London MLS System was decommissioned in May 2017 and replaced by a GNSS/GBAS system.

On the contrary, the newly developed GNSS/GBAS systems are more capable of providing safe and reliable guidance than the MLS systems, with a greatly improved flexibility in the definition of approach tracks. For example, the GBAS system supports flights (within a 3 NM radius from an airport location) with a precision approach service like ILS by using the concept of Differential GPS (DGPS). A curved approach and the control of glide path angle are possible for the GBAS, unlike for the ILS. Therefore, the efficient and flexible handling of landings is possible. Also, unlike the ILS that needs to be installed at each runway along the entering direction of flights, the GBAS system can offer information of approach guidance for several runways, using just one piece of equipment. Hence, it has economic benefits compared to the ILS. Moreover, within the past two decades, the aviation navigation has been gradually transitioning from the ground-based infrastructure to rely increasingly on the global navigation satellite systems (GNSSs). This has led the ICAO to standardize a navigation performance concept called the Performance-Based Navigation (PBN). Within the PBN, the system performance requirements for navigation equipment are specified as Required Navigation Performance (RNP) with a high level of accuracy, integrity and availability.

However, in order to provide precision instrument approaches that utilize three-dimensional angular guidance to a dedicated runway, two possibilities exist: (1) On the one hand, the so called the satellite-based augmentation system (SBAS), in which the GNSS reference stations are distributed over a wide area at precisely known locations. They measure the GNSS signals and send the data to a master control station. The master control station computes correction and integrity information, which is broadcasted to the flights via a geostationary satellite. (2) On the other hand, in the so called ground-based augmentation system (GBAS), which is used to achieve GNSS augmentation at an airport only, it is sufficient to place two to four reference stations at the airport and have a local processing facility. The correction and integrity information are transmitted to the flights via a (VHF) radio data link. In both cases, the user applies those corrections to its own GNSS measurements and computes a more precise

position. Furthermore, by using the Final Approach Segment (FAS) data block which is supported by the Geographical Information System (GIS) of a specific airport terrain and space, the aircraft's computer can then calculate the angular deviations with respect to the GIS aided reference trajectory, and the final result will be a guidance signal looking like the conventional one (ILS). (Dautermann, 2020)

Therefore, the GIS aided precise approach trajectory, which uses the signals of the GBAS Landing System (GLS), is examined through a comparison with the Non-GIS aided approach trajectories used in the current conventional ILSs. Furthermore, the available GIS infrastructure of the Budapest Airport (BUD) is detailed, showing the future investment in GBAS landing system to optimize the accuracy, integrity, availability performance, as well as to increase the capacity of the air traffic and the airport handling. Special technical focus will be on the differences between the GLS and ILS systems in terms of precise approach.

7.3 Geographic Information System (GIS) Implementation in the Aviation Domain

From a software perspective, a GIS consists of a special type of computer program capable of storing, editing, processing, and presenting geographic data and information as maps. There are several GIS software providers, such as Environmental Systems Research Institute Inc., (www.esri.com) which distributes ArcGIS, and Pitney Bowes, (www.pbinsight.com), that distributes MapInfo GIS. Though online mapping services and interfaces are provided by companies like Google, Yahoo, and Microsoft, such services are not (yet) considered fully fledged GIS platforms. (Campbell, 2011). There are also open-source GIS options, such as GRASS, (<http://grass.itc.it>), which is freely distributed and maintained by the open source community, (Campbell, 2011). All GIS software, regardless of vendor, consists of a database management system that is capable of handling and integrating two types of data: spatial data and attribute data. Spatial data refer to the real-world geographic objects of interest, such as streets, buildings, lakes and countries, and their respective locations. In addition to location, each of these objects also possesses certain traits of interest, or attributes, such as a name, number of stories, depth, or population. GIS software keeps track of both the spatial and attribute data and permits us to link the two types of data together to create information and facilitate analysis. One popular way to describe and visualize a GIS is picturing it as a cake with many layers. Each layer of the cake represents a different geographic theme, such as water

features, buildings, and roads, and each layer is stacked one on top of another, (Campbell, 2011).

As hardware, a GIS consists of a computer, memory, storage devices, scanners, printers, GPS units, and other physical components. If the computer is situated on a network, the network can also be considered an integral component of the GIS because it enables users to share data and information that the GIS uses as inputs and creates as outputs. As a tool, a GIS permits users to maintain, analyze, and share a wealth of data and information. From the relatively simple task of mapping the path of a hurricane to the more complex task of determining the most efficient garbage collection routes in a city, a GIS is used across the public and private sectors. Online and mobile mapping, navigation, and location-based services are also personalizing and democratizing GISs by bringing maps and mapping to the masses. (SaylorOrg, 2015).

Basically, the GIS provides an important support for the planning and implementation of aeronautical needs; it supports the aeronautical data production, the management, and the visualization. (ESRI, 2020) In addition, it ensures the automation, the quality assurance, and the task assistant for workflow management in creating efficient and accurate data production. That makes the data interoperability meet the ICAO standards.

By the GIS aided, especially the Visual Flight Rules (VFR) procedures can be issued easily and used efficiently, however, the Instrumental Flight Rules (IFR) procedures can be used in case of bad weather, using the signals of the Landing systems more efficiently. Furthermore, both the VFR and the IFR procedures should be certified and published for open use for the sake of the safety of flights, for example, the VFR view of Budapest in terms of digital maps is published in the Hungarian Airports official website, (www.hungaryairport.hu), as seen in Figure 60 below. An added layer in the electronic map shows the coordinates of the entrance and hold-on fixes. Globally, the Eleventh Air Navigation Conference (AN-Conf/11) in 2003 recommended that ICAO had to develop a database web that is containing all tabular material from ICAO regional air navigation plans, together with major traffic flows' charts and other regional data. Later, the ESRI's ArcGIS Server, a server-based GIS solution with client access via the Web, was chosen to meet ICAO's needs. Therefore, the first phase of the electronic Air

Navigation Planning (eANP) was deployed in 2008; it makes the ICAO Global Air Navigation Plan (GANP) database available to many users.

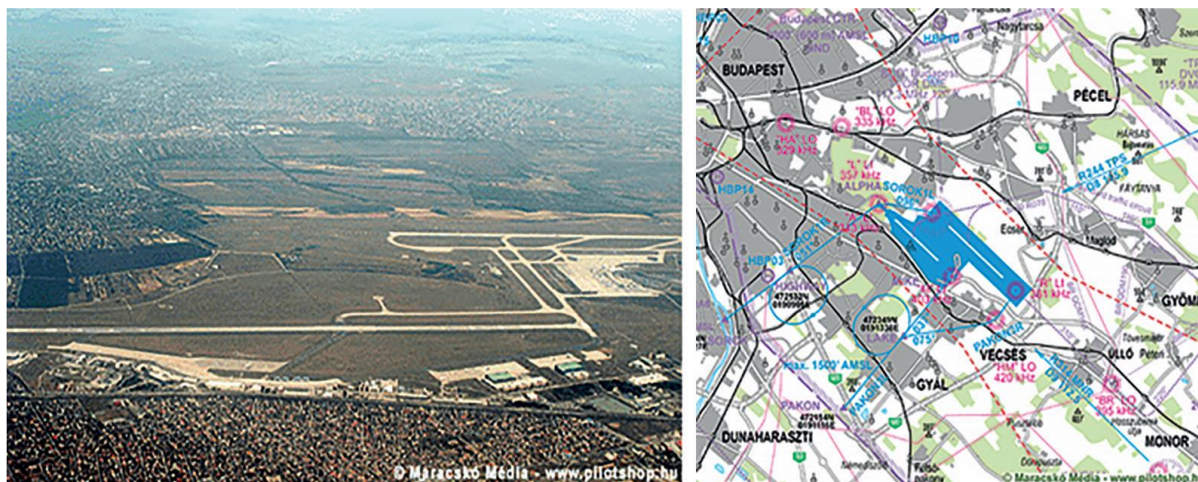


FIGURE 60: ON THE LEFT: ARIAL PHOTO OF BUD AIRPORT. ON THE RIGHT: VISUAL APPROACH CHART FOR BUD. SOURCE: ‘AIRPORT INFORMATION / VISUAL APPROACH CHART.’

The ICAO (eANP) GIS portal is a gateway combining a database and Internet based GIS technology, allowing authorized users to submit, store, update, manipulate, analyze, and chart the global air navigation planning data from a centralized ICAO server. Essentially, the eANP displays dynamic, interactive charts. Users are now able to perform many different functions besides viewing the data. They can create and view what-if scenarios of new routes, chart traffic flow information with other user-selected criteria, and update the data. Users can also fly the 3D electronic Terrain and Obstacle Databases (eTOD) in ArcGIS Explorer. In addition, the users can access the GIS portal via the internet to browse the data directly using a variety of clients. It includes the Microsoft Internet Explorer, the ESRI ArcGIS Explorer, or the ArcGIS desktop clients depending on the use of the application. The GIS portal can be accessed online at 192.206.28.81/eganp.

The global air navigation plans are available at the GIS portal, they include the Air Traffic Safety (ATSanp) charts, the Flight Information Region (FIRanp) charts, the Air Traffic Management (ATM) charts, the Aerodrome Operational Planning (AOP) satellite images, the regional charts, and many other thematic maps.

However, the GIS portal's interactive maps are gradually replacing the air navigation plans that are delivered on paper. This is beneficial to ICAO, as the data accessed via eANP is up to date and accurate, making it a more reliable means of navigation. Through eANP, shown in Figure 61 below, the air navigation systems are being implemented more efficiently at the national, the regional, the interregional, and the global levels. Hence, the Planning and implementation groups are able to take the information and expedited plans according to ICAO priorities. Having this information available online greatly facilitates updating and accessing the latest information for states, the ICAO regional offices, and other authorized users. (Nagle, 2009).

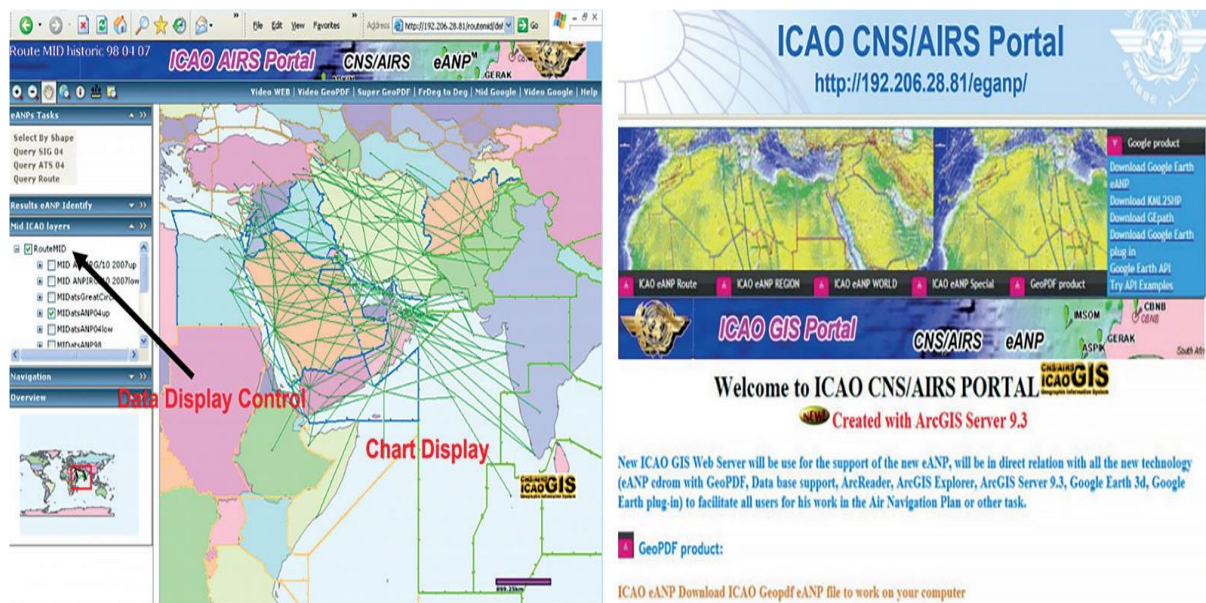


FIGURE 61: THE ARCGIS AIDED EGANP PORTAL OPERATING IN ICAO FOR AUTHORIZED USERS. SOURCE: NAGLE, 'GLOBAL AIR NAVIGATION.'

7.4 The technical differences between the GLS and the ILS insight of the GIS aiding

In terms of technical differences, the GLS system uses the GIS aided precision approach in the FAS, unlike the ILS system. It is important firstly to examine the approach path differences and developments having taken place during the transition period from ILSs to GLSs systems.

Basically, when designing the approach path, many factors should be taken into consideration to ensure a safe path in the last landing phase of a flight, the most important factor being to avoid obstacles, especially the natural non-lighted terrain; it is usually being performed by surveying the space volume within the guidance path in 3D domain. Therefore, it is essential to use the GIS tools due to its flexibility and feasibility of exploring vertical terrain around any approached runway(s).

The VFR procedures and the IFR procedures can be issued easily and used efficiently if the GIS is aided, and they can also be used in case of bad weather using the signals of the existing landing systems. Whatever the type of the used landing system was, either the ILS or the GLS, there are differences in the used signals, but both systems should be capable to support a certain level of performance, which must meet the minimum aeronautical standard requirements contained in the ICAO/FAA documents in such hard Instrument Meteorological Circumstances (IMC). In case of system failure during the FAS, if it is not possible to meet the required performance in such critical moments of bad weather, then a divergence to another airport with better conditions is necessary, and this will cause more expenses and delays in flights.

Actually, there are three modes of phases of flight: the terminal phase mode (both departure and arrival), the Enroute phase mode, and the final approach phase mode, as shown in Figure 62 below. Each phase has the operational requirements of navigation that are supported by a certain type of equipment, as said before: the radio navigation equipment (such as VOR, DME, and ILS) were and still supporting the current flights, they are gradually replaced by the GNSS technical solutions such as ABAS, GBAS, and SBAS systems.

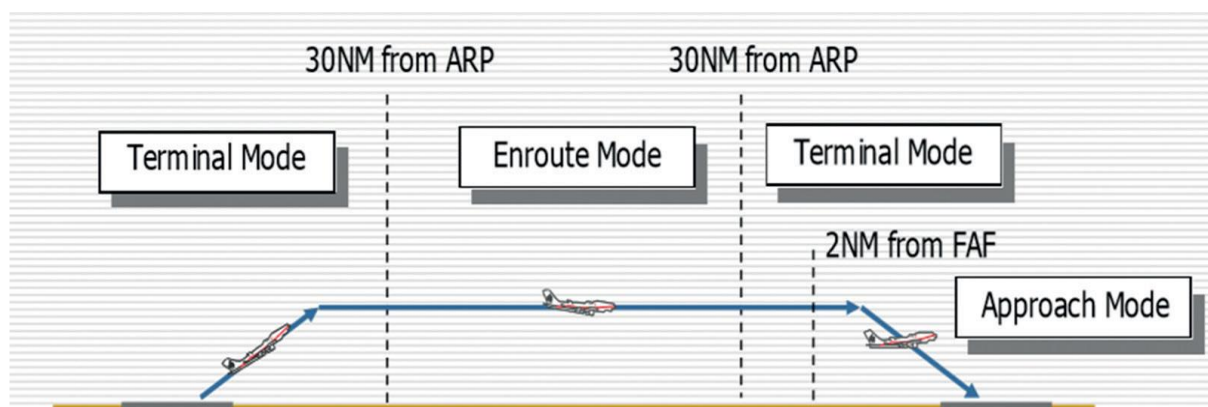


FIGURE 62: THE FLIGHT PHASES MODES. SOURCE: EDITED BY THE AUTHOR

However, in terms of both the Enroute flight phase and the terminal flight phase modes, the main difference between the Conventional Radio-Navigation, that uses the Radio signal, and the new GNSS navigation, that uses the Satellite signals, can be illustrated in Figure 63 below. The main benefits are the shorter route distance, the improved navigation performance, and the avoidance of obstacles, the noise abatement, and the more effective route structure. This will increase the capacity of traffic and decrease the expenses and the delays.

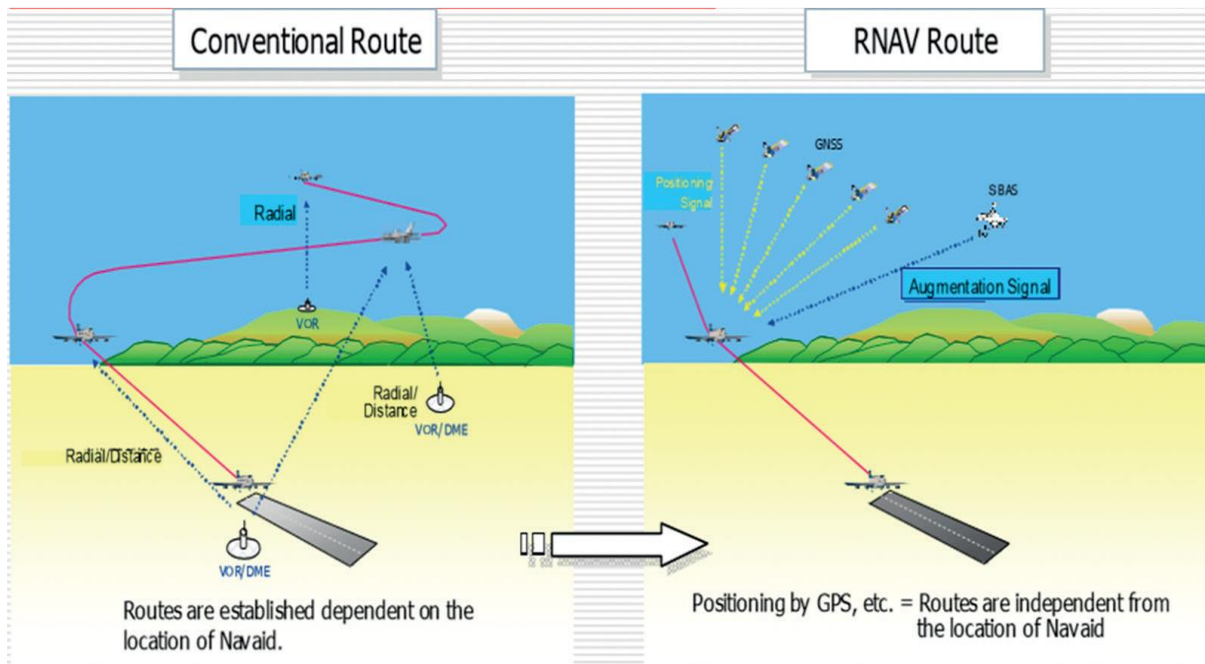


FIGURE 63: THE CONCEPTUAL DIFFERENCE BETWEEN THE RADIO NAVIGATION AND THE GNSS NAVIGATION.
SOURCE: EDITED BY THE AUTHOR

On the other hand, most critical is the last segment of flight, which is the landing phase. In this phase, the obstacle-free path is supported either by Radio-Navigational ILS system, or/and the GNSS Navigational GLS systems using the GIS aiding maps for approach. In the following paragraphs the two systems are illustrated, showing the degree of accuracy in both, assuming that both have advantages and disadvantages that should be taken into consideration. Firstly, and in brief, the ILS system uses the radio propagation of two low frequency signals (150 Hz and 90 Hz) modulated over the main VHF channel. Those two lobes are tightly and geographically linked to the main lateral path of the center line of a given runway and also to the main vertical slope of the gliding angle (nominal 3 degrees). The approaching aircraft

deviates from one side to the another side of two lobes until the Difference of Depth of Modulation (DDM) for both equals to 0, the DDM value of 0 meaning that the electronic path is totally aligned with the geographical center line of the approached runway. Therefore, it is most important that those types of equipment that are subjected to periodical flight checks for calibration processing ensure their accuracy every time they are used. Many types of flight checks can be performed, such as the initial commissioning flight check, the periodic ones, and the maintenance flight checks whenever an amplifier or antennas change. The total ILS system cannot be certified to be safely-used without those flight checks, and it should be done every year at least by a certified flight-checking agency, such as the Federal Aviation Agency (FAA).

In such a system the use of GIS aiding is not so critical, due to the fact that the radiation is well aligned with the needed safely approaching path, which is free of obstacles and clear to land. However, it uses the GIS data in the approach paper plates only, they are not so much linked together. In other words, the ILS system can still be used if there are no certified approach plates in place, because of its independence of the GIS coordinates, since it uses a separate radio propagation method in the landing process. Figure 64 below shows the main idea of the principle of operation and design of the ILS system.

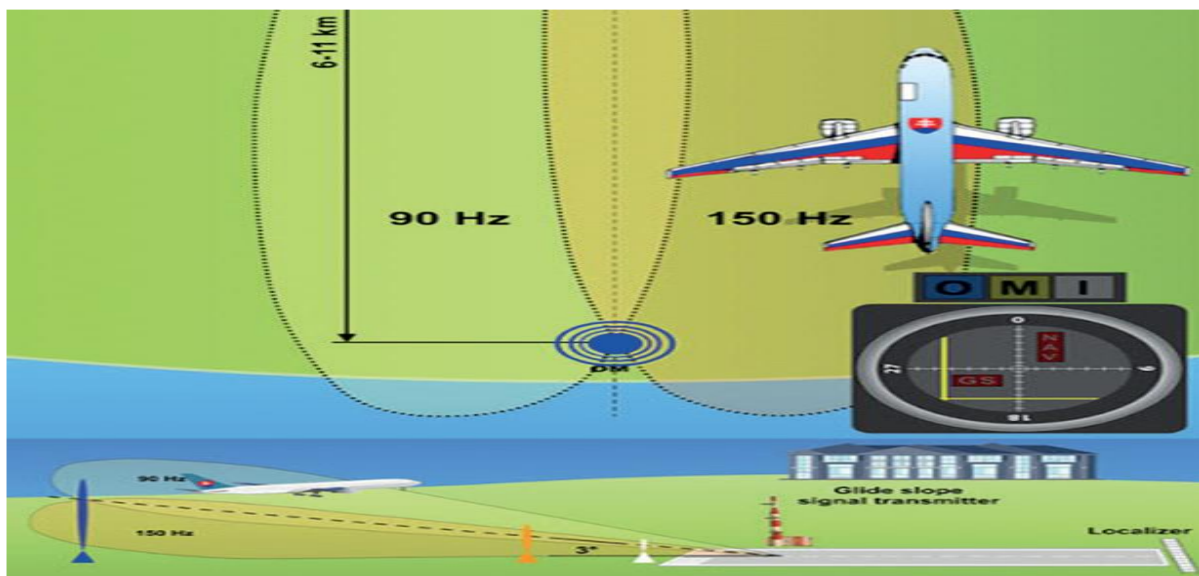


FIGURE 64: THE CONCEPTUAL LANDING PATH PROFILE BY THE RADIO NAVIGATION ILS SYSTEMS. SOURCE: EDITED BY THE AUTHOR

Furthermore, when the approach plates are in place and ready to be used, they must also be flight checked periodically to ensure their compliance with the signals radiated by the ILS

system. Hence, it can be concluded that the ILS systems are not strongly dependent on the GIS system, which is supported by the coordinates of the satellite sensors, but they aid and ease the use of the path data in the VFR flights only. Consequently, it can better describe the idea of the recommended convergence to the new GLS systems, that use the same WGS- 84 coordinates in the Approach Plates, in order to optimize the performance of the landing process and to unify the accuracy factors between both the GLS systems and the GIS-aided Approach Plates, not only in the landing phase, but also in the terminal phase of flight, which comes prior the final approach phase.

On the other hand, the GLS systems are contrary to the ILS systems. They basically use another conceptual path data of landing, which is basically dependent of the Lat. / Long coordinates, and it is fully compliant with the GIS-aided approach plates. Figure 65 below shows the conceptual navigational definition of the final path using both the ILS and the GLS systems, but it is handled differently by the GLS system, (RTCA245A, 2004).

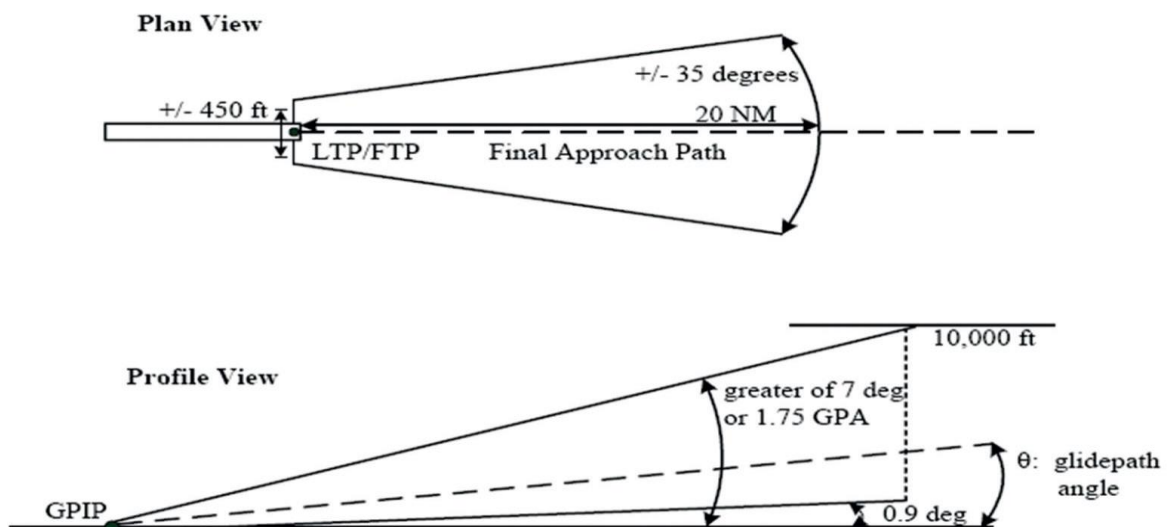


FIGURE 65: THE CONCEPTUAL LANDING PATH PROFILE. SOURCE: 'MINIMUM AVIATION'

By principle, the GLS requires that both the ground and aircraft subsystems use exactly the same ephemeris and satellite clock corrections. Moreover, since the differential principle removes all the ranging errors that are common to the ground and the aircraft subsystems, Ionospheric, Tropospheric or SBAS corrections are not applied by the two subsystems. The main functions of the GBAS Ground Subsystem are summarized as follows: (Alhosban A. , 2015).

- Provide locally relevant pseudorange corrections;
- Provide GBAS related data; and FAS data;
- Provide ranging source availability data; and integrity monitoring for ranging source.

Most importantly and related to this chapter, the GBAS ground subsystem stores data related to the runway end(s), in the form of FAS path construction data blocks. It broadcasts this data continuously for reception by the approaching aircraft. One ground subsystem can support an unlimited number of aircraft subsystems within its service volume. However, each GBAS Station has Data Processing and Integrity Units that are responsible for:

- Satellite signal monitoring; and integrity monitoring functions;
- Code carrier smoothing and differential corrections calculation;
- GBAS messages elaboration (MT1, MT2, MT4), detailed in Table 21 below.

The aircraft subsystem then corrects its own pseudorange measurements for each satellite with the differential correction data received from the ground subsystem. The corrected pseudorange measurements are then used to more accurately determine the aircraft's position relative to the selected Final Approach Segment or Final Approach Path.

Message Type Identifier	Message Name
0	Spare
1	Pseudo-range corrections
2	GBAS-related data
3	Reserved for ground-based ranging source
4	Final Approach Segment (FAS) data
5	Predicted ranging source availability
6	Reserved
7	Reserved for national applications
8	Reserved for test applications
9 – 255	Spare

TABLE 21: GBAS MESSAGES. SOURCE: 'MINIMUM AVIATION'

The Type 4 message contains one or more sets of FAS data, each defining a single precision approach. It includes the following data, among which the most important is the coordinates of the Landing Threshold Point/Fictitious Threshold Point (LTP/FTP):

- Operation type: 0 to 15
- SBAS provider ID: 0 to 15

- Airport ID
- Runway number: 0 to 36
- Runway letter
- Approach performance designator: 0 to 7
- Route indicator
- Reference path data selector: 0 to 48
- Reference path identifier
- *LTP/FTP latitude: $\pm 90.0^\circ$*
- *LTP/FTP longitude: $\pm 180.0^\circ$*
- *LTP/FTP height: -512.0 to $6\ 041.5$ m*
- *FPAP latitude: $\pm 1.0^\circ$*
- *FPAP longitude: $\pm 1.0^\circ$*
- Approach TCH (Note): 0 to 1,638.35 m (0 to 3,276.7 ft.)
- Approach TCH units' selector
- GPA: 0 to 90.0°
- Course width: 80 to 143.75 m
- Length offset: 0 to 2,032 m
- Final Approach Segment CRC

Based on the above description, it is clear that the GLS/GBAS system is fully capable of more suitable operation by the GIS-aided precision approach procedures than the conventional ILS systems. With that said, the following section will show more about how precise the landing process is, using both systems based on experimental real flight results.

7.5 Assessment of the future performance of the GBAS Landing System (GLS)

In this section, a better CAT I (GAST-C) performance of GLS systems over the ILS systems in the GIS-aided FAS segment is assumed. The rationale behind this assumption is justified by the evidence of the global and domestic practices of the authorized civil aviation controls. Many airports are currently using the GLS systems along with the ILS systems specifically in the transition period until 2030. See (GBAS installations,' Google Maps). The local civil Aviation authorities differ in the level of degree of their usages' dependent, some of them are using GLSs as main system with ILSs as alternative systems during such transition period, and others do the opposite.

However, many researches were performed on CAT II/III (GAST-D/F) performance level, but they still under certification process. Up to date, the ILS systems showed better accuracy and availability performance level than GLSs in CAT II/III requirements, although they are not using the GIS aided precision approach techniques. When the GIS aided approach paths are to be used in CAT II/III performance, then the ILSs are assumed not to be fully compliant with them, due to the fact that they are using the RF radiations other than the Satellite Coordinates supported by the GIS in WGS-84 format. Hence the GLS systems would be of a better performance instead if they were able to be certified. The GLS certification is a matter of the dual satellite constellation and dual frequency dependent, and other factors. Globally, many GBAS landing systems had been installed and operated since it was fully certified in 2012 as CAT I performance. To date, more than 130 stations were deployed all over the world, some are working properly as CAT I (GAST-C) and are fully operational. This service type supports operations equivalent to a CAT-I instrument landing system (ILS) with a minimum decision height of 200 ft. and a runway visual range of at least 550 m. It is located in Bremen (ICAO identifier EDDW) in northern Germany, and since then it is regularly used by Air Berlin, which

has equipped a large portion of their B737-NG fleet. Other airports like Zurich and Frankfurt am Main are currently installing the systems.

A number of trial GBAS stations with different levels of progress toward certification had been set up in several countries including Spain, France, Australia, Germany and Russia. Furthermore, Figure 66 below shows how much the installations have been spread worldwide.



FIGURE 66: THE GBAS LANDING SYSTEMS INSTALLATION MAP WORLDWIDE. SOURCE: 'GBAS INSTALLATIONS'

As for the local perspective, a previous study (Jeong, 2016) has recently indicated that there are differences in the ways the ILS and GBAS offer approach guidance, and in their principles and methods. In that study, a comparative analysis was performed on the accuracy of deviation between the GBAS Landing System (GLS) and ILS by means of flight tests, using the flight inspection aircraft at Gimpo International Airport in South Korea. The results of the study showed that the ILS deviation error increases as the distance between the threshold of runway and the aircraft increases; on the other hand, the GLS deviation error is stable, within the range of ± 0.5 to ± 2 m lateral and vertical deviation, respectively. The results are shown in Figure 67 below. Furthermore, many other studies in the USA, Germany, France and other countries had showed the same results, or even better results from the same aspect. This approves the

assumption that we started with above, that is, the GLS would be better in terms of accuracy if it was aided by the GIS.

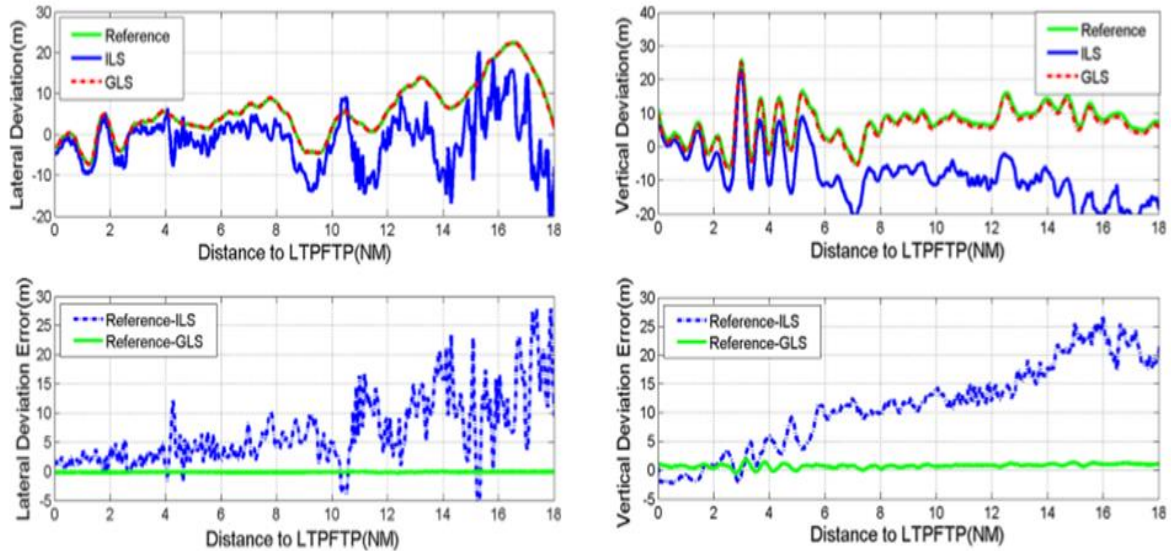


FIGURE 67: THE DEVIATION AND THE ERRORS OF THE GLS AND ILS SYSTEMS, REFERENCED TO LATERAL AND VERTICAL GUIDANCE. SOURCE: JEONG, BAE, JUN AND LEE, 'FLIGHT TEST EVALUATION.'

7.5.1 Result Analysis:

Based on the results above, it is pretty proved that the GLS system are better in CAT I performance level than the ILS systems, due to the fact that the GIS aided approaches with WGS-84 coordinate system work better with the GLSs. Based on this interpretation, we can apply these outcomes on the BUD airport in Budapest Hungary.

7.6 Special case implementation: Budapest Airport

Therefore, according to the BUD airport data listed in the official websites referenced in the website of *Hungarocontrol*, <https://ais.hungarocontrol.hu/aip/2018-05-24/>, it is clearly approved that the BUD airport approach procedures use the Radio Navigation (RNAV) performance that depend on the GIS WGS-84 coordinate system, which is implemented in both the Terminal and the Final approach modes of flight, while there is no GBAS Landing system in place yet, as per the updated Hungarocontrol website seen above. The existing operated landing system is only the ILS system. According to a previous study (Alhosban A. , 2019)on

the availability of the GBAS signals in the BUD airport as a part of the European area, a simulator tool was used for this purpose. The results showed the capacity of using the GLSS not even in CAT I performance, but also in CAT II as well. Namely, this resulted in the chance feasibility of more investment in installing a GBAS station in Budapest international Airport, for the sake of having more accurate approaches and enhanced capacity of its air traffic management. Furthermore, it can be applied in military airports for night flights as well. Figure 68 below.

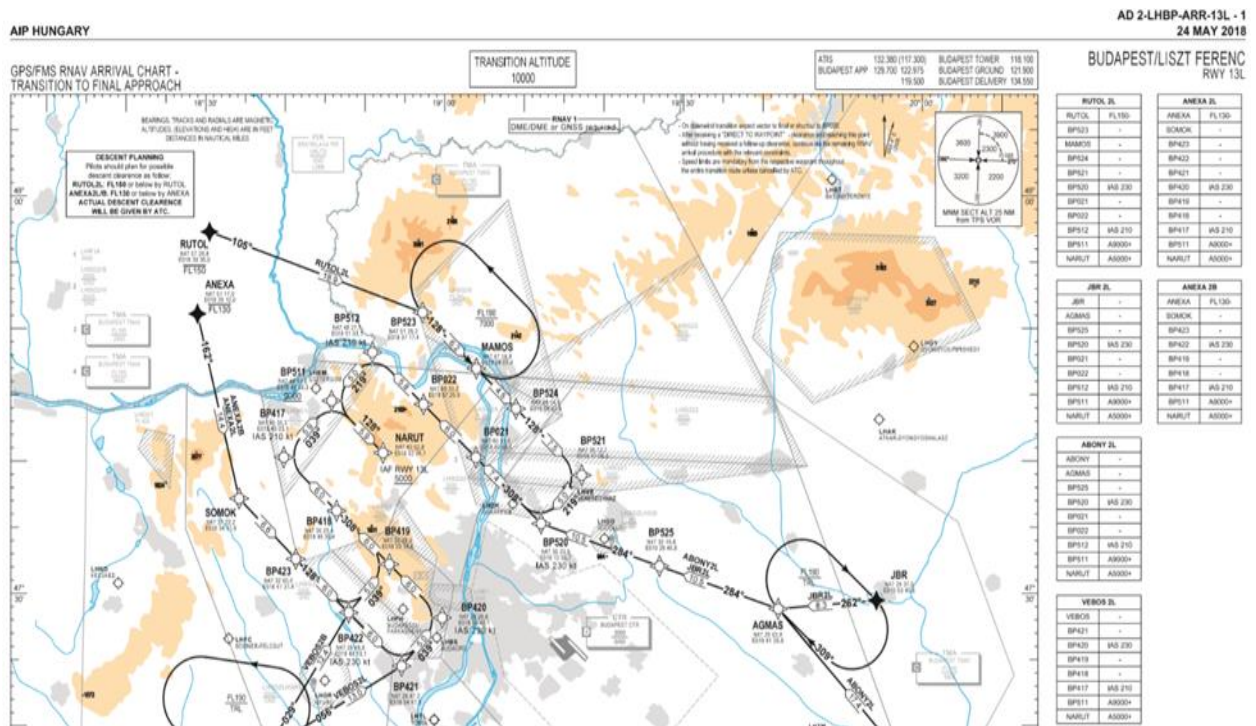


FIGURE 68: THE TERMINAL RNAV DATA FOR BUD AIRPORT 13L INCLUDING THREE HOLDING AREAS FOR TRANSITION TO FAS. SOURCE: [HTTPS:// AIS.HUNGAROCONTROL.HU/AIP/2018-05-24/2018-05-24-AIRAC/GRAPHICS/EAIP/LH_AD_2_LHBP_ARR_13L_EN.PDF](https://ais.hungarocontrol.hu/AIP/2018-05-24/2018-05-24-AIRAC/GRAPHICS/EAIP/LH_AD_2_LHBP_ARR_13L_EN.PDF)

In terms of existing infrastructure for Budapest airport BUD, the following figures, taken from the updated official website and published since May 2018, show the Terminal and the Final approach RNAV data. Hence, in Figure 66 above, there are three GIS aided holding areas in the terminal mode prior to the FAS mode for the east end 13L in the BUD airport; they can be reached by either the SBAS or GPS on-board systems in the approaching aircraft. The holding areas are used in case of heavy traffic, to delay the coming aircrafts until the runway is clear to land. Figure 69 below shows the final approach segment data. It contains four (4) Way Points (WP); the three Initial Approach Final (IAF) WPs correspond to the three potential coming

directions: the straightforward WP is named NARUT, the left one GIGAN, and the right one KESID. All the three WPs lead the approaching aircraft to the Initial Final (IF) WP, which is the start point to the FAS descending glide path, where the ILS and the GLS are used in bad weather of low visibility. All those four points are designed obstacle-free for the east direction of the runway called 13 (130 degrees to the east), as are the west approach end, 31L/R (310 degrees to the west), in order to cover both ends of the runway. For sake of simplicity and due to the similarity, the west end part of the runway was not intended to be mentioned in this dissertation.

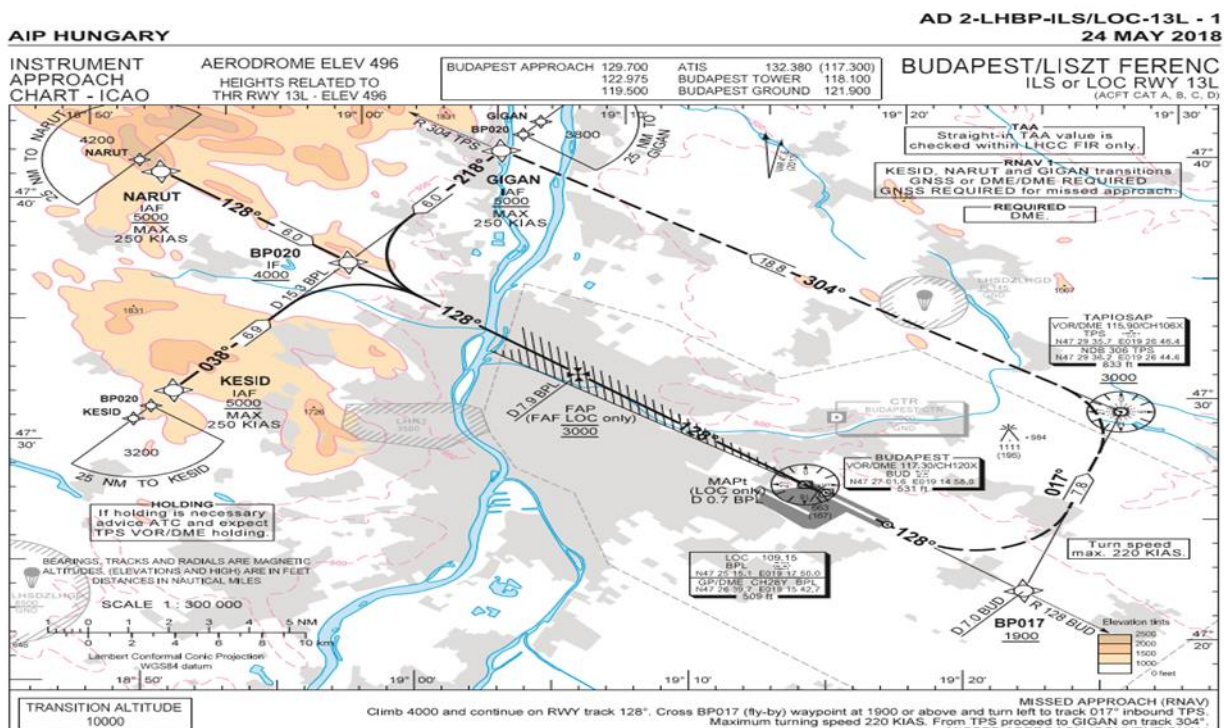


FIGURE 69: THE START OF THE FINAL APPROACH SEGMENT INSTRUMENT RNAV DATA FOR BUD AIRPORT 13L. SOURCE: https://ais.hungarocontrol.hu/aip/2018-05-24/2018-05-24-AIRAC/GRAPHICS/EAIP/LH_AD_2_LHBP_ILS_OR_LOC_13L_EN.PDF

Finally, as shown in Figure 70 below, the final approach fix (FAF) started to be used in the final segment, extended to the 13R Runway’s Touch Height (TCH) point called MAPT, which is supposed to be 200ft. above the runway threshold point as per CAT I performance in IFR flights. The direction of landing is 128 degrees, almost 130 degrees, the slope between the two points from the IF WP to the RWY13 R/L would be 3 degrees. In this final segment, the use of ILS or GLS is linked to the availability of integrity, accuracy and continuity of the system,

especially in bad weather or night flights. From this, the GLS system performance was approved to be better than the ILS systems.

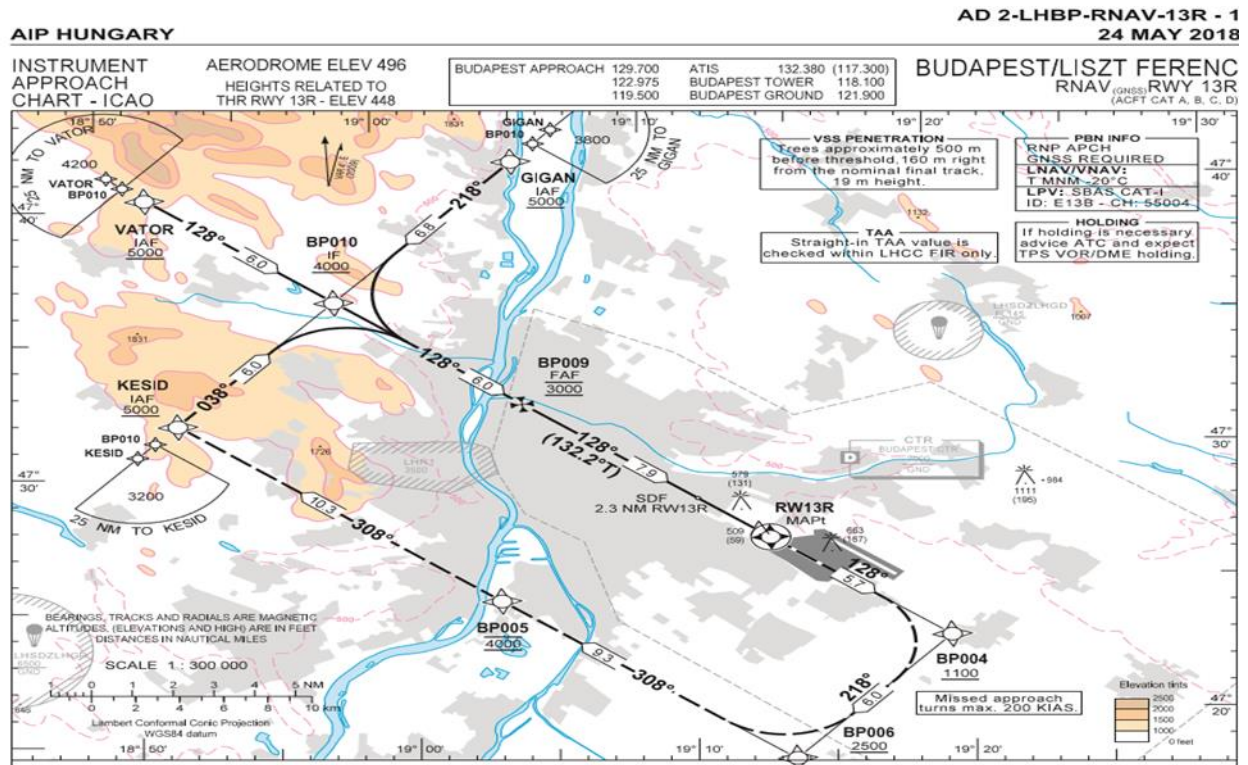


FIGURE 70: THE FINAL APPROACH SEGMENT INSTRUMENT RNAV DATA FOR BUD AIRPORT 13L. SOURCE: [HTTPS://AIS.HUNGAROCONTROL.HU/AIP/2018-05-24/2018-05-24-AIRAC/GRAPHICS/EAIP/LH_AD_2_LHBP_RNAV_13R_EN.PDF](https://ais.hungarocontrol.hu/aip/2018-05-24/2018-05-24-AIRAC/GRAPHICS/EAIP/LH_AD_2_LHBP_RNAV_13R_EN.PDF)

7.6.1 Results Analysis:

- According to the BUD airport data listed in the official websites referenced in the website of *Hungarocontrol*, <https://ais.hungarocontrol.hu/aip/2018-05-24/>, it is clearly approved that the BUD airport approach procedures use the Radio Navigation (RNAV) performance that depend on the GIS WGS-84 coordinate system, which is implemented in both the Terminal and the Final approach modes of flight, while there is no GBAS Landing system in place yet, but ILS only.
- There is a chance feasibility of more investment in installing a GBAS station in Budapest international Airport, for the sake of having more accurate approaches and enhanced capacity of its air traffic management. Furthermore, it can be applied in military airports for night flights as well.

- As per the existing infrastructure for Budapest airport BUD, the Terminal and the Final approach RNAV data shows that there are three GIS aided holding areas in the terminal mode prior to the FAS mode for the east end 13L in the BUD airport; they can be reached by either the SBAS or GPS on-board systems in the approaching aircraft, the holding areas are used in case of heavy traffic, to delay the coming aircrafts until the runway is clear to land.
- The use of ILS or GLS is linked to the availability of integrity, accuracy and continuity of the system, especially in bad weather or night flights. From this, the GLS system performance was approved to be better than the ILS systems.

7.7 Conclusions and Recommendations

- In conclusion, according to the analysis done on the availability of the GIS aiding maps for the Terminal and Final Approach modes of flights in BUD airport, using the GLS system is feasible and more accurate, not even in CAT I performance, but also in CAT II as well. This feasibility leads to the chance of more investment in installing a GBAS Landing System (GLS) station in Budapest international Airport (BUD), for the sake of having more accurate approaches and enhanced capacity of its air traffic management. Furthermore, it can be recommended that those GLS systems can be applied in military airports for night flights as well. However, there is a technical feasibility of installing a GBAS station in Budapest International Airport in the performance of GAST-D/F, it can be adopted - as many civil aviation authorities adopted – as an alternative usage of the GLS system side by side with the existing ILS system, in order to make easier the gradual transition to the potentially coming GLS systems. Many benefits can be achieved in terms of cost effectiveness, capacity increase, and enhanced performance. Also As per the existing infrastructure for Budapest airport BUD, the Terminal and the Final approach RNAV data shows that there are three GIS aided holding areas in the terminal mode prior to the FAS mode for the east end 13L in the BUD airport; they can be reached by either the SBAS or GPS on-board systems in the approaching aircraft.

7.7.1 The New Achieved Scientific Result

New scientific result # 5: I have approved that there is a feasibility of installing a GBAS station in Budapest International Airport, for the sake of having more accurate approaches and enhanced capacity of its air traffic management, In addition, I have approved that the GBAS system performance will be better than the existing ILS systems in Budapest airport, which is characterized being a new result, validated and geographically approved, it is not being conducted by any other researchers in this domain yet.

7.7.2 Recommendations

I recommend that there is a technical feasibility of installing a GBAS station in Budapest International Airport in the performance of GAST-D/F, it can be adopted - as many civil aviation authorities adopted – as an alternative usage of the GLS system side by side with the existing ILS system, in order to make easier the gradual transition to the potentially coming GLS systems. Many benefits can be achieved in terms of cost effectiveness, capacity increase, and enhanced performance.

Chapter 8: Summarized Conclusions, and Recommendations

8.1 Introduction

In this chapter, I concluded all my new achieved scientific results of this dissertation hereby, then the hypotheses were answered, and finally the practical availability of the scientific results and recommendations are stated.

8.2 The New Achieved Scientific Results

Most importantly to be mentioned is that all of this dissertation achieved scientific results were published in peer-reviewed Journals, the publications were continuously and timely performed as the progress of the research went on. The time schedule of the research during the 4-year research plan was conducted and supervised carefully, trying to mitigate all the difficulties and to overcome all the challenges that faced this work. All the efforts led to the success of showing up the following achieved new scientific results in the domain of GNSS/GBAS landing systems, which contribute directly and seriously to the aviation worthiness and safety.

The new achieved scientific results are:

1. New scientific result # 1a: Global coverage: I have approved that the global availability of the GBAS Landing System in GAST-D/F performance of 99.99% using a single constellation simulator (Galileo or GPS) is not feasible in Single Constellation/ Dual Frequency SC/DF, but Galileo is more visible when CB-DF precision configuration is reached, which is characterized being newly updated result than a recently announced in 2020 by ICAO in Annex 10/V.1/Amendment 92. It is more precise and fully validated than the previously conducted studies.

New scientific result # 1b: Regional coverage: I have innovated a regional coverage selection, and I approved that Galileo constellation is able to fulfil the aeronautical requirements of both 99.99% and 99.75% (GAST-D/E/F) over Europe sky using GBAS precise configuration of CB-DF, and it is very close (99.404%) over USA, but the GPS constellation is not able to fulfil these requirements, which is characterized being a new,

approved, validated and efficient regional operational concept of GBAS system not being conducted by any other previously studies except as individual airports.

2. The new scientific result # 2: I have developed a structural Matlab software of nearly 1000 code lines to assess the impact of the new BOC signals and filters on the MEE errors in the GPS receivers based on the theoretical multipath error equations, which is characterized being a new, validated, more comprehensive and more customized software than those being recently used by the Chinese researchers in 2020. It is more capable of being customized to assess any new GPS signal process analysis in the future.
3. New scientific result # 3: I have developed a new methodology in assessing the impact of the Electronic Attacks on the GPS signal using the Multipath analogy approach in terms of power level, time of action and data affecting, which is characterized being a new methodology and more efficient than other empirical assessing methods in GBAS protection domain. It assesses by a simulating tool to which level of protection is needed in each configuration.
4. New scientific result # 4: I have approved that the innovated Denning Geo-Encryption model and its mobility enhancement is not efficient in flight modes, it cannot be characterized to be safely used in approach and landing phases due to the high speed mobility of the landing aircrafts, vulnerable and weak GPS signal, slow navigational message update rate, and the wind-varying descent speed. But it can be used with more added value in stationary or semi-moving modes only, which is characterized being safer and less risky than the similar geo-encryption mobility model created by Alfugaha model.
5. New scientific result # 5: I have approved that there is a feasibility of installing a GBAS station in Budapest International Airport, for the sake of having more accurate approaches and enhanced capacity of its air traffic management, In addition, I have approved that the GBAS system performance will be better than the existing ILS systems in Budapest airport, which is characterized being a new result, validated and geographically approved, it is not being conducted by any other researchers in this domain yet.

8.3 Hypotheses' Answers

The answers for the hypotheses addressed in chapter 1 table 1 are as seen in table 2 below:

#	Hypothesis	Results after testing
1	Single GNSS GBAS systems are capable to achieve GAST-D/F global performance in landing operations.	No , but Regionally only
2	Galileo/GPS each alone is capable to achieve GAST-D/F regional performance in Landing operations.	<ul style="list-style-type: none"> Galileo: Yes, over Europe, and very close globally. GPS: Neither globally Nor regionally
3	Galileo is more immune to Electronic Attacks than GPS	Yes
4	GEO- Encryption is not efficient with high speed mobility of the landing aircrafts that using GNSS.	Yes
5	GNSS Landing Systems (GLSs) have better performance with Geographic Information system (GIS) approaches plates than conventional ILSs.	Yes

TABLE 22: HYPOTHESES' ANSWERS

8.4 Practical Availability of the Scientific Results and Recommendations

This dissertation long study is a continuation of a previous master study in 2006 in France, on the same aspect of assessing the Impact of GPS errors on GBAS landing System, but in Performance CAT II or GAST D. that master study recommended at that time, along with adjacent similar studies worldwide, to certify the GNSS GBAS Landing system to be operated in CAT II/GAST-D performance. Recently, in 2020, ICAO has certified it, and finally it saw the light successfully, but not in CAT III/ GAST-F performance, the CAT III /GAST –F performance is not foreseeable to be certified as per ICAO unless dual constellation (by adding Galileo GNSS system) is being used for this purpose.

Consequently, in this Dissertation research, and based on my achieved and approved scientific results, I recommend ICAO to certify the GBAS Landing system in CAT III/GAST-F performance using a single constellation of Galileo or GPS also. At least, it can be certified to

be operated regionally over Europe/or over a Single Airport like Budapest Airport using the European Galileo constellation. In addition, I encourage researchers worldwide to perform similar researches in the same domain to support my findings and recommendations.

Detailed technical recommendations are listed in each chapter in this dissertation, and they are summarized as below:

- I recommend that a further investigations in this aspect is recommended when Galileo system comes to its full operation capability of 30 satellites. As well as the modernized GPS Block III comes to its full 20 satellites capability, this would be anticipated by 2025.
- I recommend to use the developed Matlab software for researches in MEE assessment in GBAS applications. Because it is capable to be customized and improved for more purposes due to its simple structure and its dependency on different sub function that can added easily according to the needed mission
- I recommend using the analogy method of interference between the unintentional multipath error and the intentional electronic attacks in order to assess to which extent the electronic equipment could be affected constructively or destructively.
- I recommend that further investigations of such better concept of geo-encryption in flight phases should be conducted by experimental flight tests, which is beyond the capability of the scope of this PhD Dissertation.
- I recommend that there is a technical feasibility of installing a GBAS station in Budapest International Airport in the performance of GAST-D/F, it can be adopted - as many civil aviation authorities adopted – as an alternative usage of the GLS system side by side with the existing ILS system, in order to make easier the gradual transition to the potentially coming GLS systems. Many benefits can be achieved in terms of cost effectiveness, capacity increase, and enhanced performance.

With that is being said, I reach to the end of my dissertation for this PhD Degree in UPS/NKE University at Budapest Hungary.

This page is intentionally left blank

Table of Figures

FIGURE 1: THE REQUIRED AERONAUTICAL REQUIREMENTS FOR ILS/GBAS LANDING SYSTEMS [OPEN SOURCE]..	15
FIGURE 2: DISSERTATION PROGRESS (RESEARCH ACTIVITIES PHASE V _s ACADEMIC PHASE)	22
FIGURE 3 : NEW MODERN GNSS SIGNAL STRUCTURE ((B. EISSFELLER, 2007)	29
FIGURE 4. COLLISION OF THE NORWEGIAN FRIGATE “KNM HELGE INGSTAD” AFP (SEIDEL J. , 2018)	35
FIGURE 5: GBAS SYSTEM INFRASTRUCTURE OVERVIEW [EDITED BY AUTHOR].....	40
FIGURE 6: MITIGATED GAD GROUND ACCURACY DESIGNATOR CONFIGURATION [EDITED BY AUTHOR]	49
FIGURE 7: MITIGATED AAD (LEFT)/AMD (RIGHT) ACCURACY DESIGNATORS CONFIGURATION [EDITED BY AUTHOR]	49
FIGURE 8: SIMULATION GROUP TREE COMBINATIONS [EDITED BY AUTHOR]	53
FIGURE 9: AVIGA STEP 1: TRAJECTORY CALCULATION [EDITED BY AUTHOR].....	55
FIGURE 10: AVIGA STEP 2: SPECIFIC OPERATION CALCULATION [EDITED BY AUTHOR]	55
FIGURE 11: AVIGA GBAS MODEL SCHEME/ ALGORITHM [AS PER DESIGNER].....	55
FIGURE 12: MAIN RESULTS AVAILABILITY AGAINST USER MULTIPATH ERROR FOR GPS / GALILEO [EDITED BY AUTHOR]	58
FIGURE 13: 3D GLOBALLY AVAILABILITY FOR GALILEO [EDITED BY AUTHOR]	64
FIGURE 14: 2D GLOBALLY AVAILABILITY FOR GALILEO [EDITED BY AUTHOR]	64
FIGURE 15: AVAILABILITY OVER EUROPE 30N TO 70N, 5°X5° GRID FOR GALILEO [EDITED BY AUTHOR]	65
FIGURE 16: AVAILABILITY OVER EUROPE 30N TO 70N, 2°X2° GRID FOR GALILEO [EDITED BY AUTHOR]	66
FIGURE 17: AVAILABILITY OVER EXACT EUROPE 39N TO 70N, GRID 5°X5°, AND 2°X2° FOR GALILEO [EDITED BY AUTHOR].....	67
FIGURE 18: DISCRIMINATOR AFFECTED BY MULTIPATH [EDITED BY AUTHOR].....	73
FIGURE 19: LEFT PANEL: NEW MODERN GNSS SIGNAL STRUCTURE [16], RIGHT PANEL: EFFECT ON THE AUTOCORRELATION FUNCTION ACF [EDITED BY THE AUTHOR].....	75
FIGURE 20: EFFECT OF BOC AND BPSK ON THE MULTIPATH ERROR ENVELOPE MEE [OPEN SOURCE, EDITED BY AUTHOR].....	76
FIGURE 21: BLOCK DIAGRAM FOR GENERAL GNSS RECEIVER [EDITED BY AUTHOR]	77
FIGURE 22: COSTAS PLL LOOP [EDITED BY AUTHOR].....	79
FIGURE 23: NON COHERENT DLL LOOP [EDITED BY AUTHOR]	82
FIGURE 24: CORRELATION PROCESS [EDITED BY AUTHOR].....	84
FIGURE 25: COHERENT DLL LOOP [EDITED BY AUTHOR]	85
FIGURE 26: CODE ERROR ENVELOPE OF THE MULTIPATH [EDITED BY AUTHOR]	86
FIGURE 27: ERROR FINDING FUNCTION AND ENVELOPE ERROR FLOWCHART [EDITED BY AUTHOR]	88
FIGURE 28: ERROR – FINDING FUNCTION FLOW CHART [EDITED BY AUTHOR]	89
FIGURE 29: COMPARISON WITH SIMILAR SOFTWARE [EDITED BY AUTHOR]	90
FIGURE 30: BPSK, CODE MULTIPATH ERROR ENVELOPES [EDITED BY AUTHOR]	91
FIGURE 31: BOC (1, 1), CODE MULTIPATH ERROR ENVELOPES [EDITED BY AUTHOR].....	92
FIGURE 32: BOC (2, 2), CODE MULTIPATH ERROR ENVELOPES [EDITED BY AUTHOR].....	92
FIGURE 33: BPSK, PHASE MULTIPATH ERROR ENVELOPES [EDITED BY AUTHOR].....	93
FIGURE 34: BPSK, CODE MULTIPATH ERROR ENVELOPES/DIFFERENT FILTERS [EDITED BY AUTHOR].....	94
FIGURE 35: BPSK, DISCRIMINATOR DELAY DUE TO FILTER [EDITED BY AUTHOR]	95
FIGURE 36: BPSK, IMPACT OF THE FILTER BANDWIDTH [EDITED BY AUTHOR].....	96
FIGURE 37: THE NORWEGIAN FRIGATE SUFFERED NAVIGATION FAILURE [(SEIDEL, 2018)].....	101
FIGURE 38: NEWARK AIRPORT LAYOUT (EDITED BY THE AUTHOR)	103
FIGURE 39: LAYOUT OF LISZT FERENC AIRPORT AT BUDAPEST (EDITED BY THE AUTHOR)	103
FIGURE 40: GBAS SYSTEM LINKS, [EDITED BY AUTHOR]	106
FIGURE 41: GPS CODING STRUCTURE [(B. HOFMANN-WELLENHOF, 2001)].....	107
FIGURE 42: GPS SIGNAL COMPONENTS [(B. HOFMANN-WELLENHOF, 2001)]	108
FIGURE 43: NEW MODERN GNSS SIGNAL STRUCTURE [(B. EISSFELLER, 2007)]	109
FIGURE 44: GPS SIGNAL PROCESSING FLOWCHART [(B. HOFMANN-WELLENHOF, 2001)].....	110

FIGURE 45: PPDs LOW POWER WIDELY AVAILABLE [(INSIDEGNSS, GNSS JAMMING AND SPOOFING: HAZARD OR HYPE?, 2018)]	111
FIGURE 46: THE SIMULATED AREAS IN EUROPE AND USA [(ALHOSBAN A. , 2015)].....	116
FIGURE 47: SIMULATION RESULTS [EDITED BY THE AUTHOR]	117
FIGURE 48: CURVED B NAVSYS PROTOTYPE 3-D 7-ELEMENT [(ALHOSBAN A. , 2015)]	119
FIGURE 49: GALILEO AND GPS NEW FREQUENCY PLAN FOR DIFFERENT SERVICES [(OFFICIALUSGOVGPS, 2019) (ESA, GALILEO_FUTURE_AND_EVOLUTIONS, 2018)]	120
FIGURE 50: THE GEO-CODEX GEO-ENCRYPTION ALGORITHM (DENNING&SCOTT, 2003)	124
FIGURE 51: THE PVT GEO-LOCK MAPPING (DENNING&SCOTT, 2003)	125
FIGURE 52: THE SUCCESSIVE PVT GEO-LOCK WAYPOINTS: ENCRYPTED (LEFT PANEL), DECRYPTED (RIGHT PANEL) (DENNING&SCOTT, 2003)	126
FIGURE 53: THE SUCCESSIVE PVT GEO-LOCK WAYPOINTS TO SECURE THE INFORMATION IN A PREDEFINED ROUTE OF POLYGON SHAPE, (LEFT PANEL) (DENNING&SCOTT, 2003) MODEL, DIAGRAM ILLUSTRATING THE FOUR MOBILITY PARAMETERS OF AN ELLIPSE ZONE SHAPE: VELOCITY (V), DIRECTION (θ), SPEED MANOEUVRABILITY (Y -AXIS B), AND BREADTH MANOEUVRABILITY (X -AXIS A), (RIGHT PANEL) (AL-FUQAHA, 2007) MODEL.....	127
FIGURE 54: GPS CODING STRUCTURE (LEFT PANEL), GPS SIGNAL COMPONENTS (RIGHT PANEL) HOFMANN (2001).....	129
FIGURE 55: THE FLIGHT PHASES MODES (EDITED BY AUTHOR)	133
FIGURE 56: THE TERMINAL RNAV DATA FOR BUD AIRPORT 13L INCLUDING THREE HOLDING AREAS FOR TRANSITION TO FAS	133
FIGURE 57: THE START OF THE FINAL APPROACH SEGMENT INSTRUMENT RNAV DATA FOR BUD AIRPORT 13L	134
FIGURE 58: THE FINAL APPROACH SEGMENT INSTRUMENT RNAV DATA FOR BUD AIRPORT 13L	135
FIGURE 59: THE WIND IMPACT IN THE DESCENT SPEED [(AIRBUS, 2017)]	137
FIGURE 60: ON THE LEFT: ARIAL PHOTO OF BUD AIRPORT. ON THE RIGHT: VISUAL APPROACH CHART FOR BUD. SOURCE: ‘AIRPORT INFORMATION / VISUAL APPROACH CHART.’	144
FIGURE 61: THE ARCGIS AIDED EGANP PORTAL OPERATING IN ICAO FOR AUTHORIZED USERS. SOURCE: NAGLE, ‘GLOBAL AIR NAVIGATION.’	145
FIGURE 62: THE FLIGHT PHASES MODES. SOURCE: EDITED BY THE AUTHOR	146
FIGURE 63: THE CONCEPTUAL DIFFERENCE BETWEEN THE RADIO NAVIGATION AND THE GNSS NAVIGATION. SOURCE: EDITED BY THE AUTHOR	147
FIGURE 64: THE CONCEPTUAL LANDING PATH PROFILE BY THE RADIO NAVIGATION ILS SYSTEMS. SOURCE: EDITED BY THE AUTHOR	148
FIGURE 65: THE CONCEPTUAL LANDING PATH PROFILE. SOURCE: ‘MINIMUM AVIATION’	149
FIGURE 66: THE GBAS LANDING SYSTEMS INSTALLATION MAP WORLDWIDE. SOURCE: ‘GBAS INSTALLATIONS’	153
FIGURE 67: THE DEVIATION AND THE ERRORS OF THE GLS AND ILS SYSTEMS, REFERENCED TO LATERAL AND VERTICAL GUIDANCE. SOURCE: JEONG, BAE, JUN AND LEE, ‘FLIGHT TEST EVALUATION.’	154
FIGURE 68: THE TERMINAL RNAV DATA FOR BUD AIRPORT 13L INCLUDING THREE HOLDING AREAS FOR TRANSITION TO FAS. SOURCE: HTTPS://AIS.HUNGAROCONTROL.HU/AIP/2018-05-24/2018-05-24-AIRAC/GRAPHICS/Eaip/LH_AD_2_LHBP_ARR_13L_EN.PDF	155
FIGURE 69: THE START OF THE FINAL APPROACH SEGMENT INSTRUMENT RNAV DATA FOR BUD AIRPORT 13L. SOURCE: HTTPS://AIS.HUNGAROCONTROL.HU/AIP/2018-05-24/2018-05-24-AIRAC/GRAPHICS/Eaip/LH_AD_2_LHBP_ILS_OR_LOC_13L_EN.PDF	156
FIGURE 70: THE FINAL APPROACH SEGMENT INSTRUMENT RNAV DATA FOR BUD AIRPORT 13L. SOURCE: HTTPS://AIS.HUNGAROCONTROL.HU/AIP/2018-05-24/2018-05-24-AIRAC/GRAPHICS/Eaip/LH_AD_2_LHBP_RNAV_13R_EN.PDF	157

Table of Tables

TABLE 1: RESEARCH HYPOTHESES	21
TABLE 2: DISSERTATION STRUCTURE (CHAPTERS VERSUS OBJECTIVES)	22
TABLE 3. EUROPEAN RATIONALE SUMMARY [COMPILED BY THE AUTHOR]	34
TABLE 4: <i>GSL REQUIRED PERFORMANCE [EDITED BY AUTHOR]</i>	41
TABLE 5: <i>GBAS REQUIRED AVAILABILITY PERFORMANCE</i>	42
TABLE 6: <i>RANGING MEASUREMENT PERFORMANCE</i>	46
TABLE 7: <i>BASIC GBAS PERFORMANCE (LOW ACCURACY/SINGLE FREQUENCY)</i>	48
TABLE 8: <i>ADVANCED GBAS PERFORMANCE (HIGH ACCURACY/DUAL FREQUENCY)</i>	48
TABLE 9: <i>IONOSPHERIC AND TROPOSPHERIC PARAMETERS' ASSUMPTION [EDITED BY AUTHOR]</i>	50
TABLE 10: <i>COMMON PARAMETERS' ASSUMPTIONS [EDITED BY AUTHOR]</i>	51
TABLE 11: <i>THE AVERAGE TIME THAT NEEDED FOR EACH SIMULATION PROCESS [EDITED BY AUTHOR]</i>	54
TABLE 12: <i>THE PERFORMED NUMBER OF SIMULATIONS' RUNS [EDITED BY AUTHOR]</i>	54
TABLE 13: <i>THE INPUT PARAMETERS VARIATION [EDITED BY AUTHOR]</i>	56
TABLE 14: <i>THE MEANING OF THE ABBREVIATIONS OF INPUT PARAMETERS VARIATION [EDITED BY AUTHOR]</i>	56
TABLE 15: <i>GBAS AVAILABILITY FOR GALILEO CONSTELLATION [EDITED BY AUTHOR]</i>	57
TABLE 16: <i>GBAS AVAILABILITY FOR GPS CONSTELLATION [EDITED BY AUTHOR]</i>	57
TABLE 17: <i>UMPE MITIGATION LEVELS NEEDED TO MEET REQUIREMENTS PER CONFIGURATION [EDITED BY AUTHOR]</i>	59
TABLE 18: <i>S/N RATIO AGAINST EAS IN CORRELATION TECHNIQUES [(B. HOFMANN-WELLENHOF, 2001)]</i>	110
TABLE 19: <i>COMPARISON TABLE BETWEEN EAS AND MULTIPATH [EDITED BY THE AUTHOR]</i>	114
TABLE 20: <i>AMD PARAMETERS [(ALHOSBAN A. , 2015)]</i>	115
TABLE 21: <i>GBAS MESSAGES. SOURCE: 'MINIMUM AVIATION'</i>	150
TABLE 22: <i>HYPOTHESES' ANSWERS</i>	162

Table of Equations

$A = AP X AF X AM$	EQUATION 1	42
$MTBO - MTTRMTBO = 0.9992$	EQUATION 2	43
$Agnd = 1 - 1 - MTBOLLZ - MTTRMTBOLLZ + 1 - MTBOGLI - MTTRMTBOGLI = 0.99925$	EQUATION 3.....	44
$\sigma i2 = \sigma pr - groundi2 + \sigma trobo i2 + \sigma ionoi2 + \sigma airi2$	EQUATION 4	46
$\sigma air, i2 = \sigma receiver2\theta i + \sigma multipath2\theta i$	EQUATION 5.....	47
$RMSprgrdGPS\theta i \leq (a0 + a1.e - \theta i\theta o)2M + a22$	EQUATION 6	48
$RMSpr - airGPS \theta i = a0 + a1. e - \theta i4$	EQUATION 7.....	49
$RMSmultipath \theta i = a0 + a1. e - \theta i10$	EQUATION 8	49
$rt = A_o. dt - \tau_o ct - \tau_o. \cos 2\pi fL1t - \theta_o + A1. dt - \tau 1. ct - \tau 1\cos 2\pi fL1t - \theta 1$	EQUATION 9.....	72
$D= 2. H. SIN (ELEV.)$	EQUATION 10	73
$CBCS = \alpha. BOC1,1 + \beta. BCSn,1$	EQUATION 11	76
$rt = A. dt - \tau. ct - \tau. \cos 2\pi fL1t - \theta + n(t)$	EQUATION 12.....	77
$rt = A_o. dt - \tau_o ct - \tau_o. \cos 2\pi fL1t - \theta_o + A1. dt - \tau 1. ct - \tau 1\cos 2\pi fL1t - \theta 1$	EQUATION 13	78
$rt = A_o. dt - \tau_o. cft - \tau_o. \cos 2\pi f1t - \theta_o + A1. dt - \tau 1. cft - \tau 1. \cos 2\pi f1t - \theta 1$	EQUATION 14	78
$rt = A_o. dkTD - \tau_o. cfkTD - \tau_o. \cos 2\pi f1kTD - \theta_o + A1. dkTD - \tau 1. cfkTD - \tau 1. \cos 2\pi f1kTD - \theta 1$	EQUATION 15	80
$\theta - \theta = KDCO 0tVc vdv$	EQUATION 16.....	80
$Ipn = A2. dn. Kct - \tau_o. \cos \theta - \theta_o + \alpha. A2. dn. Kct - \tau 1 + \Delta \tau. \cos \theta - \theta 1 + \Delta \theta$	EQUATION 17	80
$Qpn = A2. dn. Kct - \tau_o. \sin \theta - \theta_o + \alpha. A2. dn. Kct - \tau 1 + \Delta \tau. \sin \theta - \theta 1 + \Delta \theta$	EQUATION 18	80
$Ven = Ipn. Qp(n)$	EQUATION 19.....	80
$Ven = A24. K2\tau - \tau_o. \sin(\theta - \theta_o). \cos(\theta - \theta_o)$	EQUATION 20.....	80
$Ven = A48. K2\tau - \tau_o. \sin(2(\theta - \theta_o))$	EQUATION 21	81
$Ven = Ipn. Qp(n)(Ip2(n) + Qp2(n))$	EQUATION 22.....	81
$Ven = 12. \sin(2(\theta - \theta_o))$	EQUATION 23	81
$Ven = \arctan(Qp(n)Ip(n))$	EQUATION 24.....	81
$Ven = (\theta - \theta_o)(n)$	EQUATION 25.....	81
$\epsilon \theta = \theta - \theta_o = \arctan \alpha. Kct_o - \tau_o + \Delta \tau. \sin(\Delta \theta 1)Kct_o - \tau_o + \alpha. Kct_o - \tau_o + \Delta \tau. \cos(\Delta \theta 1)$	EQUATION 26.....	81
$ILn = A2. dn. Kc\epsilon \tau - Cs2. \cos \epsilon \theta + \alpha. A2. dn. Kc\epsilon \tau - Cs2 + \Delta \tau. \cos(\epsilon \theta + \Delta \theta)$	EQUATION 27.....	82
$IEn = A2. dn. Kc\epsilon \tau + Cs2. \cos \epsilon \theta + \alpha. A2. dn. Kc\epsilon \tau + Cs2 + \Delta \tau. \cos(\epsilon \theta + \Delta \theta)$	EQUATION 28	82
$QLn = A2. dn. Kc\epsilon \tau - Cs2. \sin \epsilon \theta + \alpha. A2. dn. Kc\epsilon \tau - Cs2 + \Delta \tau. \sin(\epsilon \theta + \Delta \theta)$	EQUATION 29	82
$QEn = A2. dn. Kc\epsilon \tau + Cs2. \sin \epsilon \theta + \alpha. A2. dn. Kc\epsilon \tau + Cs2 + \Delta \tau. \sin(\epsilon \theta + \Delta \theta)$	EQUATION 30.....	82
$Ve(n) = Ipn. IEn - ILn + Qp. (QEn - QLn)$	EQUATION 31	83
$Ven = IEn + QEn - (ILn + QLn)$	EQUATION 32	83
$Ven = A24. K2\epsilon \tau + C2 - K2\epsilon \tau - C2 + \alpha 2. A24. (K2\epsilon \tau + C2 + \Delta \tau - K2\epsilon \tau - C2 + \Delta \tau)$	EQUATION 33	83
$Kc\epsilon \tau = Kc\epsilon \tau = 1 - \epsilon \tau Tc, \text{ if } \epsilon \tau \ll TcKc\epsilon \tau = 0, \text{ elsewhere}$	EQUATION 34	83
$GBOCf = 1Tcsin\pi fTcnsin(\pi fTc)\pi f\cos(\pi fTcn)2$ FOR THE SINE PHASED EVEN N	EQUATION 35	84
$GBOCf = 1Tcsin\pi fTcncos(\pi fTc)\pi f\cos(\pi fTcn)2$ FOR THE SINE PHASED ODD N	EQUATION 36	84
$En = A02. Kcf. \epsilon \tau + Cs2 + A12. Kcf. \epsilon \tau + Cs2 + \Delta \tau. \cos \Delta \theta$	EQUATION 37.....	85
$Ln = A02. Kcf. \epsilon \tau - Cs2 + A12Kcf. \epsilon \tau - Cs2 + \Delta \tau. \cos \Delta \theta$	EQUATION 38.....	85
$Ven = A02Kcf\epsilon \tau + Cs2 - A02. Kcf\epsilon \tau - Cs2 + A12. Kcf\epsilon \tau + Cs2 + \Delta \tau - A12Kcf\epsilon \tau - Cs2 + \Delta \tau \cos(\Delta \theta)$	EQUATION 39	85
$V\epsilon \tau = A02. V\epsilon \tau + A12. V\epsilon \tau + \Delta \tau. \cos \Delta \theta = 0$	EQUATION 40.....	86
$MDdB = 10 \log A1A02, \text{ So, } A1A0 = 10MDdB2 * 10$	EQUATION 41	90

FINAL DELAY = THE PROPAGATION DELAY (PSEUDORANGE) + THE MULTIPATH DELAY - FILTER DELAY
 EQUATION 42..... 94

$J/S = ERP_J - ERPS - LJ + LS + GR_J - GR$ EQUATION 43 112

$rt = A_0 \cdot dt - \tau_0 ct - \tau_0 \cdot \cos 2\pi f L1 t - \theta_0 + A1 \cdot dt - \tau 1 \cdot ct - \tau 1 \cos 2\pi f L1 t - \theta 1$ EQUATION 44 113

$RMS_{multipath\theta i} = a0 + a1 \cdot e - \theta i 10$ EQUATION 45..... 115

PVT-GEO-LOCK = ∫ (POSITION (LAT. /LONG.), VELOCITY, TIME) EQUATION 46..... 125

L1= (RK), L2=L1 (RK), AND L3=L2 (L1 (RK)) EQUATION 47 126

$J/S = ERP_J - ERPS - LJ + LS + GR_J - GR$ EQUATION 48..... 130

Appendix A-1: Bibliography and References

- Adamy, D. (2009). “*EW 103: Tactical Battlefield Communications Electronic Warfare*”, London: Artech House.
- Airbus. (2017). *control-your-speed-during-descent-approach-and-landing.pdf*. France: Product Safety department (GS). Retrieved from <https://mms-safetyfirst.s3.eu-west-3.amazonaws.com/pdf/safety+first/control-your-speed-during-descent-approach-and-landing.pdf>
- Al-Fuqaha, A. A.-I. (2007). Geo-Encryption Protocol for Mobile Networks. *Semantic Scholar, Western Michigan University. USA*, 88-89.
- Alhosban, A. (2015). “Impact of Multipath Error On the availability of Integrity In GBAS Application”,. In UNOOSA, *Outer space* (pp. 244-287). Austria: UNOOSA.
- Alhosban, A. (2019). "Electronic Warfare in NAVWAR: Impact of Electronic Attacks on GNSS / GBAS Approach Service Types C and D Landing systems and their proposed Electronic Protection Measures (EPM)". *Hadmérnök*, 238-255.
- Alhosban, A. (2019). Navigation Warfare (NAVWAR); Balancing for Position in Space GPS Vs Galileo. *Hadmernok Journal*, 163-177. doi:10.32567/hm.2019.4.10
- B. Eissfeller, V. K. (2007). Performance of GPS, GLONASS and Galileo. *researche gate*, 185–199.
- B. Hofmann-Wellenhof, H. L. (2001). “*Global Positioning System Theory and Practice*” ,*Fifth, revised edition*,. New York: Springer-Verlag Wien GmbH,.
- Beauchamp, S. (2019). GBAS: FAA Status, System Approval Process, and Operational Experience. *ICAO GBAS/SBAS Implementation Workshop, NextGen Portfolio Management & Technology office*,, 55-60.
- Beidleman, S. (2006). GPS versus Galileo: Balancing for Position in Space. *Air University Press Maxwell Air Force Base*, 23-50.
- Bernd Eissfeller, G. A. (2007). ” Performance of GPS, GLONASS and Galileo”, *ION*, Jan. 2007. *ION*, 35-55.
- Braasch. (2002). LAAS Integrated Multipath Antenna. *Institute of Navigation ION GPS VA, USA*, 21-42.
- Campbell, J. S. (2011). *Essentials of Geographic Information System*. USA: Saylor Foundation.
- Dautermann, T. –L.–G.–E. (2020). Extending access to localizer performance with vertical guidance approaches by means of an SBAS to GBAS converter GPS Solution 24 (2020), Article No. 37. DOI: <https://doi.org/10.1007/s10291-019-09>. *GPS Solution 24 (2020), Article No. 37*. DOI: <https://doi.org/10.1007/s10291-019-09>, 37-58. doi:10.1007/s10291-019-09
- Denning&Scott. (2003). Geo-Encryption: Using GPS to Enhance Data Security. *GPS World, Calhoun, Archive of Naval Postgraduate Institute*, 40-49.
- Denning, D. (2001). Is cyber terror next? understanding September. *SSRC*, 191-197.
- ESA. (2018, 10 10). *ESA / Applications / Navigation*. Retrieved from European Space Agency: https://www.esa.int/Applications/Navigation/Contract_signing_to_boost_performance_and_security_of_Galileo_services

- ESA. (2018). *Galileo Navigation*. Europe Space Agency: ESA. Retrieved from https://www.esa.int/Our_Activities/Navigation/Contract_signing_to_boost_performance_and_security_of_Galileo_services
- ESA. (2018). *Galileo_Future_and_Evolutions*. USA: navipedia.
- ESA. (2018). *Galileo_Future_and_Evolutions, The reference for Global Navigation Satellite Systems*. The reference for Global Navigation Satellite Systems. Madrid: EU. Retrieved from https://gssc.esa.int/navipedia/index.php/Galileo_Future_and_Evolutions
- ESRI. (2020). *Modernizing Nautical Chart Production: Next-Generation Charting System Based on Commercial Off-the-Shelf Solution.* ' In: *GIS Use in Map, Chart and Data Production*. ESRI. Available: www.esri.com/content/dam/esrisites/sitecore-archive/Files/Pdfs/library/bro. USA: ESRI .
- European Space Agency, ESA. (2018, 10 18). Retrieved from Galileo Future and Evolutions: https://gssc.esa.int/navipedia/index.php/Galileo_Future_and_Evolutions
- FieldManual(FM)-3-36. (2012). *Army doctrine for electronic warfare (EW) planning, available on the link : https://armypubs.us.army.mil/doctrine/index.html*. Washington Dc: NATO. Retrieved from <https://armypubs.us.army.mil/doctrine/index.html>
- G. Gluschke, M. C. (2018). *Cyber Security Policies and Critical Infrastructure Protection*. Germany: Institute for Security and Safety GmbH.
- Galileo. (2008). Galileo open service, signal in space interface control document. *European space agency/European GNSS supervisory authority*, 105-115.
- GPS. (2006, 11 21). *Official U.S. government GPS*. Retrieved from www.gps.gov: <https://www.gps.gov/policy/cooperation/russia/2006-working-group-1/>
- GPSTechnology. (2015). *special report on Navigation/GPS Technology in Military Application*. USA: Military Embedded Systems.
- Gurtov, A. P. (2018). Controller–Pilot Data Link Communication Security,. *Sensors, Vol. 18, Issue (5),1636, Sweden*, 1-12.
- Haig, Z. (2015). ELECTRONIC WARFARE IN CYBERSPACE. , 7(2). *Security and Defense Quarterly*, 22-35.
- Hronyecz, T. F. (2015). Info-Communication System Requirements for Deployable Rapid Diagnostic Laboratory Support. *AARMS*, 53-61.
- I. Sayim, H. L. (2017). Ionospheric delay prediction and code-carrier. *Aerospace*, 70, 66-75. Retrieved from <https://doi.org/10.1016/j>.
- ICAOAmendment91&92. (2020). *ICAO Annex 10, Volume I, Aeronautical Telecommunications, (2018), Amendment 91, GBAS strategy, section 7.1.2.1, and section 3.3.14 and attachment C. 2018 continued in amendment 92, (2020), Appendix C-2, pages: Att.20-29.* . Canada: ICAO.
- ICAOAnnex10. (2002). Aeronautical Telecommunication. *International Civil Aviation Organization*, 55-100.
- InsideGNSS. (2018). *GNSS Jamming and Spoofing: Hazard or Hype?* USA: space of innovation .
- InsideGNSS. (2018). *GNSS Jamming and Spoofing: Hazard or Hype?* . USA: Inside GNSS.

- IrfanSayim, H. D. (2017). Ionospheric delay prediction and code-carrier divergence testing for GBAS using neural network and GPS L1. *Elsevier Masson SAS, Aerospace science and technology.*, 33-49.
- J. Ma, Y. Y. (2020). FH-BOC: generalized low-ambiguity anti-interference spread spectrum modulation based on frequency-hopping binary offset carrier. *GPS Solutions* , 24-70.
- Jean-Pierre. (2003). Error Models for precision landing using new GNSS signals . *ION GPS/GNSS, VA, USA.*, 45-59.
- Jeong, M. B. (2016). ‘Flight test evaluation of ILS and GBAS performance at Gimpo International Airport.’ 473–483. DOI: <https://doi.org/10.1007/s10291-015-0457-1>. *GPS Solution 20 (2016)*,, 473-483. doi:10.1007/s10291-015-0457-1
- JW, B. (2001). Binary offset carrier modulations for radio navigation. *IOT Institute of Navigation*, 227-246.
- Lewis, T. (2015). *Critical Infrastructure Protection in Homeland Security, Ch. 7*. New Jersey USA: John Wiley & Sons, Inc. Hoboken.
- LockheedMartin. (2021). *The fifth satellite in the GPS III series launches June 17, 2021*. USA: Lockheed Martin.
- M. Jeong, J. B. (2016). ‘Flight test evaluation of ILS and GBAS performance at Gimpo International Airport,.’ *GPS Solution*, 473-483.
- M. Jeong, J. Bae1, H. Jun and Y. Lee. (2016). Flight test evaluation of ILS and GBAS performance at Gimpo International Airport. *Springer GPS Solution*, 473-483.
- Mathews, A. K. (2005). Working Group Meetings the18th,., *ION GNSS, VA, USA*, 21-42.
- Michael, J. L. (2015). GBAS ground monitoring requirements from an airworthiness perspective. *Springer-Verlag Berlin Heidelberg*, 75-90.
- Nagle, J. (2009). ‘*Global Air Navigation System Performance Based eANP Framework*,’ *SIP/WP/10 eANP Framework*. USA: SIP/WP/10 eANP Framework.
- Novatel. (2015). *special report on Navigation/GPS Technology in Military Application*. USA: Military Embedded Systems, Navigation Warfare Article.
- OfficialUSgovGPS. (2019). *Official U.S. government information about the Global Positioning System (GPS) and related topics*, *GPS.gov*. Washington Dc: US Government.
- Order, E. (2020). *Executive Order on Strengthening National Resilience through Responsible Use of Positioning, Navigation, and Timing Services*. Washington DC: USA.
- Rotondo, G. (2017). Processing and Integrity of DC/DF GBAS for CAT II/III Operations. Signal and Image processing. *INPT, NN: 2016INPT0130*, 65-89.
- RTCA245A. (2004). Minimum Aviation System Performance Standards for The Local Area Augmentation System (LAAS). *RTCA*, 50-200.
- S. BAŞAK, S. U. (2019). Ground Based Augmentation Ssystem (GBAS). *İstanbul Aydın Üniversitesi Dergisi - İAÜD*, 205-215. doi:10.17932/IAU.IAUD.m.13091352.2019.2/42

- SaylorOrg. (2015). 'Geographic Information Systems for Today and Beyond.' Saylor.org. https://saylordotorg.github.io/text_essentials-of-geographic-information-systems/s05-03-geographic-information-systems.html. USA: Saylor Org. Retrieved from https://saylordotorg.github.io/text_essentials-of-geographic-information-systems/s05-03-geographic-information-systems.html
- Seidel. (2018). *GPS Signal jammed in Norway and Finland, GPS signals jammed: Norway, Finland warn pilots Russia may blind their navigation systems*. Austria: Technology news.
- Seidel, J. (2018, 11 14). *GPS signals jammed: Norway, Finland warn pilots Russia may blind their navigation systems*. Retrieved from news.com.au: <https://www.news.com.au/technology/innovation/military/gps-signals-jammed-norway-finland-warn-pilots-russia-may-blind-their-navigation-systems/news-story/ee28be793012e9b9e66d59ffba439242>
- Susumu. (2017). Ionospheric delay gradient model for GBAS in the Asia-Pacific. *Springer-Verlag Berlin Heidelberg*, 66-78.
- T. Dautermann, M. F. (2012). 'Approach service type D evaluation of the DLR GBAS testbed, . *GPS Solutions*, 375-387.
- T. Dautermann, M. F. (2020). Approach service type D evaluation of the DLR GBAS testbed. *Springer GPS Solution*, 375-387.
- T. Dautermann, T. L. (2020). Extending access to localizer performance with vertical guidance approaches by means of an SBAS to GBAS converter. *Springer GPS Solution*, 36-55.
- USAF. (2019, 10 19). *US Air Force website*. Retrieved from www.losangeles.af.mil: www.losangeles.af.mil/News/Article-Display/Article/1941274/smc-and-its-government-industry-partners-successfully-launch
- X. Zhao, X. H. (2021). Improved MBOC modulations based on periodic offset subcarrier, Institute of Engineering and Technology (IET). *WILEY*, 85-105. doi:10.1049/cmu2.12195
- Yiping Jiang, C. M. (2016). Code carrier divergence monitoring for dual-frequency GBAS. *Springer-Verlag Berlin Heidelberg*, 45-61.

Appendix A-2: Author Publications.

<https://m2.mtmt.hu/gui2/?type=authors&mode=browse&sel=authors10072986>

Publication type	Value	Participation rate (%)	Points
Journal article in a peer-reviewed journal published abroad			
in an MTA „A” or „B” category journal			
<ul style="list-style-type: none"> – Ahmad Alhosban: „GPS Characterization in the Cyberspace Concept between Vulnerability and Geo-Encryption: Impact on GBAS Landing System (GLS)” <i>Revista Academiei Fortelor Terestre / Land Forces Academy Review</i> 25: 2. pp. 146-158., 13 p. (2020) DOI 10.2478/raft-2020-0018 https://www.armyacademy.ro/reviste/rev2_2020/Alhosban_Raft_2_2020.pdf – Ahmad Alhosban: „Assessing Availability of GNSS-GBAS Landing Systems in GAST -D/F Performance” <i>Advances in Military Technology</i> 17:1 (2022) DOI 10.3849/aimt.01540 (accepted for publication) 	6 points	100%	12
in an MTA „C” or „D” category journal	4 points	-	-
in a peer-reviewed journal published in Hungary			
in an MTA „A” or „B” category foreign language journal			
<ul style="list-style-type: none"> – Ahmad Alhosban: „Electronic Warfare in NAVWAR: Impact of Electronic Attacks on GNSS / GBAS Approach Service Types C And D Landing Systems and their Proposed Electronic Protection Measures (EPM)” <i>Hadmérnök</i> 14: 2. pp. 238-255., 18 p. (2019) DOI 10.32567/hm.2019.2.20 https://folyoirat.ludovika.hu/index.php/hadmernok/article/view/351/54 – Ahmad Alhosban: „Navigation Warfare (NAVWAR): Balancing the Position in Space between GPS and Galileo” <i>Hadmérnök</i>, 14: 4. pp. 163–177. 15p. (2019) DOI 10.32567/hm.2019.4.10 https://folyoirat.ludovika.hu/index.php/hadmernok/article/view/940/293 	4 points	100%	8
in an MTA „C” or „D” category foreign language journal			
<ul style="list-style-type: none"> – Ahmad Alhosban: „Assessment of the GIS-Aided Precise Approach Using the GNSS-GBAS Landing Systems”, 	3 points	100%	3

<p>Repüléstudományi Közlemények 32: 2. pp. 49–65. 17p. (2021) DOI 10.32560/rk.2020.2.4 https://folyoirat.ludovika.hu/index.php/reptudkoz/article/view/1507/4238</p>			
Publications in journals with quartile rankings			
Conference materials published in the material of an international conference (online too)			
<p>lecture published in a peer-reviewed conference material</p> <p>– Ahmad Alhosban: „<i>Impact of Multipath error on Availability of integrity in GBAS Application</i>” In: <i>International Committee on Global Navigation Satellite Systems Experts Meeting on Global Navigation Satellite Systems (GNSS) Services; Abstracts Book; pp.17-22. 6p</i> (Vienna, Austria 15 - 18 December 2015) https://www.unoosa.org/pdf/icg/2015/2015abstracts.pdf</p>	4 points	100%	4
published in the material of a Hungarian conference (online too)			
presentation in own language	1 point		
<p>abstract or poster in a foreign language</p> <p>– Ahmad Alhosban: „<i>Assessing the Availability of the Modernized GNSS to achieve GASTD/F Requirements in GBAS Landing Systems</i>” In: <i>Repüléstudományi Konferencia 2021. Book of Abstracts; pp.3-4; 2p</i> (Szolnok, Hungary 08. April 2021) https://ludevent.uni-nke.hu/event/723/book-of-abstracts.pdf</p> <p>– Ahmad Alhosban; László Bodnár: „<i>The Adopted Approach to the disaster management of Covid-19 Pandemic In Jordan /role of the National Center for Security and Crisis Management (NCSCM)</i>” In: <i>Fire Engineering & Disaster Management Prerecorded International Scientific Conference 2021. Book of abstracts; pp.489.</i> (Budapest, Hungary 23. February 2021.) https://kvi.uni-nke.hu/document/kvi-uni-nke-hu/440-konferencia.pdf</p> <p>– Ahmad Alhosban: „<i>GNSS Space Racing Beyond the Cold War Era-Technical Comparative Study</i>” In: „<i>XXIII. Tavaszi Szél Konferencia: MI és a tudomány jövője 2020</i>” Absztrakt kötet; pp.7. (Budapest, Hungary 16. October 2020.) https://www.dosz.hu/doc/dokumentumfile/2020/tavaszi-szel-2020-absztrakt-kotet-i-final.pdf</p>	1 point	100%	3.9

<p>– Ahmad, Alhosban: „NATO EU Nations’ Posture in GNSS” <i>In: Gateway of Science - Poster Contest and Exhibition; Part of the European Cyber Security Month (ECSM) and NATO70 (Budapest, Hungary 5. November 2019.)</i> https://www.uni-nke.hu/document/uni-nke-hu/2_NKE%20D%C3%96K_A%20Tudom%C3%A1ny%20Kapun%C3%A1ban.pdf</p>		100%	
Grants			
<p>participating in a University level scientific grant (1. place) – Ahmad Alhosban: „Assessing the Availability of the GNSS-GBAS Landing System in GAST –D/F Performance” Tématerületi Kiválósági Program 2020. (TKP-2020-NKA-09)</p>	1 point	100%	1
Total			31.9

Description of the other scientific activities	Timing
<p>Conference presentation: (Electronic Warfare in NAVWAR: Impact of Electronic Attacks on GNSS / GBAS Approach Service Types C and D Landing systems and their proposed Electronic Protection Measures (EPM)), Repüléstudományi Konferencia 2019. at Szolonok http://www.repulestudomany.hu/hirek/2019.04.11_RepTudKonf.html</p>	11 April 2019
<p>Conference presentation: (Galileo GNSS System: New Approach for EU Space Security), National And International Security 2019/the 10th International Scientific Conference/ Slovakia http://www.aos.sk/struktura/katedry/kbo/NMB2019/index_en.php?goen=1en</p>	24th +25th Oct. 2019
<p>Conference presentation: "New approach of instrumental landing systems using Galileo/GPS space navigation and its contribution in NATO ", Communications 2019" International scientific-professional conference./NUPS Honvéd Kulturális Központ (Budapest, 1143, Zichy Géza u. 3. https://www.uni-nke.hu/esemenyek#2019-11-14</p>	14th Nov. 2019
<p>Munich Summit Participation: GBAS availability in GAST D/F Performance were discussed with the steering committee and the high level presenters. Germany –Munich https://www.munich-satellite-navigation-summit.org/</p>	16 th and 17 th March 2021

Appendix B: Acronyms

ACSF	ATC Control and Status Function
ARNS	Aeronautical Radio Navigation Spectrum
ASIC	Application Specific Integrated Circuit
ATC	Air Traffic Control
ATM	Air Traffic Management
BER	Bit Error Rate
C/A	Coarse Acquisition
CAT	Category (of precision approach operation)
CCA	Common Cause Analysis
CMC	Code Minus Carrier
COS	Continuity Of Service
COTS	Commercial Off The Shelf
CRC	Cyclic Redundancy Check
CW	Continuous Wave
CWI	Continuous Wave Interference
D8PSK	Differential 8 Phases Shift Keying
DA/H	Decision Altitude/Height
DH	Decision Height
EATMP	European Air Traffic Management Program
ECEF	Earth Centered Earth Fixed
ECI	Earth Centered Inertial Co-ordinate System
EGNOS	European Geostationary Navigation Overlay Service
EMC	Electromagnetic Compatibility
EMI	Electromagnetic Interference
ERP	Effective Radiated Power
ESARR	Eurocontrol Safety Regulatory Requirement
ETA	Event Tree Analysis
EVM	Error Vector Magnitude
FAA	Federal Aviation Administration (United States)
FAS	Final Approach Segment
FAT	Factory Acceptance Testing
FEC	Forward Error Correction
FHA	Functional Hazard Analysis
FMEA	Failure Mode and Effects Analysis
FPAP	Flight Path Alignment Point
ft	Feet
FT	Factory Testing
FTA	Fault Tree Analysis
GAD	Ground Accuracy Designation
GBAS	Ground Based Augmentation System
GCID	GBAS Continuity Integrity Designator
GLONASS	Global (Orbiting) Navigation Satellite System
GLS	GNSS Landing System
gnd	Ground
GNSS	Global Navigation Satellite System
GPA	Glide Path Angle
GPIP	Glide Path Intercept Point
GPS	Global Positioning System
HAT	Height Above Threshold

HPOL	Horizontal Polarization
ICAO	International Civil Aviation Organization
ICD	Interface Control Document
ID	Identification
ILS	Instrument Landing System
IOD	Issue of Data
IODC	Issue of Data Clock
IODE	Issue of Data Ephemeris
IODN	Issue of Data Navigation message (SBAS)
IMEA-GA	Impact of Multipath Error on Availability of Integrity in GBAS Application
JAR	Joint Aviation Requirements
LAAS	Local Area Augmentation System (FAA)
LAL	Lateral Alert Limit
LCSF	Local Control and Status Function
LNA	Low Noise Amplifier
LPL	Lateral Protection Level
LRU	Line Replaceable Unit
LSB	Least Significant Bit
LTP/FTP Point	Landing Threshold Point/Fictitious Threshold
MASPS Specification	Minimum Aviation System Performance
MDE	Minimum Detectable Error
MDT	Maintenance Data Terminal
MERR	Maximum Error
MFR	Message Failure Rate
MI	Misleading Information
MLS	Microwave Landing System
MOPS (Eurocae) Specification	Minimum Operational Performance
MOPS (RTCA)	Minimum Operational Performance Standard
MSAS(Japan)	MTSAT Satellite-Based Augmentation System
MSB	Most Significant Bit
MTBF	Mean Time Between Failure
MTBO	Mean Time Between Outage
MTn	Message Type n
MTSAT	Multifunction Transport Satellite (Japan)
MTTR	Mean Time To Repair
NM	Nautical Mile
NSE	Navigation System Error
PPS	Pulse Per Second
PR	Pseudorange
PRC	Pseudorange Correction
PRN	Pseudo Random Noise
PSSA	Preliminary System Safety Assessment
PVT	Position, Velocity, Time
RF	Radio Frequency
RFI	Radio Frequency Interference
RMS	Root Mean Square
RNP	Required Navigation Performance
RPDS	Reference Path Data Selector
RR	Reference Receiver
RRC	Range Rate Correction

RSDS	Reference Station Data Selector
SARPS	Standards and Recommended Practices
SBAS	Space Based Augmentation System
SIS	Signal in Space
SNT	SBAS Network Time
SPS	Standard Positioning Service
SQM	Signal Quality Monitoring
SSA	System Safety Assessment
SSID	Station Slot Identifier
SV	Satellite Vehicle
TBC	To Be Confirmed
TBD	To Be Determined
TCH	Threshold Crossing Height
TDMA	Time Differential Multiple Access
TTA	Time To Alert
UTC	Universal Co-ordinated Time
UMPE	User Multipath Error
VAL	Vertical Alert –Limit
VDB	VHF Data Broadcast
VHF	Very High Frequency
VHF COM	VHF Communications Band
VHF NAV	VHF Navigation Band
VOR	VHF Omni-directional Range
VPL	Vertical Protection Level
VSWR	Voltage Standing Wave Ratio
WAAS	Wide Area Augmentation System
WGS-84	World Geodetic System 1984

Appendix C: Author CV (Resume)

Mr. Ahmad M. S. Alhosban is a PhD candidate from Jordan, He is an Ex-Air-Force Colonel Engineer, He joined the PhD Program in the Defense Electronic ICT Research field at the KMDI /NKE since 2018, and he has got Excellent grades, 4.98 out of 5. His research topic is the **Impact of GPS Navigational Errors on the Required Performance of GBAS Approach Service Type D/F (GAST-D/F) Landing Systems**. During his PhD program, Mr. Alhosban has successfully published 5 papers, from which 2 of them were abroad in Check Republic and Romania, and 3 in Hungary, 4 of them are in A/B peer-reviewed Journals and 1 in C/D Rank. He still has an extra paper in process, and he wrote a chapter in a book also under publication process. All were in the scope of his topic objectives. Mr. Alhosban also has conducted 5 international conferences, 2 of them were abroad in Slovakia and Austria, 1 was published. Also he was awarded a University level scientific grant, all were in his aspect topic. He had his master degree from ENAC University in France, Toulouse, in 2006, his aspect was Satellite-Based Communication, Navigation Surveillance Engineering for Air Traffic Management, before he had got his BSc in Electrical and Communication Engineering from Jordan in 1994, and both were in a very good grades. Mr. Alhosban was the Chief of Ground Communication Supply Branch, also he was the Founder/Chief of the ATC Engineering B.Sc. program in the Aviation Science Faculty in a Jordanian University, and he was the Commander of the Electronic Workshop's/Labs, His Total years of experience is 24 years, from which 6 years of them were in the teaching activities as a University teacher. Mr. Alhosban has lead and perform many Electronic communications and navigational projects and system installations during his service in Air Force, he also had designed and installed the video streaming system on the air force aircrafts. He supervised more than 30 flight checks of their commissions and periodic maintenance. Colonel Ahmad has joined the Jordanian Engineering Association since 1994, and he has got a consultant rank in his aspect, he also was an effective represented for the GNSS Air Navigation National Strategic Committee, hosted by the Ministry of Transportation and leaded by CARC, Civil Aviation Regularity Commission. Furthermore he represented Jordan in the ICG Expert Meeting in Vienna, Austria, Under UNOOSA, 2015. He also joined the Outer space research Group in Hungary in 2021. His Total Number of training period in U.S.A is (30 weeks). And in France is (30 weeks). And in Germany is (26 weeks). As well as Italy, Sweden and Austria for 2 weeks each. He has got the Royal Legion of Merit 2nd class medal 2016.

Personal Information:

- Name: Ahmad M. S. Alhosban
- Date of Birth: 28 July 1972, Place of Birth: Al-Mafraq, Jordan
- Nationality: Jordanian
- E-mail: ahmad_alhosban@yahoo.com



Profile of Education:

- **PhD Candidate/ 4th Year:** in ICT/Satellite GNSS Navigation Engineering, GBAS Systems, @ National University for Public Services (NUPS/NKE), Budapest, Hungary, since 2018. Excellent, 4.97 out of 5, Rank 1st.
- **Rank: JCE Consultant Engineer in Communication**, Since May 2017, from Jordanian Engineering Association. Rated highest possible degree.
- **Master Degree (MS)/Advanced (Bac+7)** in Satellite-Based Communication, Navigation, and Surveillance SB-CNS/ATM, from ENAC, Toulouse, FRANCE @ 2006, rated Very Good, 1st rank.
- **Bachelor’s Degree (BSc)** in Electrical / Communication Engineering, from Mu’tah University, KARAK, JORDAN. @ 1994, rated Very Good, 3rd rank.
- **Diploma Degree** in Military Science from JORDAN@ 1994, rated Excellent.
- **General Secondary Certificate** (Scientific Stream) from Al-Mafraq High school, Jordan, @1989/1990. Rated Excellent, 1st rank.

Languages:

- **Arabic:** Mother Tongue, fluently
- **English:** Second Language, fluently in Listening, Reading, Writing and Speaking.
- **French and Hungarian:** third Languages, Reading only.

Computer Science:

- **Programming Languages** (Matlab, Visual Basic, Fortran): Very Good
- **Spécial Programming** (MD110 Exchange, AXT Exchange, Radios, Vidéo Communications, Navigation networks, GPS networks) : Excellent

Management and Logistics: Projects’ management, Personnel management, financial management, Resources management, Electronic Workshop Commander and chief of Com/NAV/Radar Supply

University Education

University/Country	Dates	Certificate	Results
National University of Public Services (NUPS/NKE)	2018-2022 5 years	PhD Candidate ICT-GNSS Engineering	Excellent (4.97/5) 1 st Rank/25
Ecole Nationale de l’Aviation Civile (ENAC, Toulouse/France)	2005 – 2006 (1.2 year)	Advanced Master in CNS (Satellite-Based, Communication, Navigation and Surveillance)	Very good (82.5 %)/1 st rank/7
Mu’tah University, Karak/Jordan	1990-1994 (5 years)	Bachelor’s Degree in Electrical / Communication Engineering	Very Good (78.48%)/3 rd rank/13

College and School Education

College/Country	Dates	Certificate	Results
Mutah Collège, Karak/Jordan	1992-1994	Diploma Degree (Bac+2) in Military Science	Excellent (95%), 20 th rank/360
Al-Mafraq High School, Jordan,	1989-1990	General Secondary Certificate (Scientific Stream)	Excellent (91.9 %)/1 st rank
Al-Mafraq High School, Jordan,	1987-1988	Basic Elementary School Certificate	Excellent (97.8%)/1 st Rank

Special Training

College/Country	Dates	Certificate	Results
Defense Language Institute(DLI), Lackland AFB, Texas, USA	Feb/2004- May/2004	<u>Diploma</u> in Specialized English	Outstanding
Keesler AFB, Mississippi, USA	May/2004- July/2004	<u>Diploma</u> in Expedentiary Communication & Information Training (ECOT)	Distinguished

Professional Job:

Retired in Sep. 2018 as Colonel 4th Year from RJAF as: Chief of Ground Communication Supply Branch and Chief, B.Sc. of ATC Division- Aviation Science Faculty and Electronic Workshop's/Labs Commander, Total years of experience: **24 years**, Period: 1994 to 2018
Organization: Jordan Engineer Association, Period: 1994 to present

Details of positions:

Dates	Position	Place
2015-2018 Parallel job	Chief, and founder of the program of B.Sc. of ATC Division- Aviation science Faculty AABU University	Al Al-Bait University AABU
2018-2018	Chief of Ground Communication Branch	Directorate of Electronic Communications
2016-2018	Commander, Electronic Workshops and PMEL Labs	Directorate of Electronic Communications
2014 - 2016	Chief of Electronic Communication Supply Branch	Directorate of Supply
2013 - 2013	Nav aids/Radios / 1st Staff Officer	Directorate of Electronic Communication
2007 - 2013	Nav aids& Radios Maintenance Senior Field Engineer	Electronic workshops and labs
2005 - 2006	Master SB-CNS France	ENAC, Toulouse, France
2002 - 2005	Nav aids Senior Field Engineer & Instructor	Nav aids workshop/RJAF
2000 - 2002	Electronics & Communications Instructor(Teacher)	Prince Faisal College

1994 - 2000	Communication/Navigation Site Engineer	Different bases in RJAF /Jordan
-------------	--	---------------------------------

Main Performed Projects:

Project	Date	Place
Foundation and Teaching GNSS courses, Advanced GNSS and BPA courses and RNAV courses	2013-2016/ 4 courses	Queen Noor Civil Aviation Technical College(QNCATC)
Establishing Full Motion Video (FMV) Analysis Center in	2013-2015	Squadron 15/RJAF
Adding Metadata Capability to the Video stream.	2014-2015	Squadron 15/RJAF
BMS, video receiving center network over fiber from (4) receiving sites installation (10) ten video receiving sites.	2009-2012	RJAF/ JORDAN
Addressable fire alert systems installations in three sites	2007+2008	RJAF/ JORDAN
3 ILS/DME and 4 VORs installations	2008-2012	4 bases in RJAF
Telecommunication Cabling Infrastructure installations	2002-2004	KFAB and KA2AB/RJAF

Seminars:

- ✓ International and national Security Conference, Slovakia, Oct, 2019, lecturer
- ✓ Info Communication Conference, Budapest NKE, Nov.2019, lecturer
- ✓ Aviation Conference, Szolnok, Budapest, April 2019, jamming effect on GBAS Systems for CATII/III performance. lecturer
- ✓ ITU Regional Workshop on Terrestrial and Space Radio Communication Services for the Arab States, Amman - Jordan, 29 November – 1 December 2016
- ✓ ICG Expert Meeting in Vienna, Austria, Under UNOOSA, 14-18 Dec 2015, giving a GBAS presentation and publicized in website,
- ✓ GNSS Air Navigation National Strategic Committee, an effective RJAF member/representative in permanent committee to address the GNSS future in Jordan, hosted by the Ministry of Transportation and led by CARC, Civil Aviation Regularity Commission.

Special O.J.T.:

- ✓ FAA Flight Inspection for TACAN, VOR, ILS /US Air force, Jordan, 2002 to 2013, 5 weeks /year
- ✓ Total Number of training period in U.S.A and English spoken countries is (30 weeks).
- ✓ Total period in France is (30 weeks).
- ✓ Total period in Germany is (26 weeks).
- ✓ Total period in Hungary: 4 years till now

Outside visits: Hungary (4year), U.S.A (20 states) over 25 times (1.5 Year), France (1 year and 2 months), Germany (6 months), U.A.E (Dubai) 2 times, Italy, Sweden, Austria.

Medals: Legion of Merit 2nd class medal 2016

Appendix D: Matlab-Based Multipath Error Envelopes Software

```
3
4 % Matlab-based Code Multipath Error Envelopes%
5
6 clc;
7 format long;
8 clear all;
9 close all;
10
11 % GPS L1 Constants
12
13 c=299792458; % Speed of Light in Vacuum in m/s
14 F1=1575.42e6; % L1 Frequency in Hz
15 T1=1/F1; % Period of L1
16 lambda=c/F1; % Wave Length of L1
17 Fc=1023000; % Chip Frequency C/A
18
19 % Part 1: Pre-Envelope calculation stages
20
21 % Step 1 :Input parameters
22
23 Fc=input('Input Code Frequency (in MHz) Fc=');
24 BW_D=input('Input Double-sided bandwidth (in MHz) BW_D= ');
25 Cs=input('Early-Late Chip Spacing (from 0 to 1) Cs= ');
26 a=input('Relative Amplitude of the Reflected Signal(from 0 to 1) a= ');
27 mater=input('Code materialization waveform. Choose ''bpsk'' or ''boc11''
28 or ''boc22'': ', 's');
29
30 if strcmp(mater, 'bpsk')
31     bpsk=1;
32     boc11=0;
33     boc22=0;
34 elseif strcmp(mater, 'boc11')
35     bpsk=0;
36     boc11=1;
37     boc22=0;
38 elseif strcmp(mater, 'boc22')
39     bpsk=0;
40     boc11=0;
41     boc22=1;
42 else
43     fprintf('Input Error.... Repeat the simulation!');
44     return
45 end;
46
47 Filter=input('Filter type, Choose ''butterworth'' or ''chebyshev'' or
48 ''fir_boxcar'' or ''fir_hamming'': ', 's');
49
50 if strcmp(Filter, 'butterworth')
51     butterworth=1;
52     chebyshev=0;
53     fir_boxcar=0;
54     fir_hamming=0;
55 elseif strcmp(Filter, 'chebyshev')
56     butterworth=0;
57     chebyshev=1;
58
59
60
61
62
63
64
65
66
67
68
69
70
71
72
73
74
75
76
77
78
79
80
81
```

```
83
84     fir_hamming=0;
85     elseif strcmp(Filter,'fir_boxcar')
86     butterworth=0;
87     chebyshev=0;
88     fir_boxcar=1;
89     fir_hamming=0;
90     elseif strcmp(Filter,'fir_hamming')
91     butterworth=0;
92     chebyshev=0;
93     fir_boxcar=0;
94     fir_hamming=1;
95     else
96     fprintf('Input Error.... Repeat the simulation!');
97     return
98     end;
99     Fc=Fc*1e6;
100    Tc=1/Fc;
101
102    % Step 2: Autocorrelation Stage
103    % -----
104    tau=-5*Tc:Tc/500:5*Tc;
105    if bpsk==1;
106    K_auto=autocorr(tau,Tc);
107    elseif boc11==1;
108    K_auto=Auto_BOC_1_1(0,tau,Tc);
109    elseif boc22==1;
110    K_auto=Auto_BOC_2_2(0,tau,Tc);
111    end;
112
113    figure(1);
114    plot(tau,K_auto);
115    title('Autocorrelation Function');grid;hold on;
116
117    % Step 3: Filtering Stage
118
119    fc=BW_D/2;
120
121    if butterworth==1;
122    [b1,a1]=butter(6,(2*fc/300));
123    elseif chebyshev==1;
124    [b1,a1]=cheby1(3,1,(2*fc/300));
125    elseif fir_boxcar==1;
126    [b1,a1]=fir1(1000,2*fc/300,boxcar(1001));
127    elseif fir_hamming==1;
128    [b1,a1]=fir1(100,2*fc/300,Hamming(101));
129    end;
130
131    K_auto=filter(b1,a1,K_auto); plot(tau,K_auto,'g');
132    legend('Autocorrelator','Filtered Autocorrelator');
133    xlabel('Delay in seconds');pause;
134
135    % Step 4 :Early-Late Discriminator stage
136
137    Cs=Cs*Tc;
138    tau_early=(-5*Tc-Cs/2):Tc/500:(5*Tc-Cs/2);
139    tau_late=(-5*Tc+Cs/2):Tc/500:(5*Tc+Cs/2);
```

```

119     if bpsk==1;
120     K_auto_early=autocorr(tau_early,Tc);
121     K_auto_late=autocorr(tau_late,Tc);
122     elseif boc11==1;
123     lag_E=-Cs/2;
124     lag_L=Cs/2;
125     K_auto_early=Auto_BOC_1_1(lag_E,tau_early,Tc);
126     K_auto_late=Auto_BOC_1_1(lag_L,tau_late,Tc);
127     elseif boc22==1;
128     lag_E=-Cs/2;
129     lag_L=Cs/2;
130     K_auto_early=Auto_BOC_2_2(lag_E,tau_early,Tc);
131     K_auto_late=Auto_BOC_2_2(lag_L,tau_late,Tc);
132     end;
133
134     discrim_no_filt=K_auto_early-K_auto_late;% without filtering
135     K_auto_early=filter(b1,a1,K_auto_early);
136     K_auto_late=filter(b1,a1,K_auto_late);
137     figure(2); plot(tau,K_auto_early);hold
138     on; plot(tau,K_auto_late,'r');
139     title(['Early and Late Autocorrelators
140     (Cs=',num2str(1/Tc*Cs),',Fc=',num2str(Fc/1e6), 'MHz,BW=',num2str(BW_D), 'MH
141     z)']);
142     legend('Early Autocorrelator','Late Autocorrelator');
143     xlabel('Delay in Seconds');grid on;pause;
144
145     % Step 5 : Discriminator Without Multipath
146
147     discrim=K_auto_early-K_auto_late;
148
149     figure(3);
150     plot(tau,discrim);hold on;
151     plot(tau,discrim_no_filt,'g');
152     legend('Filtered Discriminator','Non Filtered Discriminator');
153     title('Discriminator Without Multipath'); title(['Discriminator Without
154     Multipath
155     (Cs=',num2str(1/Tc*Cs),',Fc=',num2str(Fc/1e6), 'MHz,BW=',num2str(BW_D), 'MH
156     z)']);
157     xlabel('Delay in Seconds');grid on;pause;
158
159
160     % Step 6 : Discriminator With Multipath
161
162     vect_delay=[0*Tc:Tc/10:1.5*Tc];
163
164     for i=1:length(vect_delay);
165     mp_delay=vect_delay(i);
166
167     tau_early_mp=(-5*Tc-Cs/2-mp_delay):Tc/500:(5*Tc-Cs/2-mp_delay);
168     tau_late_mp=(-5*Tc+Cs/2-mp_delay):Tc/500:(5*Tc+Cs/2-mp_delay);
169
170     if bpsk==1;
171     K_auto_early_mp=autocorr(tau_early_mp,Tc);
172     K_auto_late_mp=autocorr(tau_late_mp,Tc);
173     elseif      boc11==1;
174     lag_E=-Cs/2;
175     lag_L=Cs/2;
176     K_auto_early_mp=Auto_BOC_1_1(lag_E,tau_early_mp,Tc);
177     K_auto_late_mp=Auto_BOC_1_1(lag_L,tau_late_mp,Tc);

```



```

179     elseif      boc22==1;
180     lag_E=-Cs/2;
181     lag_L=Cs/2;
182     K_auto_early_mp=Auto_BOC_2_2(lag_E,tau_early_mp,Tc);
183     K_auto_late_mp=Auto_BOC_2_2(lag_L,tau_late_mp,Tc);
184     end;
185
186     K_auto_early_mp=filter(b1,a1,K_auto_early_mp);
187     K_auto_late_mp=filter(b1,a1,K_auto_late_mp);
188
189     discrim_mp=a*(K_auto_early_mp-K_auto_late_mp)*cos(pi); % Out-of-phase
190     MP
191     discrim_tot=discrim+discrim_mp;
192
193     figure(4); plot(tau, discrim);hold on;
194     plot(tau, discrim_mp, 'r');grid on;
195     title(['Discriminator With more than one Multipath Signal
196
197     (a=', num2str(a), ', Cs=', num2str(1/Tc*Cs), ', Fc=', num2str(Fc/1e6), 'MHz, BW=',
198     num2str(BW_D), 'MHz)']);
199     legend('Discriminator Without Multipath', 'Discriminator With
200     Multipath');
201
202     figure(5);
203     plot(tau, discrim);hold on;
204     plot(tau, discrim_tot, 'g');
205     title(['Discriminator With more than one Multipath Signal
206     (a=', num2str(a), ', Cs=', num2str(1/Tc*Cs), ', Fc=', num2str(Fc/1e6), 'MHz, BW=',
207     num2str(BW_D), 'MHz)']);
208     legend('Discriminator Without Multipath', 'Sum of both
209     discriminators');
210     xlabel('Delay in Seconds');grid on;
211
212     end;
213     pause;
214
215     % Part 2:Code Tracking Multipath Error Calculations %
216
217     % Step 1 : Impact on Discriminator delay due to Filter only in the
218
219     % Step 1/A : Calculating the Delay Error Due to Filter Only
220
221     tau=-5*Tc:Tc/500:5*Tc;
222     discrim=K_auto_late-K_auto_early;
223     err_filt=err_finding(discrim,tau,Tc,Cs);
224
225     figure(6);
226     plot(tau, discrim);
227     title(['Discriminator Delay Due to Filter
228     Only(Cs=', num2str(1/Tc*Cs), ', Fc=', num2str(Fc/1e6), 'MHz, BW=', num2str(BW_D)
229     , 'MHz, Error=', num2str(err_filt), 'Meters, Filter=', num2str(Filter), ')']);
230     grid;pause;
231
232     % Step 1/B: Delay Error due to filter and One multipath Signal
233
234     [discrim_tot_max, val_max]=max(discrim_tot);
237     [discrim_tot_min, val_min]=min(discrim_tot);
238     tau_max_mp=tau(val_max);
     tau_min_mp=tau(val_min);

```

```

239 win=abs(tau_max_mp-tau_avg_mp);
240 tau_mp_1=tau_avg_mp-win;tau_mp_2=tau_avg_mp+win;
241 delt_tau_mp=((tau>tau_mp_1)&(tau<tau_mp_2));
242 discrim_delt_tau_mp=discrim_tot(delt_tau_mp);
243 figure;
244 plot(tau(delt_tau_mp),discrim_delt_tau_mp);
245 title(['Discriminator delay due to filter and MP in the linear region
246 (a=',num2str(a),' ,Cs=',num2str(1/Tc*Cs),' ,Fc=',num2str(Fc/1e6),'MHz,BW=',
247 num2str(BW_D),'MHz,Filter=',num2str(Filter),'')]);
248 grid;pause;
249
250 % Step 2 :Impact on Discriminator Delay Due to Multipath only
251
252 if a==1
253 vect_delay=[0.01*Tc:0.01*Tc:2*Tc];
254 end;
255
256 if a~=1
257 vect_delay=[0*Tc:0.01*Tc:2*Tc];
258 end;
259
260 err_tau_pos=zeros(1,length(vect_delay));
261 err_tau_neg=zeros(1,length(vect_delay));
262 tau_max=zeros(1,length(vect_delay));
263 err_cross_tau=zeros(1,length(vect_delay));
264 first_neg=0;
265
266 h=waitbar(0,'Please wait ... ');
267
268 for i=1:length(vect_delay);
269 mp_delay=vect_delay(i);i
270
271 tau_early_mp=(-5*Tc-Cs/2-mp_delay):Tc/500:(5*Tc-Cs/2-mp_delay);
272 tau_late_mp=(-5*Tc+Cs/2-mp_delay):Tc/500:(5*Tc+Cs/2-mp_delay);
273
274 if bpsk==1;
275 discrim=K_auto_late-K_auto_early;
276 err_filt=err_finding(discrim,tau,Tc,Cs);
277 K_auto_early_mp=autocorr(tau_early_mp,Tc);
278 K_auto_late_mp=autocorr(tau_late_mp,Tc);
279 K_auto_early_mp=filter(b1,a1,K_auto_early_mp);
280 K_auto_late_mp=filter(b1,a1,K_auto_late_mp);
281 discrim=(K_auto_late-K_auto_early);
282 discrim_mp=a*(K_auto_late_mp-K_auto_early_mp);
283
284 elseif boc11==1;
285 lag_E=-Cs/2;
286 lag_L=Cs/2;
287 discrim=K_auto_early-K_auto_late;
288 err_filt=err_finding(discrim,tau,Tc,Cs);
289 K_auto_early_mp=Auto_BOC_1_1(lag_E-mp_delay,tau_early_mp,Tc);
290 K_auto_late_mp=Auto_BOC_1_1(lag_L-mp_delay,tau_late_mp,Tc);
291 K_auto_early_mp=filter(b1,a1,K_auto_early_mp);
292 K_auto_late_mp=filter(b1,a1,K_auto_late_mp); discrim=(K_auto_early-
293 K_auto_late); discrim_mp=a*(K_auto_early_mp-K_auto_late_mp);
294
295 elseif boc22==1;
296 lag_E=-Cs/2;
297 lag_L=Cs/2;

```

```

299         discrim=K_auto_early-K_auto_late;
300         err_filt=err_finding(discrim,tau,Tc,Cs);
301         K_auto_early_mp=Auto_BOC_2_2(lag_E-mp_delay,tau_early_mp,Tc);
302         K_auto_late_mp=Auto_BOC_2_2(lag_L-mp_delay,tau_late_mp,Tc);
303         K_auto_early_mp=filter(b1,a1,K_auto_early_mp);
304         K_auto_late_mp=filter(b1,a1,K_auto_late_mp);
305         discrim=(K_auto_early-K_auto_late);
306         discrim_mp=a*(K_auto_early_mp-K_auto_late_mp);
307     end;
308
309     waitbar(i/length(vect_delay),h);
310
311     discrim_tot_pos=discrim+discrim_mp; % MP Inphase with the LOS
312     signal(positive envelope)
313     discrim_tot_neg=discrim-discrim_mp; % MP out-of-phase with LOS
314     signal(negative envelope)
315
316     if bpsk==1; err_tau_pos(i)=err_finding(discrim_tot_pos,tau,Tc,Cs);
317     err_tau_pos(i)=err_tau_pos(i)-err_filt; % this is teh positive
318     error envelope err_tau_neg(i)=err_finding(discrim_tot_neg,tau,Tc,Cs);
319     err_tau_neg(i)=err_tau_neg(i)-err_filt; % this is the negative
320     error envelope
321
322     elseif (boc11==1 | boc22==1);
323
324     if i==1; [discrim_max,ind_max]=max(discrim_tot_pos);
325     [discrim_min,ind_min]=min(discrim_tot_pos);
326     tau_max(i)=tau(ind_max); tau_min=tau(ind_min);
327     tau_avg(i)=.5*(tau_max(i)+tau_min); win=abs(tau_max(i)-
328     tau_avg(i)); tau_1(i)=tau_avg(i)-win;
329     tau_2(i)=tau_avg(i)+win;
330
331     else
332     if (i>1 & i<6)
333     tau_max(i)=old_tau_zero;
334
335     else
336     r0=i-4;
337     A=[err_cross_tau(i-1);err_cross_tau(i-2);err_cross_tau(i-
338     3);err_cross_tau(i-4);];
339     B=[1 i-r0 (i-r0)^2 (i-r0)^3;
340     1 i-1-r0 (i-1-r0)^2 (i-1-r0)^3;
341     1 i-2-r0 (i-2-r0)^2 (i-2-r0)^3;
342     1 i-3-r0 (i-3-r0)^2 (i-3-r0)^3]; C=B\A;
343     tau_max(i)=[1 i-r0+1 (i-r0+1)^2 (i-00+1)^3]*C;
344     end;
345     end;
346
347     k=1; discrim_delt_tau=-1;
348     pos(1)=2;
349     neg=find(discrim_delt_tau<0);
350     first_neg=neg(1);
351
352
353
354
355
356
357
358

```

```
359 while(length(find(discrim_delt_tau>0))==0 |
360 length(find(discrim_delt_tau<0))==0 | pos(1)~=1);
361 delt_tau=((tau>tau_avg-k*win/500)&(tau<tau_avg+k*win/500));%
362 enlarging tau from middle towards edges
363 discrim_delt_tau=discrim_tot_pos(delt_tau); k=k+1;
364 pos=find(discrim_delt_tau>0);
365 end;
366
367 neg=find(discrim_delt_tau<0); first_neg=neg(1);
368 ind_neg=find(discrim_tot_pos==discrim_delt_tau(first_neg)); if
369 length(ind_neg)~=1;
370 ind_neg=ind_neg(1); end;
371 val_first_neg=discrim_delt_tau(first_neg);
372 ind_pos=ind_neg-1;
373 val_first_pos=discrim_delt_tau(first_neg-1);
374
375 step=Tc/300; tau_crossp=tau(ind_pos):step/100:tau(ind_neg);
376 delt_crossp=interp1([tau(ind_pos) tau(ind_neg)], [val_first_pos
377 val_first_neg],tau_crossp);
378
379 err_cross_tau(i)=tau_crossp(find(abs(delt_crossp)==min(abs(delt_crossp))))
380 );
381 old_tau_zero=err_cross_tau(i);
382 err_tau_pos(i)=c*err_cross_tau(i)-err_filt;
383
384 if i==1; [discrim_max,ind_max]=max(discrim_tot_neg);
385 [discrim_min,ind_min]=min(discrim_tot_neg);
386 tau_max(i)=tau(ind_max); tau_min=tau(ind_min);
387 tau_avg(i)=.5*(tau_max(i)+tau_min); win=abs(tau_max(i)-
388 tau_avg(i)); tau_1(i)=tau_avg(i)-win;
389 tau_2(i)=tau_avg(i)+win;
390
391 else
392 if (i>1 & i<6)
393 tau_max(i)=old_tau_zero;
394
395 else
396 r0=i-4;
397 A=[err_cross_tau(i-1);err_cross_tau(i-2);err_cross_tau(i-
398 3);err_cross_tau(i-4)];
399 B=[1 i-r0 (i-r0)^2 (i-r0)^3;
400 1 i-1-r0 (i-1-r0)^2 (i-1-r0)^3;
401 1 i-2-r0 (i-2-r0)^2 (i-2-r0)^3;
402 1 i-3-r0 (i-3-r0)^2 (i-3-r0)^3]; C=B\A;
403 tau_max(i)=[1 i-r0+1 (i-r0+1)^2 (i-00+1)^3]*C;
404 end;
405 end;
406
407 k=1; discrim_delt_tau=-1;
408 pos(1)=2;
409 neg=find(discrim_delt_tau<0);
418
```

```
419     first_neg=neg(1);
420
421     while(length(find(discrim_delt_tau>0))==0 |
422     length(find(discrim_delt_tau<0))==0 | pos(1)~=1);
423     delt_tau=((tau>tau_avg-k*win/500)&(tau<tau_avg+k*win/500));%
424     enlarging tau from middle towards edges
425     discrim_delt_tau=discrim_tot_neg(delt_tau); k=k+1;
426     pos=find(discrim_delt_tau>0);
427     end;
428
429     neg=find(discrim_delt_tau<0); first_neg=neg(1);
430     ind_neg=find(discrim_tot_neg==discrim_delt_tau(first_neg)); if
431     length(ind_neg)~=1;
432     ind_neg=ind_neg(1); end;
433     val_first_neg=discrim_delt_tau(first_neg);
434     ind_pos=ind_neg-1;
435     val_first_pos=discrim_delt_tau(first_neg-1);
436
437     step=Tc/300; tau_crossp=tau(ind_pos):step/100:tau(ind_neg);
438     delt_crossp=interp1([tau(ind_pos) tau(ind_neg)], [val_first_pos
439     val_first_neg],tau_crossp);
440
441     err_cross_tau(i)=tau_crossp(find(abs(delt_crossp)==min(abs(delt_crossp))
442     ));
443     old_tau_zero=err_cross_tau(i);
444     err_tau_neg(i)=c*err_cross_tau(i)-err_filt;
445     end;
446     end;
447
448     close(h); figure;
449     plot(vect_delay,err_tau_pos,'b');hold on;
450     plot(vect_delay,err_tau_neg,'r');grid;
451     title('Code Error Envelope');
452     xlabel('Delay in Seconds');
453     ylabel('Error in Meters'); title(['Code Multipath Error Envelope
454     (a=',num2str(a),' ,Cs=',num2str(1/Tc*Cs),' ,Fc=',num2str(Fc/1e6),'MHz,BW=',
455     num2str(BW_D),'MHz,Waveform=',num2str(mater),' ,Filter=',num2str(Filter),'
456     ')]);
457
458     % The End of The Code multipath error Envelope Matlab Program
459
460
461     % Matlab-based Phase Multipath Error Envelopes
462
463     clc;
464     format long;
465     clear all;
466     close all;
467
468     % GPS L1 Constants
469
470     c=299792458;      % Speed of Light in Vacuum in m/s
471     F1=1575.42e6;    % L1 Frequency in Hz
472     T1=1/F1;        % Period of L1
473
474
475
476
477
478
```

```
479 lamda=c/F1;      % Wave Length of L1
480 Fc=1023000;     % Chip Frequency C/A
481
482 % Part 1: Pre-Envelope calculation stages
483
484 % Step 1 : Input parameters
485
486 Fc=input('Input Code Frequency (in MHz) Fc=');
487 BW_D=input('Input Double-sided bandwidth (in MHz) BW_D= ');
488 Cs=input('Early-Late Chip Spacing(from 0 to 1) Cs= ');
489 a=input('Relative Amplitude of the Reflected Signal(from 0 to 1) a= ');
490 mater=input('Code materialization waveform. Choose 'bpsk' or 'boc11'
491 or 'boc22'): ', 's');
492
493 if strcmp(mater, 'bpsk')
494     bpsk=1;
495     boc11=0;
496     boc22=0;
497 elseif strcmp(mater, 'boc11')
498     bpsk=0;
499     boc11=1;
500     boc22=0;
501 elseif strcmp(mater, 'boc22')
502     bpsk=0;
503     boc11=0;
504     boc22=1;
505 else
506     fprintf('Input Error.... Repeat the simulation!');
507     return
508 end;
509
510 Filter=input('Filter type, Choose 'butterworth' or 'chebyshev' or
511 'fir_boxcar' or 'fir_hamming'): ', 's');
512
513 if strcmp(Filter, 'butterworth')
514     butterworth=1;
515     chebyshev=0;
516     fir_boxcar=0;
517     fir_hamming=0;
518 elseif strcmp(Filter, 'chebyshev')
519     butterworth=0;
520     chebyshev=1;
521     fir_boxcar=0;
522     fir_hamming=0;
523 elseif strcmp(Filter, 'fir_boxcar')
524     butterworth=0;
525     chebyshev=0;
526     fir_boxcar=1;
527     fir_hamming=0;
528 elseif strcmp(Filter, 'fir_hamming')
529     butterworth=0;
530     chebyshev=0;
531     fir_boxcar=0;
532     fir_hamming=1;
533 else
534     fprintf('Input Error.... Repeat the simulation!');
535     return
536 end;
537
538
539 Fc=Fc*1e6;
```



```

539 Tc=1/Fc;
540 Cs=Cc*Tc;
541 fc=BW_D/2;
542
543 % Step 2 :Early-Late Power Discriminator stage
544
545 tau=-3*Tc:Tc/300:3*Tc;
546 eps_tau_early=(-3*Tc+Cc/2):Tc/300:(3*Tc+Cc/2);
547 eps_tau_late=(-3*Tc-Cc/2):Tc/300:(3*Tc-Cc/2);
548 eps_theta=3*pi/4;
549
550 if bpsk==1;
551 I_auto_early=autocorr(eps_tau_early,Tc).*cos(eps_theta);
552 Q_auto_early=autocorr(eps_tau_early,Tc).*sin(eps_theta);
553 I_auto_late=autocorr(eps_tau_late,Tc).*cos(eps_theta);
554 Q_auto_late=autocorr(eps_tau_late,Tc).*sin(eps_theta);
555
556 elseif boc11==1; lag=-Cc/2;
557 I_auto_early=Auto_BOC_1_1(lag,eps_tau_early,Tc).*cos(eps_theta);
558 Q_auto_early=Auto_BOC_1_1(lag,eps_tau_early,Tc).*sin(eps_theta);
559 I_auto_late=Auto_BOC_1_1(lag,eps_tau_late,Tc).*cos(eps_theta);
560 Q_auto_late=Auto_BOC_1_1(lag,eps_tau_late,Tc).*sin(eps_theta);
561
562 elseif boc22==1; lag=-Cc/2;
563 I_auto_early=Auto_BOC_2_2(lag,eps_tau_early,Tc).*cos(eps_theta);
564 Q_auto_early=Auto_BOC_2_2(lag,eps_tau_early,Tc).*sin(eps_theta);
565 I_auto_late=Auto_BOC_2_2(lag,eps_tau_late,Tc).*cos(eps_theta);
566 Q_auto_late=Auto_BOC_2_2(lag,eps_tau_late,Tc).*sin(eps_theta);
567 end;
568
569 if butterworth==1;
570 [b1,a1]=butter(6,(2*fc/300));
571 elseif chebyshev==1;
572 [b1,a1]=cheby1(3,1,(2*fc/300));
573 elseif fir_boxcar==1;
574 [b1,a1]=fir1(1000,2*fc/300,boxcar(1001));
575 elseif fir_hamming==1;
576 [b1,a1]=fir1(100,2*fc/300,Hamming(101));
577 end;
578
579 I_auto_early=filter(b1,a1,I_auto_early);
580 Q_auto_early=filter(b1,a1,Q_auto_early);
581 I_auto_late=filter(b1,a1,I_auto_late);
582 Q_auto_late=filter(b1,a1,Q_auto_late);
583
584 figure(1);
585 plot(tau,I_auto_early,'b');hold on;
586 plot(tau,I_auto_late,'r');hold on;
587 plot(tau,Q_auto_early,'-b');hold on;
588 plot(tau,Q_auto_late,'-r');grid on;
589 title('Autocorrelation Functions');
590 legend('I auto early','I auto late','Q auto early','Q auto late');pause;
591
592 vect_tau_delay=[0.001*Tc:Tc/100:1.5*Tc];
593 vect_theta_delay=[.001*pi:pi/150:pi];
594
595 mp_tau_delay=zeros(1,length(vect_tau_delay));
596 mp_theta_delay=zeros(1,length(vect_theta_delay));

```

```
599
600 h=waitbar(0,'Please wait ...');
601
602 for i=1:length(vect_tau_delay);
603 mp_tau_delay=vect_tau_delay(i);
604 mp_theta_delay=vect_theta_delay(i);
605
606 eps_tau_early_mp=(-
607 3*Tc+Cs/2+mp_tau_delay):Tc/300:(3*Tc+Cs/2+mp_tau_delay);
608 eps_tau_late_mp=(-3*Tc-Cs/2+mp_tau_delay):Tc/300:(3*Tc-
609 Cs/2+mp_tau_delay);
610
611 if bpsk==1;
612
613 I_auto_early_mp=a*autocorr(eps_tau_early_mp,Tc).*cos(eps_theta+mp_theta_d
614 elay);
615
616 Q_auto_early_mp=a*autocorr(eps_tau_early_mp,Tc).*sin(eps_theta+mp_theta_d
617 elay);
618
619 I_auto_late_mp=a*autocorr(eps_tau_late_mp,Tc).*cos(eps_theta+mp_theta_del
620 ay);
621
622 Q_auto_late_mp=a*autocorr(eps_tau_late_mp,Tc).*sin(eps_theta+mp_theta_del
623 ay);
624
625 elseif boc11==1;
626 lag_E=-Cs/2;
627 lag_L=Cs/2;
628
629 I_auto_early_mp=a*Auto_BOC_1_1(lag_E,eps_tau_early_mp,Tc).*cos(eps_theta+
630 mp_theta_delay);
631
632 Q_auto_early_mp=a*Auto_BOC_1_1(lag_E,eps_tau_early_mp,Tc).*sin(eps_theta+
633 mp_theta_delay);
634
635 I_auto_late_mp=a*Auto_BOC_1_1(lag_L,eps_tau_late_mp,Tc).*cos(eps_theta+mp
636 _theta_delay);
637
638 Q_auto_late_mp=a*Auto_BOC_1_1(lag_L,eps_tau_late_mp,Tc).*sin(eps_theta+mp
639 _theta_delay);
640
641 elseif boc22==1;
642 lag_E=-Cs/2;
643 lag_L=Cs/2;
644
645 I_auto_early_mp=a*Auto_BOC_2_2(lag_E,eps_tau_early_mp,Tc).*cos(eps_theta+
646 mp_theta_delay);
647
648 Q_auto_early_mp=a*Auto_BOC_2_2(lag_E,eps_tau_early_mp,Tc).*sin(eps_theta+
649 mp_theta_delay);
650
651 I_auto_late_mp=a*Auto_BOC_2_2(lag_L,eps_tau_late_mp,Tc).*cos(eps_theta+mp
652 _theta_delay);
653
654 Q_auto_late_mp=a*Auto_BOC_2_2(lag_L,eps_tau_late_mp,Tc).*sin(eps_theta+mp
655 _theta_delay);
656
657 end;
658
659 I_auto_early_mp=filter(b1,a1,I_auto_early_mp);
```

```

659 Q_auto_early_mp=filter(b1,a1,Q_auto_early_mp);
660 I_auto_late_mp=filter(b1,a1,I_auto_late_mp);
661 Q_auto_late_mp=filter(b1,a1,Q_auto_late_mp);
662
663 I_auto_early_tot=I_auto_early+I_auto_early_mp;
664 Q_auto_early_tot=Q_auto_early+Q_auto_early_mp;
665 I_auto_late_tot=I_auto_late+I_auto_late_mp;
666 Q_auto_late_tot=Q_auto_late+Q_auto_late_mp;
667
668 E_L_discrim=(I_auto_early).^2+(Q_auto_early).^2-(I_auto_late).^2-
669 (Q_auto_late).^2;
670 E_L_discrim_tot=(I_auto_early_tot).^2+(Q_auto_early_tot).^2-
671 (I_auto_late_tot).^2-(Q_auto_late_tot).^2;
672
673 waitbar(i/length(vect_tau_delay),h);
674 end;
675
676 close(h); figure(2);
677 plot(tau,E_L_discrim);hold on;
678 plot(tau,E_L_discrim_tot,'r');
679 legend('Phase Discriminator W/O MP','Phase Discriminator With MP');
680 title('Discriminator Function');
681 xlabel('Delay in Seconds');grid on;pause;
682 % Part 2: Phase Tracking Error Calculation
683
684 % Step 1: Calculation of the delay implied by the filter
685
686 err_filt=err_finding(E_L_discrim,tau,Cs,Tc);
687 err_filt=err_filt/c;
688
689 figure(3);
690 plot(tau,E_L_discrim);
691 title(['Phase Discriminator Delay Due to Filter
692 Only(Cs=',num2str(1/Tc*Cs),' ,Fc=',num2str(Fc/1e6),'MHz,BW=',num2str(BW_D)
693 , 'MHz,Error=',num2str(err_filt*c),'Meters)']);
694 grid;pause;
695
696
697 % Step 2: Calculation of the delay implied by the multipath over 1.5*Tc
698
699 vect_tau_delay=[0.01*Tc:Tc/500:1.5*Tc];
700 vect_theta_phase=-pi:pi/5:pi;
701
702 eps_tau_early=0;
703 eps_tau_late=0;
704 eps_theta=0;
705
706 h=waitbar(0,'Please wait ...');
707
708 for i=1:length(vect_tau_delay);i
709 for j=1:length(vect_theta_phase);j
710 mp_tau_delay=vect_tau_delay(i);
711 mp_theta_delay=vect_theta_phase(j);
712
713 eps_tau_early_mp=(-
714 3*Tc+Cs/2+mp_tau_delay):Tc/300:(3*Tc+Cs/2+mp_tau_delay);
715 eps_tau_late_mp=(-3*Tc-Cs/2+mp_tau_delay):Tc/300:(3*Tc-
716 Cs/2+mp_tau_delay);

```

```
719 %intializtion of the while loop
720 last_eps_tau_early=eps_tau_early+Tc;
721 last_eps_tau_late=eps_tau_late+Tc;
722 last_eps_theta=eps_theta+pi/2;
723
724 while((abs(last_eps_theta-eps_theta)>pi/100) & (abs(last_eps_tau_early-
725 eps_tau_early)>Tc/100) & (abs(last_eps_tau_late- eps_tau_late)>Tc/100));
726
727 last_eps_tau_early=eps_tau_early;
728 last_eps_tau_late=eps_tau_late;
729 last_eps_theta=eps_theta;
730
731 if bpsk==1;
732
733 I_auto_early=autocorr(eps_tau_early,Tc).*cos(eps_theta);
734
735 Q_auto_early=autocorr(eps_tau_early,Tc).*sin(eps_theta);
736
737 I_auto_late=autocorr(eps_tau_late,Tc).*cos(eps_theta);
738
739 Q_auto_late=autocorr(eps_tau_late,Tc).*sin(eps_theta);
740
741 I_auto_early=filter(b1,a1,I_auto_early);
742 Q_auto_early=filter(b1,a1,Q_auto_early);
743 I_auto_late=filter(b1,a1,I_auto_late);
744 Q_auto_late=filter(b1,a1,Q_auto_late);
745
746 %mp_theta_delay=0 %for the inphase mutlipath
747
748 I_auto_early_mp=a*autocorr(eps_tau_early_mp,Tc).*cos(eps_thet
749 a+mp_theta_delay);
750 Q_auto_early_mp=a*autocorr(eps_tau_early_mp,Tc).*sin(eps_thet
751 a+mp_theta_delay);
752 I_auto_late_mp=a*autocorr(eps_tau_late_mp,Tc).*cos(eps_theta+
753 mp_theta_delay);
754 Q_auto_late_mp=a*autocorr(eps_tau_late_mp,Tc).*sin(eps_theta+
755 mp_theta_delay);
756
757 I_auto_early_mp=filter(b1,a1,I_auto_early_mp);
758 Q_auto_early_mp=filter(b1,a1,Q_auto_early_mp);
759 I_auto_late_mp=filter(b1,a1,I_auto_late_mp);
760 Q_auto_late_mp=filter(b1,a1,Q_auto_late_mp);
761
762 I_auto_early_tot_pos=I_auto_early+I_auto_early_mp;
763 %for inphase positive side :
764 Q_auto_early_tot_pos=Q_auto_early+Q_auto_early_mp;
765 I_auto_late_tot_pos=I_auto_late+I_auto_late_mp;
766 Q_auto_late_tot_pos=Q_auto_late+Q_auto_late_mp;
767
768 E_L_discrim=(I_auto_early).^2+(Q_auto_early).^2- (I_auto_late).^2-
769 (Q_auto_late).^2; % without multipath
770
771 E_L_discrim_tot_pos=((I_auto_early_tot_pos).^2+(Q_auto_early_tot_pos).^2-
772 (I_auto_late_tot_pos).^2-(Q_auto_late_tot_pos).^2);
773
774
775 err_tau_pos(i,j)=err_finding(E_L_discrim_tot_pos,tau,Cs,Tc);
776 err_tau_pos(i,j)=err_tau_pos(i)/c-err_filt; %without filter error
778
```

```
779
780
781 eps_tau_mp_pos=err_tau_pos(i,j)+mp_tau_delay;
782 K_auto_mp_pos=autocorr(eps_tau_mp_pos,Tc); % as an
783 approximation filter is removed here
784 K_auto_pos=autocorr(err_tau_pos(i,j),Tc);
785
786
787 err_theta_pos(i,j)=atan((a*K_auto_mp_pos*sin(mp_theta_delay))/(K_auto_pos
788 +a*cos(mp_theta_delay)*K_auto_mp_pos));
789 err_theta_pos(i,j)=err_theta_pos(i,j)/2/pi*lamda; %in meters
790 end;
791
792 if (boc11==1 | boc22==1);
793 if boc11==1;
794 lag=-Cs/2;
795
796 I_auto_early=Auto_BOC_1_1(lag,eps_tau_early,Tc).*cos(eps_theta);
797
798 Q_auto_early=Auto_BOC_1_1(lag,eps_tau_early,Tc).*sin(eps_theta);
799
800 I_auto_late=Auto_BOC_1_1(lag,eps_tau_late,Tc).*cos(eps_theta);
801
802 Q_auto_late=Auto_BOC_1_1(lag,eps_tau_late,Tc).*sin(eps_theta);
803 end;
804
805 if boc22==1;
806 lag=-Cs/2;
807
808 I_auto_early=Auto_BOC_2_2(lag,eps_tau_early,Tc).*cos(eps_theta);
809
810 Q_auto_early=Auto_BOC_2_2(lag,eps_tau_early,Tc).*sin(eps_theta);
811
812 I_auto_late=Auto_BOC_2_2(lag,eps_tau_late,Tc).*cos(eps_theta);
813
814 Q_auto_late=Auto_BOC_2_2(lag,eps_tau_late,Tc).*sin(eps_theta);
815 end;
816
817 I_auto_early=filter(b1,a1,I_auto_early);
818 Q_auto_early=filter(b1,a1,Q_auto_early);
819 I_auto_late=filter(b1,a1,I_auto_late);
820 Q_auto_late=filter(b1,a1,Q_auto_late);
821
822
823 if boc11==1; lag_E=-Cs/2;
824 lag_L=Cs/2;
825 I_auto_early_mp=a*Auto_BOC_1_1(lag_E-
826 mp_tau_delay,eps_tau_early_mp,Tc).*cos(eps_theta+mp_theta_delay
827 ); Q_auto_early_mp=a*Auto_BOC_1_1(lag_E-
828 mp_tau_delay,eps_tau_early_mp,Tc).*sin(eps_theta+mp_theta_delay
829 ); I_auto_late_mp=a*Auto_BOC_1_1(lag_L-
830 mp_tau_delay,eps_tau_late_mp,Tc).*cos(eps_theta+mp_theta_delay)
831 ;
832 Q_auto_late_mp=a*Auto_BOC_1_1(lag_L-
833 mp_tau_delay,eps_tau_late_mp,Tc).*sin(eps_theta+mp_theta_delay)
834 ;
838
```

```

839     end;
840
841     if boc22==1; lag_E=-Cs/2;
842     lag_L=Cs/2;
843     I_auto_early_mp=a*Auto_BOC_2_2(lag_E-
844     mp_tau_delay,eps_tau_early_mp,Tc).*cos(eps_theta+mp_theta_delay
845     );
846     Q_auto_early_mp=a*Auto_BOC_2_2(lag_E-
847     mp_tau_delay,eps_tau_early_mp,Tc).*sin(eps_theta+mp_theta_delay
848     ); I_auto_late_mp=a*Auto_BOC_2_2(lag_L-
849     mp_tau_delay,eps_tau_late_mp,Tc).*cos(eps_theta+mp_theta_delay)
850     ;
851     Q_auto_late_mp=a*Auto_BOC_2_2(lag_L-
852     mp_tau_delay,eps_tau_late_mp,Tc).*sin(eps_theta+mp_theta_delay)
853     ;
854     end,
855
856     I_auto_early_mp=filter(b1,a1,I_auto_early_mp);
857     Q_auto_early_mp=filter(b1,a1,Q_auto_early_mp);
858     I_auto_late_mp=filter(b1,a1,I_auto_late_mp);
859     Q_auto_late_mp=filter(b1,a1,Q_auto_late_mp);
860
861     I_auto_early_tot_pos=I_auto_early+I_auto_early_mp;
862     Q_auto_early_tot_pos=Q_auto_early+Q_auto_early_mp;
863     I_auto_late_tot_pos=I_auto_late+I_auto_late_mp;
864     Q_auto_late_tot_pos=Q_auto_late+Q_auto_late_mp;
865
866     E_L_discrim=(I_auto_early).^2+(Q_auto_early).^2-(I_auto_late).^2-
867     (Q_auto_late).^2; % without multipath
868     E_L_discrim_tot_pos=((I_auto_early_tot_pos).^2+(Q_auto_early_tot_pos).^2-
869     (I_auto_late_tot_pos).^2-(Q_auto_late_tot_pos).^2);
870
871     if i==1; [discrim_max,ind_max]=max(E_L_discrim_tot_pos);
872     [discrim_min,ind_min]=min(E_L_discrim_tot_pos);
873     tau_max(i)=tau(ind_max);
874     tau_min=tau(ind_min);
875     tau_avg(i)=.5*(tau_max(i)+tau_min); win=abs(tau_max(i)-
876     tau_avg(i)); tau_1(i)=tau_avg(i)-win;
877     tau_2(i)=tau_avg(i)+win;
878
879     else
880     if (i>1 & i<6)
881     tau_max(i)=old_tau_zero;
882
883     else
884     r0=i-4;
885     A=[err_cross_tau(i-1);err_cross_tau(i-
886     2);err_cross_tau(i-3);err_cross_tau(i-4)];
887     B=[1 i-r0 (i-r0)^2 (i-r0)^3;
888     1 i-1-r0 (i-1-r0)^2 (i-1-r0)^3;
889     1 i-2-r0 (i-2-r0)^2 (i-2-r0)^3;
890     1 i-3-r0 (i-3-r0)^2 (i-3-r0)^3]; C=B\A;
891     tau_max(i)=[1 i-r0+1 (i-r0+1)^2 (i-00+1)^3]*C;
892     end;
893     end;
898

```

```
899
900 k=1; discrim_delt_tau=-1; pos(1)=2;
901 neg=find(discrim_delt_tau<0);
902 first_neg=neg(1);
903
904 while(length(find(discrim_delt_tau>0))==0 |
905 length(find(discrim_delt_tau<0))==0 | pos(1)~=1);
906 delt_tau=((tau>tau_avg- k*win/500)&(tau<tau_avg+k*win/500));% enlarging
907 tau from middle towards edges
908 discrim_delt_tau=E_L_discrim_tot_pos(delt_tau);
909 k=k+1;
910 pos=find(discrim_delt_tau>0);
911 end;
912
913 neg=find(discrim_delt_tau<0);
914 first_neg=neg(1);
915
916 ind_neg=find(E_L_discrim_tot_pos==discrim_delt_tau(first_neg));
917 if length(ind_neg)~=1;
918 ind_neg=ind_neg(1);
919 end; val_first_neg=discrim_delt_tau(first_neg);
920 ind_pos=ind_neg-1; val_first_pos=discrim_delt_tau(first_neg-
921 1);
922
923 step=Tc/300;
924 tau_crossp=tau(ind_pos):step/100:tau(ind_neg);
925 delt_crossp=interp1([tau(ind_pos) tau(ind_neg)], [val_first_pos
926 val_first_neg],tau_crossp);
927
928 err_cross_tau(i)=tau_crossp(find(abs(delt_crossp)==min(abs(delt_crossp))
929 ));
930 old_tau_zero=err_cross_tau(i);
931 err_tau_pos(i,j)=err_cross_tau(i)-err_filt;
932
933 eps_tau_mp_pos=err_tau_pos(i,j)+mp_tau_delay;
934
935 if boc11==1;
936 lag=-Cs/2;
937
938 K_auto_mp_pos=Auto_BOC_1_1(lag,eps_tau_mp_pos,Tc); % as an
939 approximation filter is removed here
940 K_auto_pos=Auto_BOC_1_1(lag,err_tau_pos(i,j),Tc);
941 end;
942
943 if boc22==1;
944 lag=-Cs/2;
945
946 K_auto_mp_pos=Auto_BOC_2_2(lag,eps_tau_mp_pos,Tc); % as an
947 approximation filter is removed here also
948 K_auto_pos=Auto_BOC_2_2(lag,err_tau_pos(i,j),Tc);
949 end;
950
951 err_theta_pos(i,j)=atan((a*K_auto_mp_pos*sin(mp_theta_delay))/(K_auto_pos
952 +a*cos(mp_theta_delay)*K_auto_mp_pos));
953 err_theta_pos(i,j)=err_theta_pos(i,j)/2/pi*lamda; %in meters
958
```



```

959         end;
960         end;
961     end;

962     waitbar(i/length(vect_tau_delay),h);
963 end;
964

965 close(h);
966 figure(4);
967 for i=1:length(vect_tau_delay)
968     for j=1:length(vect_theta_phase)
969         plot(vect_tau_delay(i)/Tc,err_theta_pos(i,j));hold on;
970     end;
971 end;
972 title(['Phase Multipath Error Envelope
973 (a=',num2str(a),' ,Cs=',num2str(1/Tc*Cs),' ,Fc=',num2str(Fc/1e6),'MHz,BW=',
974 num2str(BW_D),'MHz,Waveform=',num2str(mater),'')]);
975 xlabel('Dealy in Chips');grid on;
976 ylabel('Phase Error in (Meters)');
977
978 % The End of The Phase Envelope Matlab Program
979
980
981 SUB-FUNCTIONS
982
983 1/4 -autocorr.m
984
985 function K=autocorr(tau,Tc)
986 K(tau<=-Tc)=0;
987 K((tau>-Tc)&(tau<=0))=1-(abs(tau((tau>-Tc)&(tau<=0)))/Tc);
988 K((tau>0)&(tau<Tc))=1-(abs(tau((tau>0)&(tau<Tc)))/Tc);
989 K(tau>=Tc)=0;
990
991 2/4 - Auto BOC 1 1.m
992
993 function K=Auto_BOC_1_1(Cs,tau,Tc);
994 n=1; q=1; % BOC(1,1)
995 F0 = 1.023*1e6; % Local Frequency to generate Fs and Fc
996 Fs = n*F0; % Sub-carrier Frequency
997 Ts=1/Fs;
998 Fc = q*F0; % Spreading Code Frequency
999 Tc = 1/Fc;
1000 Lc=1023*Tc; %Length of one code period in seconds
1001 tfin=Lc; %Simulation time
1002 t=[-5*Tc:Tc/500:5*Tc]; %Simulation time vector
1003 Fe=500*Fc;
1004 df=Fe/length(tau);
1005 f=-Fe/2:df:Fe/2-df;
1006 dsp=(1./(Tc*pi^2.*f.^2)).*sin(pi.*f*Tc).^2.*tan(pi.*f*Tc/2).^2.*exp(-
1007 2*pi*sqrt(-1).*f*Cs);% DSP of BOC(1,1)
1008 temp = real(fftshift(iff(fftshift(dsp))));
1009 A=max(temp);
1010 K=1/A*temp;
1018
3/4 - Auto BOC 2 2.m

function K=Auto_BOC_2_2(Cs,tau,Tc);
n=2; q=2; % BOC(2,2)

```

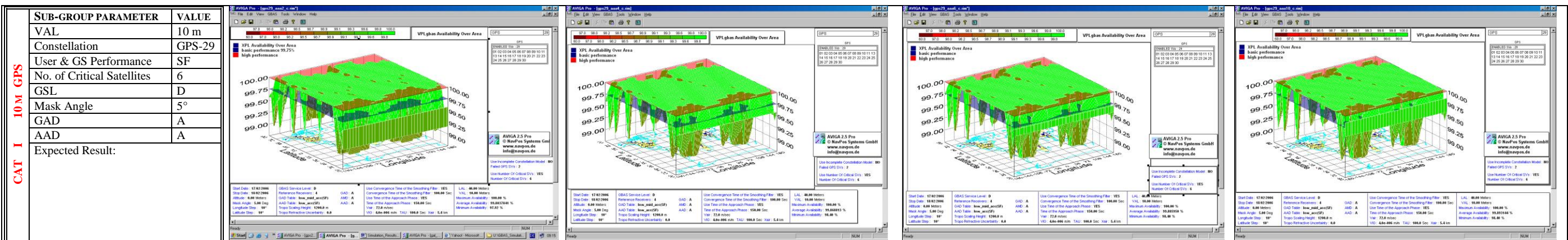
```
1019 Ts = 1/Fs;
1020 Fc = q*F0;           % Spreading Code Frequency is(2.046 MHz)
1021 Tc = 1/Fc;
1022 Lc=1023*Tc;         %Length of one code period in seconds
1023 tfin=Lc;           %Simulation time
1024 t=[-5*Tc:Tc/500:5*Tc]; %Simulation time vector
1025 Fe=500*Fc;
1026 df=Fe/length(tau);
1027 f=-Fe/2:df:Fe/2-df;
1028 dsp=(1./(Tc*pi^2.*f.^2)).*sin(pi.*f*Tc).^2.*tan(pi.*f*Tc/2).^2.*exp(-
1029 2*pi*sqrt(-1).*f*Cs);% DSP of BOC(2,2)
1030 temp = real(fftshift(iffshift(fftshift(dsp))));
1031 A=max(temp);
1032 K=1/A*temp;
1033
1034
1035 4/4 - err finding.m
1036
1037 function R=err_finding(discrim,tau,Tc,Cs)
1038 Fc=1.023;
1039 c=299792458;         % light speed in vacuum m/s
1040 Fc=Fc*1e6;          % chip code rate C/A code
1041 Tc=1/Fc;
1042 [discrim_max,ind_max]=max(discrim);
1043 [discrim_min,ind_min]=min(discrim);
1044 tau_max=tau(ind_max);
1045 tau_min=tau(ind_min);
1046 tau_avg=.5*(tau_max+tau_min);
1047 win=abs(tau_max-tau_avg);
1048 tau_1=tau_avg-win;
1049 tau_2=tau_avg+win;
1050
1051 j=1;
1052 delt_tau=((tau>tau_1)&(tau<tau_2)); % linear region
1053 discrim_delt_tau=discrim(delt_tau);
1054 pos=find(discrim_delt_tau>0);
1055
1056 while(length(find(discrim_delt_tau>0))==0 |
1057 length(find(discrim_delt_tau<0))==0 | pos(1)~=1);
1058 delt_tau=((tau>tau_avg-j*win/500)&(tau<tau_avg+j*win/500));%
1059 enlarging tau from middle towards edges
1060
1061 j=j+1;
1062 discrim_delt_tau=discrim(delt_tau);
1063 pos=find(discrim_delt_tau>0);
1064 end;
1065
1066 neg=find(discrim_delt_tau<0); first_neg=neg(1);
1067 ind_neg=find(discrim==discrim_delt_tau(first_neg));
1068 if length(ind_neg)~=1;
1069 ind_neg=ind_neg(1);
1070 end;
1071 val_first_neg=discrim_delt_tau(first_neg);
1072 ind_pos=ind_neg-1;
1073 val_first_pos=discrim_delt_tau(first_neg-1);
1074
1075 step=Tc/100;
1076 tau_crossp=tau(ind_pos):step/100:tau(ind_neg);
1077
```

```
delt_crossp=interp1([tau(ind_pos) tau(ind_neg)], [val_first_pos
val_first_neg],tau_crossp);
err_cross_tau=tau_crossp(find(abs(delt_crossp)==min(abs(delt_crossp)))));

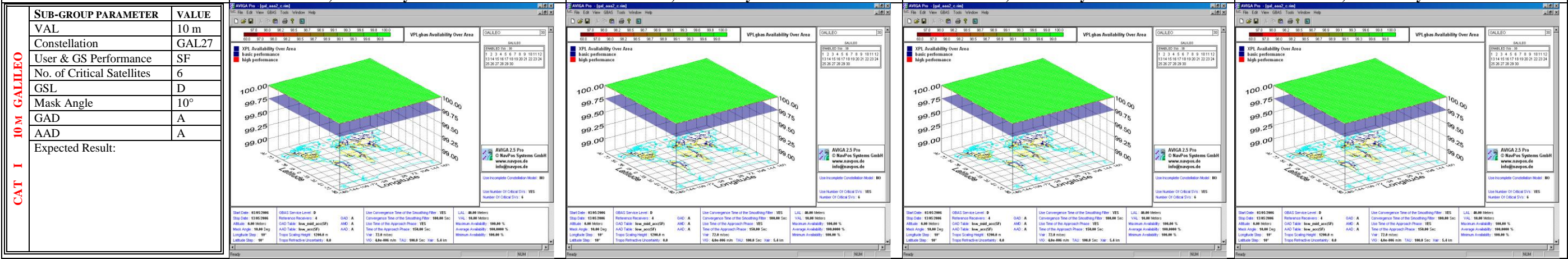
delay=err_cross_tau; % this is the filter delay in seconds
error=c*delay; % this is the filter delay error in meters
R=error
```

Appendix E: Outputs of the Simulation Runs

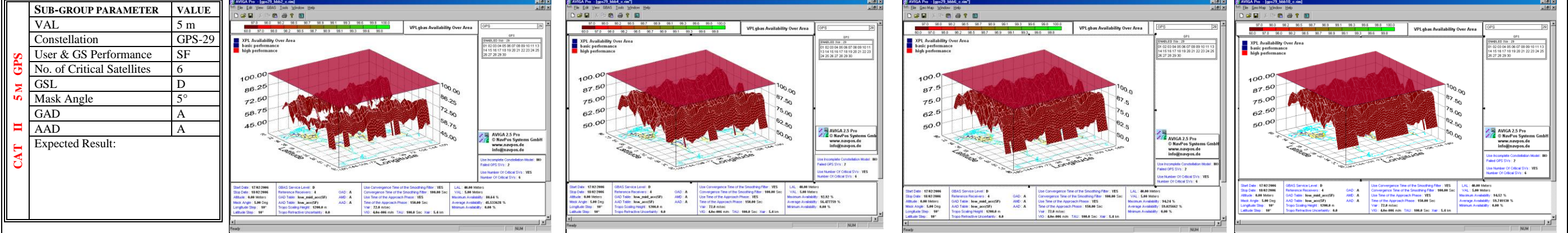
Appendix E: Simulations Results for the Impact of GPS Navigational Errors on the Required Performance of GBAS Approach Service Type D/F (GAST-D/F)



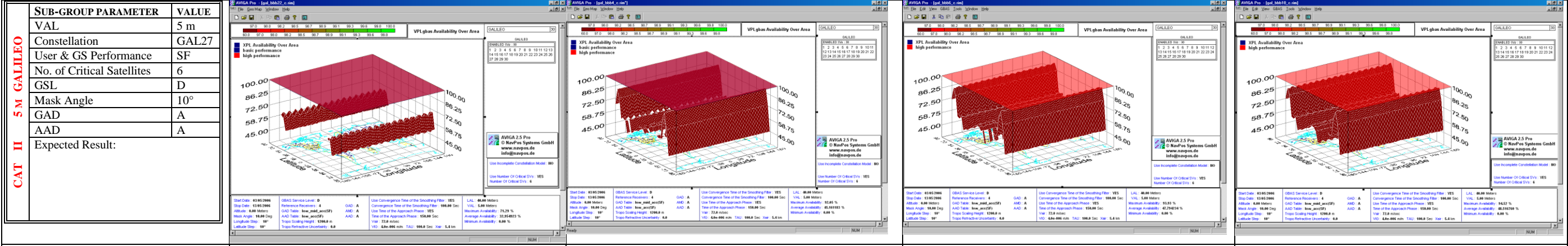
Multipath error :XPL Global Availability



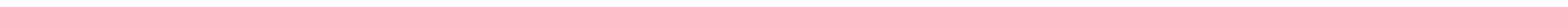
Multipath error: XPL Global Availability



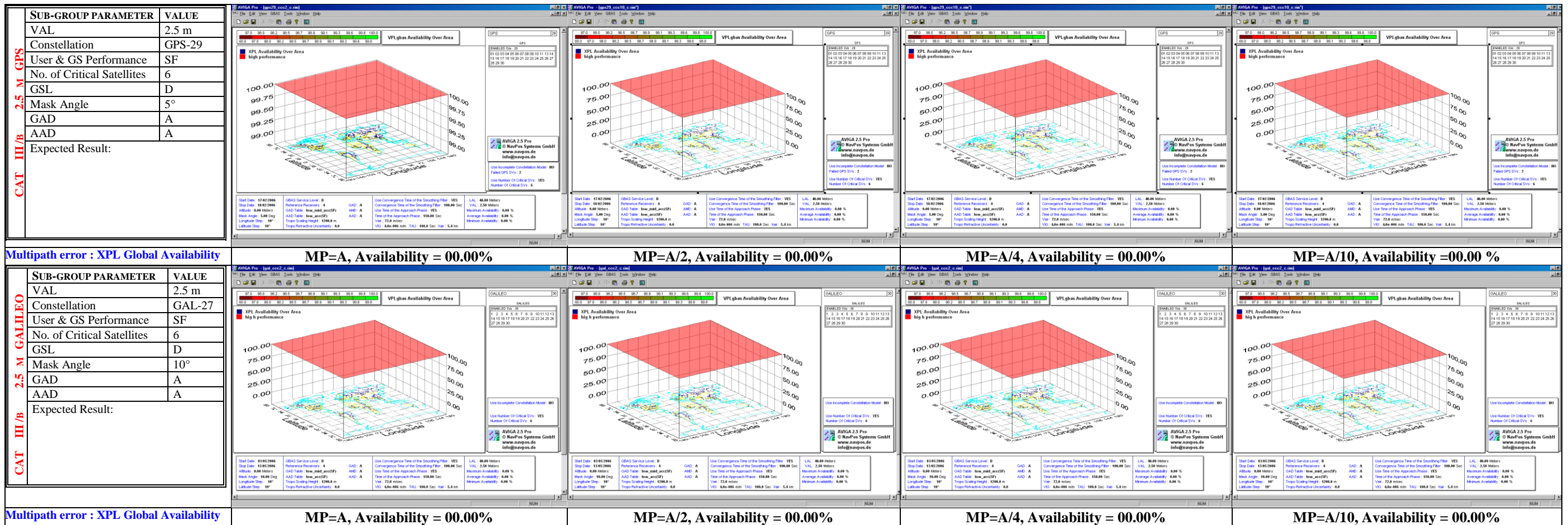
Multipath error :XPL Global Availability



Multipath error: XPL Global Availability



Appendix E: Simulations Results for the Impact of GPS Navigational Errors on the Required Performance of GBAS Approach Service Type D/F (GAST-D/F)



Appendix E: Simulations Results for the Impact of GPS Navigational Errors on the Required Performance of GBAS Approach Service Type D/F (GAST-D/F)

CAT I 10M GPS	SUB-GROUP PARAMETER	VALUE
	VAL	10 m
	Constellation	GPS-29
	User & GS Performance	DF
	No. of Critical Satellites	6
	GSL	D
	Mask Angle	5°
GAD	A	
AAD	A	
Expected Result:		

Multipath error :XPL Global Availability

CAT I 10M GALILEO	SUB-GROUP PARAMETER	VALUE
	VAL	10 m
	Constellation	GAL27
	User & GS Performance	DF
	No. of Critical Satellites	6
	GSL	D
	Mask Angle	10°
GAD	A	
AAD	A	
Expected Result:		

Multipath error :XPL Global Availability

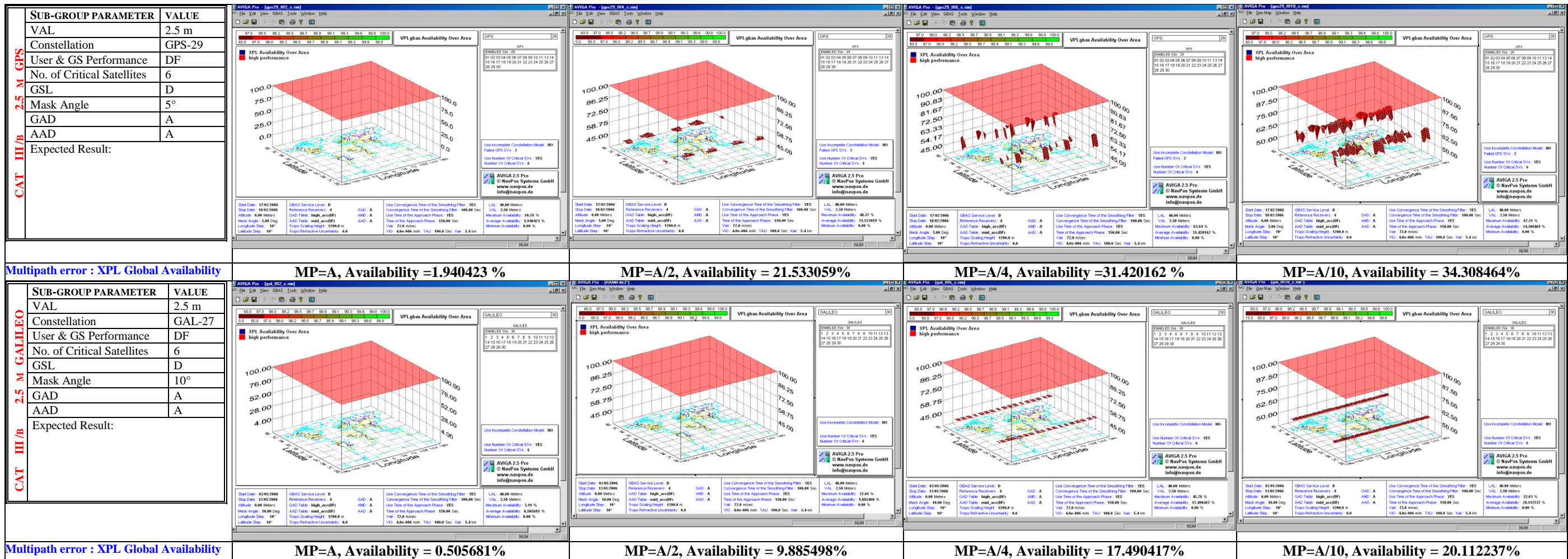
CAT II 5M GPS	SUB-GROUP PARAMETER	VALUE
	VAL	5 m
	Constellation	GPS-29
	User & GS Performance	DF
	No. of Critical Satellites	6
	GSL	D
	Mask Angle	5°
GAD	A	
AAD	A	
Expected Result:		

Multipath error :XPL Global Availability

CAT II 5M GALILEO	SUB-GROUP PARAMETER	VALUE
	VAL	5m
	Constellation	GAL27
	User & GS Performance	DF
	No. of Critical Satellites	6
	GSL	D
	Mask Angle	10°
GAD	A	
AAD	A	
Expected Result:		

Multipath error :XPL Global Availability

Appendix E: Simulations Results for the Impact of GPS Navigational Errors on the Required Performance of GBAS Approach Service Type D/F (GAST-D/F)



Appendix E: Simulations Results for the Impact of GPS Navigational Errors on the Required Performance of GBAS Approach Service Type D/F (GAST-D/F)

SUB-GROUP PARAMETER	VALUE
VAL	10 m
Constellation	GPS-29
User & GS Performance	SF
No. of Critical Satellites	6
GSL	D
Mask Angle	5°
GAD	B
AAD	B
Expected Result:	

Multipath error :XPL Global Availability

SUB-GROUP PARAMETER	VALUE
VAL	10 m
Constellation	GAL27
User & GS Performance	SF
No. of Critical Satellites	6
GSL	D
Mask Angle	10°
GAD	B
AAD	B
Expected Result:	

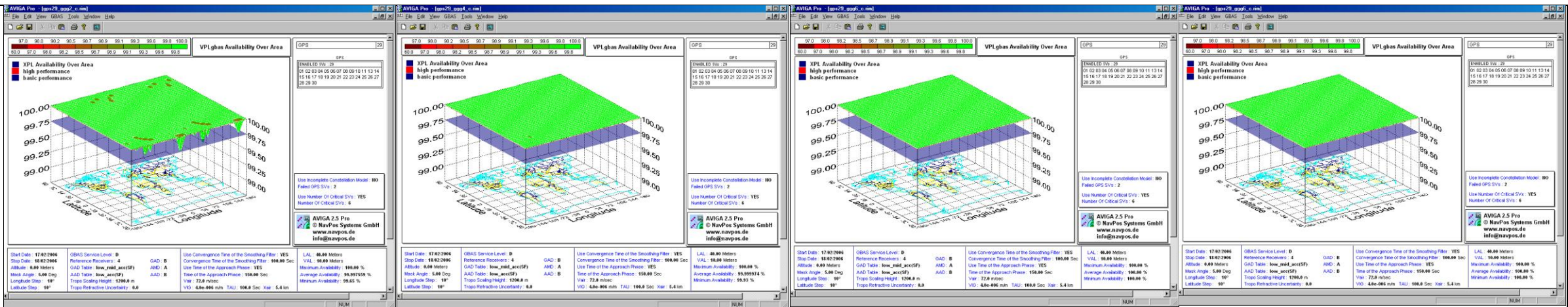
Multipath error: XPL Global Availability

SUB-GROUP PARAMETER	VALUE
VAL	5 m
Constellation	GPS-29
User & GS Performance	SF
No. of Critical Satellites	6
GSL	D
Mask Angle	5°
GAD	B
AAD	B
Expected Result:	

Multipath error :XPL Global Availability

SUB-GROUP PARAMETER	VALUE
VAL	5 m
Constellation	GAL27
User & GS Performance	SF
No. of Critical Satellites	6
GSL	D
Mask Angle	10°
GAD	B
AAD	B
Expected Result:	

Multipath error: XPL Global Availability

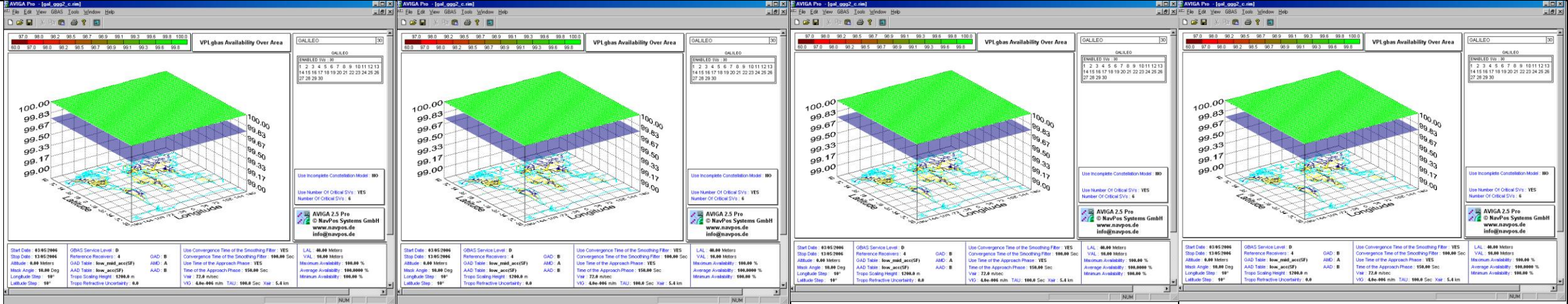


MP=A, Availability =99.997559%

MP=A/2, Availability =99.999974 %

MP=A/4, Availability = 100.000%

MP=A/10, Availability =100.00 %

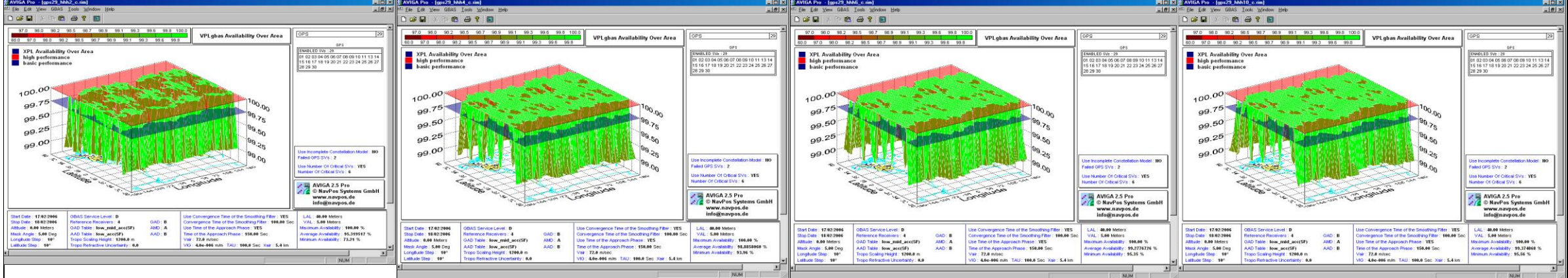


MP=A, Availability =100.00%

MP=A/2, Availability = 100.00%

MP=A/4, Availability = 100.00%

MP=A/10, Availability = 100.00%

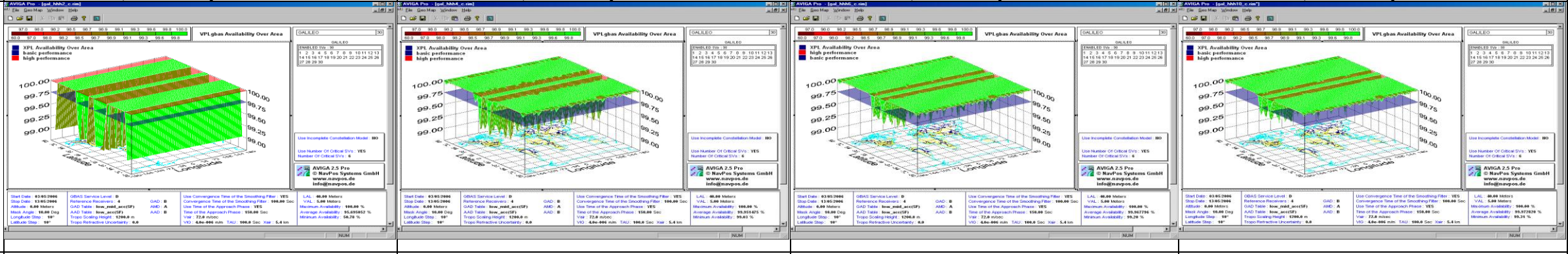


MP=A, Availability = 95.319517%

MP=A/2, Availability = 98.885806%

MP=A/4, Availability = 99.277672 %

MP=A/10, Availability = 99.374868%



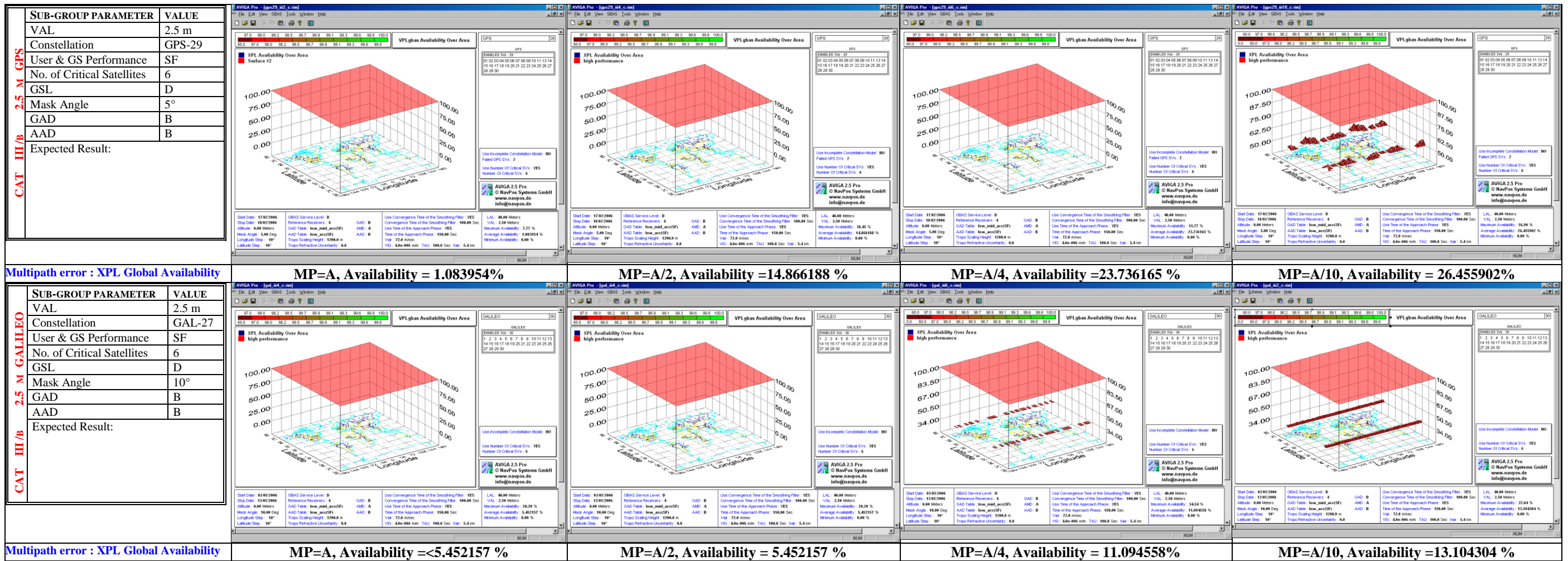
MP=A, Availability =95.695052%

MP=A/2, Availability =99.951475 %

MP=A/4, Availability = 99.967796%

MP=A/10, Availability =99.972820%

Appendix E: Simulations Results for the Impact of GPS Navigational Errors on the Required Performance of GBAS Approach Service Type D/F (GAST-D/F)



Appendix E: Simulations Results for the Impact of GPS Navigational Errors on the Required Performance of GBAS Approach Service Type D/F (GAST-D/F)

SUB-GROUP PARAMETER	VALUE
VAL	10 m
Constellation	GPS-29
User & GS Performance	DF
No. of Critical Satellites	6
GSL	D
Mask Angle	5°
GAD	B
AAD	B
Expected Result:	

Multipath error :XPL Global Availability

SUB-GROUP PARAMETER	VALUE
VAL	10 m
Constellation	GAL27
User & GS Performance	DF
No. of Critical Satellites	6
GSL	D
Mask Angle	10°
GAD	B
AAD	B
Expected Result:	

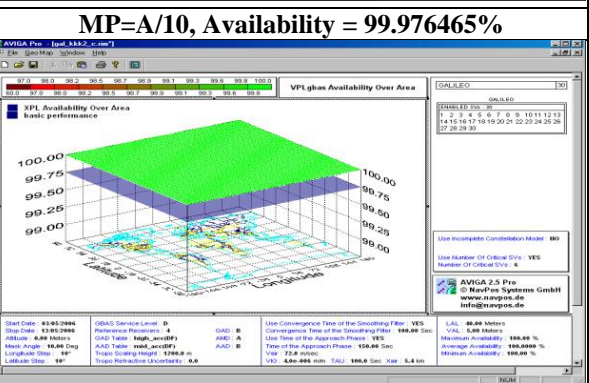
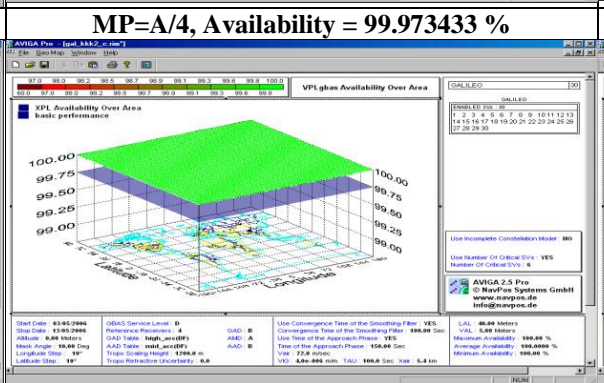
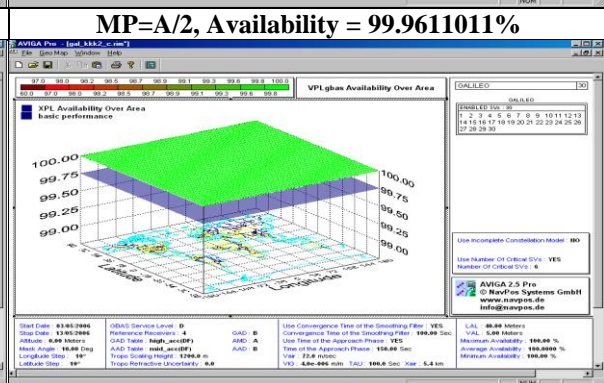
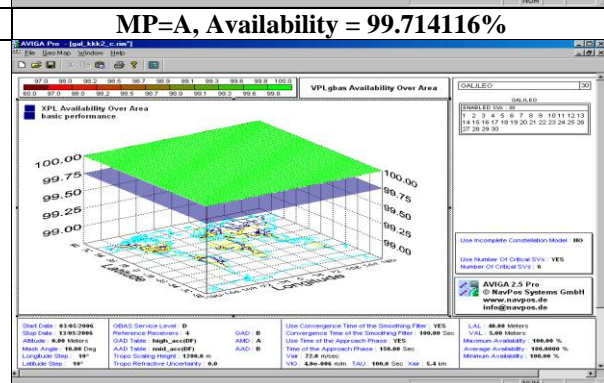
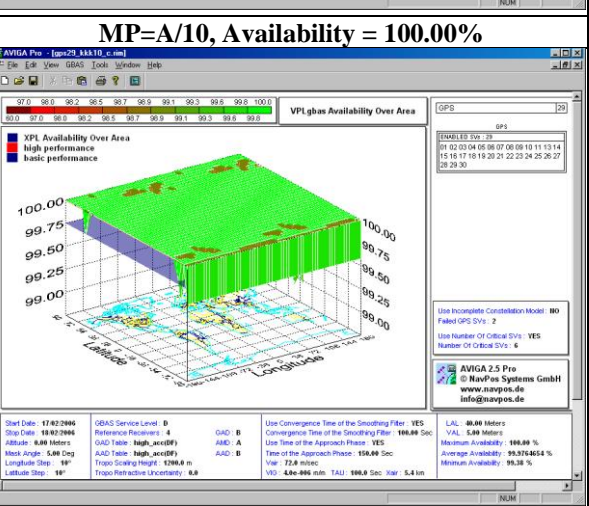
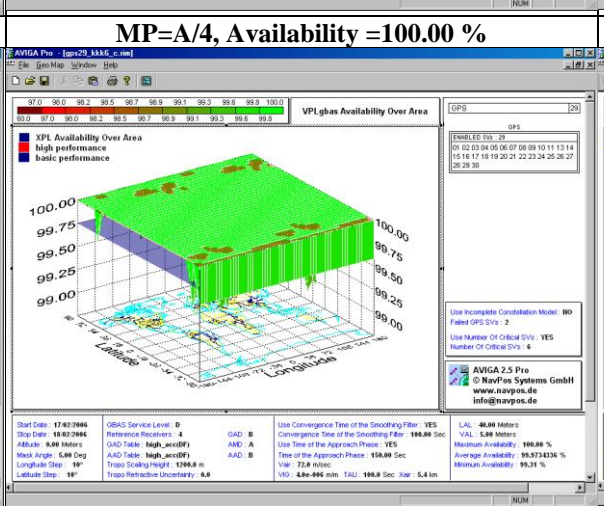
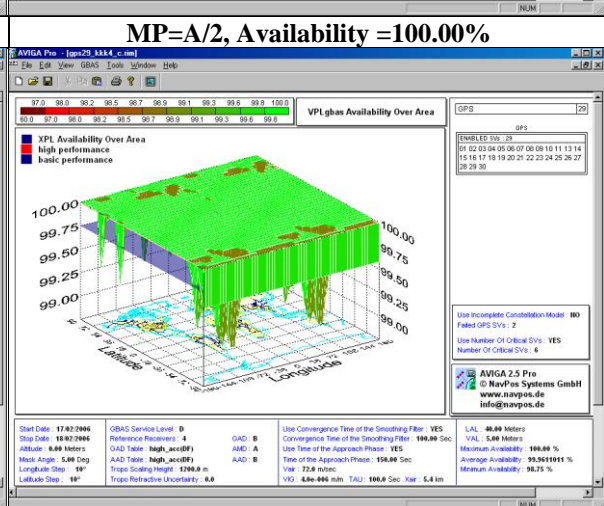
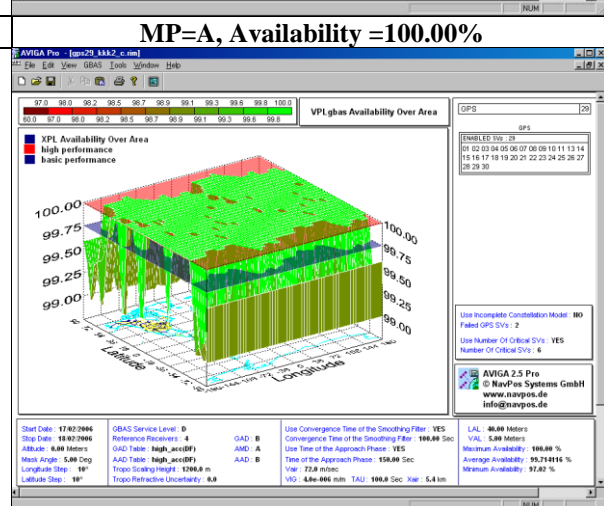
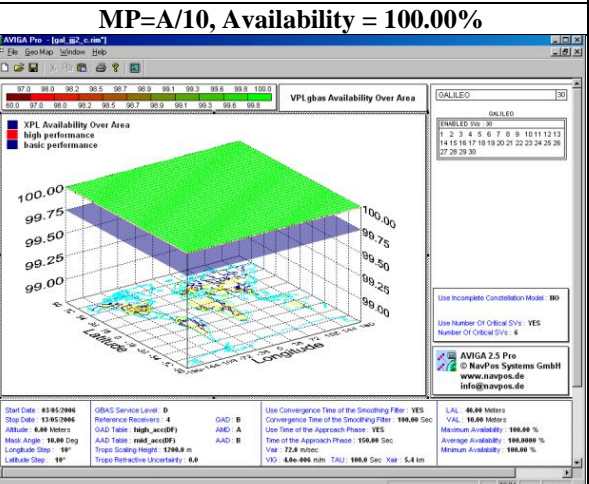
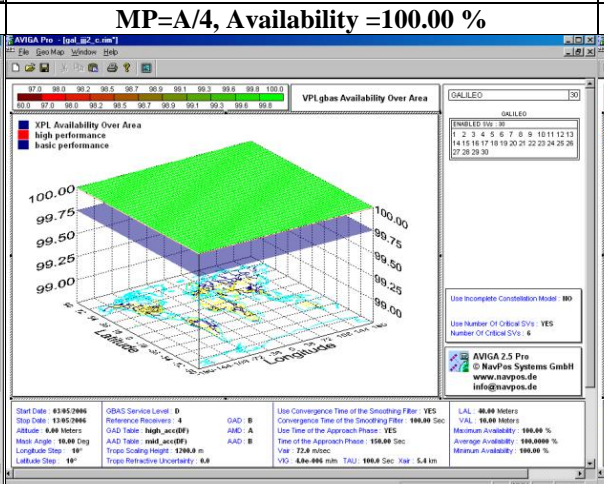
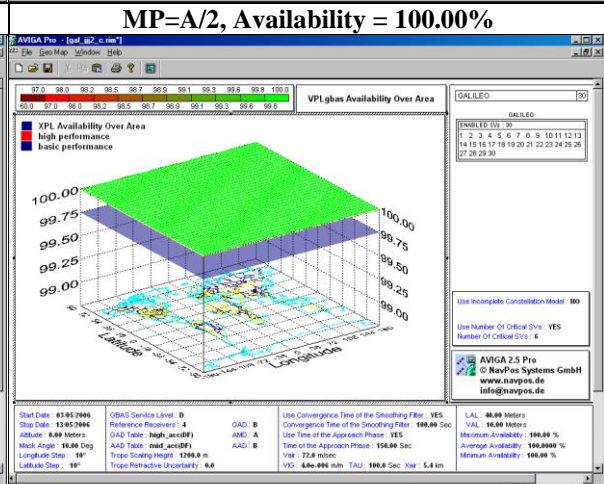
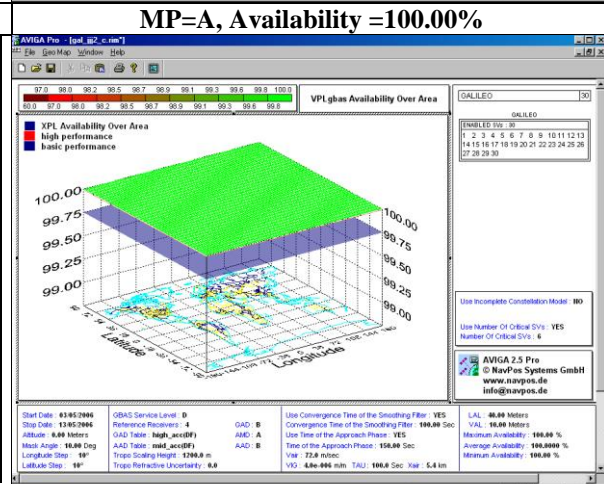
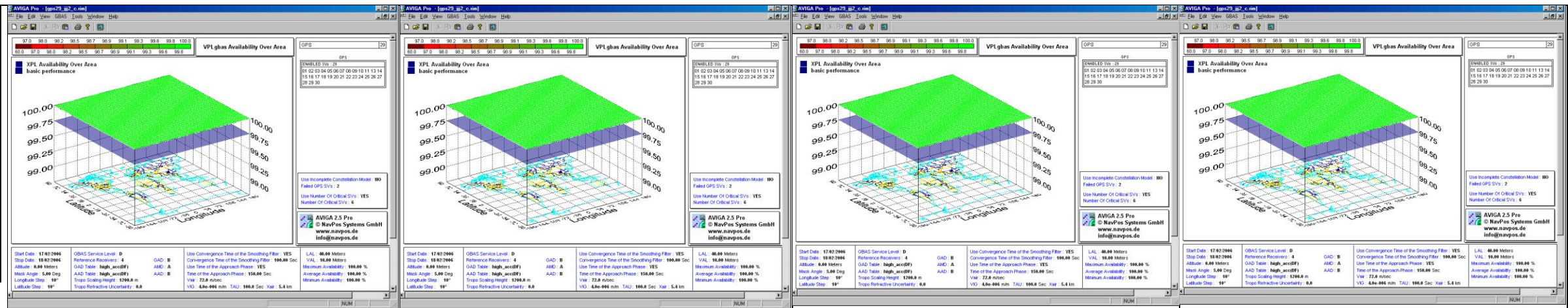
Multipath error :XPL Global Availability

SUB-GROUP PARAMETER	VALUE
VAL	5 m
Constellation	GPS-29
User & GS Performance	DF
No. of Critical Satellites	6
GSL	D
Mask Angle	5°
GAD	A
AAD	A
Expected Result:	

Multipath error :XPL Global Availability

SUB-GROUP PARAMETER	VALUE
VAL	5 m
Constellation	GAL27
User & GS Performance	DF
No. of Critical Satellites	6
GSL	D
Mask Angle	10°
GAD	B
AAD	B
Expected Result:	

Multipath error :XPL Global Availability



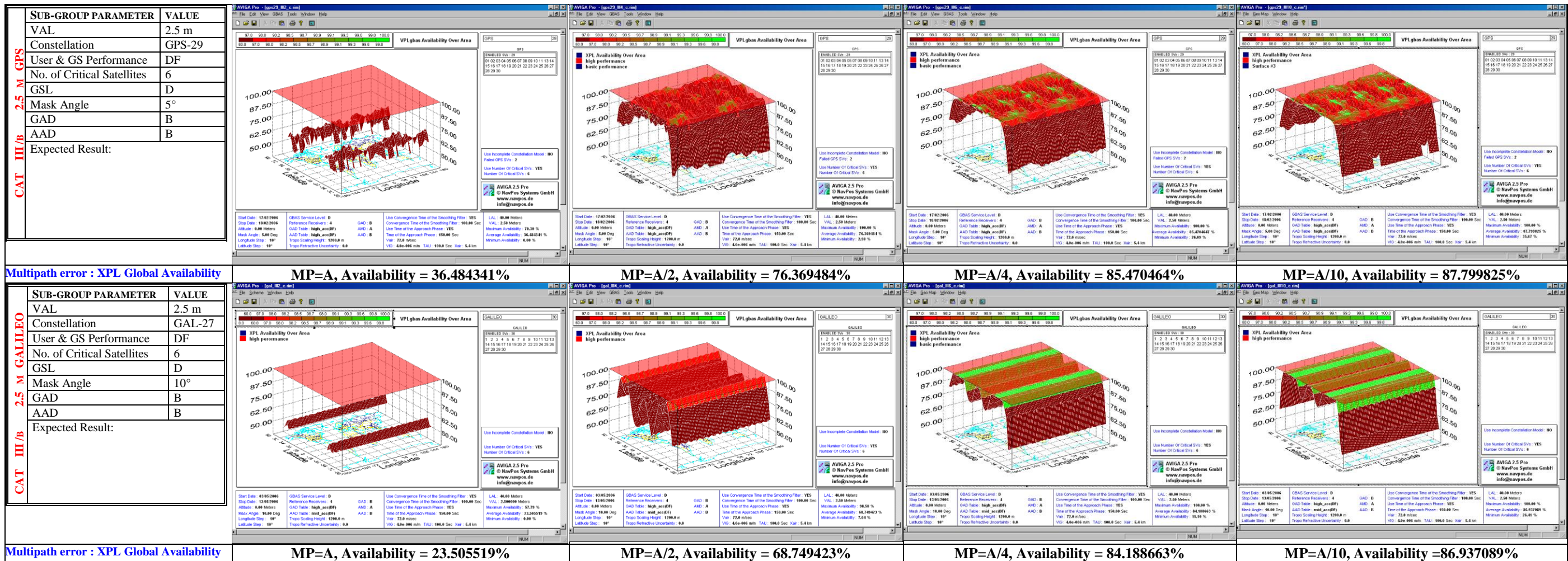
MP=A, Availability = 100.00%

MP=A/2, Availability = 100.00%

MP=A/4, Availability = 100.00%

MP=A/10, Availability = 100.00%

Appendix E: Simulations Results for the Impact of GPS Navigational Errors on the Required Performance of GBAS Approach Service Type D/F (GAST-D/F)



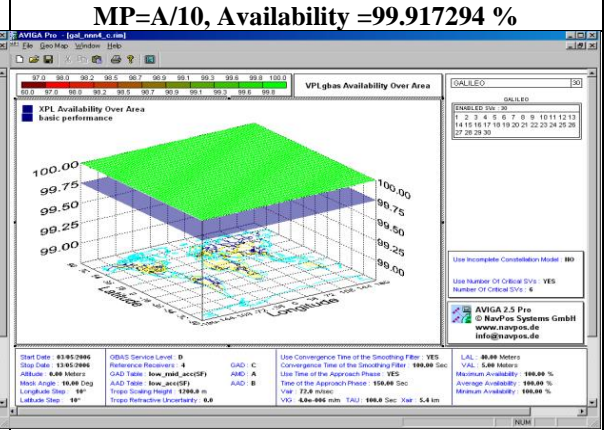
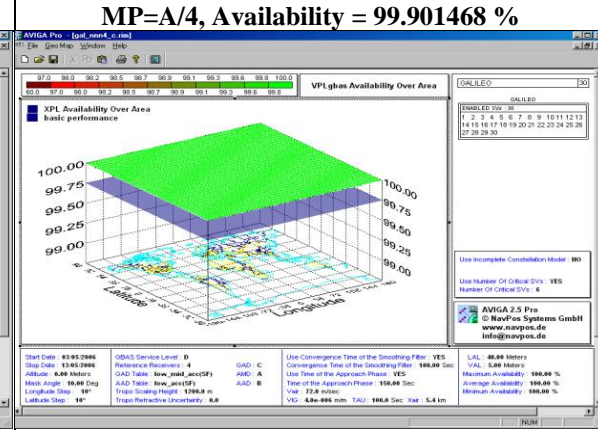
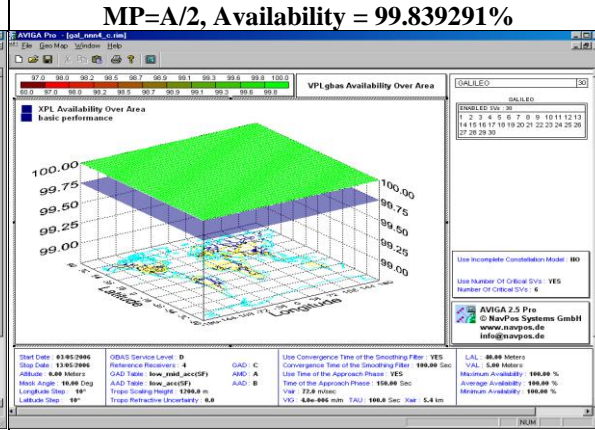
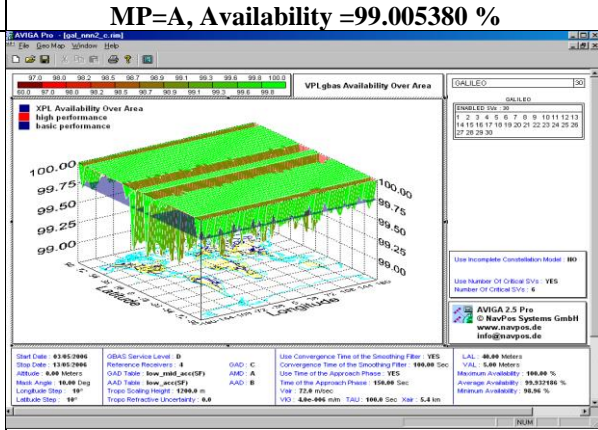
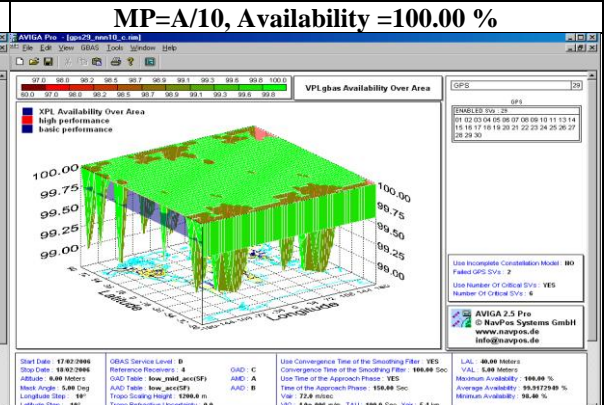
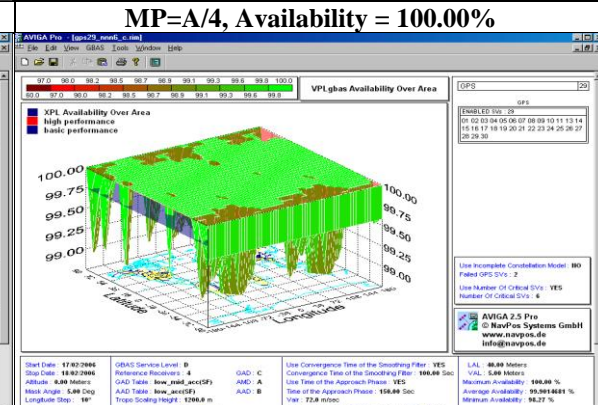
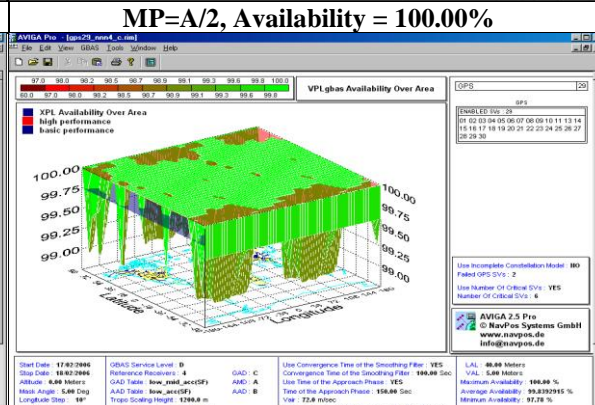
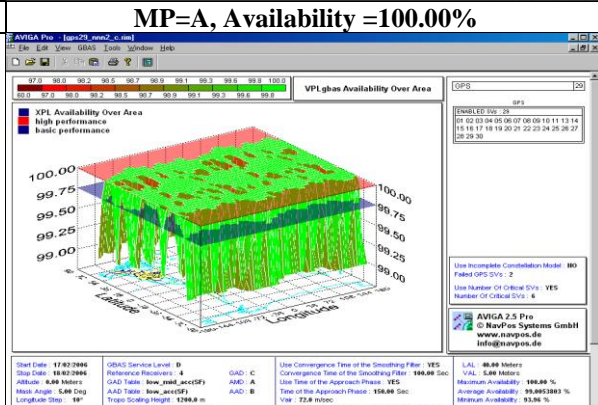
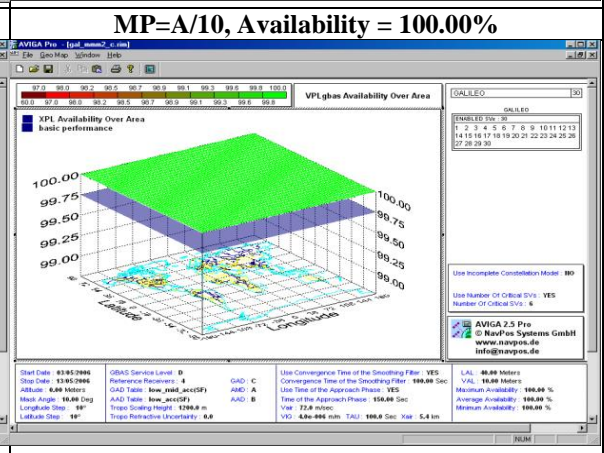
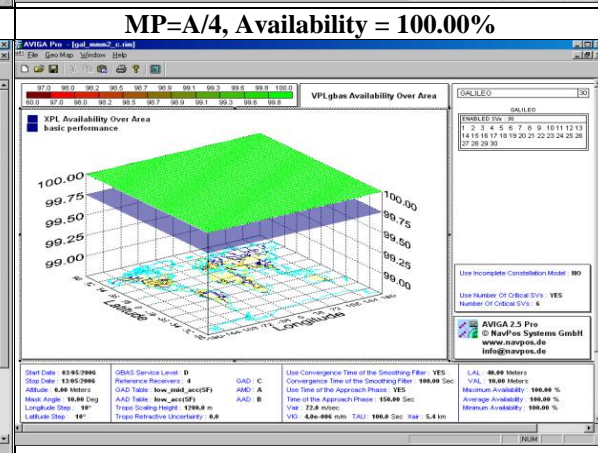
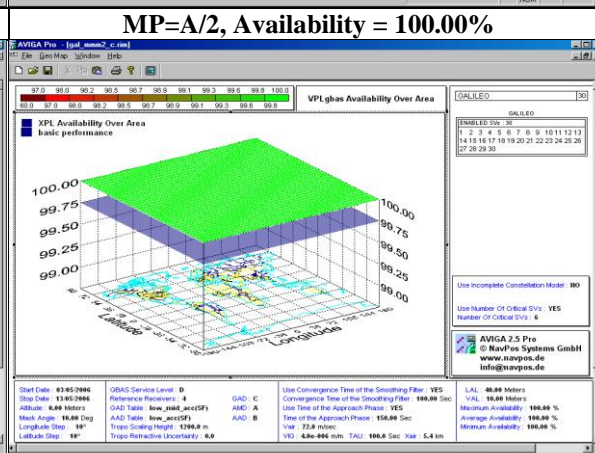
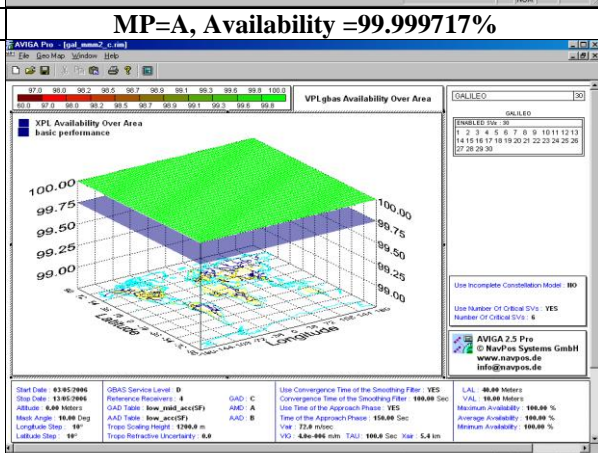
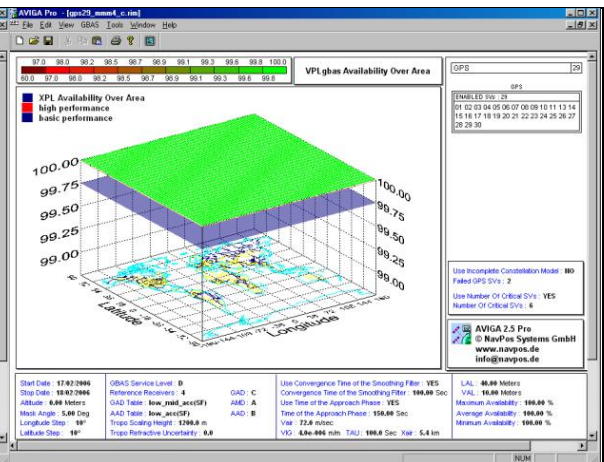
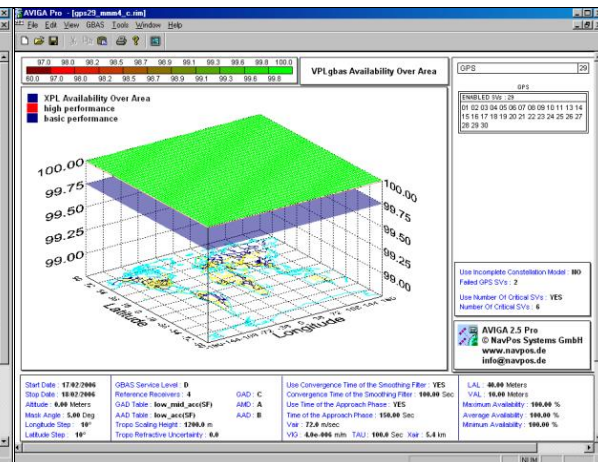
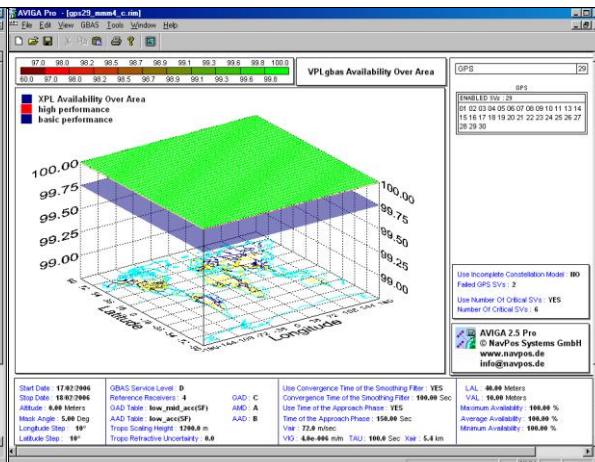
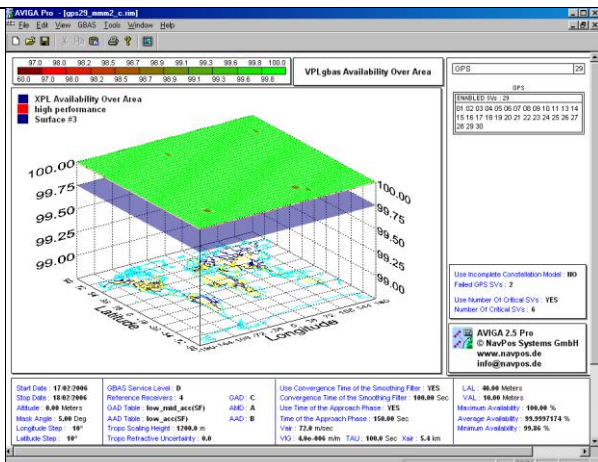
Appendix E: Simulations Results for the Impact of GPS Navigational Errors on the Required Performance of GBAS Approach Service Type D/F (GAST-D/F)

SUB-GROUP PARAMETER	VALUE
VAL	10 m
Constellation	GPS-29
User & GS Performance	SF
No. of Critical Satellites	6
GSL	D
Mask Angle	5°
GAD	C
AAD	B
Expected Result:	

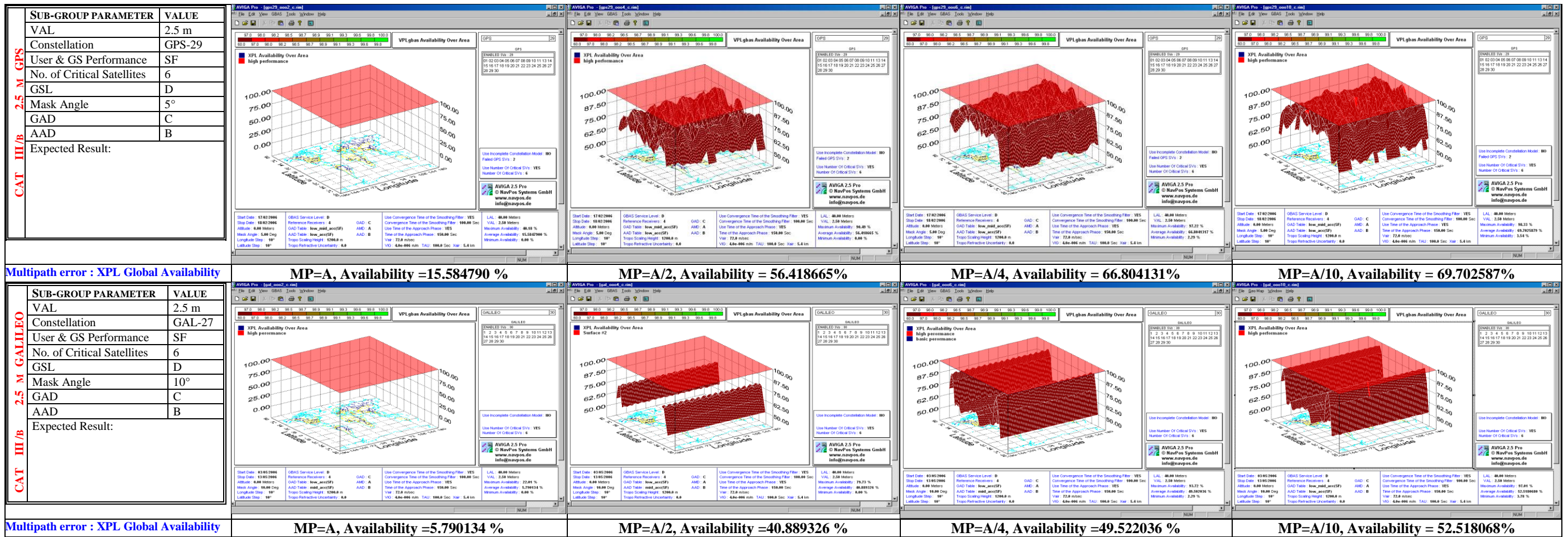
SUB-GROUP PARAMETER	VALUE
VAL	10 m
Constellation	GAL27
User & GS Performance	SF
No. of Critical Satellites	6
GSL	D
Mask Angle	10°
GAD	A
AAD	A
Expected Result:	

SUB-GROUP PARAMETER	VALUE
VAL	5 m
Constellation	GPS-29
User & GS Performance	SF
No. of Critical Satellites	6
GSL	D
Mask Angle	5°
GAD	C
AAD	B
Expected Result:	

SUB-GROUP PARAMETER	VALUE
VAL	5 m
Constellation	GAL27
User & GS Performance	SF
No. of Critical Satellites	6
GSL	D
Mask Angle	10°
GAD	C
AAD	B
Expected Result:	



Appendix E: Simulations Results for the Impact of GPS Navigational Errors on the Required Performance of GBAS Approach Service Type D/F (GAST-D/F)

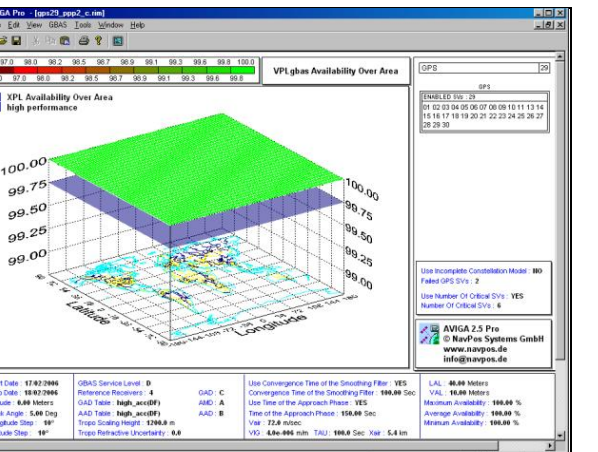
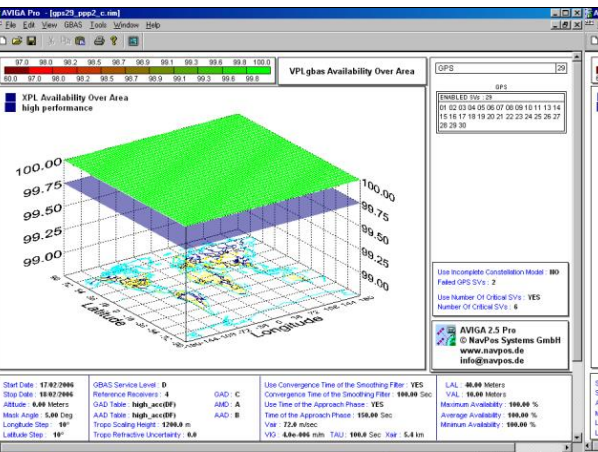
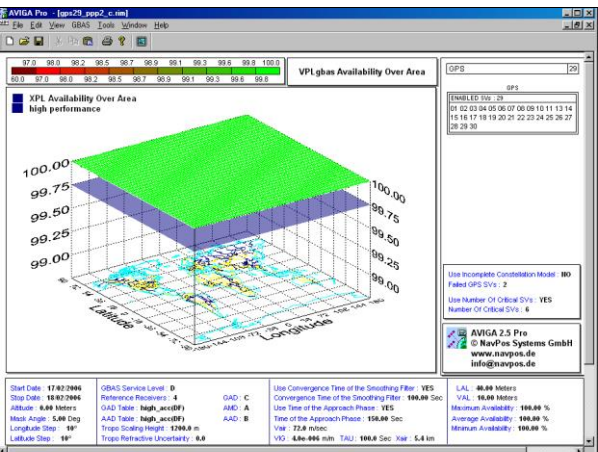
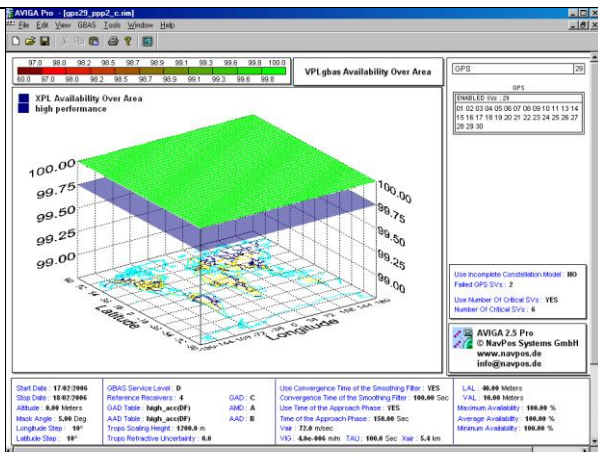


Appendix E: Simulations Results for the Impact of GPS Navigational Errors on the Required Performance of GBAS Approach Service Type D/F (GAST-D/F)

SUB-GROUP PARAMETER	VALUE
VAL	10 m
Constellation	GPS-29
User & GS Performance	DF
No. of Critical Satellites	6
GSL	D
Mask Angle	5°
GAD	C
AAD	B
Expected Result:	

Multipath error :XPL Global Availability

SUB-GROUP PARAMETER	VALUE
VAL	10 m
Constellation	GAL27
User & GS Performance	DF
No. of Critical Satellites	6
GSL	D
Mask Angle	10°
GAD	C
AAD	B
Expected Result:	

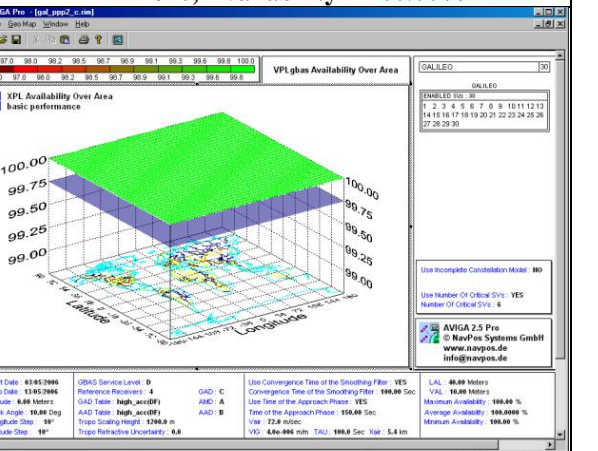
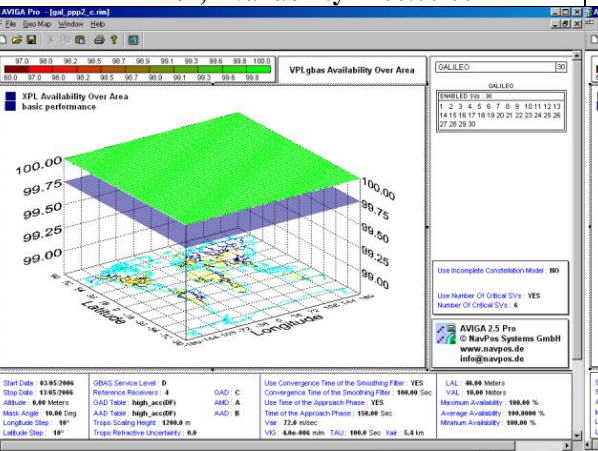
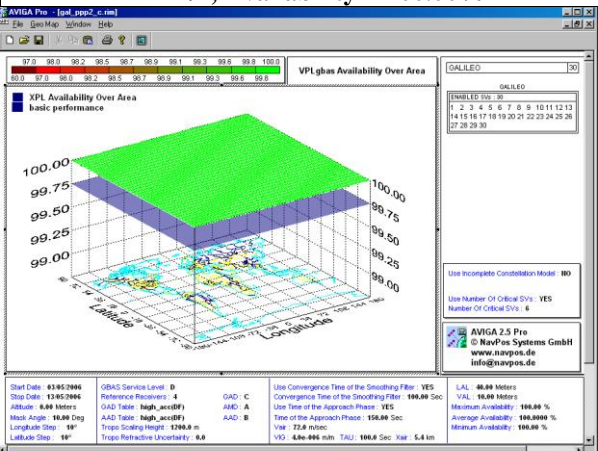
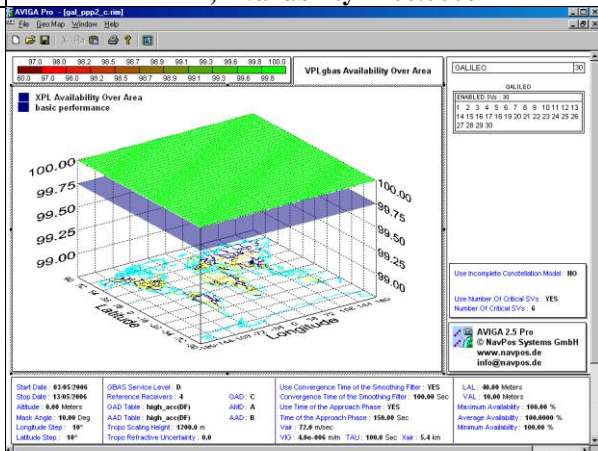


MP=A, Availability =100.00%

MP=A/2, Availability = 100.00%

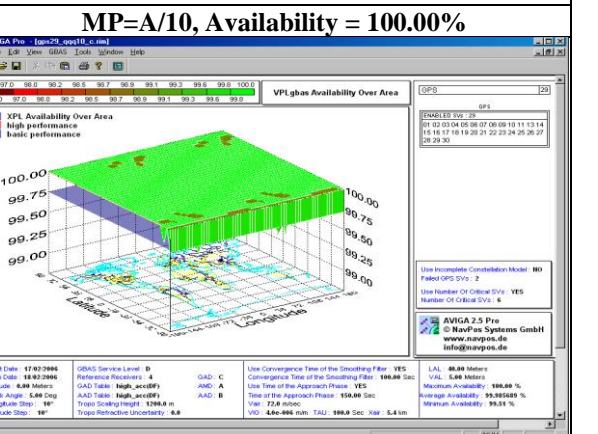
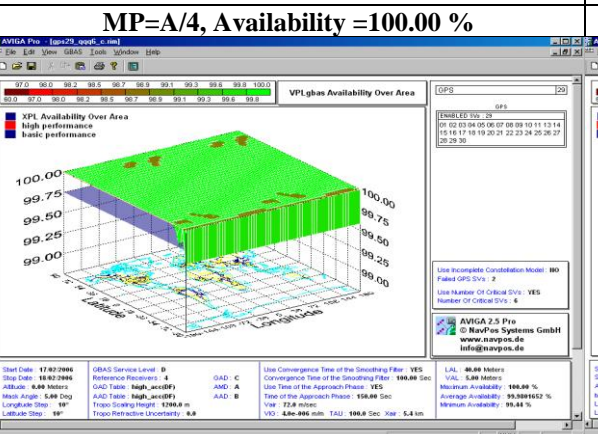
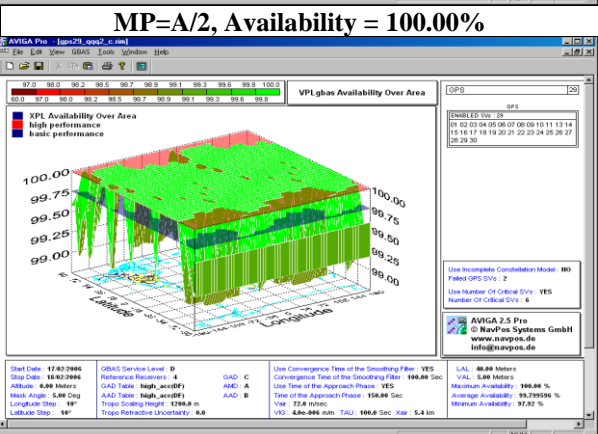
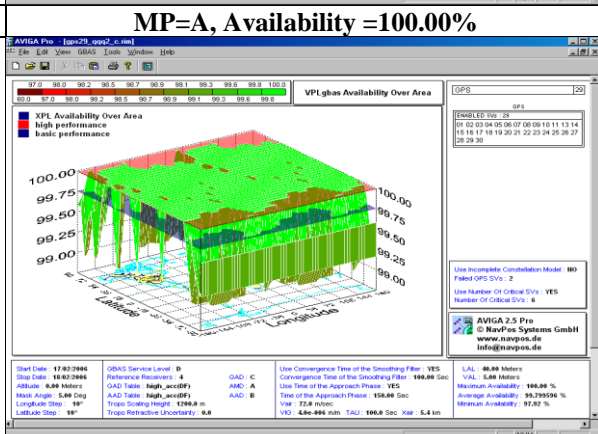
MP=A/4, Availability =100.00 %

MP=A/10, Availability = 100.00%



Multipath error: XPL Global Availability

SUB-GROUP PARAMETER	VALUE
VAL	5 m
Constellation	GPS-29
User & GS Performance	DF
No. of Critical Satellites	6
GSL	D
Mask Angle	5°
GAD	C
AAD	B
Expected Result:	

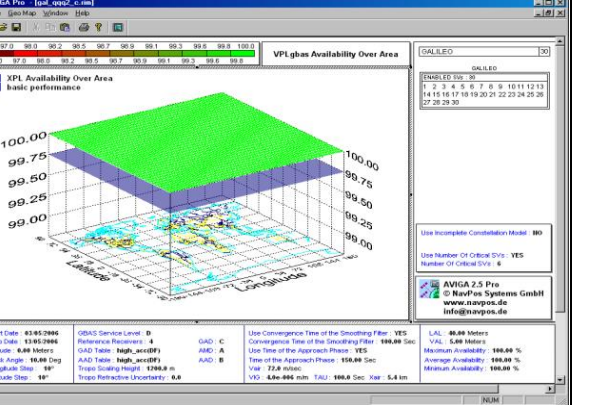
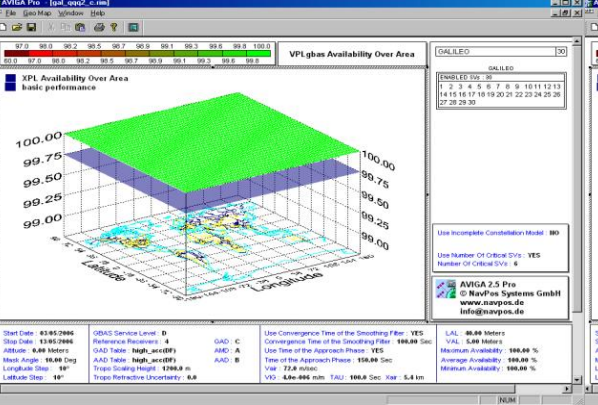
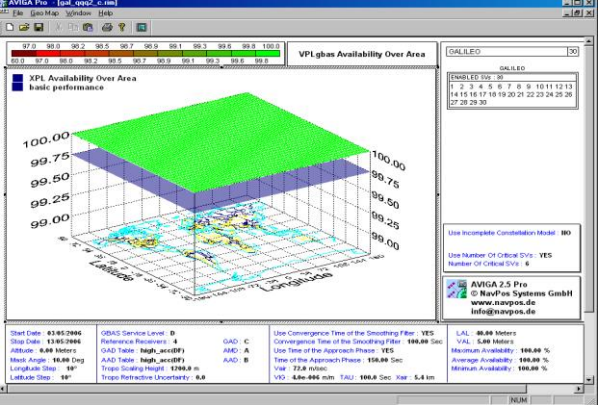
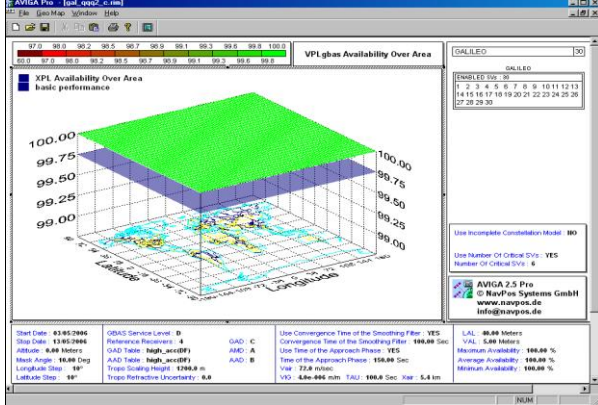


MP=A, Availability = 99.799596%

MP=A/2, Availability = 99.971943%

MP=A/4, Availability = 99.980165 %

MP=A/10, Availability = 99.985689%



Multipath error: XPL Global Availability

MP=A, Availability =100.00%

MP=A/2, Availability = 100.00%

MP=A/4, Availability = 100.00%

MP=A/10, Availability = 100.00%

Appendix E: Simulations Results for the Impact of GPS Navigational Errors on the Required Performance of GBAS Approach Service Type D/F (GAST-D/F)

